



Thermo-responsive Graft Copolymers based on Poly(Methyl Vinyl Ether) : from Synthesis to Evaluation

Ondine Confortini

Promotor : Prof. Dr. Filip Du Prez

GHENT UNIVERSITY
Faculty of Sciences
Department of Organic Chemistry
Polymer Chemistry Research Group

Academic Year 2008-2009

Thesis submitted to obtain the grade of Doctor in Sciences: Chemistry

**Thermo-responsive Graft Copolymers based on
Poly(Methyl Vinyl Ether) : from Synthesis to Evaluation**

Ondine Confortini

Polymer Chemistry Research Group
Department of Organic Chemistry
Ghent University
Belgium

ACADEMIC DISSERTATION

Thesis submitted to obtain the degree of Doctor in Sciences: Chemistry

*To be presented with the permission of the Faculty of Science of the Ghent University for
public criticism in Auditorium A of the Department of Organic Chemistry,
on April 30th, 2009, at 15h00.*

Ghent 2009

Supervisor

Professor Filip Du Prez
Polymer Chemistry Research Group
Ghent University
Belgium

Reviewers

Professor Heikki Tenhu
Laboratory of Polymer Chemistry
University of Helsinki
Finland

and

Professor Bruno Van Mele
Department of Physical Chemistry and Polymer Science
Free University of Brussels
Belgium

Jury

Professor Filip Du Prez (promoter, UGent)
Professor Heikki Tenhu (University of Helsinki, Finland)
Professor Bruno Van Mele (Free University of Brussels, Belgium)
Professor Em. Eric Goethals (UGent, Belgium)
Professor Peter Dubrueel (UGent, Belgium)

Acknowledgments

First of all, I wish to express my deepest gratitude to my supervisor, Professor Filip Du Prez for offering me the opportunity to take part in this project, which opened the doors of the fascinating world of nanotechnology. While allowing me considerable freedom, he also taught me how to manage it. I will keep an unforgettable memory of the solid scientific methodology he taught me. I am grateful for his scientific guidance, encouragement, and patience during these years. I wish to thank him for offering me the possibility to spend the most instructive and challenging period of my life in Ghent.

I am grateful to Professor Em. Eric Goethals for having welcomed me as a foreign master student, for the possibility to start to work in his laboratory, and for learning me to write my first international publication.

I am grateful to Professor Jean-Paul L  n   in the University of Rouen who found me my master training in Ghent, which finally permitted me to obtain the degree of Doctor in Sciences with Professors Eric Goethals and Filip Du Prez.

It is an honour for me that Professor Heikki Tenhu and Professor Bruno Van Mele accepted to be the reviewers of this work. I thank Professors Eric Goethals and Peter Dubruel for the examination of this work and I am pleased that Professor Katrien Strubbe is the president of this jury.

This manuscript is the result of numerous collaborations that made the realization of an interdisciplinary study possible.

I am very grateful to Professor Heikki Tenhu in the University of Helsinki for offering me the excellent facilities in Dynamic Light Scattering (DLS), High Sensitivity Differential Scanning Calorimetry (HS-DSC) and Pressure Perturbation Calorimetry (PPC). I am also grateful to Dr. Vladimir Aseyev for offering me his expertise in DLS, and Dr. Antti Laukkanen for HS-DSC and PPC. Your guidances in editing the manuscripts were most helpful!

I am very grateful to Professor Bruno Van Mele in the Free University of Brussels for his interest in my work and for offering me the opportunity to characterize the thermo-responsive properties of my graft copolymers by Modulated Temperature Differential Scanning Calorimetry (MTDSC). I also thank him for the constructive and interesting criticism of the manuscript. I would also like to thank Dr. Kurt Van Durme, Dr. Jun Zhao and Dr. Guy Van Assche for all the help with the measurements by MTDSC.

I specially thank Professor Rudy Willem and Dr. Monique Biesemans in the Free University of Brussels for their valuable discussion and help concerning the evaluation of the grafting degree of my graft copolymers, and who permit me to use their MATLAB program.

I would also specially thank Professor Uwe Beginn in the University of Aachen in Germany for his long discussion about the different methods to determine the monomer reactivity ratios and who permits me to used his BASIC program.

I would like to thank Professor Etienne Schacht and Dr. Veska Toncheva in UGent for the critical aggregate concentration (CAC) measurements, and Mr Roeland Myngheer for the PEO synthesis.

I would like to thank Professor V. Zubov and Dr. N. Bulychev in the University of Moscow for his interest in my work and for the dye stabilization of my PMVE-*g*-PEO/water system.

I also wish to thank my short-term colleagues in the University of Helsinki for making my stay very enjoyable by creating a friendly and helpful atmosphere in the laboratory. I will never forget this typical Sauna party!

I would like to thank all the former and current members of the Department of Organic Chemistry: Professors, technicians and colleagues, for making it such a pleasant place to work. Especially thanks to Beatrice Verdonck and Peggy Van De Velde who learned me the base of the polymer synthesis and the living cationic polymerization. I wish to thank Nadya, Laurence, Céline, Malgosia, Dilek, Dennis, Tianzhu and Irene for their friendship.

Finally, I wish to owe my warmest thanks to my parents, Jacques and friends for their endless love, encouragement and belief in me.

Financial support from UGent and the European Scientific Foundation (ESF) are gratefully acknowledged.

Brussels, April 2009

Ondine Confortini

Introduction and Aim.....	1
PART I : Functionalized Random Copolymers of Hydrophilic and Hydrophobic Vinyl Ether Monomers Obtained by Living Cationic Copolymerizations.....	9
Content of Part I.....	10
Abstract.....	12
Chapter 1 : Theory of Living Cationic Polymerization of Vinyl Ethers.....	13
Chapter 2 : Theory of the Determination of the Reactivity Ratios of Random Copolymers.....	31
Chapter 3 : Synthesis of Vinyl Ether Copolymers by Cationic Copolymerizations.....	41
PART II : Design of Novel Thermo-responsive Poly(Methyl Vinyl Ether)-<i>g</i>-Poly(Ethylene Oxide) Graft Copolymers via the 'Grafting onto' Method.....	75
Content of Part II.....	76
Abstract.....	78
Chapter 4 : Theoretical Aspects of Graft Copolymers.....	79
Chapter 5 : Synthesis and Molecular Characterization of Poly(Methyl Vinyl Ether)- <i>g</i> -Poly(Ethylene Oxide) Graft Copolymer.....	89
Chapter 6 : Thermo-responsive Properties of PMVE- <i>g</i> -PEO Graft Copolymers.....	105
PART III : Well-defined Stimuli-responsive Graft Copolymer Structures by Combination of the 'Grafting From' Method and ATRP....	143
Content of Part III.....	144
Abstract.....	146
Chapter 7 : Theory of Controlled Radical Polymerization.....	147
Chapter 8 : Synthesis of Poly(Methyl Vinyl Ether) based Graft Copolymers via 'Grafting From' Method.....	161
Chapter 9 : Properties of Thermo-responsive PMVE- <i>g</i> -PS Graft Copolymer.....	191
PART IV : Experimental Part.....	207
Content of Part IV.....	208
IV.1. Reagents and Materials.....	209
IV.2. Analytical Methods: Measurements.....	211
IV.3. Syntheses.....	225
Conclusion.....	241
Appendix I : COPOINT Program.....	249
Appendix II : Basic Program for the Tidwell-Mortimer Method.....	251
Appendix III : Determination of the Degree of Functionalization of PMVE- <i>g</i> -PEO by Elemental Analysis and the Non-linear Least-squares Analysis.....	253
Appendix IV : Abbreviations	259

INTRODUCTION

What is strongest than the stone or softest than water? Nevertheless, soft water corrodes the stone so strong. The perseverance.

Ovide

Introduction and Aim

Introduction

The range of research into the so-called *stimuli-responsive polymers*, also referred to as *smart polymers*, has been considerably extended in recent years. Investigations in this area are at the leading edge of modern science [1-7]. Smart polymers are polymers that undergo reversible sharp physical or chemical modifications in response to specific changes in their environment (figure I1, table I1). The microscopic changes are apparent at the macroscopic level as precipitation formation in a solution or an order of magnitude decrease or increase in hydrogel size or solvent content. As living processes are based on such responses to stimuli, these smart macromolecules are the compounds of choice to study and mimic biological systems. Therefore, a lot of research work has been devoted to the conception of stimuli-responsive polymers used in composite systems responding to temperature, pH, ionic strength, chemicals, electric or magnetic fields, light, etc.

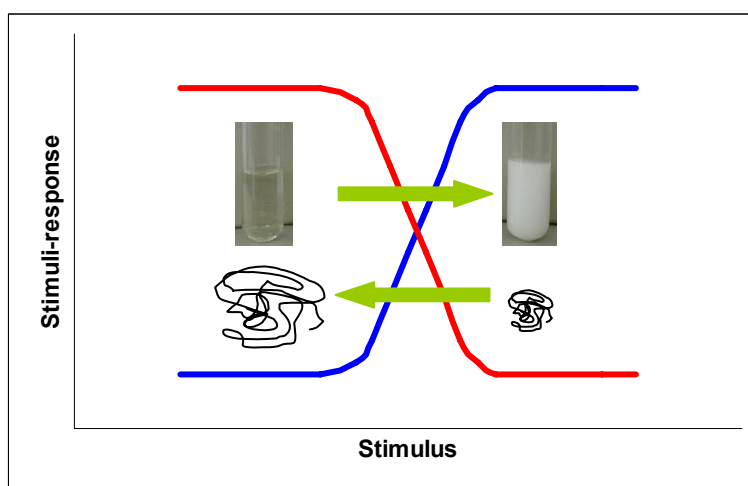


Figure I1. Sketch of smart behaviour of polymers.

The practical importance of smart polymers is extremely wide and versatile. They can radically change quite a variety of technological processes. Smart polymers are sometimes called materials of the XXI century and have been extensively used in diverse fields, such as in membrane activities [5, 8], chromatography [3,6,9], fabrication of sensors and actuators [10] and artificial muscles [11]. They can also be used in the treatment and diagnosis of various diseases. They are employed for making polymeric systems for controlled release of drugs [12-16] and their targeted delivery to a certain site of the human body [12,14-16], immobilization of various biologically active substances for the purpose of their storage and further utilization [12,15,17], removal of toxins from solutions [15,18], and creation of new effective systems for immune assay

(antibody-antigen interaction under homogeneous conditions) [19]. On the basis of smart polymers, controllable polymeric systems were created, which undergo transitions from a homogeneous to a heterogeneous state by the action of small changes in the environment. This made it possible to develop advanced technologies for isolating and purifying biologically active substances [1-2,20], which is of primary importance; concentrating metal ions [21]; separating organic substances [1,21]; and dewatering gels and suspensions [22]. Most of the polymers presented previously are responsive to only one kind of stimulus, but for some applications, independent responsiveness to several factors, such as temperature and pH, may be required.

Table I1. Several types of stimuli used in the area of responsive polymers.

<i>Physical</i>	<i>Chemical</i>	<i>Biomedical</i>
Temperature	pH	Enzyme substrates
Ionic strength	Specific ions	Affinity ligands
Solvents	Chemical agents	Other biomedical agents
Electric and magnetic fields		
Radiation (UV, visible light, ultrasonic)		
Mechanical stress and strain		

Poly(methyl vinyl ether) (PMVE) is an example of a non-ionic polymer with thermo-responsive behaviour and is easily transformed into a polymer gel by high energy radiation, such as γ -ray or electron beam. Moreover, PMVE can be synthesized by living cationic polymerization, allowing to combine it with a variety of other polymer segments in a controlled way (**Chapter 1**). An aqueous solution of PMVE exhibits phase separation in water at a *Lower Critical Solution Temperature* (LCST) equal to physiological temperatures (37°C). This means that PMVE is soluble in cold water, but precipitates upon heating above the cloud point temperature (T_{cp}). A PMVE gel also shows thermo-responsive characteristics: it swells below and shrinks above the T_{cp} . Water-swollen PMVE gels and PMVE fibrous gels having macroporous structure were used as an artificial muscle model, an automatic separation system, an artificial finger model and a photosensitive device [23]. Also, block copolymers with PMVE in water solutions have showed microphase separation [24] and thermo-responsive micellization behaviour. Amphiphilic block copolymers, in which PMVE has been combined with poly(isobutyl vinyl ether) (PIBVE) or poly(octadecyl vinyl ether) (PODVE), show high stabilization activity for aqueous dispersions of the hydrophobic organic pigments copper phthalocyanine and carbon black, as demonstrated in the own research group [25]. PMVE grafted on polystyrene (PS) surfaces caused temperature-dependent surface properties [26]. Amphiphilic dendrigrafts with PMVE and PS could be used to complex or transport selectively compounds dispersed in water media and extract them by temperature increase [27].

Aim

In our research group, PMVE was already studied in its linear form but also in combination with other polymer segments, such as *block copolymers* (PMVE-*b*-PIBVE and PMVE-*b*-PIBVE-*b*-PMVE) [25,32], and *random copolymers* (P(MVE-*co*-ODVE)) [33]. As in the last ten years, important research activity has been devoted to the design, synthesis, characterization and controlled self-organization of well-defined stimuli-responsive graft copolymer systems [28-31], our study was undertaken to investigate possible routes to generate graft copolymers of this thermo-responsive PMVE. We describe herein the preparation of such PMVE graft copolymers by using both *grafting onto* (**Chapter 5**) and *grafting from* (**Chapter 8**) approaches to attach the copolymers as nearly monodisperse side chains of controlled molecular weight.

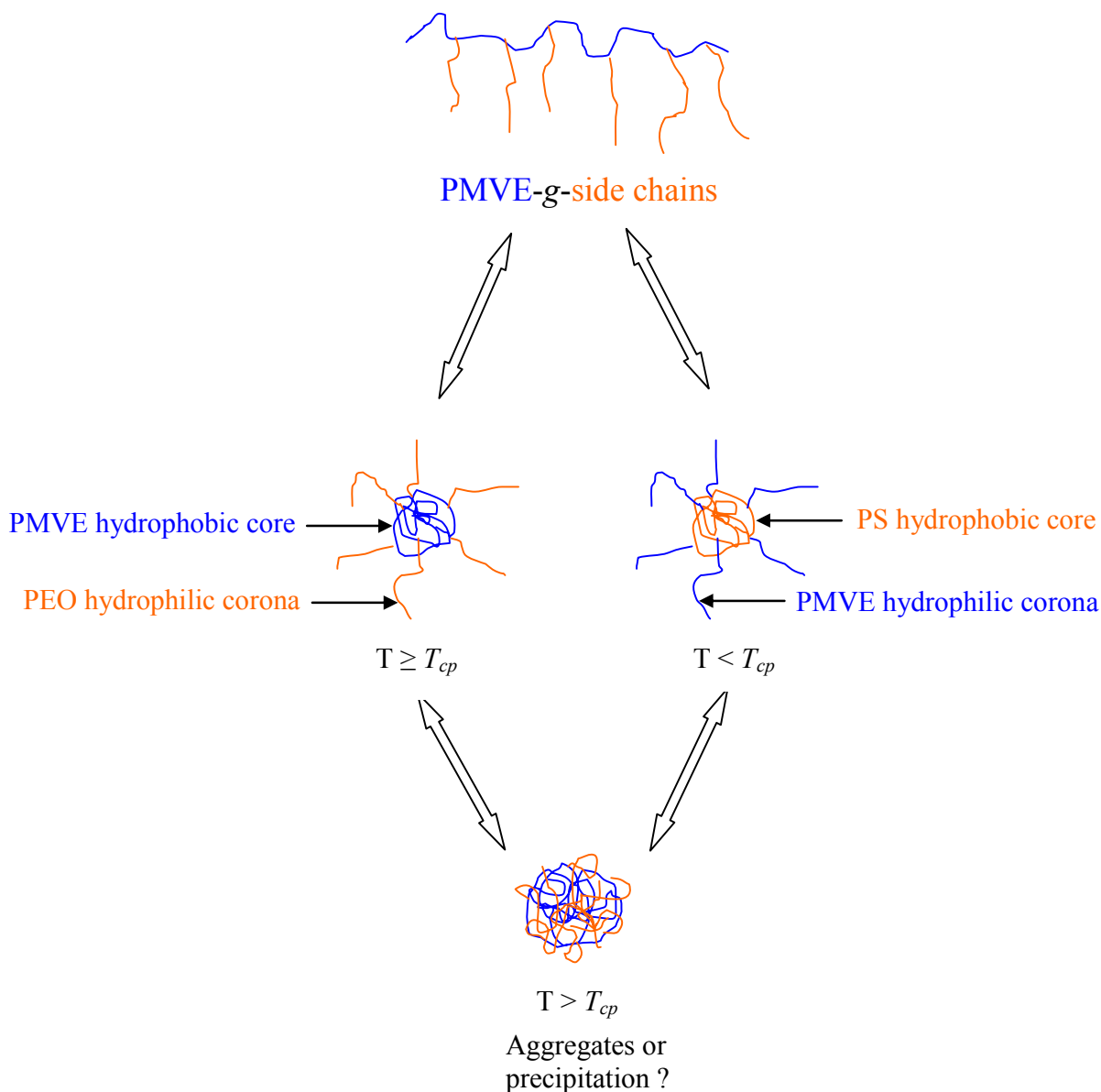
The PhD thesis is divided in three parts, each of which is preceded by a theoretical part:

1) In the first part of the research, the objective was to develop novel PMVE-based *copolymers* by means of cationic copolymerization techniques with the aim to produce a backbone for the graft copolymers with a statistical structure (**Chapter 3**). For this reason, random copolymerizations of MVE with a small quantity of 2-chloro-ethyl vinyl ether (CEVE) by living cationic polymerization techniques have been investigated. Poly(2-chloroethyl vinyl ether) (PCEVE) is a versatile reactive polymer that introduces functional groups capable of nucleophilic substitution reactions of its pendent groups with a variety of functionalized polymers. Controlled/'living' polymerization methods offer the best way to prepare well-defined polymers, i.e. with controlled molecular weights, low polydispersities and terminal functionalities, in systems with small contribution of side reactions.

2) In the second step, it was the aim to achieve grafting the PMVE backbone via the *grafting onto* procedure, which is based on the covalent binding of preformed linear PEO chains to the main chain. This first route to hydrophilic branched polymers containing a PMVE backbone consists in grafting amino-terminated PEO chains onto reactive chlorine pendent groups located on the backbone (**Chapter 5**). Compared to the *grafting from* procedure, this strategy based on the linking of an elementary macromolecular backbone allows a more accurate characterization of the resulting copolymers since the building blocks can be characterized separately. Thus, these polymers are well-defined with regard to the molecular weights of the backbone and the branches, as well as the number of branches. They can have narrow molecular weight distribution and the branches are randomly distributed over the PMVE chain.

Then, the thermo-responsive properties of these new graft copolymers with hydrophilic side chains were studied as a function of different parameters such as length and number of the side chains (**Chapter 6**). Thus, these graft copolymers could function as simple, fast and reversible

smart systems (see scheme A1). Although the application of these systems was not part of this research, they could be applied as surfactants, dispersants and stabilizers for colloidal suspensions or controlling the rheology of aqueous formulations, as was already demonstrated for a variety of other segmented polymer structures in our research group.



Scheme A1. Possible modes of aggregates formation for thermo-responsive PMVE graft copolymers in aqueous solution with PEO hydrophilic and PS hydrophobic side chains.

3) In the last part, two different graft copolymers on PMVE backbone were performed via the *grafting from* procedure, which consists in growing PS or PtBMA grafts directly from the backbone (**Chapter 8**). Following the second approach, graft copolymers with PS or PtBMA branches have been prepared from poly(methyl vinyl ether-co-(2-chloroethyl vinyl ether)) (P(MVE-co-CEVE)) with a suitable atom transfer radical polymerization (ATRP) initiator. ATRP [34] is a process, which has been used to prepare graft copolymers by both *grafting through* and *grafting from* methods, where complexes of transition metals such as copper [35], ruthenium [36], iron [37] or nickel [38], are utilized in conjunction with alkyl halides (**Chapter 7**). In our synthesis, the

remaining pendant chlorines, substituted by 2,2,2-tribromoethanol (TBE) as ATRP initiator, were reacted with a stoichiometric amount of N,N,N',N'',N'''-pentamethyldiethylene-triamine (PMDETA) and copper (Cu(II)) catalyst system on one hand, and with nickel dibromide triphosphine (NiBr₂(PPh₃)₂) metal catalyst on the other hand, giving rise to ATRP initiating sites for styrene and *tert*-butyl methacrylate (tBMA) polymerization. After activation of TBE via ATRP, it is the goal to prepare thermo-responsive graft copolymers. One main drawback of the grafting from procedure lies in the impossibility to characterize precisely the structure of the resulting copolymers since neither the exact number of branches added nor their molar mass can be accurately determined. Note that PMVE graft copolymers with PS side chains (as PEO, see above) will undergo solubility changes in water in response to temperature changes.

Finally, the thermo-responsive properties if these novel graft copolymers were studied (**Chapter 9**). From specifically designed graft copolymers, containing a thermo-responsive backbone and hydrophobic side chains, we should expect that they would be able to generate micelles or aggregates with thermo-responsive core or corona (see scheme A1).

References

- [1] Kumar A., Srivastava A., Galaev I.Y., Mattiasson B., *Prog. Polym. Sci.*, **2007**, 32, 1205.
- [2] Lochhead R.Y., *Cosmetics and Toiletries*, **2006**, 121, 73.
- [3] Capadona J.R., Shanmuganathan K., Tyler D.J., Rowan S.J., Weder C., *Science*, **2008**, 319, 1370.
- [4] Rinaudo M., Osada Y., *L'Actualité Chimique*, **2006**, 300, 31.
- [5] Lequeieu W., Shtanko N., Du Prez F.E., *J. Membr. Sci.*, **2005**, 256, 64.
- [6] Lynen F., Heijl J., Du Prez F.E., Brown R., Szucs R., Sandra P., *Chromatographia*, **2007**, 66, 143.
- [7] Dai L., in '*Intelligent Macromolecules for Smart Devices: From Materials Synthesis to Device Applications*', Springer-Verlag: London, **2004**.
- [8] (a) Borchering H., Hicke H.G., Jorcke D., Ulbricht M., *Ann. NY Acad. Sci.*, **2003**, 984, 470. (b) Ramamoorthy M., Ulbricht M., *J. Membr. Sci.*, **2003**, 217, 207. (c) Ulbricht M., *J. Chromatogr. B*, **2004**, 804, 113.
- [9] (a) Kokufuta E., *Adv. Polym. Sci.*, **1993**, 110, 157. (b) Hoffman A.S., Stayton P.S., Bulmus V., Chen G., Chen J., Cheung C., Chilkoti A., Ding Z., Dong L., Fong R., Lackey C.A., Long C.J., Miura M., Morris J.E., Murthy N., Nabeshima Y., Park T.G., Press O.W., Shimoboji T., Shoemaker S., Yang H.J., Monji N., Nowinski R.C., Cole C.A., Priest J.H., Harris J.M., Nakamae K., Nishino T., Miyata T., *J. Biomed. Mater. Res.*, **2000**, 52, 577. (c) Jeong B., Gutowska A., *Trends in Biotechnology*, **2002**, 20 (7), 305.
- [10] (a) Vidal F., Popp J.F., Plesse C., Chevrot C., Teyssié D., *J. Appl. Polym. Sci.*, **2003**, 90, 3569. (b) Randriamahazaka H., Plesse C., Vidal F., Gauthier C., Chevrot C., Teyssié D., *Proc. SPIE Conference on Smart Structures and Materials*, **2004**, 5385, 294. (c) Vidal F., Plesse C.,

- Teyssié D., Chevrot C., *Synt. Met.*, **2004**, *142*, 287. (d) Dimitrov I., Trzebicka B., Müller A.H.E., Dworak A., Tsvetanov C.B., *Prog. Polym. Sci.*, **2007**, *32*, 1275.
- [11] (a) Kakugo A., Sugimoto S., Gong J.P., Osada Y., *Adv. Materials*, **2002**, *14*, 1124. (b) Kakugo A., Shininaka K., Matsumoto K., Gong J.P., Osada Y., *Bioconjugate Chem.*, **2003**, *14*, 1185. (c) Kakugo A., Sugimoto S., Shikinata K., Gong J.P., Osada Y., *J. Biomater. Sci.*, **2005**, *16(2)*, 203. (d) Kakugo A., Shininaka K., Takekawa N., Sugimoto S., Osada Y., Gong J.P., *Biomacromolecules*, **2005**, *6(2)*, 845.
- [12] Plate N.A., Valuev L.I., Valuev I.L., *Nauka Ross.*, **1998**, *103*, 21.
- [13] (a) Hoffman A., *J. Controlled Release*, **1987**, *6*, 297. (b) Valuev L.I., Zefirova O.N., Odydenova I.V., Platé N.A., *J. Bioact. Compat. Polym.*, **1994**, *9*, 55.
- [14] Kabanov V.Y., *Usp. Khim*, **1998**, *67*, 886.
- [15] Hoffman A., Afrassiabi A., Dong L., *J. Controlled Release*, **1986**, *4*, 213.
- [16] (a) Stayton P.S., Ding Z., Hoffman A.S., *Methods Mol. Bio.*, **2004**, *283*, 37. (b) Bajpai A.K., Shukla S.K., Bhanu S., Kankane S., *Prog. Polym. Sci.*, **2008**, *33*, 1088.
- [17] Xue Shen Wu., Hoffman A., Yager P., *J. Polym. Sci., Part A: Polym. Phys.*, **1992**, *30*, 2121.
- [18] Crenshaw B., Burnworth M., Khariwala D., Hiltner P.A., Mather P.T., Simha R., Wede C., *Macromolecules*, **2007**, *40*, 2400.
- [19] Monji N., Hoffman A., *Appl. Biothechnol.*, **1987**, *14*, 107.
- [20] A. Suzuki, in 'Phase Transitions in Gels Induced by Interaction with Stimuli', Berlin: Springer, **1993**, vol. II, p. 226.
- [21] Taiguchi Y., Kishi R., Ichijo H., Hirasa O., *Kobunshi Ronbunshu*, **1993**, *50*, 905.
- [22] Freitas R., Cluster E., *Chem. Eng. Sci.*, **1987**, *42*, 97.
- [23] Kishi R., Ichijo H., Hirasa O., *J. Int. Mat. Syst. Struct.*, **1993**, *4*, 533.
- [24] Yamauchi K., Hasegawa H., Hashimoto T., Köhler N., Knoll K., *Polymer*, **2002**, *43*, 3563.
- [25] Bulychev N.A., Arutunov I.A., Zubov V.P., Verdonck B., Zhang T., Goethals E.J., Du Prez F.E., *Macromol. Chem. Phys.*, **2004**, *205*, 2457.
- [26] Kawaguchi D., Tanaka K., Kajiyama T., Takahara A., Tasaki S., *Macromolecules*, **2003**, *36*, 6824.
- [27] Schappacher M., Puteaux J.L., Lefevre C., Deffieux A., *J. Am. Chem. Soc.*, **2005**, *127*, 2990.
- [28] (a) Verdonck B., Goethals E.J., Du Prez F.E., *Macromol. Chem. Phys.*, **2003**, *204*, 2090. (b) Ph.D. of Verdonck B., in 'Ontwikkeling van Thermo-responsieve Polymeersurfactanten op Basis van Pol(Methyvinylether)', Ghent University, Belgium, **2004**. (c) Mpoukouvalas K., Floudas G., Verdonck B., Du Prez F.E., *Phys. Rev. E*, **2005**, *72*, 011802.
- [29] (a) Zhang X., Reyntjens W., Goethals E.J., *Polym. Int.*, **2000**, *49*, 277. (b) Ph.D. of Rentjens W.G.S., in 'Thermoresponsieve Materialen op Basis van Poly(Vinylethers)', Ghent University, Belgium, **2001**.
- [30] Wenzel A., Yamgishita H., Kitamoto D., Endo A., Haraya K., Nakane T., Hanai N., Matsuda H., Kamuswetz H., Paul D., *J. Membr. Sci.*, **2000**, *179*, 69.
- [31] Shim J.K., Lee Y.B., Lee Y.M., *J. Appl. Polym. Sci.*, **1999**, *74*, 75.

- [32] Bernaerts K.V., Fustin C.-A., Bomal-D'Haese C., Gohy J.-F., Martins J.C., Du Prez F.E., *Macromolecules*, **2008**, *41*, 2593.
- [33] (a) Patil N.V., *Bioprocess Int.*, **2006**, *4(8)*, 42. (b) Wang W., Chen L., *J. Appl. Polym. Sci.*, **2007**, *104*, 1482. (c) Fulghum T.M., Estillore N.C., Vo C.-D., Armes S.P., Advincula R.C., *Macromolecules*, **2008**, *41*, 429. (d) Gupta S., Agrawal M., Uhlmann P., Simon F., Oertel U., Stamm M., *Macromolecules*, **2008**, *41*, 8152.
- [34] Patten T.E., Matyjaszewski K., *Adv. Mat.*, **1998**, *10*, 901.
- [35] Wang J.S., Matyjaszewski K., *J. Am. Chem. Soc.*, **1995**, *117*, 5614.
- [36] Kato M., Kamigaito M., Sawamoto T., *Macromolecules*, **1995**, *28*, 1721.
- [37] Matyjaszewski K., Wei M., Xia J., McDermott N.E., *Macromolecules*, **1997**, *30*, 8161.
- [38] Uegaki H., Kotani Y., Kamigaito M., Sawamoto M., *Macromolecules*, **1997**, *30*, 2249.

PART I

Functionalized Random Copolymers of Hydrophilic and Hydrophobic Vinyl Ether Monomers Obtained by Living Cationic Copolymerizations

Parts of these chapters have been published as articles:

¹ Confortini O., Verdonck B., Goethals E.J., *e-polymers*, **2004**, no. 43.

² Confortini O., Du Prez F.E., *Macromol. Chem. Phys.*, **2007**, *208*, 1871.

Chapter 1 : Theory of Living Cationic Polymerization of Vinyl Ethers	13
1.1. Poly(Vinyl Ethers)	13
1.1.1. Introduction	13
1.1.2. Physical Properties	14
1.1.2.1. The Homopolymers	14
1.1.2.2. The Copolymers	14
1.1.3. Health and Safety Factors	15
1.2. The Classical Carbocationic Polymerization	15
1.2.1. The initiation	15
1.2.2. The Propagation	16
1.2.3. Chain Transfer, Termination and Other Side Reactions	17
1.2.3.1. Chain Transfer and Termination	17
1.2.3.2. Side Reactions due to the presence of Water	17
1.2.4. Role of a Proton Trap : the THA	19
1.2.5. The Interplay Among Basic Elements of a Cationic System	19
1.3. Living Cationic Polymerization	20
1.3.1. Definition and Characteristics of Living Polymerization	20
1.3.2. Discovery	21
1.3.3. Initiating Systems : Three General approaches	22
1.3.4. The Propagation	23
1.3.5. The Termination	24
1.3.6. The Quasi-Living Polymerization	24
1.4. Design of Macromolecular Architectures by Living Cationic Polymerization	24
1.4.1. End-Functionalized Polymers	24
1.4.2. Macromonomers	25
1.4.3. Pendant-Functionalized Polymers	26
1.4.4. Block Copolymers	27
1.4.5. Multi-Armed and Star-Shaped Polymers	27
1.5. References	27
Chapter 2 : Theory of the Determination of the Reactivity Ratios of Random Copolymers	31
2.1. Introduction	31
2.2. Types of Copolymerization Behavior	31
2.3. Estimation of Monomer Reactivity Ratios	33
2.3.1. The Linear Methods	33
2.3.2. The Non-Linear Methods	34
2.3.3. Variation of Copolymer Composition with Conversion or Meyer-Lowry Method	37
2.5. Conclusion	38
2.6. References	38
Chapter 3 : Synthesis of Vinyl Ether Copolymers by Cationic Copolymerizations	41
3.1. Introduction	41
3.2. Mechanism of the Copolymerizations	43

3.3. Compositions of the Copolymers by ¹H NMR	45
3.3.1. Homopolymers	47
3.3.2. Copolymers	47
3.4. Synthesis of Copolymers of Isobutyl Vinyl Ether and 2-Chloroethyl Vinyl Ether with Methyl Vinyl Ether Starting from a Mono-functional Initiator	49
3.4.1. Experimental Conditions for Synthesis of P(MVE- <i>co</i> -IBVE)	50
3.4.2. Experimental Conditions for Synthesis of P(MVE- <i>co</i> -CEVE)	51
3.4.3. Livingness.....	56
3.5. Synthesis of Copolymers of Methyl Vinyl Ether and Isobutyl Vinyl Ether with 2-Chloroethyl Vinyl Ether Starting from a Bi-functional Initiator	58
3.5.1. The Homopolymerizations.....	58
3.5.2. The Copolymerizations	58
3.6. Determination of the Monomer Reactivity ratios	61
3.6.1. Monomer Reactivity Ratios of P(MVE- <i>co</i> -IBVE)	61
3.6.1.1. The Linear Methods.....	61
3.6.1.2. The Non-Linear Methods.....	62
3.6.2. Monomer Reactivity Ratios of P(MVE- <i>co</i> -CEVE)	64
3.6.2.1. Extended <i>Kelen-Tüdös</i> method.....	64
3.6.2.2. The Non-Linear Methods.....	64
3.6.3. Copolymerization Curves: Evolution of the Composition with the Overall Conversion.....	65
3.7. Physical Properties	68
3.7.1. The Glass Transition Temperature	68
3.7.2. Solubility	68
3.8. Conclusion	70
3.9. References	70

Abstract

This present study focuses on the new living cationic random copolymerization of methyl vinyl ether (MVE) or isobutyl vinyl ether (IBVE) and 2-chloroethyl vinyl ether (CEVE) to obtain functionalized poly(isobutyl vinyl ether) (PIBVE) and thermo-responsive poly(methyl vinyl ether) (PMVE). The random copolymers poly(IBVE-co-MVE), poly(MVE-co-CEVE) and poly(IBVE-co-CEVE) were synthesized in toluene using 1,1-diethoxyethane (DEE) and 1,1,3,3-tetraethoxypropane (TEoP) as mono- and bi-functional initiator respectively. The acetal was added to trimethylsilyliodide (TMSI) to form the initiating system, and then copolymerizations were activated by zinc iodide (ZnI_2). The kinetics of copolymerization were investigated for each monomer from series of at least nine reactions for which the initial monomer molar ratios ranged from 0.1 to 0.9. The copolymer compositions were determined by NMR. The copolymerizations were found to be living under specific conditions.

The monomer reactivity ratios for the copolymerization were determined using linearization methods such as Fineman-Ross, Kelen-Tüdös and extended Kelen-Tüdös methods. Also, non-linear methods were employed by the use of the COPOINT program and the reactivity ratios obtained were compared. The values of the monomer reactivity ratios showed that poly(IBVE-co-MVE) copolymers have a moderate gradient-type structure with a strong tendency to alternate whereas the poly(MVE-co-CEVE) copolymers have a tendency toward an alternating structure. Moreover, the glass transition temperatures (T_g 's) of copolymers were determined and the theoretical T_g 's of homopolymers were deduced. Solubility of the homopolymers and copolymers were also studied using different solvents at 20°C.

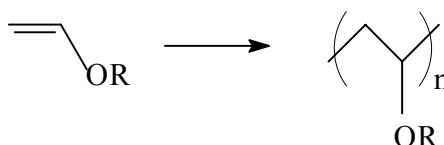
Chapter 1

Theory of Living Cationic Polymerization of Vinyl Ethers

1.1. Poly(Vinyl Ethers)

1.1.1. Introduction

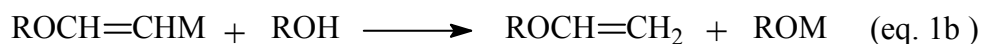
Poly(vinyl ethers) (PVEs) are compounds with the general formula:



where R is an alkyl group such as methyl (MVE), ethyl (EVE), isobutyl (IBVE) or octadecyl. MVE, EVE, IBVE and *n*-butyl vinyl ether (*n*BuVE), are the commercially available VEs for reason of physical and chemical properties [1-3]. PVEs are produced exclusively by polymerization of vinyl ether monomers [4].

In 1878, the first reaction of PVEs (prepared by Wislicenius) was recognized as a chain reaction involving a cationic polymerization initiated by I^+ and chain growth via carbonium ions. In the 1920's, the monomeric vinyl ether became readily available by Reppe vinylation of alcohols with acetylene (under basic conditions at temperature of 120-180°C [5-7], scheme 1.1) and grew in industrial importance. After 1930, VEs and PVEs were produced on an industrial scale, initially at the Ludwigshafen works of the I.G. Farbenindustrie (now BASF), and since 1940 at the General Aniline and Film Corporation (GAF) in the United States, and later also by Union Carbide (UCC) in the United States.

Today, PVE homopolymers are only produced by BASF and Polymer Source in Canada; UCC and GAF have ceased production.



Scheme 1.1. Synthesis of VE: vinylation of alcohols. A likely mechanism for the reaction involves addition of the metal alcoholate to the triple bond (eq.1a) in the rate-controlling step followed by metal-alcohol exchange (eq.1b) [5].

1.1.2. Physical Properties

1.1.2.1. The Homopolymers

The physical properties of the PVEs depend on molecular weight, the nature of the alkyl group, the nature of the initiator, stereospecificity and crystallinity. They may be formed as viscous, sticky liquid, rubbery or brittle solids. PVEs with long alkyl side chains are waxy. The economically most important use of PVEs is in the adhesives industry, mostly as modifying additives for other (cheaper) raw materials. PVEs find wide application as adhesives, surface coatings, lubricants, greases, elastomers, melting compounds, fibers and films as well as in chemical processing.

Properties of PCEVE [1, 8-11]:

PCEVE is used as X-Ray-beam resist; chlorine substituents on the alkoxy side chains improve sensitivity and resolution. PCEVE is hydrophobic, elastomeric and particularly used to be substituted ($T_g = -35\text{ }^\circ\text{C}$).

Properties of PIBVE [1,5,10-11]:

This polymer is used either in the dry state or as a solution in an organic solvent. It has excellent adhesion to plastics, metals, and coated surfaces and finds applications as an adhesion promoter and plasticizer in pressure-sensitive tapes and labels, as well as in various adhesive compositions and surface coatings. PIBVE is produced as a highly viscous oil and as a soft resin, but also as a secondary emulsion in water for mixing with other aqueous polymer emulsions.

Properties of PMVE [1,5,10-12]:

PMVE is a polymer that undergoes a LCST (see **Chapter 6**) (37°C) governed by the hydrophilic-hydrophobic-balance (HLB). Such polymer is sometimes referred to as “thermo-shrinking”, and gets particular interest because of the abrupt nature of its phase transition and the fact that the transition is reversible, which allows repeated “thermal-switching”. PMVE has extensive uses in adhesives and coatings, as a non-migrating plasticizer, and as tackifier [5]. It can be used as a hot-melt adhesive, as a pigment-wetting agent, and as a plasticizer for printing inks. The polymer also has uses as a stabilizer in emulsion polymerization. The three important commercial applications for PMVE are for viscosity control and dry-film flexibility in UV photoresist coating solutions; as tackifier and adhesion promoter for acrylic pressure-sensitive adhesives used as tapes, labels and decals; and as semipermeable membrane for reverse osmosis [12].

1.1.2.2. The Copolymers

PVEs are compatible with a wide variety of other polymers and copolymers. Principle applications for the most important commercial alkyl VEs with one or two other monomers that have appeared in the literature since 1970-1971 are listed in table 1.1. They are used as auxiliary materials for adhesives and paints, and in many industries [13-14].

Table 1.1. Some Commercial VE Copolymers.

Polymer	Supplier	Application
Poly(MVE-co-maleic anhydride-co-divinyl ether of 1,4-butanediol)	GAF	Textile print paste Thickener
Poly(MVE-co-MA)	GAF ICI	Adhesives, coatings, pharmaceuticals
Poly(MVE-co-monoethyl maleate)		Thermographic copying material
Poly(MVE-co-monoethyl maleate)		Printability
Poly(IBVE-co-vinyl chloride)	BASF	Marine paints, electrostatic image-developing powders, binding resin
Poly(IBVE-co-monoethyl maleate)		Aerosol, hairspray, resin
Poly(CEVE-co-N-vinylpyrrolidone)		Photochemical cross-linking of polymers to immobilize enzymes

1.1.3. Health and Safety Factors

For the common PVEs known for nearly 50 years (MVE, EVE, IBVE and ODVE), no effects which are hazardous to health have so far been found. In animal experiments, they are classified as non-irritating to the skin and non-mutagenic.

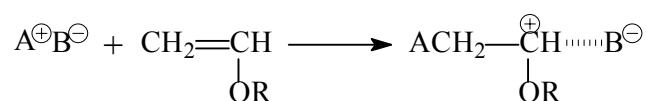
PMVE is not a primary irritant or a sensitizer. White rats and guinea pigs tolerate 90-100 cm³/kg of a 25% aqueous solution in oral toxicity tests. Oral toxicity values for white rats are 29g/kg body weight for the polymers tested.

1.2. The Classical Carbocationic Polymerization

The polymerization of alkyl VEs has been known for a long time [15], and several polymers are or have been produced commercially. The polymerization of VEs is possible only by cationic mechanism from the electron-donating nature of the ether substituent. The systematic study of the kinetics of VE polymerization was started in 1947 by Eley and co-workers [16] who polymerized *n*-BuVE with SnCl₄ [15], iodine [17], AgClO₄ [18] and PhCCl [18]. The British research group eventually established the cationic chain polymerization mechanism for VEs, consisting of initiation, propagation, chain transfer and termination.

1.2.1. The Initiation

The initiation step in the cationic polymerization of VEs is an electrophilic addition of a cation A⁺, derived from an initiator A⁺B⁻, across a VE double bond, to form a monomeric carbocation (scheme 1.2).



Scheme 1.2. Formation of a carbocation by the initiation step.

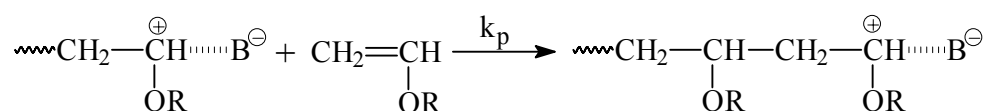
Because of their high reactivity, VEs can be polymerized by a variety of acidic compounds, including those which are too weakly acidic to initiate cationic polymerization of styrene, isobutene and other less reactive vinyl monomers. Typical examples are summarized in table 1.2.

Table 1.2. The initiators.

<i>Initiator</i>	<i>Examples</i>	<i>References</i>
Protonic acids (Brønsted acids)	CF ₃ SO ₃ H, HClO ₄ , CF ₃ COOH	28
Metal halides (Lewis acids)	SnCl ₄ , FeCl ₃ , ZnCl ₂ , BF ₃ , BF ₃ OEt ₂	29
Halogenated metals alkyls	RAICl ₂ , R ₂ AlCl, RMgX; R = alkyl, X = halogen	
Cation-forming salts	Ph ₃ C ⁺ SnCl ₅ ⁻ , C ₇ H ₇ ⁺ SbCl ₆ ⁻ , MeCO ⁺ ClO ₄ ⁻	30-31
Halogens	I ₂ , IBr	30, 32
Modified Ziegler-Natta catalysts	Et ₃ Al-VCl ₄ -iBu ₃ Al-THF	3, 25
Solid acids	Cr ₂ O ₃ , Al ₂ (SO ₄) ₃ -H ₂ SO ₄	33
High-energy radiation	γ-ray	23, 34

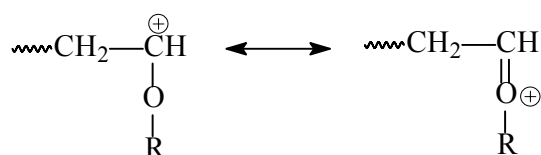
1.2.2. The Propagation

The propagating reaction in VE polymerization is assumed to proceed via a carbocation as a growing species (scheme 1.3, where B⁻ is the counteranion derived from an initiator).



Scheme 1.3. Propagation of PVEs.

The reactivity of monomer with initiator and propagating cation depends on the electron-donating power of the pendant group through inductive effect (Me < Et < *i*Pr < *t*Bu). In general, the stronger electron donating effect of the alkyl group leads to higher propagating rate constant (*k_p*). VE monomers with more branched alkyl group exhibit higher reactivity than those monomers with straight pendant chain (MVE < EVE < *i*PrVE < *t*BuVE). The alkyl substituents in VEs may affect their reactivity also through the resonance effect, mediated by the intervening ether oxygen (scheme 1.4).



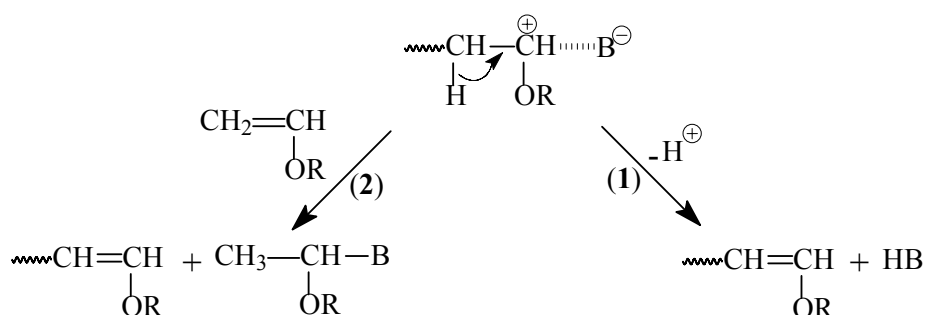
Scheme 1.4. The resonance effect.

1.2.3. Chain Transfer, Termination and Others Side reactions

1.2.3.1. The Chain Transfer and Termination

Despite its long history over a century, cationic vinyl polymerization has been regarded as most difficult to control. This long-standing view stems from the fact that the chain carrier of cationic polymerization is an inherently unstable carbocation, which tends to undergo frequent chain transfer reactions among others.

Before the discovery of living cationic polymerization, the cationic polymerization of VEs hardly ever produced high molecular weight polymers unless carried out at very low temperature. The major reason is the occurrence of chain transfer reactions as described in scheme 1.5, in which a β -proton is transferred to the counteranion (1) or an incoming monomer (2) [30].



Scheme 1.5. Chain transfer reactions to counteranion (1) and an incoming monomer (2).

The chain transfer processes mostly involve the elimination of the cation's β -proton, which is acidic due to the vicinal positive charge.

In contrast, the termination reaction is much less important in comparison with transfer reaction, which means that the polymerization will be controllable if the chain transfer reactions can be hampered or eliminated.

Thus, conventional cationic polymerizations, such as that of styrene with boron trifluoride etherate, are too poorly reproducible and controllable to give polymers with well-defined architectures and molecular weights.

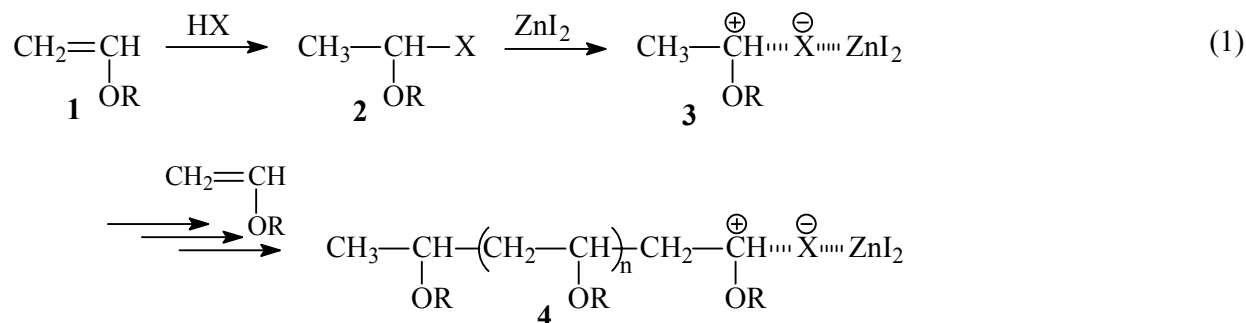
1.2.3.2. Side Reactions due to the Presence of Water

Moreover, residual water in the reaction medium can result in some other side reactions [31]. It is well-known that unavoidable water traces are present in TMSI, which is the initiator used in our syntheses of VEs in **Chapter 3** [32]. The formation of side products of low average-number molecular weight (M_n) during the living cationic polymerization of VE with a phthalimide [33] and benzoate [34] pendant group was found, and the structure of the oligomers were determined. Kodaira *et al.* have proposed a mechanism for these side reactions (scheme 1.6) where the formation of the side products originates in the reaction of the growing end with impurity water [E].

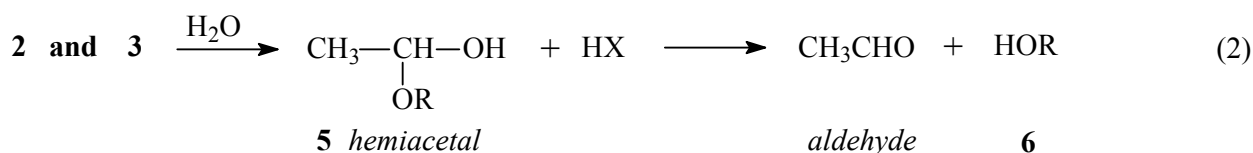
The HX/ZnI_2 (HX is a Lewis Acid) initiator produced living polymer (4). However, some of the propagating species (2 and 3) reacted with water as an impurity and caused the pendant elimination via a hemiacetal compound (5) to give an alcohol (6) [35]. An oligomer (7) was formed by the reaction of the monomeric propagating species (2 and 3), with 6 thus produced. 6 also

terminated some of **4** and formed an acetal terminal (**8**) similar to that of (**7**). The rest of the living polymer chains (**4**) terminated with methanol as a terminating agent to give the polymer with the methoxide-type acetal terminal (**9**). Both reactions leading to **7** and **8** (eq. 3 and 4, respectively) originated in the reaction of the propagating species (**2** and **3**) with casual water that produced **6**. The reactions shown by eq. 2-4 are essentially chain-transfer reactions.

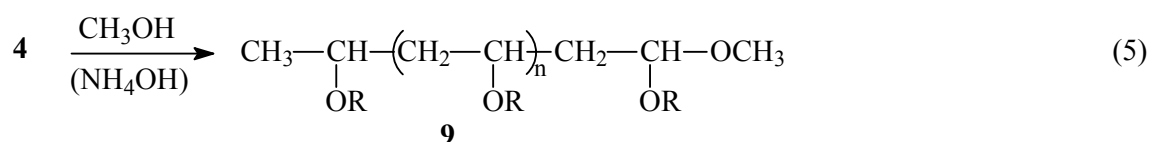
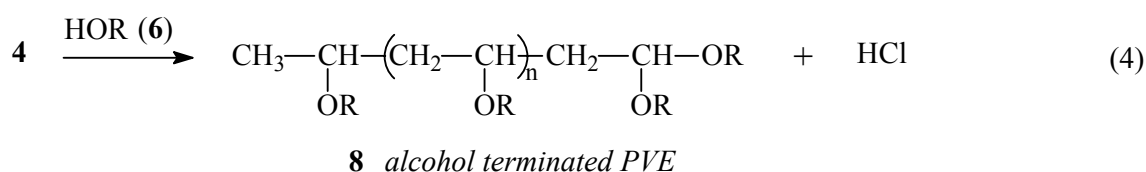
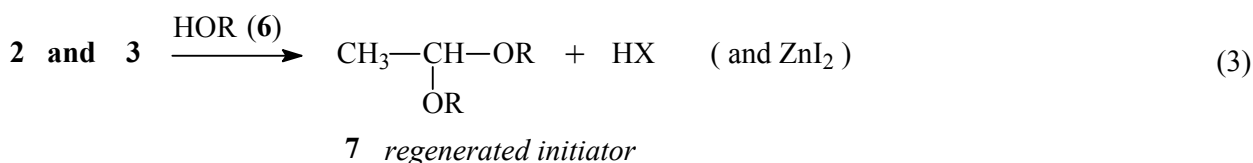
I: initiation with L.A. and activation with ZnI_2



II: aldehyde formation in the presence of water traces



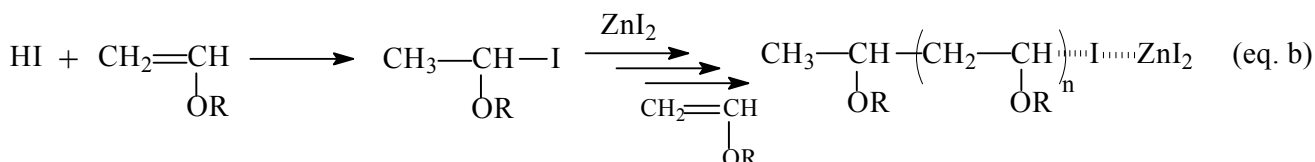
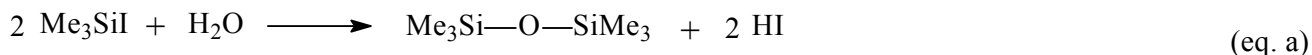
III: termination of group chains by alcohol (chain transfer reaction)



Scheme 1.6. Side reactions due to the presence of water traces during the initiation step of the VEs polymerization.

On the other hand, Deffieux *et al.* [36], in the syntheses of high molar mass of PCEVE, have provided the evidence for the occurrence of a monofunctional side initiation. In line with this observation, the latter has been attributed to the hydrolysis of TMSI by protonic impurities which leads to the *in situ* formation of HI (scheme 1.7, eq. a). It is worth mentioning that for IBVE and styrene polymerizations initiated by trimethylsilyl trifluoromethanesulfonate [37] and trimethylsilyl

diphenylphosphate [38], it has been shown that initiation does not proceed by direct electrophilic addition of TMSX on the monomer unsaturation, but involves protonic acids species formed through the hydrolysis of TMSX by residual moisture. In that case, the present hydrogen iodide would add onto the VE monomer and inevitably induce the formation of monofunctional chains (scheme 1.7, eq. b) in addition to the expected bifunctional ones.

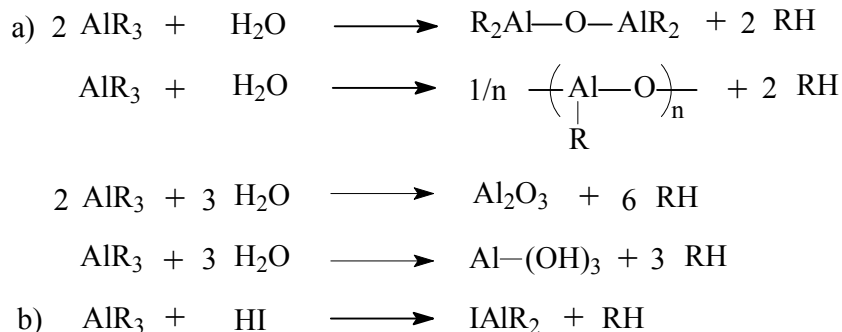


Scheme 1.7. Hydrolysis of TMSI (eq. a), HI initiation of VEs: formation of the monofunctional initiation by the presence of adventitious water present in the bulk (eq. b) [36].

1.2.4. Role of a Proton Trap: the THA

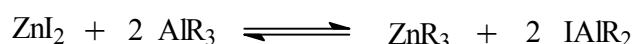
Deffieux proved that, despite the rigorous drying conditions used, the formation of a fraction of monofunctional initiation by HI, generated by a partial hydrolysis of TMSI by water [36], can not be avoided under conventional conditions (as it will be explained in **Chapter 3**).

In order to control the polymerization and to suppress the side reactions (formation of second chain transfer with a monofunctional initiator), tetrahexylaluminium (THA) was added as a proton trap, which reacts rapidly with water [39] and protonic acids [40], as exemplified in scheme 1.8.



Scheme 1.8. Reaction of trialkylaluminium (AlR_3) with water (a) and with protonic acids (b) [39].

Although the living character of the polymerizations is preserved, another side reaction can exist, namely the reaction between AlR_3 and ZnI_2 , which reduces the efficiency of the ZnI_2 [41] (scheme 1.9). Consequently, the highest DP_n for the homopolymer PCEVE, which could be obtained, was equal to 300 [41].



Scheme 1.9. Ligand exchange between zinc iodide and trialkylaluminium.

1.2.5. The Interplay Among Basic Elements of a Cationic System

For a given cationic polymerization system of VEs, the nature and the whole process of polymerization will be governed by four or five basic elements: the initiator system, the monomer,

the solvent, the reaction temperature and a fifth, less precise one, namely the concentration of possible impurities, mainly residual water [42].

The variable associated with the initiator is its electrophilicity or acidity, but also its stability and leaving properties of the counteranion of the active species, or both. With respect to living cationic polymerization, the optimized matching of the initiator, the activator and (or) a third useful component in the initiating system should be another important variable. The role of the solvent is reflected by its polarity and the possible specific solvating properties. Generally, high polarity of the solvent will lead to uncontrollable polymerization. Even the change in the concentration of monomer in the system can influence the nature of the cationic polymerization, which results from the change in polarity of the system. Changes in temperature can result in the purely kinetic modification and the nature of the initiating and propagating species in the polymerization process. Finally, the amount of residual moisture must be considered, and recently there have been some studies about its influence on the living polymerization [2,43].

Thus, the cationic initiators require high-purity monomers and solvents, clean apparatus, and the absence of water is particularly important [19,36]. It is recommended that the VEs are stored under a nitrogen atmosphere to minimize contact with air and moisture. VEs are hydrolyzed in the presence of aqueous acids to acetaldehyde and the respective alcohols. The reaction is acid catalyzed, and the VEs are comparatively stable in the presence of base. In general, if protected from contact with water and acidic materials, or if properly stabilized, the VEs may be stored using the safety precautions.

1.3. Living Cationic Polymerization

1.3.1. Definition and Characteristics of Living Polymerization

The term living polymerization was originally used to describe a chain-growth polymerization free in which chain-breaking reactions are absent [42]. In such an ideal system, after initiation is completed, growing or propagating chains would only propagate and would not participate in transfer or termination, with the consequence that all macromolecules in the system are capable of growth as long as monomer is present. Therefore, the living process is one of the best methods thus far available for precise control of polymer structure and molecular weight. But practically, it is impossible for a polymerization to be perfectly living. Polymerizations are considered living if they retain their capacity of growth for a time needed for the completion of a desired task.

It has been proposed, by IUPAC Macromolecular Division, that the following experimental criteria should be applied in diagnostic characteristics for living polymerization [30,42,44]:

- ✓ the number-average molecular weight (M_n) of the polymer is directly proportional to the conversion of the monomer
- ✓ the polymerization proceeds until all of the monomer has been consumed, further addition of monomer results in continued polymerization

- ✓ the number of polymer molecules (and active centers) is constant, which is sensibly independent of monomer conversion
- ✓ the molecular weight can be controlled by the stoichiometry of the reaction
- ✓ the produced polymer has narrow molecular weight distribution (M_w/M_n) when initiation is fast
- ✓ block copolymers can be prepared by sequential monomer addition
- ✓ chain end functionalized polymers can be prepared by end-capping reactions.

The major experimental evidence of a living polymerization is the linear increase of the M_n with polymer yield.

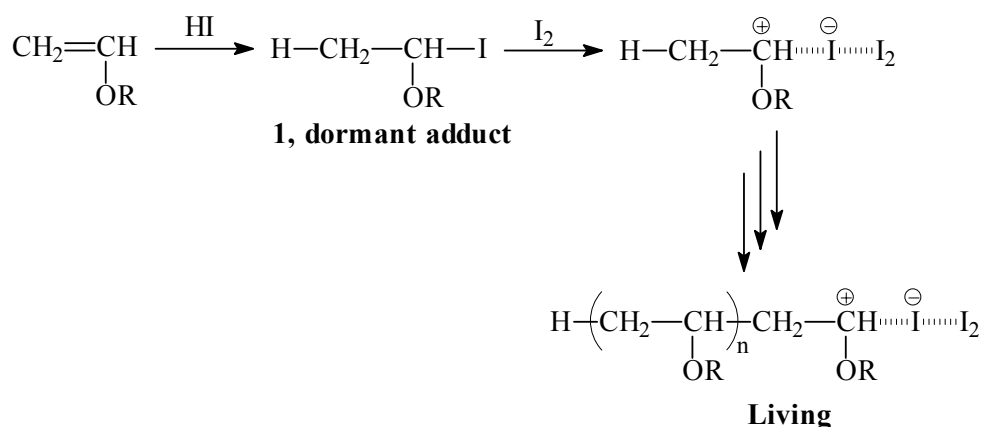
1.3.2. Discovery

Following some findings [45], Higashimura and Sawamoto reported in 1983 the first truly living cationic polymerization of alkyl vinyl ethers initiated with the combination of the HI/I₂ initiating system [24,30,46-47].

Besides the common features of living polymerizations, such as the direct proportionality of the M_n s of polymers and the resumption of polymerization and further growth of polymer molecular weights upon addition of new monomer feeds, the characteristics of the HI/I₂-mediated living polymerization include the following:

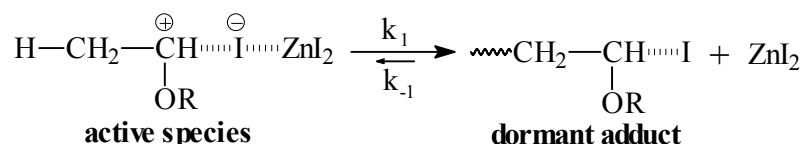
- ✓ Hydrogen iodide alone does not initiate polymerization but quantitatively forms a dormant adduct (scheme 1.10).
- ✓ An efficient polymerization takes place when molecular iodine is added to a mixture of **1** and excess monomer
- ✓ The number-average degree of polymerization (DP_n) of the polymers depends on monomer conversion and, more importantly, the molar ratio of monomer to HI.
- ✓ The concentration of iodine does not affect polymer molecular weight, but its increase accelerates the polymerization.

From these and other facts, the living polymerization with the HI/I₂ system is now understood to proceed, as shown in scheme 1.10 [47].



Scheme 1.10. Living polymerization with HI/I₂ as initiating system.

Thus, the initially formed adduct **1** acts as an initiator, whose dormant carbon-iodine bond is activated electrophilically by molecular iodine to begin living propagation. In this regard, the iodine is a Lewis acid (L.A.) called the “activator” or “coinitiator”. Collectively, we call such combinations of an initiator and activator “initiating systems”. According to this polymerization mechanism, the living nature and fine control of the polymerization are attributed to the stabilization of the growing carbocation by the nucleophilic interaction of the iodine-based binary counteranion, which decreases the positive charge at the growing cation, thereby reducing the acidity of its β -proton and eventually suppressing chain transfer (scheme 1.11).



Scheme 1.11. Equilibrium between active and dormant species.

1.3.3. Initiating Systems: Three General Approaches

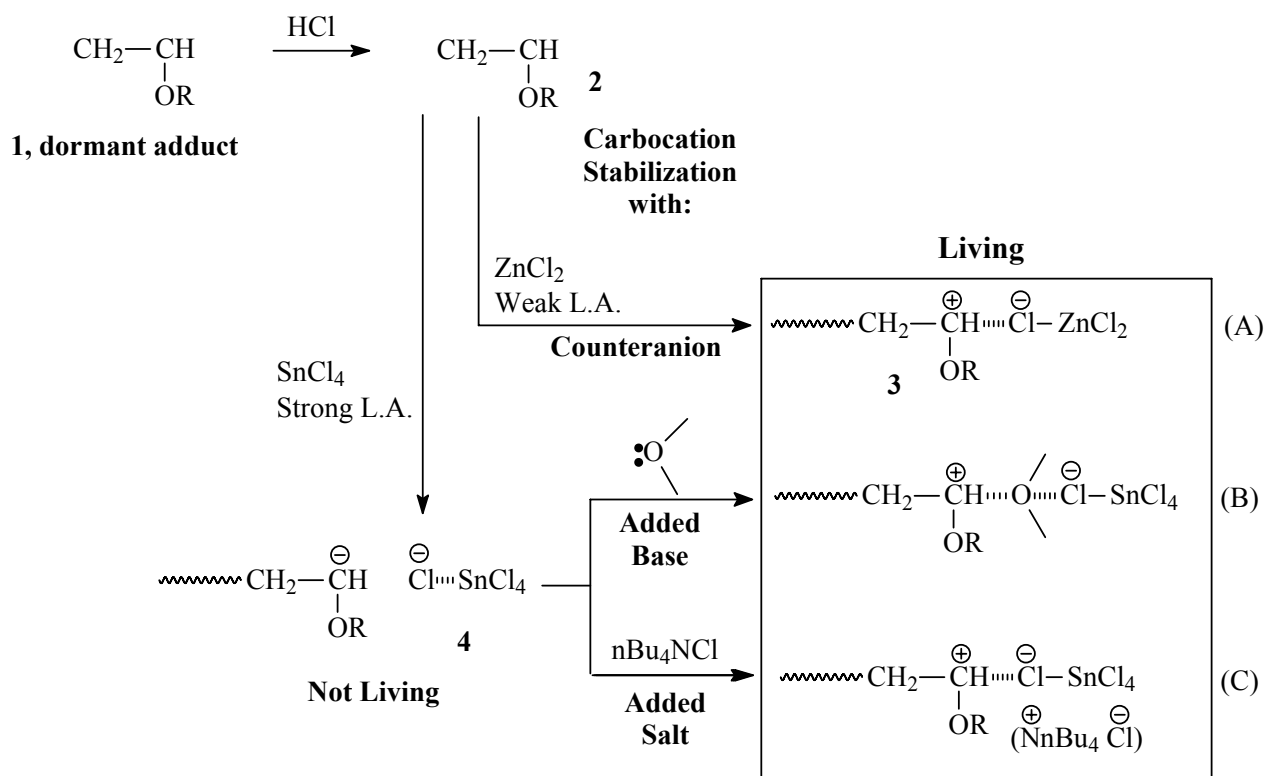
A wide variety of initiating systems have been developed on the basis of the principal of nucleophilic stabilization of growing carbocations. More specifically, three methodologies have emerged that employ different “nucleophiles” in order to stabilize the otherwise unstable carbocationic intermediates (scheme 1.12):

- ✓ Initiating Systems Based on Nucleophilic Counteranions: Protonic Acid/Metal Halide Systems (HB/MX_n) (eq. A)
- ✓ Added Lewis Bases (eq. B)
- ✓ Added Onium Salts (eq. C)

The first method, based on “nucleophilic counteranions”, is particularly suited for the synthesis of bifunctionally growing living polymer [48] and also for polymerization of VE and these graft copolymers used for our work in **Chapter 3**.

The generalization of the initiator/activator mechanism for the HI/I₂-initiation system (scheme 1.10) leads to the design of variety of initiating systems that can also induce controlled/living cationic polymerization of vinyl ethers and related monomers via the “carbocation stabilization by nucleophilic counteranions” [42] (scheme 1.12, eq. A). The carbocation species **2** is considered to be stabilized via the nucleophilic interaction of a counteranion (Cl-ZnCl₂⁻) derived from the initiating system. These mechanistic considerations also provide us with some guidelines to select initiators and activators suitable for the HCl/ZnCl₂ initiating systems.

Thus, the *initiator*, the protonic acids HCl should be such that they carry nucleophilic anions Cl⁻ which form dormant adduct (like **1**) quantitatively with vinyl monomers but should not initiate uncontrolled polymerization by themselves. Such protonic acids include hydrogen halides and carboxylic acids.



Scheme 1.12. Three general methods for living cationic polymerization based on the “nucleophilic stabilization of growing carbocations”. (scheme taken from [30])

The *activator*, the metal halides ZnCl_2 should be mild Lewis acids that do not initiate cationic polymerization, even in the presence of water but are electrophilic enough to activate the carbon-Cl terminal to give stabilized growing species [49].

When compared with the now classical HI/I_2 counterpart, an advantage of these HB/MX_n initiating systems is that some of them (HI/ZnI_2 , in particular) permit living cationic polymerization to proceed at room temperature [50], as well as easy handling and commercial availability of the components. An alternative synthesis of another initiator, α -iodo-ether, for the living cationic polymerization, is the reaction between an acetal and trimethylsilyl iodide activated with ZnI_2 , which will be used in our work for the PVE copolymerizations (**Chapter 3**).

1.3.4. The Propagation

The propagation center during the monomer insertion process, which leads to polymerization [51], has an ionic character.

The α -halogeno ether polymer ends are to be inactive for the polymerization, and can be partially ionized and enable the propagation. The reaction between ionic and covalent forms of the polymer ends is a fast equilibrium.

1.3.5. The Termination

It may be seen that, in cationic polymerization, as in human life, polymers are born (initiated); grow (propagation) into longer molecules by reacting with numerous monomers, and are killed (by chain-transfer and termination). In contrast, there is a reaction where polymers remains “alive” for a long time, and this is accordingly called “living polymerization”, that is, a chain-growth polymerization that is free from chain transfer, termination and other undesirable side reactions.

1.3.6. The Quasi-Living Polymerization

Kennedy *et al.* developed a ‘*quasi-living polymerization*’ method. When a vinyl monomer is added slowly but continuously to an initiator solution, a polymerization reaction occurs. Due to low concentration of monomer, the chain transfer and other side reactions are effectively suppressed, resulting from a polymerization phenomenologically similar to living polymerization.

1.4. Design of Macromolecular Architectures by Living Cationic Polymerization

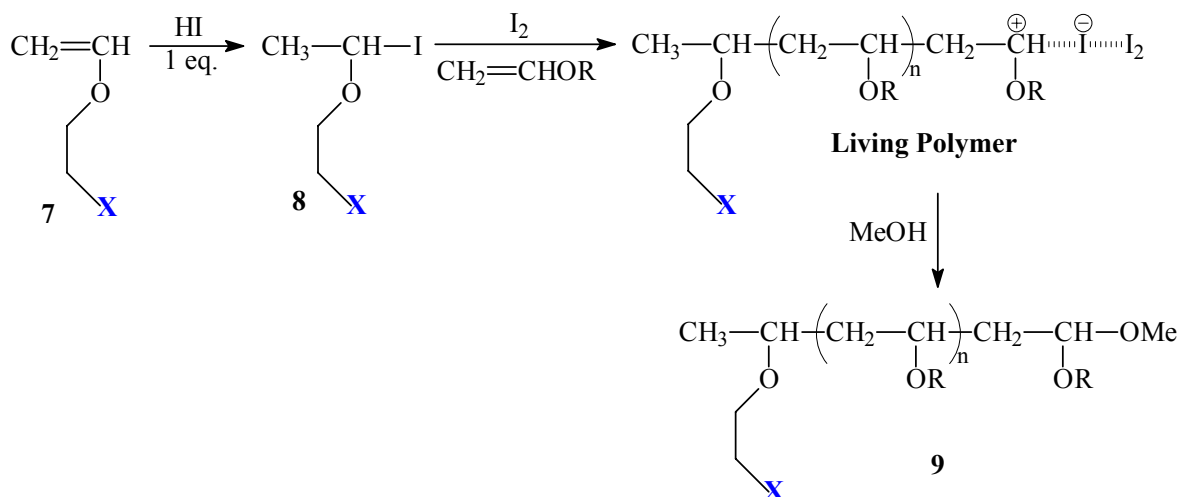
The VE family consists of a large group of members ranging from the highly hydrophobic monomer such as CEVE or IBVE, to thermo-responsive water-soluble monomer such as MVE and to the crystallizable ODVE. On the other hand, the living polymerization method can provide us PVEs with well-defined architecture, M_n and narrow M_w/M_n . Through the simple initiation, termination and further reaction for the polymeric products, various functional groups can be introduced to the chain ends or the pendant groups of polymer. Based on the combination of the versatility of monomer properties and convenient manipulation of the living polymerization of VEs, many efforts have been made to synthesize and develop PVEs with new architectures.

1.4.1. End-Functionalized Polymers

The absence of chain transfer and termination in living polymerization provides straightforward and versatile methods to attach a variety of functional groups to polymer chain ends. The synthesis of end-functionalized polymers by living polymerization is usually achieved via either an initiation or a termination reaction [52].

* The “Initiator Method”

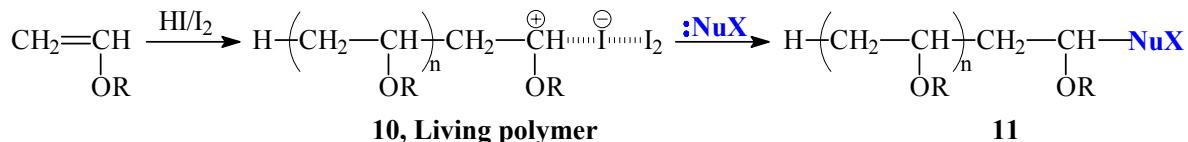
The first method, the “initiator method”, utilizes an initiator, the hydrogen iodide-vinyl ether adduct (**8**), that induces living polymerization of VEs (other than **7**) in the presence of iodine via the activation of its C-I bond. The product (**9**) carries a functional “head” (α -end) group X derived from the initiator (scheme 1.13). The “initiator method” has thus led to a variety of α -end functionalized polymers [53].



Scheme 1.13. The “initiator method”.

* *The “Termination Method”*

The second method, the “terminator method”, employs an end-capping **:NuX** (a nucleophilic terminator) with a functional group to be attached to the ω -end (tail) of the polymer (**10**). Under suitable conditions, the living end of (**10**) is so stable and selective that it combines to **:NuX** without forming an alkenic by-product ($\sim\text{CH}=\text{CHOR}$) via β -proton elimination [54-55] (scheme 1.14).



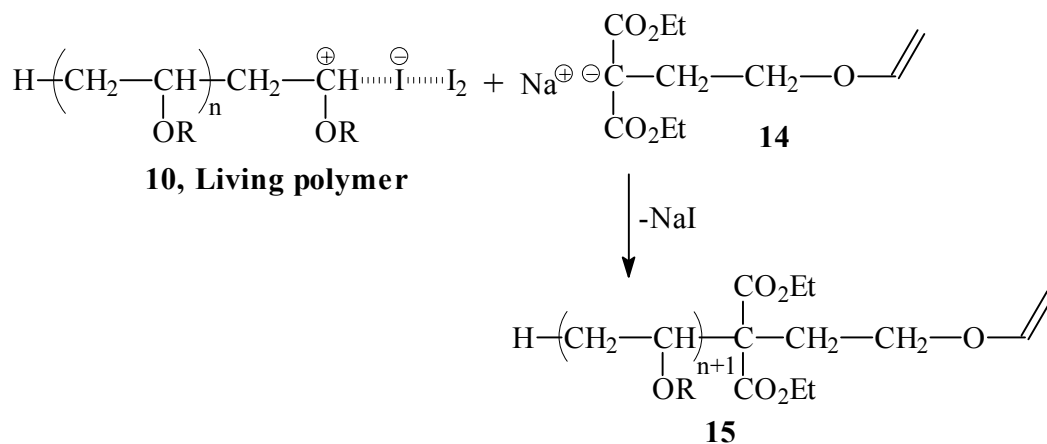
Scheme 1.14. The “Termination method”.

* *Telechelic Polymers*

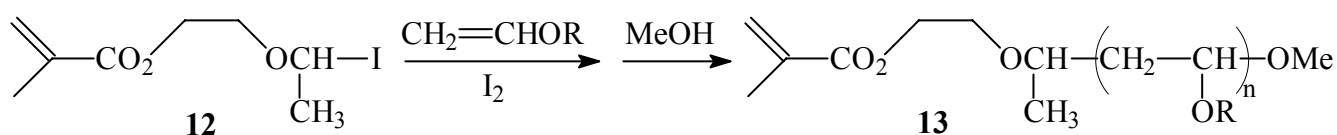
As readily expected, combination of the initiator and the terminator methods yields telechelic (α , ω -bifunctional) polymers of VEs [54,56] and *p*-methoxystyrene [57], where the two terminal groups may be identical (homotelechelic) [54,57-58] or different (heterotelechelic) [57,59].

1.4.2. Macromonomers

A polymerizable functional group can be attached to the end of the PVE [56,58,60-61] chain either by initiation or termination. For example, quenching the HI/I₂-initiated living polymer (**10**) with functional anion (**14**) leads to VE-capped PVEs (**15**) [62] (scheme 1.15). Macromonomer (**13**) with a methacrylate end is prepared by living polymerization of VEs with the initiator (**12**) derived from methacrylate vinyl monomer [63] (scheme 1.16). The macromonomers (**13**) and (**15**) are characterized by their perfect number-average end-functionality ($F_n \approx 1.0$), narrow M_w/M_n and controlled M_n .



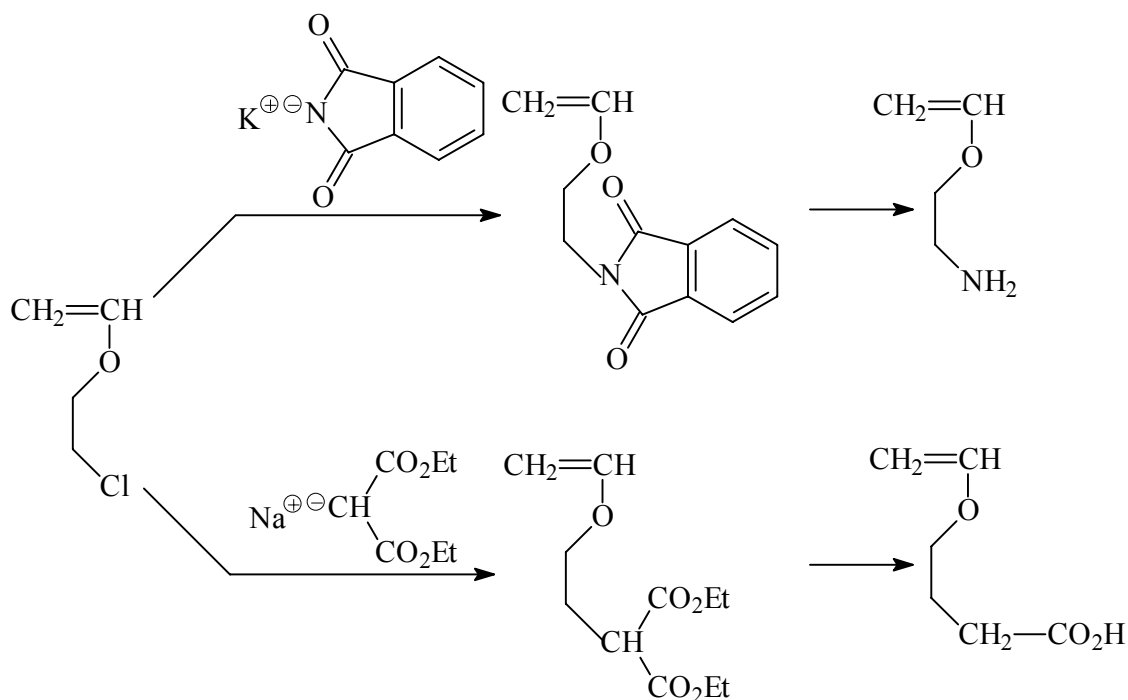
Scheme 1.15. Macromonomer with end-capping.



Scheme 1.16. Macromonomer with a methacrylate.

1.4.3. Pendant-Functionalized Polymers

One of the best methods to synthesize well-defined polymers with pendant functional groups is the living polymerization of monomers carrying appropriate substituents (sometimes in protected forms). Scheme 1.17 presents some examples of VEs from commercially available CEVE by substitution reactions of its chloroalkyl group [9,64]. These processes provide the basis of the synthesis of amphiphilic, block or graft copolymers.



Scheme 1.17. VEs with pendant-functional group.

1.4.4. Block Copolymers

Living polymerization is most frequently employed for the synthesis of block copolymers where two or more monomers are polymerized sequentially [46,54,62]. This use of bifunctional initiating systems leads also to amphiphilic AB [46,49,65-66] and ABA [15,49-50] block copolymers, which may be soluble in water and surface active. Depending on the order of addition in the sequential living polymerization, triblock copolymers containing a hydrophobic center block and hydrophilic outer blocks, or vice versa, are obtained. It is known [67] that ABA-type triblock copolymers differ in solubility characteristics from the corresponding AB diblock copolymers having the same A/B composition ratio.

It is also possible to apply the sequential monomer addition method for the synthesis of block copolymers containing blocks from different types of monomers [68-70].

1.4.5. Multi-Armed and Star-Shaped Polymers

Besides the controlled architectures of linear and functionalized polymers, increasing interest has recently been focused on macromolecules with unique three-dimensional structures or spatial shapes, especially multi-armed and star-shaped polymers [58,71-72]. A typical case for the successful use of multi-functional initiator is the preparation of tri-armed PIBVE [48,52].

1.5. References

- [1] Hort V., Gasman R.C., *'Encyclopedia of Chemical Technology'*, 3rd Ed., John Wiley & Sons, Inc., New-York, **1989**, vol. 17, p. 446-521.
- [2] Goethals E.J., Du Prez F., *Prog. Polym. Sci.*, **2007**, 32, 220.
- [3] Reyntjens W.G.S., Goethals E.J., *Polym. Adv. Technol.*, **2001**, 12, 107.
- [4] Yield N.D., Loranz D.H., in *'Vinyl and Dienes Monomers'*, **1962**, part 1, chap 7, p. 365.
- [5] Reppe W. (to I.G. Farbenindustrie A.G.), *U.S. Pat.*, **1934**, 1, 927-959; *Chem. Abstr.*, **1934**, 28, 4431.
- [6] (a) Favorskii A.E., Shostakovskii M.F., *J. Gen. Chem. (URSS)*, **1943**, 13, 1. (b) Hagemeyer H.J., Blood A.E., Heller J.D., (to Eastman Kodak), *U.S. Pat.*, **1966**, 3, 265, 675; *Fr. Pat.*, **1964**, 1, 352, 522; *Chem. Abstr.*, **1965**, 61, 9604. (c) Schildknecht C., *'Vinyl and Related Polymers'*, John Wiley & Sons, Inc., New York, **1952**, p. 593-597.
- [7] Reppe W. and al., *Ann. Chem.*, **1956**, 601, 81.
- [8] Higashimura T., Yamamoto K., *Makromol. Chem.*, **1974**, 175, 1139.
- [9] (a) Sinaizingde G., Verna A., Liu Q., Brink A., Bronk J.M., *Makromol. Chem., Macromol. Symp.*, **1991**, 42, 329. (b) Nuyken O., Rieß G., Loontjens J.A., Van Der Linde R., *Macromolecular Reports*, **1995**, A32 (Suppls. 1&2), 217 and A32 (Suppls. 4), 459. (c) Schappacher M., Deffieux A., *Macromol. Chem. Phys.*, **1997**, 198, 3953. (d) Nuyken O., Ingrish S., *Macromol. Chem. Phys.*, **1998**, 199, 711. (e) Van De Velde P., Goethals E.J., Du Prez F., *Polym. Int.*, **2003**, 52, 1589.
- [10] Orwoll R.A., in *'Physical Properties of Polymer Handbook'*, edited by J.E. Mark, AIP Press, Woodbury, New York, Chp. 7, **1996**.

- [11] Kricheldorf H.R., Nuyken O., Swift G., in 'Handbook of Polyme Synthesis', in "Plastics Engineering Series", 2nd Ed., Lavoisier Library 2000-2009, Vol. 70, **2005**.
- [12] (a) Clarson S.J., in 'Polymer Data Handbook', Oxford University Press, Inc., **1999**, p 956. (b) pmve.com.
- [13] Nakumura S., Misaka Y. (to kurita Water Industries), *Jpn. Kokai*, **1978**, 7828, 083.
- [14] (a) Cerchiara T., Luppi B., Chidichimo G., Bigucci F., Zecchi V., *Eu. Polym. Pharma. Biopharma.*, **2005**, 61, 195. (b) Labuschagne P.W., Germishuizen W.A., Verryn S.M.C., Moolman F.S., *E.J.P.*, **2008**, 44, 2146. (c) Wong T.W., Wanab S., Anthony Y., *Int. J. Pharma.*, **2008**, 37, 154.
- [15] Eley D.D., Pepper D.C., *Trans. Faraday Soc.*, **1947**, 43, 12.
- [16] Eley D.D., in 'The Chemistry of Cationic Polymerization', ed. P.H. Plesch, Pergamon Press, London, **1963**, chap 9.
- [17] Eley D.D., Richards A.W., *Trans. Faraday Soc.*, **1949**, 45, 425.
- [18] Eley D.D., Richards A.W., *Trans. Faraday Soc.*, **1949**, 45, 436.
- [19] (a) Bolza F., Treolar F.E., *Macromol. Chem.*, **1980**, 181, 839. (b) Bilakes N.M., in 'Encyclopedia of Polymer Science and Technology', Wiley-Interscience, New York, **1971**, vol. 14, p. 511.
- [20] (a) McElvain S.M., *Chem. Rev.*, **1949**, 45, 453. (b) Schildknecht C.E., Zoss A.O., Grosser F., *Ind. Eng. Chem.*, **1949**, 41, 2691. (c) Coombes J.D., Eley D.D., *J. Chem. Soc.*, **1957**, 3700. (d) Imai H., Saegusa T., Furukawa J., *Makromol. Chem.*, **1965**, 61, 92. (e) Kruglova V.A., Liporich V.G., Tyukavkina N.A., *Vysokomol. Soedin. Ser.*, **1967**, A9, 932.
- [21] (a) Palos I., Cadenas-Pliego G., Knjazhanski S.Y., Jiménez-Regalado E.J., De Casas E.G., Ponce-Ibarra V.H., *Polym. Degrad. Stab.*, **2005**, 50, 264. (b) Yoshida T., Tsujino T., Kanaoka S., Aoshima S., *J. Polym. Sci., Part A: Polym. Chem.*, **2005**, 43, 468.
- [22] Ledewith A., Sherrington D.C., *Adv. Polym. Sci.*, **1975**, 19, 1.
- [23] Crivello J.V., *Adv. Polym. Sci.*, **1984**, 62, 1.
- [24] (a) Wislicenus J., Liebigs J., *Ann. Chem.*, **1878**, 92, 106. (b) Eley D.D., Saunders J., *J. Chem. Soc.*, **1954**, 1668. (c) Hayashi Ka., Hayashi Ko., Okamura S., *J. Polym. Sci., Part A: Polym. Chem.*, **1971**, 9, 2305.
- [25] Li A.-L., Zhang W., Lang H., Lu J., *Polymer*, **2004**, 45, 6533.
- [26] (a) Mosley S.A. (Union Carbide Co.) *US Pat.*, **1951**, 2 549 921; *Chem. Abstr.*, **1951**, 45, 5972d. (b) Okamura S., Higashimura T., Watanabe T., *Makromol. Chem.*, **1961**, 50, 137. (c) Higashimura T., Watanabe T., Okamura S., *Kobunshi Kagaku*, **1963**, 20, 680. (d) Lal J., McGrath J.E., *J. Polym. Sci., Part A: Polym. Chem.*, **1964**, 2, 3369. (e) Aoki S., Nakamura K., Otsu T., *Makromol. Chem.*, **1968**, 115, 282.
- [27] Chung Y.J., Squire D.R., Stannett V., *Polymer*, **1975**, 16, 527.
- [28] (a) Kubota H., Kobanov V.Ya., Squire D.R., Stannett V., *J. Macromol. Sci., Chem. Ed.*, **1978**, A12, 1299. (b) Hsieh W.C., Kubota H., Squire D.R., Stannett V., *J. Polym. Sci., Chem. Ed.*, **1980**,

- A18, 2773. (c) Deffieux A., Hsieh W.C., Squire D.R., Stannett V., *Polymer*, **1981**, 22, 1575. (d) Huang X., Unno H., Anekata T., Hirasa O., *J. Chem. Eng. Jpn.*, **1987**, 20, 123.
- [29] Schmidt T., Janik I., Kadłubowski S., Ulański P., Rosiak J.M., Reichelt R., Arndt K.-F., *Polymer*, **2005**, 46, 9908.
- [30] Sawamoto M., *Trends Polym. Sci.*, **1993**, 1, 111.
- [31] Rahman M.S., Hashimoto T., Kodaira T., *J. Polym. Sci., Part A: Polym. Chem.*, **2000**, 39, 4362.
- [32] D'Agosto F., Charreyre M.T., Delolme F., Dessalces G., Cramail H., Deffieux A. et al., *Macromolecules*, **2002**, 35, 7911.
- [33] Hashimoto T., Ibuki H., Sawamoto M., Higashimura T., *J. Polym. Sci., Part A: Polym. Chem.*, **1988**, 26, 3361.
- [34] (a) Rahman Md., Hashimoto T., Kodaira T., *J. Polym. Sci., Part A: Polym. Chem.*, **2000**, 38, 4362. (b) Katayama H., Kamigaito M., Sawamoto M., *J. Polym. Sci., Part A: Polym. Chem.*, **2001**, 39, 1249.
- [35] (a) Kresge A., *J. Acc. Chem. Res.*, **1987**, 20, 364. (b) Kresge A.J., Ubyesz D., *J. Phys. Org. Chem.*, **1994**, 32, 316.
- [36] (a) Bennevault V., Larrue F., Deffieux A., *Macromol. Chem. Phys.*, **1995**, 196, 3075. (b) Bennevault V., Larrue F., Deffieux A., *Macromol. Chem. Phys.*, **1996**, 197, 2603.
- [37] (a) Lin C.H., Matyjaszewski K., *J. Polym. Sci., Polym. Chem.*, **1990**, 28, 1771. (b) Cho C.G., Feit B.A., Webster O.W., *Macromolecules*, **1992**, 25, 2081.
- [38] Hall H.K., Padias Jr.A.B., Atsumi M., Way T.F., *Macromolecules*, **1990**, 23, 678.
- [39] (a) Rochow E.G., Hurd D.T., Lewis R.N., in *'The Chemistry Organometallic Compounds'*, John Wiley, New York, **1957**, p. 134. (b) Ishida S-I., *J. Polym. Sci.*, **1962**, 62, 1.
- [40] Nagata W., Yoshioda M., *Tetrahedron Lett.*, **1966**, 18, 1913.
- [41] (a) Pitzer K.S., Gutowsky H.S., *J. Am. Chem. Abstr.*, **1946**, 68, 2204. (b) Ziegler K., *Chem. Abstr.*, **1961**, 55, 3435. (c) in *'Aluminium Alkyls'*, Texas Alkyls, Inc., Stauffer Company, Wesport, Conn., **1976**.
- [42] Matyjaszewski K., in *'Cationic Polymerizations: Mechanisms, Synthesis and Applications'*, Marcel Dekker, New-York, **1996**.
- [43] Bernaerts K.V., Du Prez F.E., *Polymer*, **2005**, 46, 8469.
- [44] (a) Sawamoto M., *Prog. Polym. Sci.*, **1991**, 16, 111. (b) Kennedy J.P., *Trends Polym. Sci.*, **1995**, 3, 386. (c) Puskas J.E., Kaskas G., *Prog. Polym. Sci.*, **2000**, 25, 403. (d) Sigwalt P., Moreau M., *Prog. Polym. Sci.*, **2006**, 31, 44.
- [45] (a) Higashimura T., Kishio O., *Polym. J.*, **1977**, 9, 87. (b) Higashimura T., Mitsuhashi M., Sawamoto M., *Macromolecules*, **1979**, 12, 178.
- [46] Miyamoto M., Sawamoto M., Higashimura T., *Macromolecules*, **1984**, 17, 2228.
- [47] Higashimura T., Miyamoto M., Sawamoto M., *Macromolecules*, **1985**, 18, 611.
- [48] Higashimura T., Sawamoto M., *Adv. Polym. Sci.*, **1984**, 62, 49.
- [49] Sawamoto M., Higashimura T., *Makromol. Chem., Macromol. Symp.*, **1992**, 54, 41.

- [50] Sawamoto M., Higashimura T., *Makromol. Chem., Macromol. Symp.*, **1992**, 55, 41.
- [51] Peng L., in 'Acetals as Transfer Agents in the Carbocationic Polymerization of Vinyl Ether', Ph-D from the University in Ghent, Belgium, **1996**.
- [52] Kamigaito M., Maeda Y., Sawamoto M., Higashimura T., *Macromol.*, **1993**, 26, 1643.
- [53] (a) Shohi H., Sawamoto M., Higashimura T., *Polym. Bull.*, **1989**, 21, 357. (b) Hashimoto T., Takeuchi E., Sawamoto M., Higashimura T., *J. Polym. Sci., Part A : Polym. Chem.*, **1990**, 28, 1137. (c) Sawamoto M., Hasebe T., Kamigaito M., Higashimura T., *J.M.S. Pure Appl. Chem.*, **1994**, A31, 937.
- [54] Sawamoto M., Enoki T., Higashimura T., *Macromolecules*, **1987**, 20, 1.
- [55] (a) Sawamoto M., Enoki T., Higashimura T., *Polym. Bull.*, **1987**, 18, 117. (b) Van Meirvenne D., Haucourt N., Goethals E.J., *Polym. Bull.*, **1990**, 23, 185. (c) Goethals E.J., Haucourt N., Verheyen A., Habimana J., *Makromol. Chem., Rapid Commun.*, **1990**, 11, 623. (d) Lievens S.S., Goethals E.J., *Polym. Int.*, **1996**, 41, 437.
- [56] Shobi H., Sawamoto M., Higashimura T., *Macromolecules*, **1992**, 25, 58.
- [57] (a) Shohi H., Sawamoto M., Higashimura T., *Macromolecules*, **1992**, 25, 53. (b) Shohi H., Sawamoto M., Higashimura T., *Makromol. Chem.*, **1992**, 193, 1783.
- [58] (a) Goethals E.J., Reyntjens W., Zhang X., Verdonck B., Loontjens T., *Macromol. Symp.*, **2000**, 157, 93. (b) Reyntjens W., Jonckere L., Goethals E.J., Du Prez F., *Macromol. Symp.*, **2001**, 164, 293.
- [59] Schappacher M., Deffieux A., *Macromolecules*, **1991**, 24, 2140.
- [60] Bernaerts K.V., Fustin C.-A., Bomal-D'Haese C., Gohy J.-F., Martins J.C., Du Prez, *Macromolecules*, **2008**, 41, 2593.
- [61] (a) Minoda M., Yamada K., Miyazaki M., Ohno K., Fukuda T., Miyamoto T., *ICR Annual Report*, **2008**, 5, 30. (b) *WO/2007/136574*.
- [62] Sawamoto M., Enoki T., Higashimura T., *Polym. Bull.*, **1986**, 16, 117.
- [63] Aoshima S., Ebara K., Higashimura T., *Polym. Bull.*, **1985**, 14, 425.
- [64] Yoshida T., Kanaoka S., Aoshima S., *J. Polym. Sci., Part A: Polym. Chem.*, **2005**, 43, 5357.
- [65] (a) Patrikios C., Forder C., Armes S.P., Billingham N.C., *J. Polym. Sci.*, **1996**, 34, 1529. (b) Forder C., Patrikios C.S., Armes S.P., Billingham N.C., *Macromolecules*, **1997**, 30, 5758.
- [66] Forder C., Patrikios C.S., Armes S.P., Billingham N.C., *Macromolecules*, **1997**, 30, 5759.
- [67] Kotaka T., Tanaka T., Inagaki H., *Polym. J.*, **1972**, 3, 327.
- [68] Verdonck B., Goethals E.J., Du Prez F., *Macromol. Chem. Phys.*, **2003**, 204, 2090.
- [69] (a) Labeau M.P., Cramail H., Deffieux A., *Macromol. Chem. Phys.*, **1998**, 199, 335. (b) Heischkel Y., Schmidt H-W., *Macromol. Chem. Phys.*, **1998**, 199, 869. (c) Bernaerts K.V., Du Prez F.E., *Prog. Polym. Sci.*, **2006**, 31, 671.
- [70] Yamanchi K., Hasegawa H., Hashimoto T., Köhler N., Knoll K., *Polymer*, **2002**, 43, 3563.
- [71] Schappacher M., Putaux J.L., Lefebvre C., Deffieux A., *J. Am. Chem. Soc.*, **2005**, 127, 2990.
- [72] Jeo H.J., Tak J.-P., Kim J.H., Youk J.H., *EPJ*, **2008**, 44, 2737.

Chapter 2

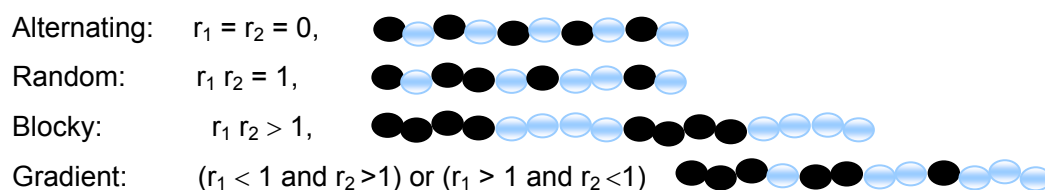
Theory of the Determination of the Reactivity Ratios of Random Copolymers

2.1. Introduction

Copolymerization is a term which is usually restricted to the polymerization of two or more vinyl monomers to give chains that contains all the monomer units arranged along the chain in a random manner. Only the case of two monomers is described here because our work is concerned with the synthesis of two vinyl monomers. These systems are mostly described theoretically for radical copolymerizations, but Kennedy is the only one who also described it for the cabocationic copolymerization [1]. In all cases, it could be also directly applied for cationic and anionic copolymerizations.

2.2. Types of Copolymerization Behavior

The properties of copolymers depend not only on the comonomer composition but also on the sequence distribution of the constituent comonomers which can range from alternating through random to blocky:



Of course, these copolymer types represent 'extremes' of structure. In practice, many so-called statistical copolymers actually show some tendency for their individual comonomers to alternate or block together.

The copolymerization curves are calculated from the Lewis-Mayo equation (eq. 2.1) for various values of the parameters r_1 and r_2 .

$$F_1 = \frac{f_1^2(r_1 - 1) + f_1}{f_1^2(r_2 + r_1 - 2) + 2f_1(1 - r_2) + r_2} \quad (\text{eq. 2.1})$$

The ordinate (F_1) represents the composition of the increment of copolymer formed from the monomer mixture having the composition (f_1) given along the abscissa axis (figure 2.1).

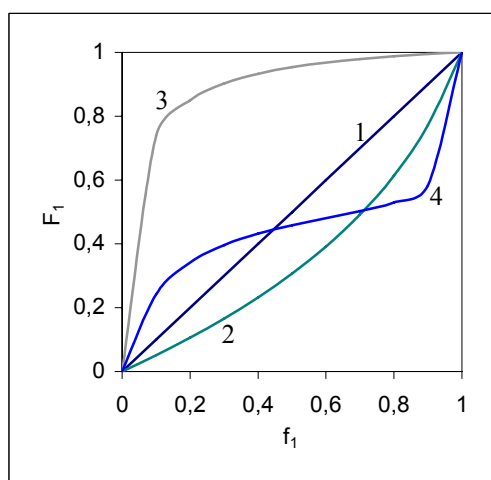


Figure 2.1. Copolymer curves with different reactivity ratios: (1) $r_1 = r_2 = 1$, (2) $r_1 = 0.35$ and $r_2 = 2.05$, (3) $r_1 = 20$ and $r_2 = 0.015$, and (4) $r_1 = 0.048$ and $r_2 = 0.238$.

* The straight line for $r_1 = r_2 = 1$ represents the trivial case in which $k_{11} = k_{12}$ and $k_{22} = k_{21}$, for which the two monomers are equally reactive with each radical.

* Wall introduced the term ideal copolymerization for the case $r_1 r_2 = 1$, in recognition of the analogy to vapor-liquid equilibria for ideal liquid mixtures. It is also apparent that the sequence of monomer units in an ideal copolymer must be necessary random. That is to say, the likelihood of occurrence of an M_1 unit immediately following an M_2 unit is the same as for an M_1 to follow an M_1 unit. The probability of either unit at any place in the chain is always equal to its mole fraction in an ideal copolymer.

* If both r_1 and r_2 are very small ($r_1 < 1$ and $r_2 < 1$), a copolymer is obtained in which the monomers alternate with near perfect regularity along the chain.

* In the case in which both ratios are greater than unity ($r_1 > 1$ and $r_2 > 1$, and therefore also $r_1 r_2 > 1$), there is a tendency to form a block copolymer in which there are blocks of both monomers in the chain.

* In the case that one of the reactivity ratios exceeds unity while the other is less than unity ($r_1 > 1$ and $r_2 < 1$), no critical (azeotropic) composition exists.

* If one of the monomers is very much more reactive than the other ($r_1 \gg r_2$), the two monomers tend to polymerize consecutively.

2.3. Estimation of Monomer Reactivity Ratios

Monomer reactivity ratios are used to predict sequence distributions as discussed in the previous section. A variety of methods have been developed to determine the reactivity ratios, which can be divided in two classes: the linear and non-linear methods. Recently, some reviews have been reported [2-6]. Due to the complex mathematics, only the main ideas have been summarized in this section.

2.3.1. The Linear Methods [2-3, 5, 7-10]

Most of these methods are based on the assumption that for conversions up to approximately 5% the ratio of the two monomers in the feed does not change appreciably. Well-known procedures of this kind are the *Mayo-Lewis* [7], the *Fineman-Ross* [8] as well as the *Kelen-Tüdös* method [9] and its extended one [10].

1) The Fineman-Ross Method [8]

Fineman and Ross reformulated the Mayo-Lewis equation (eq. 2.1) to give

$$\frac{(\rho-1)}{R} = r_1 - r_2 \frac{\rho}{R^2} \quad (\text{eq. 2.2})$$

$$\text{with } \rho = \frac{[M_1]}{[M_2]} \quad \text{and} \quad R = \frac{d[M_1]}{d[M_2]}$$

In the *Fineman-Ross* method, $(\rho-1)/R$ is plotted against $(r_1 - r_2\rho/R^2)$, and r_1 and r_2 are obtained as the slope and the intercept on the abscissa of the straight line, respectively.

2) The Kelen-Tüdös Method [9]

Using the equations of *Fineman-Ross*, the experimental points are often not equally distributed on the resulting curve, but are rather concentrated at the initial part, which can result in rather large uncertainties in the estimate for the reactivity ratios. Kelen and Tüdös suggested an alternate form of the copolymerization, introducing two new parameters G and F to obtain

$G = r_1F - r_2$, where the transformed variables are

$$G = (y-1)\frac{x}{y} \quad \text{and} \quad F = \frac{x^2}{y} \quad (\text{with } x = \rho \text{ and } y = R)$$

The disadvantage of the *Fineman-Ross* method may, however, be abolished by the following graphically valuable linear equation $\frac{G}{(\alpha+F)} = \left(r_1 + \frac{r_2}{\alpha}\right)\frac{F}{\alpha+F} - \frac{r_2}{\alpha}$ (eq. 2.3)

where α ($\alpha > 0$) is the geometrical mean value of the smallest F_m , and the largest F_M , (F -values) which gives $\alpha = \sqrt{F_m F_M}$. By introducing $\eta = \frac{G}{\alpha+F}$ and $\xi = \frac{F}{\alpha+F}$, equation (eq. 2.3)

$$\text{yields: } \eta = \left(r_1 + \frac{r_2}{\alpha}\right)\xi - \frac{r_2}{\alpha} \quad (\text{eq. 2.4})$$

The variable ξ cannot take any positive values, only those in interval [0.1]. Thus plotting the η

values calculated from the experimental data as a function of ξ , we obtain a straight line, which extrapolated to $\xi = 0$ and to $\xi = 1$ gives $-r_2/\alpha$ and r_1 (both as intercepts).

3) The Extended Kelen-Tüdös Method [10]

The Extended Kelen-Tüdös method considers the drift in the comonomer and copolymer compositions with conversion. This method is the most reliable since one may simply use the reactivity ratio values with a small error up to 60% conversion. The Extended Kelen-Tüdös method is expressed by the equation (eq. 2.4) introducing two new values to F and G :

$$F = \frac{y}{z^2} \quad \text{and} \quad G = \frac{(y-1)}{z}, \quad \text{with} \quad z = \frac{\log(1-\zeta_1)}{\log(1-\zeta_2)}$$

where ζ_1 and ζ_2 represent the molar conversion of each monomer

$$\zeta_2 = w \frac{(\mu + x)}{(\mu + y)} \quad \text{and} \quad \zeta_1 = \frac{y}{x} \zeta_2$$

$$\text{with } x \text{ and } y \text{ defined as } x = \frac{[M_1]}{[M_2]} \quad \text{and} \quad y = \frac{[dM_1]}{[dM_2]}$$

In these relations, w denotes weight conversions of the copolymerization, and $\mu = \mu_2/\mu_1$ is the ratio between the molecular weights of the two monomers (e.g., $M_{MVE} = 58.08 \text{ g.mol}^{-1}$ and $M_{CEVE} = 106.55 \text{ g.mol}^{-1}$).

2.3.2. The Non-Linear Methods [3-7, 11-15]

Because the 'independent' variable of these linear equations is not really independent, and the variance of the dependent variable is not constant [16], the statistically soundest method to determine r_1 and r_2 is to fit the copolymerization equation by means of non-linear least square difference procedures [2]. A widespread version of this method is the 'error-in-variable' model (e.g., *Tidwell and Mortimer model* [12], *terminal model* [3, 7, 11], *penultimate model* [13], *depropagation model* [14] or *complex participation model* [15]) that performs a decent statistical analysis on the presented data and calculates error limits and confidence intervals of the obtained copolymerization parameters [17].

An overview of all models and used equations is given in table 2.1. A non-linear method is the only proper way to analyze copolymer composition data and to determine reactivity ratios and has thus also been applied in our research.

1) Tidwell and Mortimer Model [12]

Tidwell and Mortimer non-linear least-square method is only valuable at low conversions (< 10%) in contrast to the other non-linear methods. *Tidwell and Mortimer model* compares several calculation methods with the following sum of squares (SS) criterion for the suitability of a set of reactivity ratios to fit an experiment with n points:

$$SS = \sum_{i=1}^n (m_1^{\text{exp}} - m_1^{\text{cal}})^2$$

Table 2.1. Copolymerization equations and copolymerization parameters for non-linear methods. (Table taken from ref. [6])

Model name	Propagation steps	Copolymerization equation	Parameter set r_i
Terminal Model	$\begin{aligned} \rightsquigarrow M_1^\bullet + M_1 &\xrightarrow{k_{11}} \rightsquigarrow M_1M_1^\bullet \\ \rightsquigarrow M_1^\bullet + M_2 &\xrightarrow{k_{12}} \rightsquigarrow M_1M_2^\bullet \\ \rightsquigarrow M_2^\bullet + M_1 &\xrightarrow{k_{21}} \rightsquigarrow M_2M_1^\bullet \\ \rightsquigarrow M_2^\bullet + M_2 &\xrightarrow{k_{22}} \rightsquigarrow M_2M_2^\bullet \end{aligned}$	$\frac{d[M_1]}{d[M_2]} = \frac{[M_1]}{[M_2]} \cdot \frac{r_1 \cdot [M_1] + [M_2]}{r_2 \cdot [M_2] + [M_1]}$	$\begin{aligned} r_1 &= k_{11}/k_{12} \\ r_2 &= k_{22}/k_{21} \end{aligned}$
Penultimate Behavior	$\begin{aligned} \rightsquigarrow M_1M_1^\bullet + M_1 &\xrightarrow{k_{111}} \rightsquigarrow M_1M_1M_1^\bullet \\ \rightsquigarrow M_1M_1^\bullet + M_2 &\xrightarrow{k_{112}} \rightsquigarrow M_1M_1M_2^\bullet \\ \rightsquigarrow M_2M_1^\bullet + M_1 &\xrightarrow{k_{211}} \rightsquigarrow M_2M_1M_1^\bullet \\ \rightsquigarrow M_2M_1^\bullet + M_2 &\xrightarrow{k_{212}} \rightsquigarrow M_2M_1M_2^\bullet \\ \rightsquigarrow M_2M_2^\bullet + M_2 &\xrightarrow{k_{222}} \rightsquigarrow M_2M_2M_2^\bullet \\ \rightsquigarrow M_2M_2^\bullet + M_1 &\xrightarrow{k_{221}} \rightsquigarrow M_2M_2M_1^\bullet \\ \rightsquigarrow M_1M_2^\bullet + M_2 &\xrightarrow{k_{122}} \rightsquigarrow M_1M_2M_2^\bullet \\ \rightsquigarrow M_1M_2^\bullet + M_1 &\xrightarrow{k_{121}} \rightsquigarrow M_1M_2M_1^\bullet \end{aligned}$	$\frac{d[M_1]}{d[M_2]} = \frac{1 + \frac{r_1' \cdot Q_{12} \cdot (r_1 \cdot Q_{12} + 1)}{r_1' \cdot Q_{12} + 1}}{1 + \frac{r_2' \cdot (r_2 + Q_{12})}{Q_{12} \cdot (r_2' + Q_{12})}} \quad Q_{12} = \frac{[M_1]}{[M_2]}$	$\begin{aligned} r_1 &= k_{111}/k_{112} \\ r_1' &= k_{211}/k_{212} \\ r_2 &= k_{222}/k_{221} \\ r_2' &= k_{122}/k_{121} \end{aligned}$
Depropagation model	<p><i>Terminal model and</i></p> <p><u>CASE I</u></p> $\rightsquigarrow M_1M_2M_2^\bullet \rightleftharpoons \rightsquigarrow M_1M_2^\bullet + M_2$ <p>$\rightsquigarrow M_1M_2^\bullet$ does not propagate</p> <p><u>CASE II</u></p> $\rightsquigarrow M_1M_2M_2M_2^\bullet \rightleftharpoons \rightsquigarrow M_1M_2M_2^\bullet + M_2$ <p>neither $\rightsquigarrow M_1M_2^\bullet$ nor $\rightsquigarrow M_1M_2M_2^\bullet$ depropagate</p>	$\frac{d[M_1]}{d[M_2]} = r_1 \cdot Q_{12} + 1 - \alpha \quad \alpha = \frac{1}{2} \cdot \left(A - \sqrt{A^2 - 4[M_2] \cdot K} \right)$ $A = 1 + [M_2] \cdot K + \frac{[M_1] \cdot K}{r_2} \quad Q_{12} = \frac{[M_1]}{[M_2]}$ $\frac{d[M_1]}{d[M_2]} = \frac{\{1 + r_1 \cdot Q_{12}\} \cdot \left\{ \alpha \gamma + \frac{\alpha}{1 - \alpha} \right\}}{\alpha \gamma - 1 + \frac{1}{(1 - \alpha)^2}} \quad \gamma = 1 + \frac{Q_{12}}{r_2} - \frac{\alpha}{[M_2] \cdot K} \quad Q_{12} = \frac{[M_1]}{[M_2]}$	$\begin{aligned} r_1 &= k_{11}/k_{12} \\ r_2 &= k_{22}/k_{21} \\ r_3 &= K [M_1] \\ r_4 &= K [M_2] \end{aligned}$
Complex participation	<p><i>Terminal model and</i></p> $M_1^\circ + M_2^\circ \xrightleftharpoons{K} M_1M_2$ <p>M° refers to uncomplexed monomer</p> $\begin{aligned} M_1^\bullet + \overline{M_2M_1} &\xrightarrow{k_{1C1}} M_1^\bullet \\ M_1^\bullet + \overline{M_1M_2} &\xrightarrow{k_{1C2}} M_2^\bullet \\ M_2^\bullet + \overline{M_1M_2} &\xrightarrow{k_{2C2}} M_2^\bullet \\ M_2^\bullet + \overline{M_2M_1} &\xrightarrow{k_{2C1}} M_1^\bullet \end{aligned}$	$\frac{d[M_1]}{d[M_2]} = \frac{1 + \left(\frac{r_2}{r_2'} + \frac{r_2''}{r_2''} \right) r_B + A}{1 + \frac{[M_2]}{[M_1]} r_2' + \left(2 \cdot \frac{r_2}{r_2'} + \frac{r_2''}{r_2''} \right) r_B + A}$ $\frac{d[M_2]}{d[M_1]} = \frac{1 + \left(\frac{r_1}{r_1'} + \frac{r_1''}{r_1''} \right) r_A + B}{1 + \frac{[M_1]}{[M_2]} r_1' + \left(2 \cdot \frac{r_1}{r_1'} + \frac{r_1''}{r_1''} \right) r_A + B}$ $A = \frac{1 + r_B \cdot \frac{r_2}{r_2'} \cdot \frac{r_1'}{r_1''} \cdot r_A}{1 + r_A \cdot \frac{r_1'}{r_1''} \cdot \frac{r_1''}{r_1''} \cdot r_A}$ $B = \frac{1 + r_A \cdot \frac{r_1'}{r_1''} \cdot \frac{r_2}{r_2''} \cdot r_B}{1 + r_B \cdot \frac{r_2}{r_2'} \cdot \frac{r_2''}{r_2''} \cdot r_B}$	$\begin{aligned} r_1 &= k_{11}/k_{12} \\ r_1' &= k_{11}/k_{1C1} \\ r_1'' &= k_{11}/k_{1C2} \\ r_2 &= k_{22}/k_{21} \\ r_2' &= k_{22}/k_{2C2} \\ r_2'' &= k_{22}/k_{2C1} \\ r_A &= K [M_1] \\ r_B &= K [M_2] \end{aligned}$

where m_i^{exp} stands for the copolymer composition determined experimentally for experiment i and m_i^{cal} stands for the copolymer composition calculated with the estimated reactivity ratios at M_{10}/M_{20} for experiment i .

The joint confidence intervals (JCI) [18], within which the correct values are believed to exist, conveys some idea of the reliability of the experiment and data. The approximate 95% JCI are delimited by the set of values r_{ij} which satisfy the following equation:

$$JCI = SS + \frac{2 \times SS}{n-2} F_{(2,n-2)}^{\text{tab}}$$

The curve-fitting method involves calculating differences $\Delta = (m_1^{\text{exp}} - m_1^{\text{cal}})^2$ and searching for reactivity ratios by plotting r_i taking $\Delta \rightarrow 0$. The theoretical curves are computed on the basis of an initial rough estimate of r_1 and r_2 (using *Fineman-Ross* and/or *Kelen-Tüdös* methods) and its refinement is made by successive iterations, so as to minimize the sum of mean-square deviations from the theoretical curve of the experimental points (m_{1i}^{exp}):

$$SS = \sum_{i=1}^{\text{exp}} \left[m_{1i}^{\text{exp}} - \frac{M_{1i}^2 (r_1 - 1) + M_{1i}}{M_{1i}^2 (r_1 + r_2 - 2M_{1i}(1 - r_2)) + r_2} \right]^2$$

2) Terminal Model (or the First-Order Markov) [3, 7, 11]

In this model, copolymers composition is only dependent on the identity of the monomer unit at the growing end, and independent of the chain composition preceding the last unit.

[feed]₀ ≠ [feed]₁ ≠ [feed]₂...

N.B.: good method when r_1 and r_2 are not so different:

$r_1 < 1$ and $r_2 < 1$ or $0 < r_1 r_2 \geq 1$ (ideal, alternation tendency or gradient tendency toward alternation).

3) Deviations from Terminal Copolymerization Model (the Penultimate Behavior, the Depropagation Model and the Complex Participation Model) [5-6, 13-15]

The derivation of the *Terminal* (of *first-order Markov*) copolymer composition equation is based on two important assumptions: one of a kinetic nature and the other of a thermodynamic nature. The first is that the reactivity of the propagating species is independent of the identity of the monomer unit, which precedes the terminal unit. The second is the irreversibility of the various propagation reactions.

• Penultimate Behavior (or the Second-Order Markov) [13]

The behaviour of some comonomer systems indicates that the reactivity of the propagating species is affected by the next-to-last (penultimate) monomer unit. If one of the comonomers (or both) has stronger polar substituents, the reactivities of the growing free carbocations can be affected by the penultimate unit. According to Coote and Davis [19], the penultimate model provides an improved description of the copolymer compositions and sequences. There are eight possible chain propagation reactions:

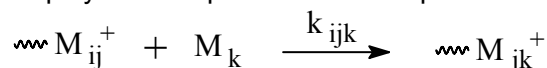


Table 2.1. Copolymerization equations and copolymerization parameters for non-linear methods. (Table taken from ref. [6])

Model name	Propagation steps	Copolymerization equation	Parameter set r_i
Terminal Model	$\begin{aligned} \rightsquigarrow M_1^\bullet + M_1 &\xrightarrow{k_{11}} \rightsquigarrow M_1M_1^\bullet \\ \rightsquigarrow M_1^\bullet + M_2 &\xrightarrow{k_{12}} \rightsquigarrow M_1M_2^\bullet \\ \rightsquigarrow M_2^\bullet + M_1 &\xrightarrow{k_{21}} \rightsquigarrow M_2M_1^\bullet \\ \rightsquigarrow M_2^\bullet + M_2 &\xrightarrow{k_{22}} \rightsquigarrow M_2M_2^\bullet \end{aligned}$	$\frac{d[M_1]}{d[M_2]} = \frac{[M_1]}{[M_2]} \cdot \frac{r_1 \cdot [M_1] + [M_2]}{r_2 \cdot [M_2] + [M_1]}$	$\begin{aligned} r_1 &= k_{11}/k_{12} \\ r_2 &= k_{22}/k_{21} \end{aligned}$
Penultimate Behavior	$\begin{aligned} \rightsquigarrow M_1M_1^\bullet + M_1 &\xrightarrow{k_{111}} \rightsquigarrow M_1M_1M_1^\bullet \\ \rightsquigarrow M_1M_1^\bullet + M_2 &\xrightarrow{k_{112}} \rightsquigarrow M_1M_1M_2^\bullet \\ \rightsquigarrow M_2M_1^\bullet + M_1 &\xrightarrow{k_{211}} \rightsquigarrow M_2M_1M_1^\bullet \\ \rightsquigarrow M_2M_1^\bullet + M_2 &\xrightarrow{k_{212}} \rightsquigarrow M_2M_1M_2^\bullet \\ \rightsquigarrow M_2M_2^\bullet + M_2 &\xrightarrow{k_{222}} \rightsquigarrow M_2M_2M_2^\bullet \\ \rightsquigarrow M_2M_2^\bullet + M_1 &\xrightarrow{k_{221}} \rightsquigarrow M_2M_2M_1^\bullet \\ \rightsquigarrow M_1M_2^\bullet + M_2 &\xrightarrow{k_{122}} \rightsquigarrow M_1M_2M_2^\bullet \\ \rightsquigarrow M_1M_2^\bullet + M_1 &\xrightarrow{k_{121}} \rightsquigarrow M_1M_2M_1^\bullet \end{aligned}$	$\frac{d[M_1]}{d[M_2]} = \frac{1 + \frac{r_1' \cdot Q_{12} \cdot (r_1 \cdot Q_{12} + 1)}{r_1' \cdot Q_{12} + 1}}{1 + \frac{r_2' \cdot (r_2 + Q_{12})}{Q_{12} \cdot (r_2' + Q_{12})}} \quad Q_{12} = \frac{[M_1]}{[M_2]}$	$\begin{aligned} r_1 &= k_{111}/k_{112} \\ r_1' &= k_{211}/k_{212} \\ r_2 &= k_{222}/k_{221} \\ r_2' &= k_{122}/k_{121} \end{aligned}$
Depropagation model	<p><i>Terminal model and</i></p> <p><u>CASE I</u></p> $\rightsquigarrow M_1M_2M_2^\bullet \rightleftharpoons \rightsquigarrow M_1M_2^\bullet + M_2$ <p>$\rightsquigarrow M_1M_2^\bullet$ does not propagate</p> <p><u>CASE II</u></p> $\rightsquigarrow M_1M_2M_2M_2^\bullet \rightleftharpoons \rightsquigarrow M_1M_2M_2^\bullet + M_2$ <p>neither $\rightsquigarrow M_1M_2^\bullet$ nor $\rightsquigarrow M_1M_2M_2^\bullet$ depropagate</p>	$\frac{d[M_1]}{d[M_2]} = r_1 \cdot Q_{12} + 1 - \alpha \quad \alpha = \frac{1}{2} \cdot \left(A - \sqrt{A^2 - 4[M_2] \cdot K} \right)$ $A = 1 + [M_2] \cdot K + \frac{[M_1] \cdot K}{r_2} \quad Q_{12} = \frac{[M_1]}{[M_2]}$ $\frac{d[M_1]}{d[M_2]} = \frac{\{1 + r_1 \cdot Q_{12}\} \cdot \left\{ \alpha \gamma + \frac{\alpha}{1 - \alpha} \right\}}{\alpha \gamma - 1 + \frac{1}{(1 - \alpha)^2}} \quad \gamma = 1 + \frac{Q_{12}}{r_2} - \frac{\alpha}{[M_2]K} \quad Q_{12} = \frac{[M_1]}{[M_2]}$	$\begin{aligned} r_1 &= k_{11}/k_{12} \\ r_2 &= k_{22}/k_{21} \\ r_3 &= K [M_1] \\ r_4 &= K [M_2] \end{aligned}$
Complex participation	<p><i>Terminal model and</i></p> $M_1^\circ + M_2^\circ \xrightleftharpoons{K} M_1M_2$ <p>M° refers to uncomplexed monomer</p> $\begin{aligned} M_1^\bullet + \overline{M_2M_1} &\xrightarrow{k_{1C1}} M_1^\bullet \\ M_1^\bullet + \overline{M_1M_2} &\xrightarrow{k_{1C2}} M_2^\bullet \\ M_2^\bullet + \overline{M_1M_2} &\xrightarrow{k_{2C2}} M_2^\bullet \\ M_2^\bullet + \overline{M_2M_1} &\xrightarrow{k_{2C1}} M_1^\bullet \end{aligned}$	$\frac{d[M_1]}{d[M_2]} = \frac{1 + \left(\frac{r_2}{r_2'} + \frac{r_2''}{r_2''} \right) r_B + A}{1 + \frac{[M_2]}{[M_1]} r_2 + \left(2 \cdot \frac{r_2}{r_2'} + \frac{r_2''}{r_2''} \right) r_B + A}$ $\frac{d[M_2]}{d[M_1]} = \frac{1 + \left(\frac{r_1}{r_1'} + \frac{r_1''}{r_1''} \right) r_A + B}{1 + \frac{[M_1]}{[M_2]} r_1 + \left(2 \cdot \frac{r_1}{r_1'} + \frac{r_1''}{r_1''} \right) r_A + B}$ $A = \frac{1 + r_B \cdot \frac{r_2}{r_2'} \cdot \frac{r_1}{r_1''} \cdot r_A}{1 + r_A \cdot \frac{r_1}{r_1'} \cdot \frac{r_2}{r_2''} \cdot r_B}$ $B = \frac{1 + r_A \cdot \frac{r_1}{r_1'} \cdot \frac{r_2}{r_2''} \cdot r_B}{1 + r_B \cdot \frac{r_2}{r_2'} \cdot \frac{r_1}{r_1''} \cdot r_A}$	$\begin{aligned} r_1 &= k_{11}/k_{12} \\ r_1' &= k_{11}/k_{1C1} \\ r_1'' &= k_{11}/k_{1C2} \\ r_2 &= k_{22}/k_{21} \\ r_2' &= k_{22}/k_{2C2} \\ r_2'' &= k_{22}/k_{2C1} \\ r_A &= K [M_1] \\ r_B &= K [M_2] \end{aligned}$

where m_i^{exp} stands for the copolymer composition determined experimentally for experiment i and m_i^{cal} stands for the copolymer composition calculated with the estimated reactivity ratios at M_{10}/M_{20} for experiment i .

The joint confidence intervals (JCI) [18], within which the correct values are believed to exist, conveys some idea of the reliability of the experiment and data. The approximate 95% JCI are delimited by the set of values r_{ij} which satisfy the following equation:

$$JCI = SS + \frac{2 \times SS}{n-2} F_{(2,n-2)}^{\text{tab}}$$

The curve-fitting method involves calculating differences $\Delta = (m_1^{\text{exp}} - m_1^{\text{cal}})^2$ and searching for reactivity ratios by plotting r_i taking $\Delta \rightarrow 0$. The theoretical curves are computed on the basis of an initial rough estimate of r_1 and r_2 (using *Fineman-Ross* and/or *Kelen-Tüdös* methods) and its refinement is made by successive iterations, so as to minimize the sum of mean-square deviations from the theoretical curve of the experimental points (m_{1i}^{exp}):

$$SS = \sum_{i=1}^{\text{exp}} \left[m_{1i}^{\text{exp}} - \frac{M_{1i}^2 (r_1 - 1) + M_{1i}}{M_{1i}^2 (r_1 + r_2 - 2M_{1i}(1 - r_2)) + r_2} \right]^2$$

2) Terminal Model (or the First-Order Markov) [3, 7, 11]

In this model, copolymers composition is only dependent on the identity of the monomer unit at the growing end, and independent of the chain composition preceding the last unit.

[feed]₀ ≠ [feed]₁ ≠ [feed]₂...

N.B.: good method when r_1 and r_2 are not so different:

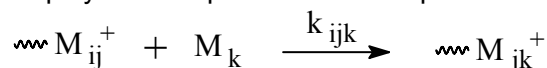
$r_1 < 1$ and $r_2 < 1$ or $0 < r_1 r_2 \geq 1$ (ideal, alternation tendency or gradient tendency toward alternation).

3) Deviations from Terminal Copolymerization Model (the Penultimate Behavior, the Depropagation Model and the Complex Participation Model) [5-6, 13-15]

The derivation of the *Terminal* (of *first-order Markov*) copolymer composition equation is based on two important assumptions: one of a kinetic nature and the other of a thermodynamic nature. The first is that the reactivity of the propagating species is independent of the identity of the monomer unit, which precedes the terminal unit. The second is the irreversibility of the various propagation reactions.

• Penultimate Behavior (or the Second-Order Markov) [13]

The behaviour of some comonomer systems indicates that the reactivity of the propagating species is affected by the next-to-last (penultimate) monomer unit. If one of the comonomers (or both) has stronger polar substituents, the reactivities of the growing free carbocations can be affected by the penultimate unit. According to Coote and Davis [19], the penultimate model provides an improved description of the copolymer compositions and sequences. There are eight possible chain propagation reactions:



Chapter 3

Synthesis of Vinyl Ether Copolymers by Cationic Copolymerizations

3.1. Introduction

The chemical structure of a copolymer depends not only on the two monomer units forming the macromolecule, but also on how such units are distributed along macromolecular chains [1]. This distribution is a direct consequence of each monomer's reactivity in the copolymer molecule [2]. In radical copolymerization, the reactivity of a free radical depends on the nature of the side groups linked to the radical carbon. With respect to this structural feature, there are three important factors influencing the monomer reactivity ratio in radical copolymerization of vinyl monomers: electronic delocalization, polarity and the volume of the side group. All these factors can be studied by analyzing the reaction between functionalized vinyl monomers to obtain the corresponding functionalized vinyl copolymers, which are understood as macromolecular compounds formed by monomer units containing groups of different nature.

Copolymerization is one of the important techniques adopted in effecting systematic changes in the polymer properties and is especially employed in the production of commercial polymers. In the commercial use of copolymerization it is usually desirable to obtain a copolymer with the narrowest possible distribution of compositions, since polymer properties (and therefore utilization) are often highly dependent on copolymer composition. Two approaches are simultaneously used to minimize heterogeneity in the copolymer composition. One is the choice of comonomers. Choosing a pair of monomers whose copolymerization behaviour is such that F_1 is not too different from f_1 is highly desirable as long as that copolymer has the desired properties. The other approach is to maintain the feed composition approximately constant by the batchwise or continuous addition of the more reactive monomer. The control composition differs from the feed.

A number of studies have reported on the copolymerization of VEs with other vinyl monomers by cationic mechanism. However, there have been few reports on the

copolymerization of VEs with other VEs [3-6]. Dunphy [4] has copolymerized CEVE with IBVE and ODVE using stannic chlorine as catalyst and determined the monomer reactivity ratios. Khomutov [5] has determined the monomer reactivity ratios in the copolymerization of *n*BVE with ethyl and isopropyl VE in the presence of sulfuric acid-aluminium sulfate. Fueno [7] has copolymerized substituted phenyl VEs by stannic chlorine to study the Hammett's relations in the copolymerization.

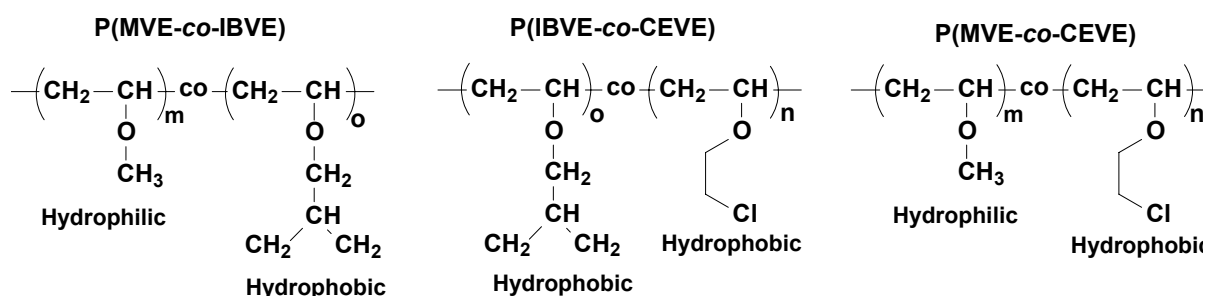
In a paper from our research group, preceding my PhD, the copolymerization of ODVE with IBVE has been reported [8]. The crystallinity of the PODVE fraction was slightly decreased by the incorporation of the hydrophobic IBVE. In our case, a well-known example belonging to the class of thermo-responsive polymers, PMVE, was chosen because it sustains its water solubility up to 37°C [9]. The fact that MVE is a gas at room temperature and the high heat of polymerization ($1400\text{kJ}\cdot\text{kg}^{-1}$) are probably the reasons why only few studies on the living cationic polymerization of MVE have been reported. Thermo-responsiveness has also been observed for other copolymers containing hydrophilic and hydrophobic units such as partially hydrolyzed poly(vinyl acetate) [10], poly(diacetone acrylamide-*co*-hydroxyethyl acrylate) [11], poly((*N*-phenylacrylamide)-*co*-(*N,N*-dimethylacrylamide)) [12], poly((methyl 2-acetamidoacrylate)-*co*-(methyl methacrylate)) [13] produced by free radical polymerization, which can be regarded as copolymers because of their random sequences of hydrophilic and hydrophobic moieties [14].

The thermo-responsive PMVE, widely studied by ourselves [15-18] and others [19-21], features not only excellent thermo-responsive properties but has also a predetermined structure with control over molecular weight and narrow polydispersity. However, until now, only a few random copolymerizations of VEs under suitable conditions for living polymerization have been described [8,22]. In spite of the uncontrolled distribution of monomer units in statistical copolymers, random copolymerization may be important because of its simplicity and practicality. None of them contained reactive groups that would allow for further modification or the construction of segmented copolymer structures.

One of the objectives of this study was to synthesize new thermo-responsive random copolymers combining thermo-responsiveness of PMVE with other physical properties in subsequent studies such as the addition of hydrophobic units of IBVE and CEVE. The other objective of this preliminary study was to develop a method to introduce reactive groups in PMVE and PIBVE. This will allow us in a later stage to introduce other polymer segments on the PVE backbone. For that reason, the copolymerization of MVE or IBVE with IBVE or CEVE was considered (scheme 3.1), through living cationic polymerization.

A series of studies dealing with the controlled cationic polymerization of VEs has shown the important possibilities offered by this procedure for the synthesis of mono- and bi-functional initiators [23-24]. Two different approaches have been used. In the first one, the VE polymerization is performed in the presence of a mono-functional initiator [23], and in the second method, by a bi-functional initiator [24]. Thus PVE chains can grow in two ways. In the present

study, the living cationic copolymerizations of VE (MVE or IBVE) with other VE (IBVE or CEVE) with the use of these initiating systems have been investigated, leading to new copolymers (scheme 3.1).



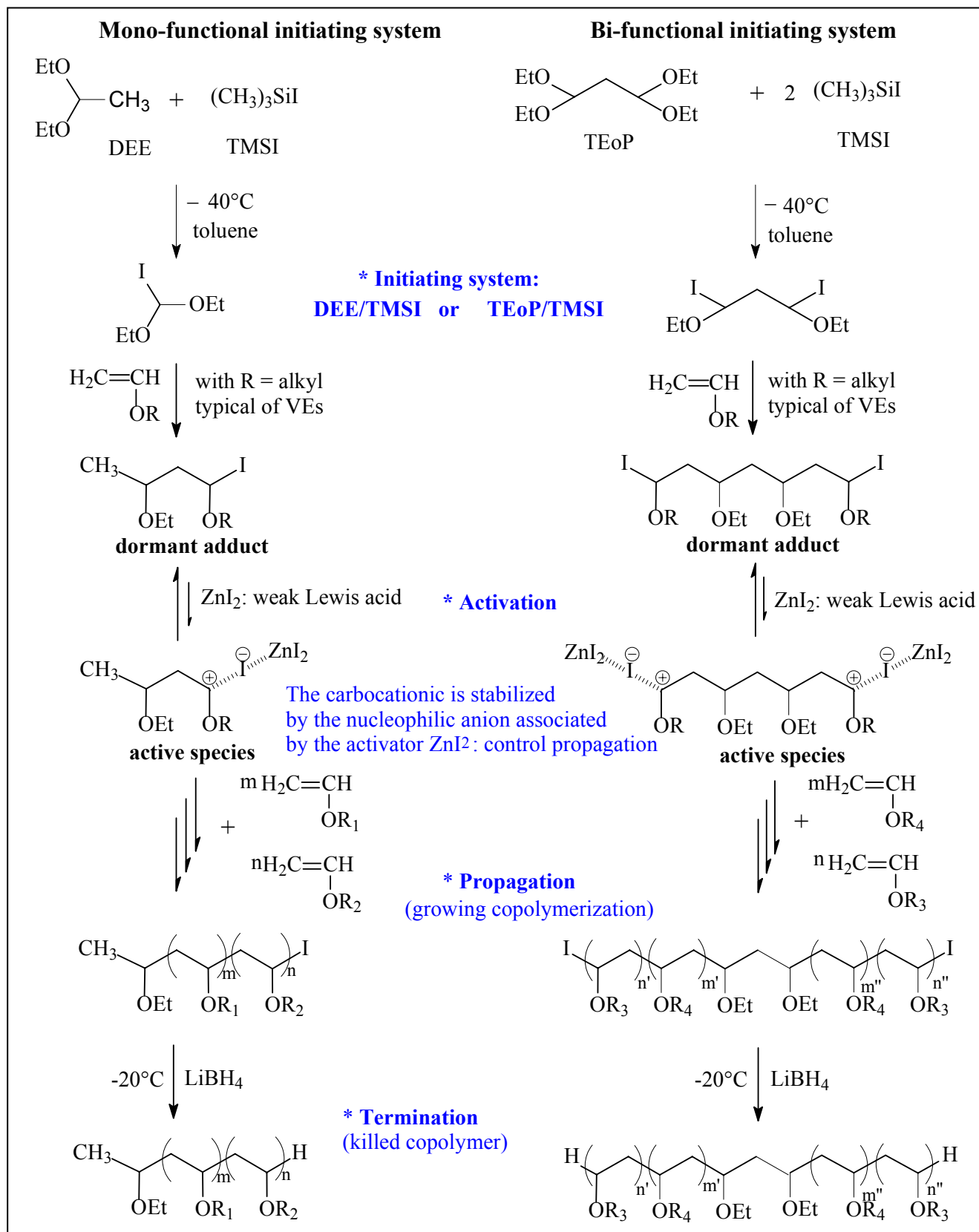
Scheme 3.1. Structure of poly(methyl vinyl ether-co-isobutyl butyl vinyl ether) (P(MVE-co-IBVE)), poly(isobutyl vinyl ether-co-(2-chloroethyl vinyl ether)) (P(IBVE-co-CEVE)) and poly(methyl vinyl ether-co-(2-chloroethyl vinyl ether)) (P(MVE-co-CEVE)).

This chapter first describes the preparation of VE copolymers with low molecular weight. In the second part, the synthesis of higher M_n using the same strategy is examined, providing experimental evidences for the occurrence of side reactions during the polymerization. Their characterization, the search for experimental conditions that allow their control and their livingness are also presented. In the third part, the monomer reactivity ratios of MVE, IBVE and CEVE comonomers have been evaluated using not only linearization methods (Fineman-Ross [25], Kelen-Tüdös [26] and Extended Kelen-Tüdös [27] methods) but also non-linearization methods (Tidwell and Mortimer model [28], terminal model [29], penultimate model [30], depropagation model [31] or complex participation model [32]). And finally, the physical properties, glass transition temperature (T_g) and solubility, were studied.

3.2. Mechanism of the Copolymerizations

The last 15 years, two initiating systems were developed that has led to a breakthrough in the synthesis of VEs. This has made the synthesis of VE much easier than in the past. In 1994, Haucourt and Goethals [23, 33-34] have developed a new initiating system based on a mono-functional acetal, the DEE, TMSI and ZnI_2 which provided the possibility to polymerize VEs in a living way. This initiating system is preferred over the originally used HI/I_2 system because of its easier purification procedure and higher stability.

In our work, the living random copolymers of IBVE or CEVE with MVE are synthesized with this mono-functional initiating system. The complete copolymerization is presented in scheme 3.2. On the other hand, the bifunctional initiating system based on a reaction of bis-acetal TEOp with TMSI was also used for the random cationic copolymerizations of MVE or IBVE with CEVE (scheme 3.2). The last system, which leads to living bi-functional chains, was also investigated by Defieux *et al* [24] for the homopolymerization of CEVE.



Scheme 3.2. Reaction scheme for the synthesis of VEs with mono and bi-functional initiators by living random cationic copolymerizations; $\text{R}_1 = \text{CH}_3$, $\text{R}_2 = \text{CH}_2\text{-CH}(\text{CH}_3)_2$ or $\text{CH}_2\text{-CH}_2\text{-Cl}$, $\text{R}_3 = \text{CH}_2\text{-CH}_2\text{-Cl}$ and $\text{R}_4 = \text{CH}_3$ or $\text{CH}_2\text{-CH}(\text{CH}_3)_2$.

In general, the copolymers have been synthesized by living cationic copolymerization of two monomers. The initiator was formed by the reaction of an acetal (DEE) or a bis-acetal (TEoP) with TMSI at -40°C in toluene (see details in experimental part). Their combination with TMSI enables to make an α -iodoether or a bis-iodoether initiator. A related experimental detail which should be noted is that, because of the highly active nature of this initiator, a rather low temperature (-40°C) was used for both procedures. Since it has been reported that TMSI is not able to initiate alone the polymerization of VEs [33,35], the latter compound was introduced in slight excess, about 1.2 equivalent per acetal function, to ensure a complete conversion of the acetal group.

The copolymerization is then triggered by ZnI_2 , which leads to mono-functional and bifunctional living chains by adding successively the monomers. In order to suppress the formation of side end groups, which would inevitably lead to a decrease of the polymer functionality, the PVEs active ends were deactivated by adding the living polymer solution into a large volume of lithium borohydride (LiBH_4) in tetrahydrofuran (THF) at low temperatures (-20°C). This produces non-reactive, stable end-groups. As a precaution, an excess of borohydride was decomposed with water before the temperature was increased.

It was reported that living/controlled cationic polymerizations of VEs with polar functional groups involved some chain transfer reactions that led to the broadening of the M_w/M_n 's of the polymers [36]. These chain transfer reactions via β -proton elimination [37-38] are described in **Chapter 1**. In the case of VE polymerization, transfer cannot be detected at a low polymerization degree but is clearly observed for higher M_n (co)polymers.

3.3. Compositions of the Copolymers by ^1H NMR

In this section, the starting group (DEE or TEoP) analysis by ^1H NMR was used to determine the DP_n of the copolymers and their compositions. There is one characteristic group in the initiator residue that can be used for this determination: the starting methyl group (protons i, figure 3.1). The DP_n of the homopolymer and copolymer was calculated from the ratio of the normalized areas of a characteristic group of the monomer repeat unit divided by either of this initiator. Before presenting the ^1H NMR spectra of the copolymers, the ^1H NMR spectra of the three homopolymers were introduced to indicate the characteristic groups in each monomer repeat unit. The composition of the copolymers was also determined by the ^1H NMR spectra of P(MVE-co-IBVE), P(MVE-co-CEVE) and P(IBVE-co-CEVE). ^1H NMR spectra of PMVE, PCEVE and PIBVE homopolymers are presented in figure 3.1, and their copolymers in figure 3.2. The spectra of these copolymers are a combination of their homopolymers spectra, indicating the successful copolymerization of the two monomers.

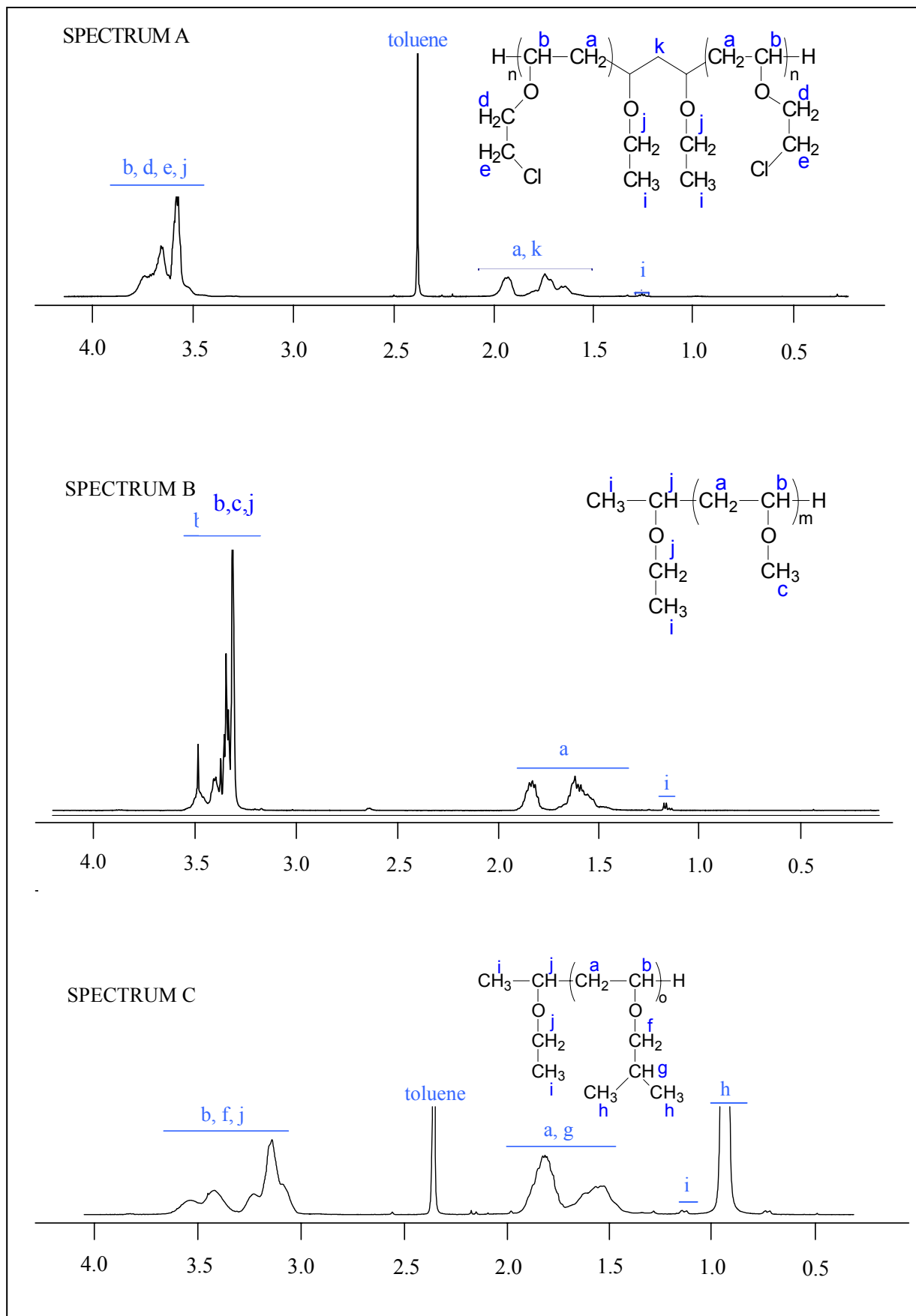


Figure 3.1. ^1H NMR spectra of PCEVE (A), PMVE (B) and PIBVE (C) in CDCl_3 .

3.3.1. Homopolymers

Each spectrum in figure 3.1 contains the six terminal methyl protons *i* at 1.1 – 1.2 ppm. The methylene unit of the three homopolymers (protons *a*) appears in the area I_{CH_2} between 1.5 – 2.0 ppm. The β -methyl protons adjacent to the oxygen atom, as an ether function, of PMVE (protons *b* and *c*) give rise to the signal area I_{MVE} between 3.2 – 3.55 ppm, while those adjacent to the oxygen of PCEVE (protons *b*, *d* and *e*) appear in the range area I_{CEVE} between 3.5 – 3.9 ppm, while also those of PIBVE (protons *b* and *f*) appear in the range area I_{IBVE} between 3 – 3.6 ppm. Moreover, IBVE units are also characterized in area I_{CH_3} by a single peak (protons *h*) at 0.9 ppm. The DP_n of the homopolymers was calculated by both methods in the case of the bi-functional initiator:

* $DP_n \text{ PMVE} = m = ((I_{MVE} - 4H) / 4H) / I_H = ((I_{CH_2} - 2H) / 2H) / I_H$, number of the repeating units of MVE

* $DP_n \text{ PCEVE} = n = ((I_{CEVE} - 4H) / 5H) / I_H = ((I_{CH_2} - 2H) / 2H) / I_H$, number of the repeating units of CEVE

* $DP_n \text{ PIBVE} = o = ((I_{IBVE} - 4H) / 3H) / I_H = ((I_{CH_2} - 2H) / 3H) / I_{CH_2} = I_{CH_3} / 6H / I_H$, number of the repeating units of IBVE

with $I_H = i/6H$, I_H : one proton integration (*i*: area of the signal at 1.18 ppm). The DP_n 's calculation from the mono and bi-functional initiators, and replacing the I_H value by $i/6H$ are summarized in table 3.1.

Table 3.1. DP_n of PMVE, PCEVE and PIBVE determined by 1H NMR.

DP_n	DEE/TMSI initiator	TEoP/TMSI initiator
MVE	$m = \frac{6I_{MVE} - 3i}{4i} = \frac{3I_{CH_2}}{i}$	$m = \frac{3I_{MVE} - 2i}{2i} = \frac{3I_{CH_2} - i}{i}$
CEVE	$n = \frac{6I_{CEVE} - 3i}{5i} = \frac{3I_{CH_2}}{i}$	$n = \frac{6I_{CEVE} - 4i}{5i} = \frac{3I_{CH_2} - i}{i}$
IBVE	$o = \frac{2I_{IBVE} - i}{i} = \frac{2I_{CH_2}}{i} = \frac{I_{CH_3}}{i}$	$o = \frac{6I_{IBVE} - 4i}{3i} = \frac{6I_{CH_2} - 2i}{3i} = \frac{I_{CH_3}}{i}$

3.3.2. Copolymers

The copolymer composition profile for the comonomer CEVE (MVE or IBVE) can be defined as the instantaneous molar fractional incorporation of CEVE into the growing polymer chains, $F_{CEVE, inst}$:

$$F_{CEVE, inst} = \frac{X_{CEVE}}{X_{CEVE} + X_{MVE}} \quad \text{and} \quad F_{CEVE, inst} = \frac{X_{CEVE}}{X_{CEVE} + X_{IBVE}}$$

Commonly, the copolymer composition and the M_n were determined by the 1H NMR spectra of the copolymers (figure 3.2). As for the homopolymers, all spectra contain the same signal at 1.1-1.2 ppm (*i*), which corresponds to six protons of the β -methyl as an ether function, derived from the DEE/TMSI or TEoP/TMSI initiator residue. As there is only a slight overlap between the peaks of both polymers, it is possible to calculate the composition of the copolymer based on the following relation:

$$X_{CEVE} = \frac{n}{m+n} \quad \text{and} \quad X_{CEVE} = \frac{n}{o+n}$$

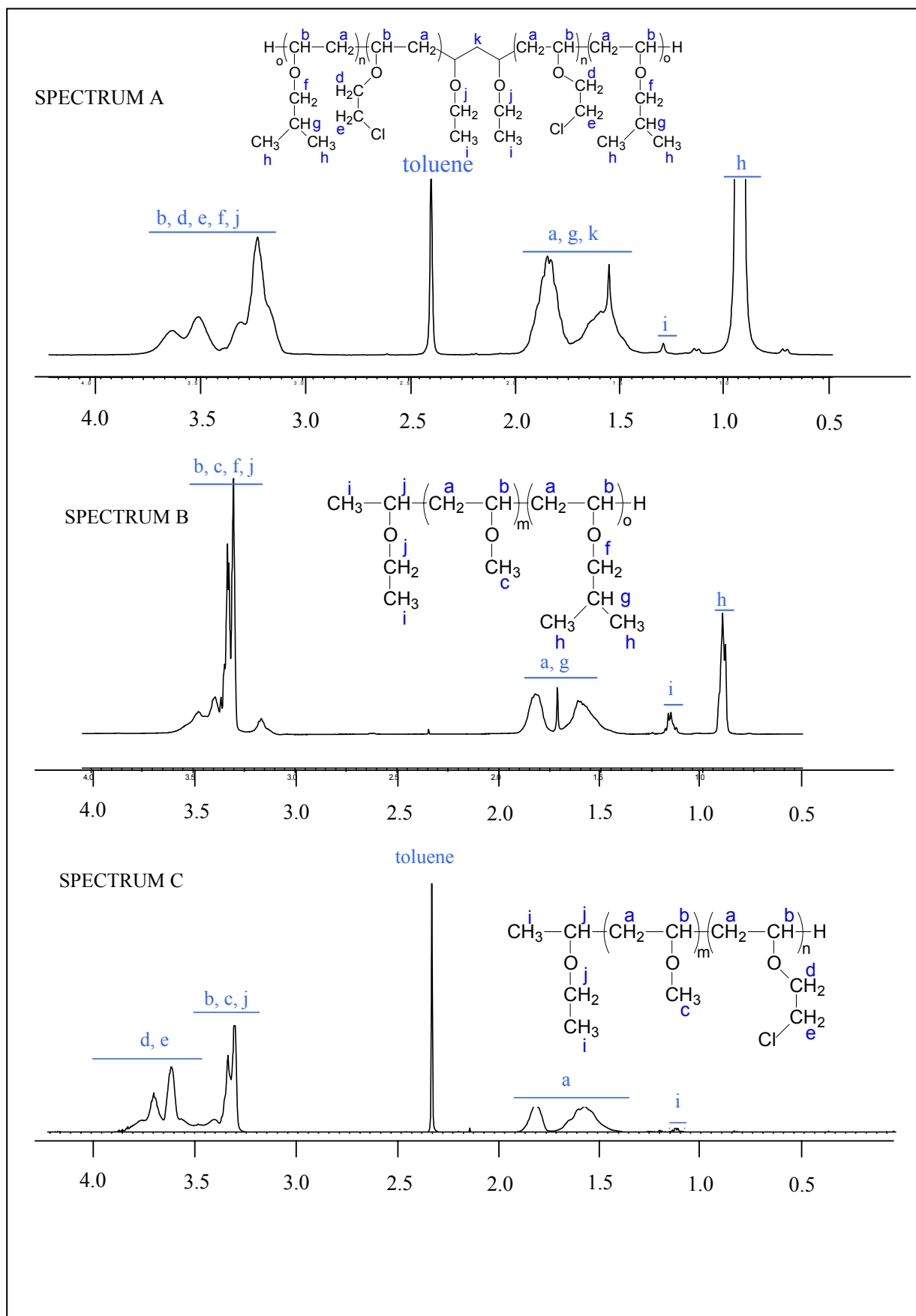


Figure 3.2. ^1H NMR spectra of P(MVE-co-IBVE) with 44/56 ratio (A), P(IBVE-co-CEVE) (B) and P(MVE-co-CEVE) with 50/50 ratio (C) in CDCl_3 .

Moreover, M_n was calculated by $M_n = m \times M_{MVE} + n \times M_{CEVE} + 73 + 1$ with 73 and 1 being the molecular weight of the starting-group of DEE/TMSI and that of the end-group; or by

$M_n = m \times M_{MVE} + n \times M_{CEVE} + 102 + 2$ with 104 and 2 being molecular weight of the starting-group of TEOp/TMSI and that of the end-group.

The details of these calculations are described in **Part IV**. The results are summarized in table 3.2.

Table 3.2. DP_n of the copolymers determined by ¹H NMR.

DP _n	DEE/TMSI initiator	TEOp/TMSI initiator
P(MVE-co-CEVE)	$m = \frac{3I_{CH2} - n}{i}$ $n = \frac{3}{2i}(I_{MVE} + I_{CEVE} - 2I_{CH2} - 8i)$	$m = \frac{3I_{CH2} - n - 1}{i}$ $n = \frac{6}{i}(I_{MVE} + I_{CEVE} - 2I_{CH2})$
P(MVE-co-IBVE)	$o = \frac{I_{CH3}}{i}$ $m = \frac{3}{4i}\left(2I_{MVE} + 2I_{IBVE} - I_{CH3} - \frac{1}{i}\right)$	$o = \frac{I_{CH3}}{i}$ $m = \frac{3}{2i}\left(I_{MVE} + I_{IBVE} - 2I_{CH3} - \frac{2}{3}\right)$
P(IBVE-co-CEVE)	$o = \frac{I_{CH3}}{i}$ $n = \frac{6}{5i}(I_{IBVE} + 2I_{CEVE} - 3I_{CH3} - 3i)$	$o = \frac{I_{CH3}}{i}$ $n = \frac{6}{5i}(I_{IBVE} + I_{CEVE} - I_{CH3} - 4i)$

3.4. Synthesis of copolymers of Isobutyl Vinyl Ether and 2-Chloroethyl Vinyl Ether with Methyl Vinyl Ether, Starting from a Mono-functional Initiator

The procedure developed in this work for preparing functional vinyl ether copolymers involves first forming a DEE-TMSI adduct as the initiator, then adding the VE, MVE or IBVE for example, with CEVE comonomers in conjunction with ZnI₂ for the propagation steps. Some previous studies showed that low temperatures (0°C for PMVE [15-18,39-41], -40°C for PCEVE [42-45] and -5°C for PIBVE [15,17,39]) are best suited for the living cationic homopolymerizations of MVE and CEVE by DEE/TMSI/ZnI₂ initiator system (table 3.3).

Table 3.3. Results of homopolymerizations of PMVE and PCEVE in toluene by DEE/TMSI/ZnI₂.

Polymer	T _{reaction}	DP _n	[A] ₀ /[I] ₀	M _{n th} ^a	M _{n SEC} ^b	M _w /M _n ^b	References
				(g mol ⁻¹)	(g mol ⁻¹)		
PMVE	0°C	64	1/10	3 800	3 600	1.10	[19]
		64	1/5	3 800	3 700	1.20	[55]
		153	1/4	8 900	7 800	1.14	[21]
PCEVE	- 40°C	15	1/10	1 680	1 710	1.08	
		40	1/10	4 350	3 220	1.05	[30]
		100	1/10	10 770	5 100	1.26	
PIBVE	- 5°C	61	1/200	6240	6100	1.05	[19]
	0°C	81	1/200	8260	8160	1.08	[12]

a) $M_{n \text{ theor}} = ([A]_0/[I]_0) \times M_0 + 73 + 1$ (M_0 : the molecular weight of CEVE (106.55 g mol⁻¹), of MVE (55.08 g mol⁻¹) and of IBVE (100.15 g mol⁻¹); 73 the molecular weight of starting group and 1 that of the end group) in g.mol⁻¹. b) Measured by SEC calibrated with polystyrene standards.

3.4.1. Experimental Conditions for Synthesis of P(MVE-co-IBVE)

The composition, M_n and M_w/M_n of copolymers obtained from different monomer feed compositions with a $[M]_0/[I] = 100$ and isolated after 4 h polymerization, are summarized in table 3.4. It was observed that, for polymerizations with high MVE fraction, considerably higher amounts of the activator ZnI₂ were necessary to ensure high conversions, compared to polymerizations with low MVE fraction. This is believed to be due to the higher tendency of ZnI₂ to complexation of MVE and/or PMVE compared to IBVE and/or PIBVE.

Table 3.4. Copolymerization of MVE and IBVE: M_n and M_w/M_n copolymers obtained after 4 h.

IBVE/MVE mole ratio	[I] ₀ /[A] ₀ ^a	Yield ^b %	o/m ^c	DP _n ^d	M _n		M _w /M _n ^f
					¹ H NMR	SEC ^e	
10/90	10	70	11/54	65	4 310	5 050	1.16
20/80	10	72	16/50	66	4 580	5 250	1.12
30/70	10	75	23/45	68	4 990	5 500	1.16
40/60	10	74	31/39	70	5 440	5 900	1.08
50/50	20	80	40/33	73	6 000	6 400	1.08
60/40	40	79	55/24	79	6 970	7 250	1.06
70/30	50	86	65/18	83	7 620	7 950	1.04
80/20	100	91	74/14	88	8 290	8 500	1.06
90/10	100	98	89/7	96	9 390	9 550	1.07

a) $[DEE]_0/[ZnI_2]_0$. b) Yield = end weight / theoretical weight, calculated for complete conversion of both monomers. c) o: PIBVE units, m: PMVE units; values determined by ¹H NMR. d) Total degree of polymerization with $DP_n = o + m$. e) Calibrated by polystyrene standards. f) Determined by SEC.

Values of M_n , obtained from SEC, are systematically somewhat higher than those determined from ¹H NMR analysis, especially for copolymers with high MVE content. This is attributed to the fact that polystyrene was used as standard for SEC calibration. The values

obtained from NMR are in reasonable agreement with the values calculated assuming fast and quantitative initiation followed by a living copolymerization. The polydispersities of the copolymers are lower than 1.16, which is in accordance with a living polymerization mechanism.

3.4.2. Experimental Conditions for Synthesis of P(MVE-co-CEVE)

The experimental conditions for the synthesis of the P(MVE-co-CEVE) copolymers had be optimized in order to obtain a copolymer structure with high degree of randomness and livingness.

* Choice of the Temperature

A first series of copolymerization experiments was performed, varying the temperature from -40°C to 0°C, with constant initial concentration of monomer ($[M]_0 = 1.036$ M). From these results listed in table 3.5, the influence of the temperature on the final composition of the copolymer and the M_n can be observed.

Table 3.5. Synthesis and characteristics of poly(MVE-co-CEVE) with feed ratio of MVE/CEVE = 95/5 (mol-%) and theoretical molecular weight $M_{n\text{ theor}} = 3\ 000\ \text{g}\cdot\text{mol}^{-1}$ for 100% conversion with $[M]_0/[DEE]_0 = 50$ and $[DEE]_0/[ZnI_2]_0 = 50$.

T °C	Overall conv ^a (%)	Time of polymerization (min)	m/n ^b	$M_{n\text{ theor}}$ (g/mol)	$M_{n\text{ NMR}}^c$ (g/mol)	$M_{n\text{ SEC}}^d$ (g/mol)	M_w/M_n^d
-40	13	380	86/14	400	550	900	1.06
-20	76	375	88/12	2 360	1 900	2 850	1.10
-15	89	390	88/12	2 760	2 100	3 000	1.12
0	75	135	94/6	2 330	2 300	3 350	1.16

a) Conversion = final weight/ initial weight. b) m/n = (molar ratio of MVE / molar ratio of CEVE) in copolymer, composition determined by ¹H NMR at the end of the reaction. c) Determined by ¹H NMR at the end of the reaction. d) Determined by GPC calibrated on PS standards.

The products exhibited narrow average molecular weight distributions at all temperatures with the same concentration of activator ($[DEE]_0/[ZnI_2]_0 = 50$), which is in apparent agreement with a clean and well-controlled polymerization process. Attempts to polymerize P(MVE-co-CEVE) with this initiating system at -40°C, such as for the PCEVE homopolymerization, yielded only 13% conversion after a long reaction time (380 min). Increasing the temperature to -15°C improved the polymerization, resulting in polymers with polydispersity lower than 1.2 and in high conversions (89%). Between -20°C and -40°C, CEVE always polymerized faster than MVE. When the polymerization temperature was increased to 0°C, the reaction becomes three times faster while keeping the polydispersity low. The $M_{n\text{ NMR}}$ was found to be close to $M_{n\text{ theor}}$, and the copolymer composition (94/6) was near the monomer feed composition (95/5), indicating a random copolymerization with living characteristics.

* *Effect of the Concentration of the Activator ZnI_2*

A series of kinetic experiments has been carried out with different concentrations of activator. Table 3.6 shows the results of a representative set of experiments.

Table 3.6. M_n and M_w/M_n variations versus $[I]_0/[A]_0$, of poly(MVE-co-CEVE) with $m/n = 60/40$, in toluene at 0°C , $M_n \text{ theor} = 3\,950 \text{ g}\cdot\text{mol}^{-1}$, $[M]_0 = 1.036\text{M}$.

$[DEE]_0/[ZnI_2]_0$ ^a	After 1 min			After 2 h 15 min		
	Conv ^b (%)	$M_n \text{ NMR}$ ^b ($\text{g}\cdot\text{mol}^{-1}$)	M_w/M_n ^c	Conv ^b (%)	$M_n \text{ NMR}$ ^b ($\text{g}\cdot\text{mol}^{-1}$)	M_w/M_n ^c
10	56	2 000	1.33	65	2 550	1.41
20	28	1 100	1.18	56	2 200	1.27
50	18	700	1.03	75	2 960	1.14

a) $[DEE]_0/[ZnI_2]_0$. b) Determined by ^1H NMR. c) Determined by SEC calibrated with polystyrene standards.

Polymerization rates, M_n and M_w/M_n appeared to be directly related to the concentration of the activator $[ZnI_2]_0$ and was governed by the $[DEE]_0/[ZnI_2]_0$ ratio. In general, the reaction decreases for lower concentrations of activator, leading to a better control of the polymerization. The best conditions have been identified for $[DEE]_0/[ZnI_2]_0 = 50$ because at this concentration, the required fast and quantitative initiation results in lowest M_w/M_n (1.14) for a conversion of 75%. As M_w/M_n is smaller for the lower activator concentration, it can be deduced that progressive deactivation controls the M_w/M_n . Nevertheless, experiments were undertaken to confirm the rapid initiation process.

* *Kinetics*

Figure 3.3 shows the plot of $\ln([M]_0/[M])$ versus time for the copolymerization of MVE and CEVE for a composition $m/n = 90/10$ with the ratio $[DEE]_0/[ZnI_2]_0$ equal to 50.

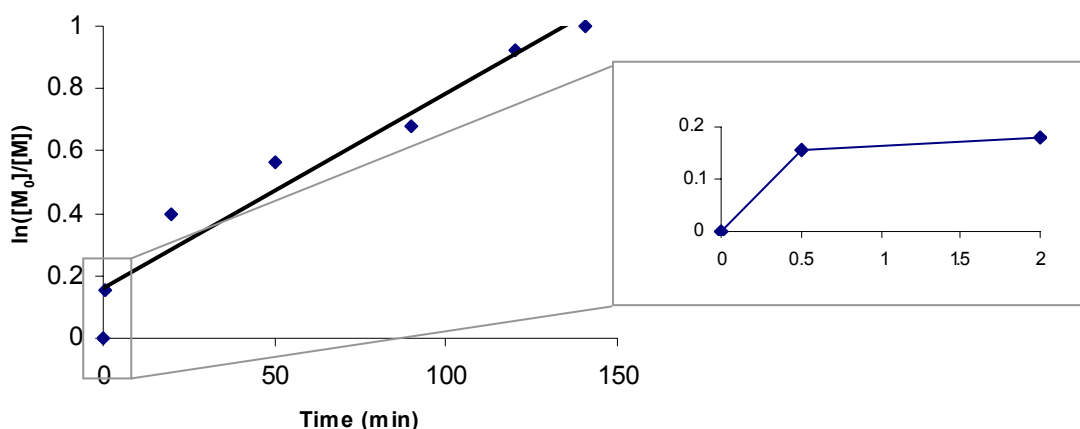
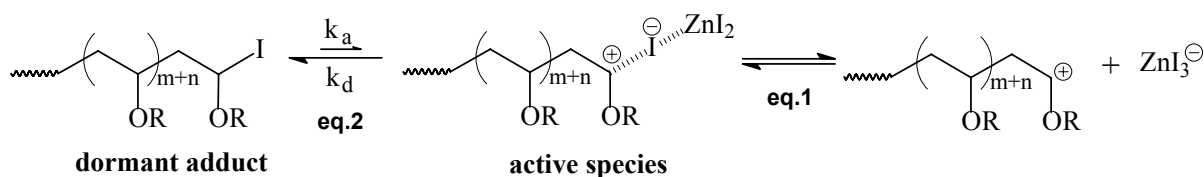


Figure 3.3. Semilogarithmic kinetic plot of poly(MVE-co-CEVE) with $m/n = 90/10$, $[DEE]_0/[ZnI_2]_0 = 50$, in toluene at 0°C with $[M]_0 = 1.036\text{M}$.

This experiment indicates that the polymerization proceeds to 86% conversion within 140 min. These data compare well with the results presented by Ohmura *et al.* [46], and by Armes *et al.* [19] for the homopolymerization of MVE. In the first stage, the speed of the initiation was very fast and high conversions (37% corresponding to $\ln[M]_0/[M] = 0.16$) were reached in less than 30 seconds. This demonstrates that the equilibrium between the activated/deactivated species (see **eq. 2** in scheme 3.3) is not yet obtained and that the rate of initiation is much higher than the propagation rate in the presence of a small quantity of ZnI_2 . This acceleration suggests that the added halogen interacts with the iodine atom at the propagating end formed by DEE/TMSI and thereby weakens its interaction with the terminal carbon (**eq. 1** in scheme 3.3). In the second stage, the polymerization slows down and the conversion increases linearly with time.



Scheme 3.3. Equilibrium between dormant adduct and active species ($\text{R} = \text{CH}_3$ or $\text{CH}_2\text{CH}_2\text{Cl}$).

The M_n versus conversion curve shown in figure 3.4 presents two set of M_n data for the copolymers, respectively determined from SEC and from ^1H NMR spectroscopy. The conversion in this plot represents the total consumed amount of both monomers.

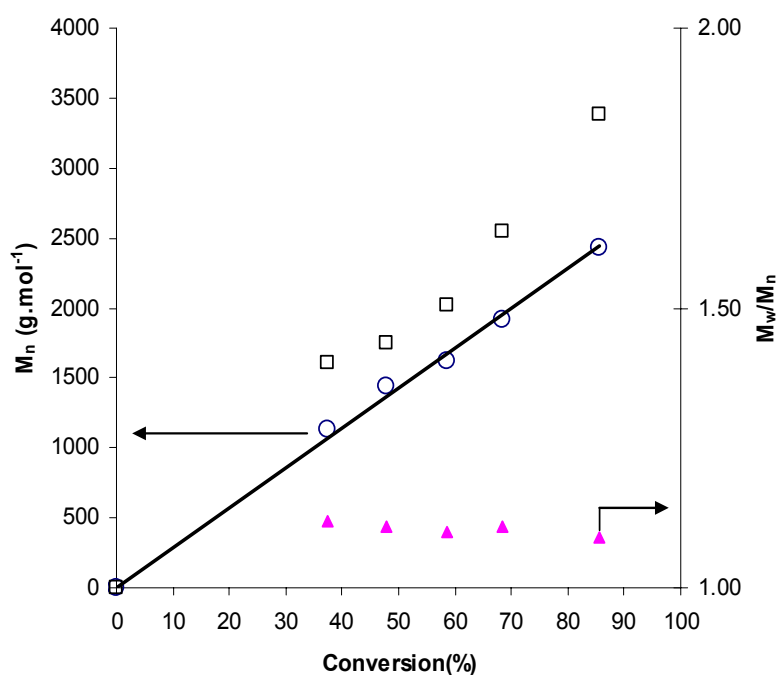


Figure 3.4. Variation of M_n NMR (\circ), M_n SEC (\square) and M_w/M_n (\blacktriangle) with conversion for the copolymerization of MVE and CEVE with $M_n^{\text{theor}} = 2\,500\text{ g.mol}^{-1}$, in toluene at 0°C , $[\text{DEE}]_0/[\text{ZnI}_2]_0 = 50$, $[\text{M}]_0 = 1.036\text{ M}$. The solid straight line indicates the calculated M_n for living polymers from the monomer/initiator ratio.

The M_n of the copolymer increases in direct proportion to monomer conversion. The polydispersities are narrow and decrease from 1.12 to 1.09 with increasing conversion, indicating

the livingness of the copolymerization. The M_n values determined from the starting-group analysis by ^1H NMR spectroscopy are close to the expected M_n . The discrepancy between the M_n 's derived from size exclusion chromatography (SEC) and the expected values are ascribed to hydrodynamic differences between P(MVE-co-CEVE) and polystyrene standards for SEC calibration.

In principle, this result could also be explained by partial dimerization of these copolymer chains during the termination step. This has been observed earlier by Loontjens *et al.* [47] for poly(ethyl vinyl ether) (PEVE) chains during the termination reaction, and also for PMVE chains by Armes *et al.* [19]. They showed that, when the concentration of the terminating reagents was dramatically reduced, a bimodal molecular weight distribution was observed by SEC. However, the SEC traces for the P(MVE-co-CEVE) copolymers are unimodal and narrow, which suggests that dimerization did not occur in a detectable amount.

The molecular characteristics of the poly(MVE-co-CEVE) copolymers with different degree of polymerization (DP_n) have been collected in table 3.7.

Table 3.7. Copolymerization of poly(MVE-co-CEVE) at 0°C, at different M_n with $[M]_0/[I]_0 = 50$.

MVE/CEVE Ratio(mol/mol)	$DP_{n\text{ theor}}^a$	Time of polymerization (min)	Overall conv (%)	$DP_{n\text{ exp}}^b$	$DP_{n\text{ NMR}}^c$	M_w/M_n^d
10/90	50	120	55	28	33	1.08
90/10	50	120	75	37	36	1.10
90/10	100	390	86	86	39	1.20
90/10	150	480	90	136	40	1.28

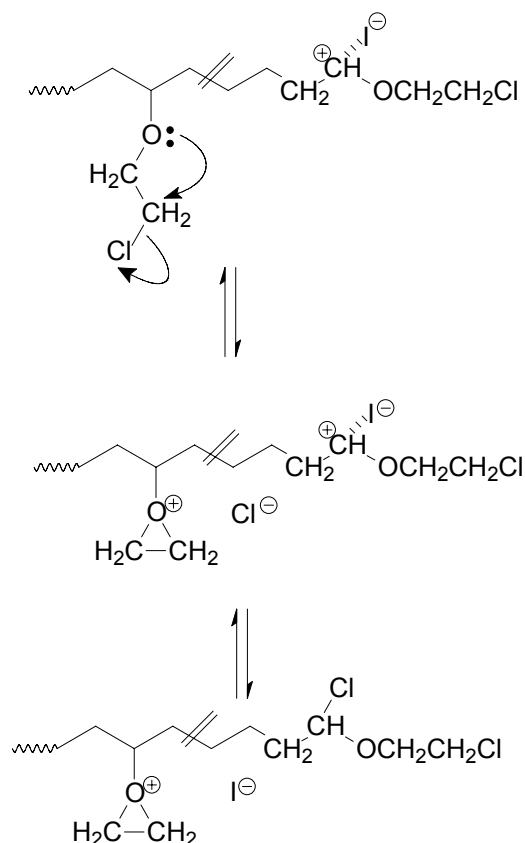
a) Calculated by $DP_{n\text{ theor}} = ([MVE]_0 \times M_{MVE} + [CEVE]_0 \times M_{CEVE}) / [DEE]_0$. b) Determined by gravimetry. c) Determined by ^1H NMR. d) Polydispersity determined by SEC calibrated with polystyrene standards

$DP_{n\text{ NMR}}$ of the copolymers remained in good agreement with $DP_{n\text{ exp}}$ until $DP_{n\text{ theor}} = 50$. After two hours, the conversion with the copolymers synthesized with a high content of CEVE (90%, entry 1) is smaller than the one with 90% of MVE (entry 2). This already indicates that MVE is more reactive than CEVE according to **Chapter 1**.

For higher values of $DP_{n\text{ theor}}$, the $DP_{n\text{ NMR}}$ differs significantly from $DP_{n\text{ exp}}$ values, while polydispersity and reaction time increase. Thus, the polymerization becomes less controllable and higher molecular weight copolymers can not be obtained. In fact, the same behaviour was observed for the homopolymerization of CEVE [42] and is ascribed to the occurrence of transfer reactions [41,48].

The reason for such transfer reactions is the acidity of the β -H atoms next to the carbocationic centre [37-38] (see **Chapter 1**). Because of their electron deficiency, the protons can readily be abstracted by monomers, counteranions or other basic components, which is clearly observed for higher molecular weight polymers. Moreover, Sherrington [49] has also observed that the polymer yield of PCEVE is always low and another termination reaction must be present. This most likely

involves the readily ionisable chlorine atom in the alkoxy substituent. In the polymer the electron pairs of the oxygen are no longer conjugated as in the unsaturated monomer, and are therefore much more basic. As a result, these may participate in a neighbouring group type reaction to produce a chloride ion (scheme 3.4). The latter is highly nucleophilic and will readily terminate electrophilic active centres. The oxonium ion so formed is likely to be inactive in the kinetic lifetimes of these vinyl polymerizations. Clearly, this termination process must compete with transfer mechanisms as the main chain limiting reaction. The same phenomenon was observed for the polymerization of CEVE with cycloheptatrienyl hexachloroantimonate [49], hydronium ion [50] and dichlorocarbene [51] as catalysts.



Scheme 3.4. Side reaction of PCEVE by ionisable chlorine atom.

From these data, it is concluded that P(MVE-co-CEVE) with predictable M_n and narrow M_w/M_n can be prepared up to a DP_n equal to 50.

After determining the experimental conditions, a series of copolymerizations has been carried out, using various MVE/CEVE molar ratios from 90 to 10, and a constant monomer/initiator molar ratio equal to 50.

Table 3.8 compares the experimental M_n _{NMR} and the theoretical M_n _{theor} values corresponding to the actual monomer conversion. The experimental data summarized in table 3.8 clearly indicate a well-controlled copolymerization process with narrow M_w/M_n (1.03-1.16) and a good agreement between the M_n _{theor} and the M_n _{NMR}.

Table 3.8. Monomer composition in the feed and in the copolymers of MVE and CEVE, $[DEE]_0/[ZnI_2]_0 = 50$, $[M]_0/[DEE]_0 = 50$ and $[M]_0 = 1.036$ M.

Feed ratio MVE/CEVE (mol/mol)	Copolymer Ratio MVE/CEVE (mol/mol) ^a	Overall conversion (%)	M_n (g.mol ⁻¹) after 2 hours			
			Theor ^b	¹ H NMR	SEC ^c	M_w/M_n ^c
10/90	7/93	68	3 500	3 300	4 000	1.10
20/80	12/88	66	3 240	3 250	3 900	1.12
30/70	21/79	64	2 990	3 200	3 850	1.13
40/60	38/62	65	2 880	2 640	3 750	1.14
50/50	47/53	63	2 630	2 650	3 750	1.11
60/40	54/46	64	2 520	2 300	3 600	1.18
70/30	62/38	60	2 220	2 300	3 400	1.16
80/20	74/26	58	2 000	2 200	3 100	1.03
90/10	91/9	57	1 830	2 000	2 700	1.08

a) fraction unit number of PMVE and PCEVE in copolymers, values determined by ¹H NMR at the end of the reaction. b) $M_{n, theor} = (([MVE]_0 \times M_{MVE} + [CEVE]_0 \times M_{CEVE}) / [DEE]_0) + S + E$ (with $S = 73$ gmol⁻¹ the initiator fragment, and $E = 1$ gmol⁻¹ the hydrogen end-group). c) Calibrated with polystyrene standards in chloroform.

3.4.3. Livingness

The livingness of the copolymers was determined by SEC analysis. The SEC traces of the copolymer samples are shown in figure 3.5.

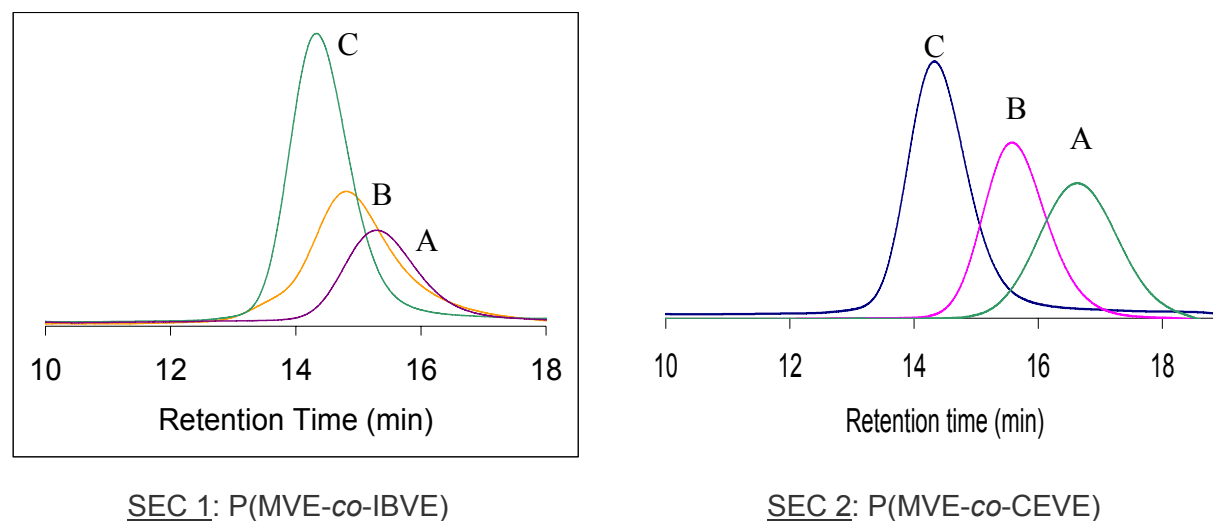


Figure 3.5. SEC analyses in CHCl₃, SEC 1 of P(MVE-co-IBVE) with MVE/IBVE = 56/44, after 15 min (A), after 1 h (B), and after 4 h (C); and SEC 2 of P(MVE-co-CEVE) with 70/30, after 15 seconds (19 % conversion, $M_n = 700$ g.mol⁻¹, $M_w/M_n = 1.09$) (A), after 18 minutes (41 % conversion, $M_n = 1\ 500$ g.mol⁻¹, $M_w/M_n = 1.12$) (B), and after 2 h 44 (84 % conversion, $M_n = 3\ 100$ g.mol⁻¹, $M_w/M_n = 1.16$) (C).

In order to confirm the livingness of this copolymerization, a series of copolymerizations has been carried out, using various MVE/CEVE molar ratios from 90 to 10, and a constant monomer/initiator molar ratio equal to 50. The experimental data summarized in table 3.8 clearly

indicate a well-controlled copolymerization process with narrow M_w/M_n (1.03 – 1.16) (figure 3.5), no ‘tailing’ to low molecular weight and the absence of any homo-PMVE, homo-PIBVE or homo-PCEVE in the final products.

As further evidence of living copolymerization of the mixture of MVE or IBVE with CEVE, a first batch of a mixture of MVE with CEVE (0.086 mol) is polymerized, and 2h50' later, a second amount of this mixture of monomers (0.050 mol) was added. As a result, SEC traces, presented in figure 3.6, clearly show that, upon addition of the second batch of comonomers, the SEC peak shifts toward higher molecular weight.

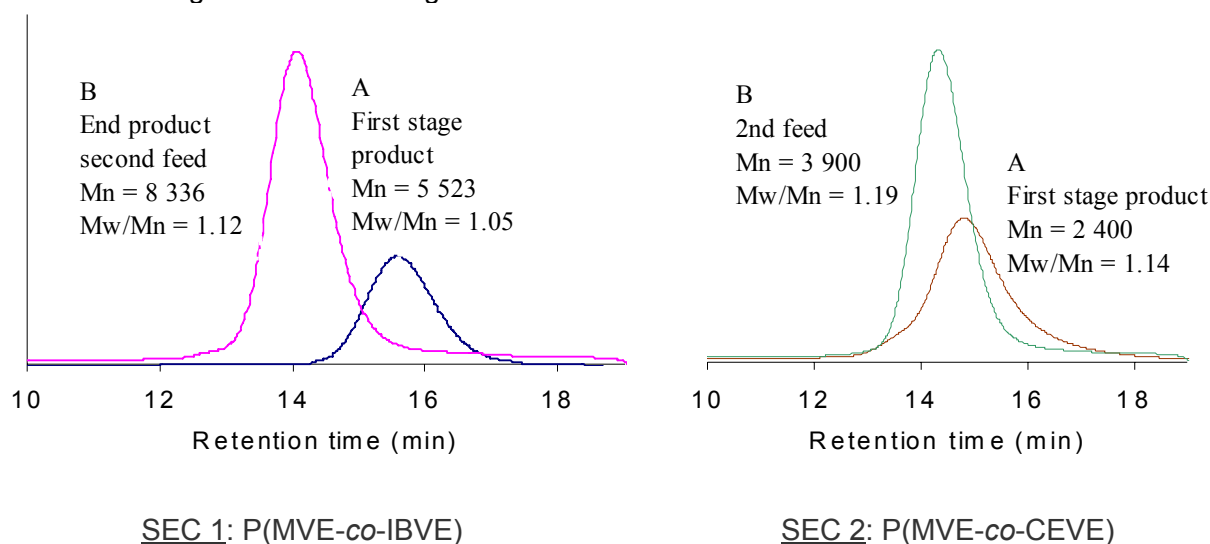


Figure 3.6. SEC results of two-stage copolymerization with: SEC 1, an MVE/IBVE (70/30 mol ratio) second monomer addition 3h30' after initiation of the first polymerization; and SEC 2, an MVE/CEVE (60/40 mol ratio) second monomer feed addition after 2h50' after initiation of the first polymerization.

Moreover, the straight line in figure 3.7 shows that the DP_n increases linearly with conversion, which is in agreement with the living character of the polymerization.

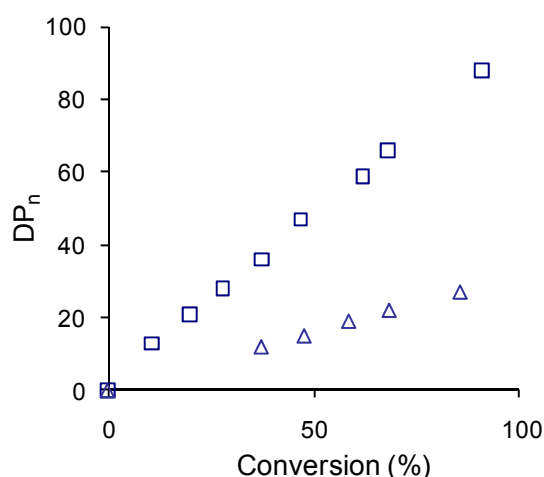


Figure 3.7. DP_n of P(MVE-co-IBVE) (□) and of P(MVE-co-CEVE) (△) as a function of conversion.

These criteria are also observed for the copolymerization of IBVE and CEVE. All these results evidence that the copolymerizations of MVE with IBVE and CEVE can be considered to be living.

3.5. Synthesis of Copolymers of Methyl Vinyl Ether and Isobutyl Vinyl Ether with 2-Chloroethyl Vinyl Ether, Starting from a Bi-functional Initiator

Observing the low molecular weights by using the above mentioned initiating system, the next step of the research was to synthesize copolymers with higher M_n in order to increase the space between the chlorine groups and to permit the easier grafting of side chains on the backbone in a later stage (**Chapter 5** and **8**). For this, the same strategy was followed with a bi-functional acetal initiator system (TEoP/TMSI/ZnI₂) in the presence of a proton trap, THA (see **Chapter 1**). In the last decade, progress has been accomplished by Deffieux *et al.* [24] in the controlled cationic polymerization of CEVE with high M_n until 20 000 g/mol by adding THA.

3.5.1. The Homopolymerizations

First, all homopolymerizations were compared in order to obtain the best reaction conditions for the random copolymerisations. In analogy with the polymerization of PCEVE by Deffieux [24], PMVE and PIBVE homopolymerizations were synthesized with a bi-functional initiator system TEOp/TMSI/ZnI₂. As it can be seen in table 3.9, the homopolymers have experimental molar masses in agreement with the theoretical values and narrow M_w/M_n (> 1.2). Because of the presence of THA, this study resulted in a relatively high DP_n . In the case of CEVE homopolymerization, high conversion was only obtained at 0°C, which means that at the same reaction temperature, IBVE is more reactive than CEVE.

Table 3.9. Results of the homopolymerizations after 3 hours with $DP_{n\ theor} = 300$ and $[ZnI_2]_0/[TEoP]_0=1/33$.

Polymer	T ^a °C	$M_{n\ theor}$ ^b g/mol	$M_{n\ SEC}$ ^c g/mol	M_n ^{1H NMR} g/mol	Yield ^d %	$DP_{n\ exp}$ ^e	M_w/M_n ^c
PCEVE	-30	32 080	7 480	8 730	23	81	1.14
PCEVE	0	32 080	22 490	29 510	100	276	1.15
PIBVE	-30	30 150	37 500	33 604	100	335	1.19
PMVE	0	17 000	15 650	16 076	75	275	1.13

a) temperature of the reaction. b) $M_{n\ theor} = 102+2+M_{monomer}*[monomer]/[I]_0$ (102: starting-group of polymer, 2: end-group of polymer, $M_{monomer}$: molecular weight of monomer (100 for IBVE and 106.55 for CEVE, $[I]_0 = [TMOp]_0$). c) determined with polystyrene standards in chloroform. d) yield = weight product/theoretical weight. e) $DP_{n\ exp}$ is determined by ¹H NMR.

After optimization of the reaction conditions for the homopolymerisations, this brings us to the syntheses of the statistical copolymers of CEVE with MVE or IBVE.

3.5.2. The Copolymerizations

* Copolymerization of P(IBVE-co-CEVE)

Copolymers with different ratios were synthesized as shown in table 3.10.

Table 3.10. Results of the copolymerizations with $DP_{n\text{ theor}} = 300$.

CEVE/IBVE		T ^c	[A] ₀ /[I] ^d	M _{n theor} ^e	M _{n SEC} ^f	Time ^g	Yield ^h	DP _{n exp} ⁱ	M _w /M _n ^f
n ₀ /o ₀ ^a	n/o ^b	°C		g/mol	g/mol	h	%		
92/8	82.9/17.1	-30	1/20	30 300	5 570	4	17	55	1.19
92/8	83.4/16.6	-15	1/33	30 300	14 230	3	46	141	1.16
13/87	3.7/96.3	-30	1/33	30 400	35 640	4	77	366	1.34
13/87	4.4/95.6	-30	1/33	30 400	28 770	3	59	288	1.20
25/75	12/88	-30	1/33	30 630	23 750	3	42	238	1.21

a) monomer feed with n_0/o_0 the initial ratio of CEVE/IBVE (mol/mol). b) o: PIBVE unit number, n: PCEVE unit number; values determined by ¹H NMR. c) temperature of the reaction. d) $[A]_0 = [ZnI_2]_0$, $[I]_0 = [TMOp]_0$. e) $M_{n\text{ theor}} = 102+2+100*[IBVE]/[I]_0*C_1+106.55*[CEVE]/[I]_0*C_2$ (102: starting-group of polymer, 2: end-group of polymer, 100: molecular weight of IBVE, 106.55: molecular weight of CEVE, C_1 and C_2 are defined as the IBVE and CEVE fractions, respectively, in the copolymer). f) determined with polystyrene standards in chloroform. g) time at the end of reaction. h) yield = weight product/weight theoretic. i) $DP_{n\text{ exp}}$ is determined by SEC. $DP_{n\text{ exp}} = m + n \approx M_{n\text{ SEC}}/100$.

Even if the reaction temperature for the synthesis of PCEVE is 0°C, the copolymerizations were synthesized at -30°C because of the higher reactivity of IBVE. For high IBVE concentrations (87%), it is concluded that P(IBVE-co-CEVE) with predictable M_n and narrow M_w/M_n can be prepared up to a DP_n equal to 300. After 3 hours, the polydispersity of the copolymers with a large content of IBVE units was increased with the time of reaction. It was explained by the side reaction between THA and ZnI_2 , which occurs above a DP_n of about 300 (see the double peak on the figure 3.8). The same phenomena have been observed for the PCEVE homopolymer by Deffieux *et al.* [24]. That is why the time of reaction was fixed at 3 hours (see the single peak on the figure 3.8). According to the SEC profile, this reaction limits the clean synthesis of high molar mass bifunctional P(IBVE-co-CEVE). When the CEVE content increased, the DP_n decreased slowly in direct proportion to the CEVE ratio until 55 for 92 CEVE mol-%. In order to increase the reactivity of CEVE, one experiment was made at -15°C (the average temperature reaction), but only 50% of monomers was polymerized.

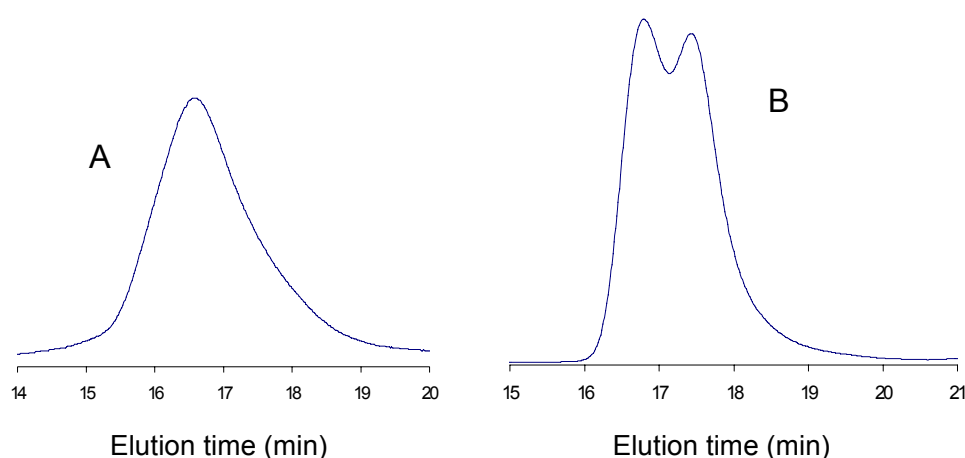


Figure 3.8. SEC chromatograms of P(IBVE-co-CEVE) (13/87) prepared with THA, after 3 h, $M_n = 28\,770\text{ g mol}^{-1}$ ($DP_n = 286$), $M_w/M_n = 1.2$ (A), and after 4 h, $M_n = 35\,640\text{ g mol}^{-1}$ ($DP_n = 355$), $M_w/M_n = 1.34$ (B).

Because the comonomers cannot be synthesized at the same temperature as a result of a high difference of reactivity, the monomer reactivity ratios were impossible to determine.

* *Copolymerization of P(MVE-co-CEVE)*

The characteristics of a series of P(MVE-co-CEVE) with different molar ratios ranging from 10 to 90, are collected in table 3.11.

Table 3.11. Results of the copolymerizations performed in the presence of THA (0.1 M) in toluene at 0°C, $[ZnI_2]_0/[TMoP]_0 = 1/33$, $[TMSI]_0/[TMoP]_0 = 1.2$ eq., $[M]_0 = 0.83$ M.

MVE/CEVE Mol ratio	$M_{n\ th}$ g/mol	$M_{n\ exp}$		$DP_{n\ exp}$	Yield %	M_w/M_n^c
		$^1H\ NMR^b$	SEC ^c			
93/7	18 550	17 630	29 420	285	35	1.09
78/22	20 730	19 890	28 410	288	34	1.17
55/45	24 070	23 520	31 360	293	35	1.15
36/64	26 840	26 460	33 070	296	31	1.18
11/89	30 470	29 450	34 650	290	33	1.13

a) $DP_n = ([M]_0/[I]_0) \times$ conversion. b) $DP_{n\ PMVE} = m$, $DP_{n\ PCEVE} = n$. c) Determined by SEC with polystyrene standards.

As it can be observed, a satisfactory agreement is observed between the experimental M_n and the theoretical values calculated on the basis of one chain formed per precursor molecules. P(MVE-co-CEVE) of DP_n up to 300 with narrow M_w/M_n were synthesized. Besides, the M_w/M_n 's are narrow in apparent agreement with a well-controlled bi-functional polymerization process. Therefore, in the presence of THA, it is possible to obtain a clean bifunctional polymerization up to relatively high M_n .

* *Livingness*

As shown in tables 3.10 and 3.11 in the majority of cases, the M_w/M_n are lower than 1.2, as expected for a living polymerization. A series of experiments were carried out to determine the livingness of the copolymerization. The same procedure was used as for the synthesis with the mono-functional initiator (see above). In all cases, the M_n increased in direct proportion to monomer conversion with narrow M_w/M_n , even after the second monomer feed addition. The straight line in figure 3.9 shows that the M_n increases linearly with conversion, which is in agreement with the living character of the polymerization.

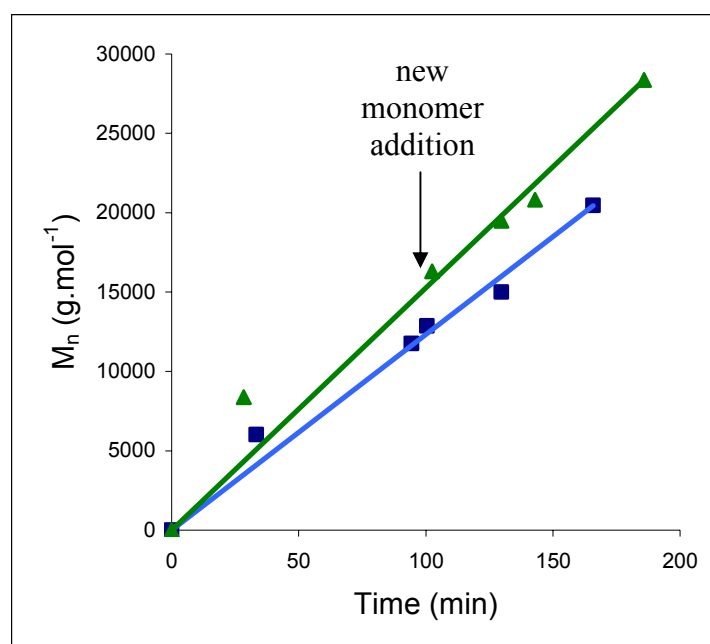


Figure 3.9. Conversion dependence of the M_n for P(IBVE-co-CEVE) (▲) and (PMVE-co-CEVE) (■) with the conversion before and after the second monomer addition.

Knowing that well-defined copolymers could be obtained, it was studied how the MVE and CEVE units were distributed over the copolymer chains.

3.6. Determination of the Monomer Reactivity Ratios

For determining the monomer reactivity ratios, a series of copolymerizations with varying monomer feed compositions, has been carried out and terminated at lowest conversion as possible (between 5 and 40 %). The composition of copolymers, as a function of comonomer feed ratio, was acquired from their ^1H NMR spectra. The results were used to determine the copolymerization reactivity parameters by linear and non-linear methods. To understand the copolymerization behaviour, the monomer reactivity ratios of IBVE, MVE and CEVE were estimated first by graphical methods according to *Fineman-Ross* [25], *Kelen-Tüdös* [26] and *Extended Kelen-Tüdös* [27] methods (see **Chapter 2**). Secondly, monomer reactivity ratios were determined by non-linear least-square methods (*Tidwell and Mortimer model* [28], *terminal model* [29], *penultimate model* [30], *depropagation model* [31] or *complex participation model* [32]) (see **Chapter 2**).

3.6.1. Monomer Reactivity Ratios of P(MVE-co-IBVE)

3.6.1.1. The Linear Methods

In case of P(MVE-co-IBVE), monomer feed compositions were obtained at low conversion (> 8%). For that reason, the two linear methods, the *Fineman-Ross* [25] and the *Kelen-Tüdös* methods [26] were chosen to determine the reactivity ratios r_{MVE} and r_{IBVE} .

* *Fineman-Ross Method*

Figure 3.10 shows the Fineman-Ross plot where the reactivity ratios r_1 and r_2 for the monomer pair M_1 (IBVE) and M_2 (MVE) can be determined by the linear equation : $(F-1)/f = r_1 - r_2 F/f^2$ (see **Chapter 2**). The values obtained by the *Fineman-Ross* method are $r_{IBVE} = 0.98$ and $r_{MVE} = 0.38$.

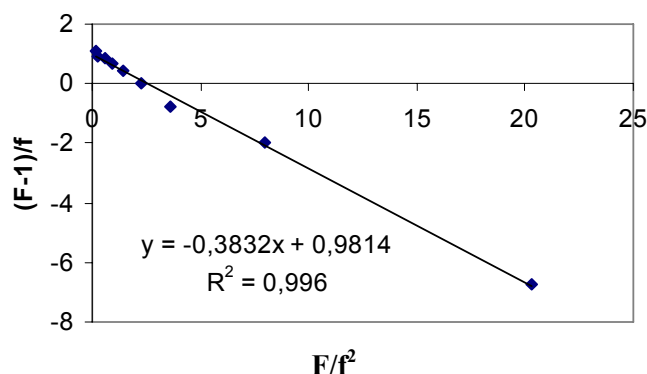


Figure 3.10. Determination of reactivity ratios by the *Fineman-Ross* method: $(F-1)/f = r_1 - r_2 F/f^2$.

* *Kelen-Tüdös Method*

The *Kelen-Tüdös* method (see **Chapter 2**), which is considered to be more reliable, was also applied. A plot of the data according to the *Kelen-Tüdös* method is shown in figure 3.11. The reactivity parameters obtained are $r_{IBVE} = 1.08$ and $r_{MVE} = 0.43$.

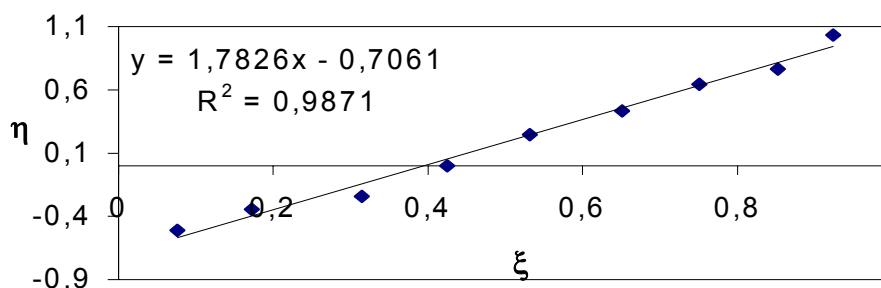


Figure 3.11. Determination of monomer reactivity ratios by the *Kelen-Tüdös* method.

3.6.1.2. The Non-Linear Methods

The monomer reactivity ratios determined by conventional linearization methods are only approximate and are usually employed as good starting values for non-linear parameter estimation schemes. Several non-linear methods have been attempted to determine more reliable values of monomer reactivity ratios [28-32]. Hence the computer program COPOINT [52] is used to determine more reliable values of monomer reactivity ratios (**Appendix I**). Moreover, the *Tidwell and Mortimer* model [28] could also be resolved by an EXCEL Visual Basic program (**Appendix II**). For the *Tidwell and Mortimer* model, the starting values r_{MVE} and r_{CEVE} obtained by *Kelen-Tüdös* method were chosen to run the Visual Basic program. The 95% JCI region for the determined r_{MVE} and r_{CEVE} values using the *Tidwell and Mortimer* model is shown in figure 3.12. The JCI was used as a measure of the accuracy to which the values obtained by the linearization methods compare with respect to the theoretical values predicted from the experimental data.

This plot indicates good agreement between the different calculations used to determine the monomer reactivity ratios.

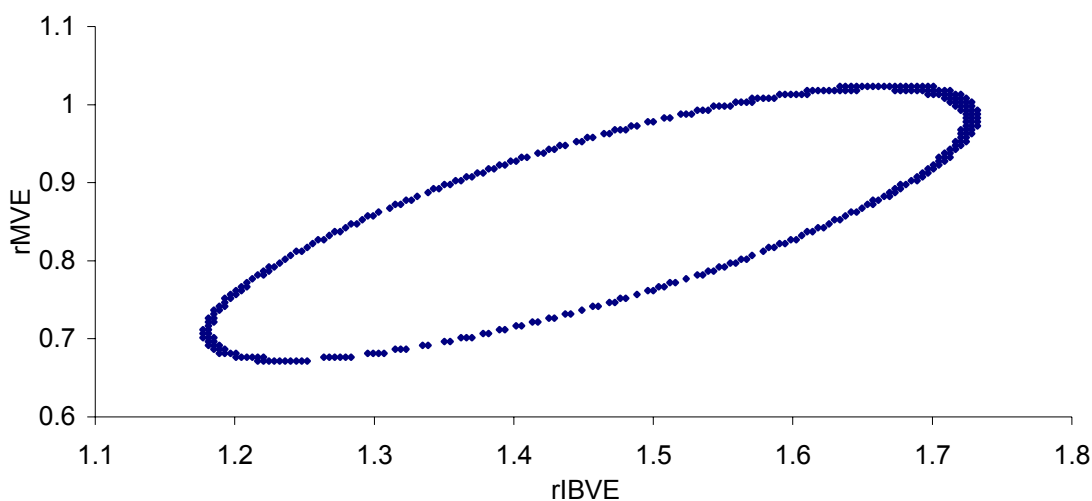


Figure 3.12. 95% JCI region of estimated r_{MVE} and r_{CEVE} values by EXCEL Visual Basic program for P(MVE-co-CEVE).

The results obtained by these programs are listed in table 3.12.

Table 3.12. Results of reactivity ratios obtained by COPOINT and EXCEL programs of non-linear methods with $\Phi(\vec{r})$ being the square difference error sum from experimental and the calculated copolymer compositions.

Method	Error sum $\Phi(\vec{r})$	Copolymerization parameters
<i>Tidwell and Mortimer model</i>	$4.90 * 10^{-3}$	$1.00 < r_1 = 1.42 < 2.00$ $0.40 < r_2 = 0.83 < 1.40$
<i>Terminal model</i>	$(6.32 \pm 2.96) * 10^{-6}$	$0.95 < r_1 = 1.44 < 2.10$ $0.81 < r_2 = 0.82 < 0.84$
<i>Penultimate model</i>	$7.54 * 10^{-6} \pm 2.71 * 10^{-4}$	$1.36 < r_1 = 2.71 < 3.42$ $4.92 < r_1' = 5.02 < 5.13$ $1.17 < r_2 = 1.20 < 1.22$ $3.68 < r_2' = 3.76 < 3.83$

On the basis of the values listed in table 3.12, both reactivity ratios changed with the method used. Depending on the user's choice COPOINT equations (1) to (5) (**Appendix I**), the reactivity ratios are different. The larger the estimated error of a data point, the lower its contribution to $\Phi(\vec{r})$ as well as to the final copolymerization parameters. COPOINT enables us to decide which of the selected models give the best numerical approximation. These reactivity ratios values were compared according to results obtained by COPOINT and EXCEL programs in table 3.12. It is clear that the best model according to the error sum is the *terminal model* which gives similar results as the *Tidwell and Mortimer model*.

3.6.2. Monomer Reactivity Ratios of P(MVE-co-CEVE)

3.6.2.1. Extended Kelen-Tüdös Method

Since the composition information was gathered over a narrow composition range, neither linearization methods for the determination of reactivity ratios could be used at low conversions. The *Extended Kelen-Tüdös* [27] method considers the drift in the comonomer and copolymer compositions with conversion. This method is the most reliable since one may simply use the linear graphic technique to calculate the reactivity ratio values with a small error up to 50% conversion. Because for the living cationic copolymerizations, only data at relatively high conversion (~ 40%), already after 30 seconds, could be obtained due to the high initiation rate, the *Extended Kelen-Tüdös* method has been applied.

Table 3.13 summarizes the monomer compositions in the feed ($[M_1]$, $[M_2]$), and the resulting copolymer ($[dM_1]$, $[dM_2]$) and the corresponding x , y , η and ξ parameters obtained from the following equation (**Chapter 2**): $\eta = (r_{\text{CEVE}} + r_{\text{MVE}}/\alpha)\xi - r_{\text{MVE}}/\alpha$.

Table 3.13. Characterization data for the copolymerization of P(MVE-co-CEVE) by *Extended Kelen-Tüdös* method, at 0°C, $[I]_0/[A]_0 = 50$ and $\alpha = 1.269$.

$[M_1]/[M_2]^a$	$[dM_1]/[dM_2]^b$	$M_{n, \text{NMR}}^c$ (g.mol ⁻¹)	Conversion ^d %	ξ	η
1/9	1/5	700	21	0.940	0.376
7/3	6/10	1 500	46	0.739	0.201
4/6	4/5	850	32	0.598	0.097
5/5	7/6	1 050	39	0.489	-0.068
6/4	8/5	900	40	0.363	-0.202
3/7	7/3	600	26	0.252	-0.337
9/1	7/1	500	21	0.060	-0.477

a) $[M_1]$ and $[M_2]$ are respectively the comonomer concentrations in the feed of MVE and CEVE. b) $[dM_1]$ and $[dM_2]$ are respectively the comonomer concentrations of MVE and CEVE in the copolymer after about 30 seconds, $[dM_1]/[dM_2]$ is determined by ¹H NMR. c) M_n calculated at the beginning of the reaction (between 15 and 30 seconds) by ¹H NMR. d) Conversion of the copolymer at the beginning of the reaction (between 15 and 30 seconds).

The composition of the copolymers is close to that of the reaction mixture when the copolymers are rich in MVE. The reactivity ratios obtained are $r_{\text{CEVE}} = 0.48 \pm 0.04$ and $r_{\text{MVE}} = 0.76 \pm 0.05$.

3.6.2.2. The Non-Linear Methods

The monomer reactivity ratios of P(MVE-co-CEVE) were also calculated using the computer COPOINT program. Only the most reliable results are compiled in table 3.14.

Table 3.14. Results of reactivity ratios obtained by COPOINT program of non-linear methods with $\Phi(\vec{r})$ being the square difference error sum from experimental and the calculated copolymer compositions.

<i>Method</i>	<i>Error sum</i> $\Phi(\vec{r})$	<i>Copolymerization parameters</i>
<i>Terminal model</i>	$(1.14 \pm 2.02) * 10^{-6}$	$0.62 < r_1 = 0.72 < 0.94$ $0.44 < r_2 = 0.45 < 0.53$
<i>Penultimate model</i>	$1.61 * 10^{-5} \pm 1.07 * 10^{-4}$	$0.90 < r_1 = 0.92 < 0.94$ $4.92 < r_1' = 5.02 < 5.13$ $0.31 < r_2 = 0.52 < 0.74$ $3.68 < r_2' = 3.76 < 3.83$
<i>Depropagation model</i>	$1.72 * 10^{-5} \pm 1.11 * 10^{-4}$	$0.80 < r_1 = 0.98 < 1.16$ $0.51 < r_2 = 0.52 < 0.53$ $9.20 < r_3 = 9.39 < 9.58$ $1.69 < r_4 = 1.73 < 1.76$
<i>CASE I</i>		

It seems that the terminal model with $r_1 = 0.72$ and $r_2 = 0.45$ yields the lowest error sum $\Phi(\vec{r})$. Moreover, these values are the closest to the Extended Kelen-Tüdös method, which prove that is a also good model. Also the penultimate and the depropagation CASE I models give values close to the terminal one.

3.6.3. Copolymerization Curves: Evolution of the Composition with the Overall Conversion

* Curve of P(MVE-co-IBVE)

The copolymerization curve, obtained from $r_{MVE} = 0.82$ and $r_{IBVE} = 1.43$, is shown in figure 3.13.

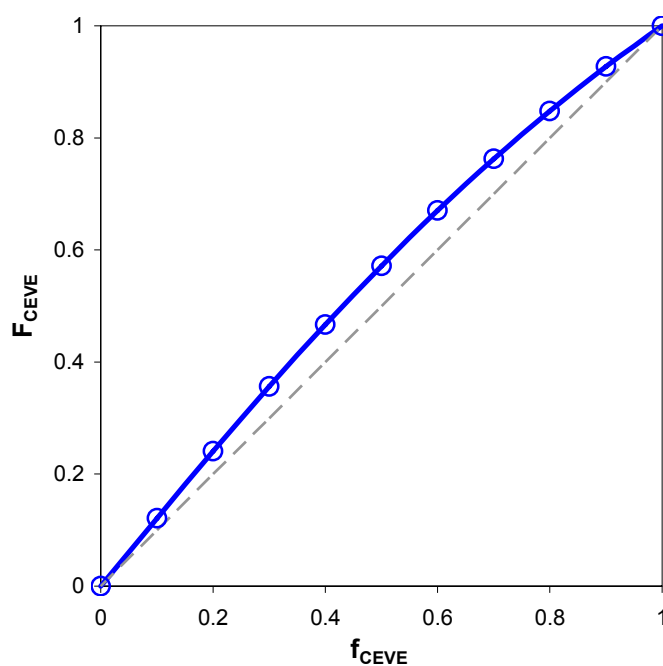


Figure 3.13. Plot of the variation of copolymer composition (F_{IBVE}) with comonomer composition (f_{IBVE}) with $r_{IBVE} = 1.43$ and $r_{MVE} = 0.82$ obtained by the *terminal* model.

Due to the living character of the copolymerization and taking into account the r_{MVE} and r_{IBVE} values, the P(MVE-co-IBVE), obtained after complete conversion, should show a moderate gradient-type structure toward strong tendency to alternate.

* Curve of P(MVE-co-CEVE)

The best reactivity ratios obtained are $r_{CEVE} = 0.45$ and $r_{MVE} = 0.72$ determined by the *terminal* model, which indicates that the sequence distribution of the product is random. The higher value for PMVE originates from the higher relative stability of the propagating species of MVE compared to the one of CEVE that contains an electron withdrawing group. As a result of the changing concentrations of each monomer, $F_{CEVE, inst}$ varies in the course of the reaction, thus the average local fraction of one comonomer varies along the length of the chain. Figure 3.14 shows the composition of the copolymer as a function of the CEVE fraction in the feed.

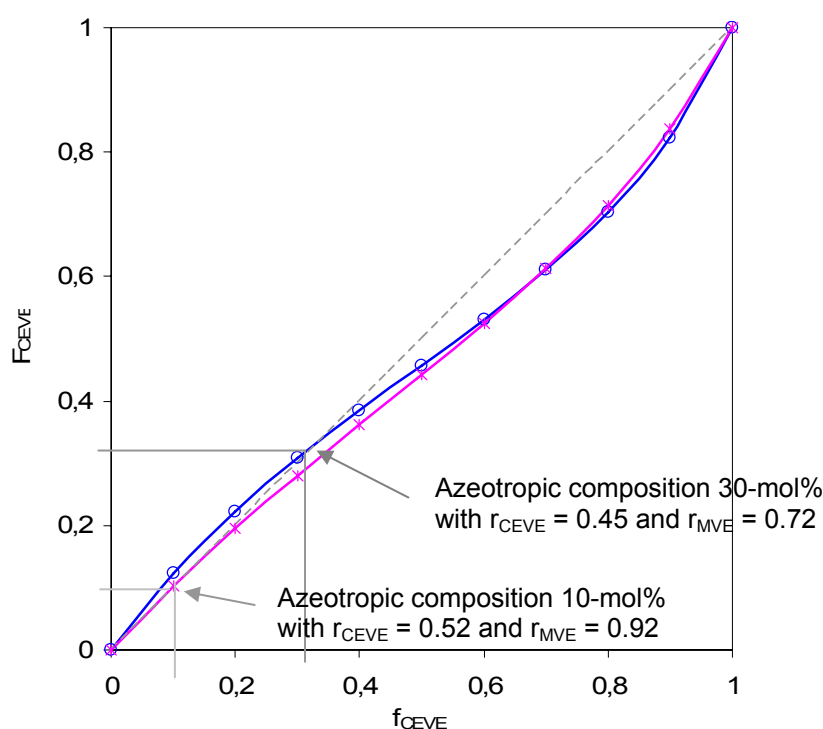


Figure 3.14. The curves plot the variation of the copolymer composition F_{CEVE} with comonomer composition f_{CEVE} . Curve (O) is drawn with $r_{CEVE} = 0.45$ and $r_{MVE} = 0.72$ from the *terminal* model, and the curve (*) with $r_{CEVE} = 0.52$ and $r_{MVE} = 0.92$ from the *penultimate* model.

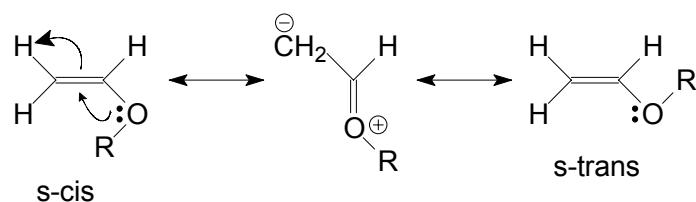
The plot of copolymer composition versus initial monomer composition is sigmoidal and it crosses the ideal line at $F_{CEVE} = f_{CEVE} = 0.3$. The values of the reactivity ratios obtained involve that the copolymerization has an azeotropic concentration at 30 mol-% of CEVE in the reaction mixture with the *Extended Kelen-Tüdös* and *terminal* models, whereas an azeotropic concentration is observed at 10 mol-% of CEVE with the *penultimate* and *depropagation CASE I* models. For both concentrations, polymerization proceeds without change in composition during the reaction, meaning that the average local concentration of the comonomers does not vary along the length of the chain. Moreover, the curve is close to the Bernoullian (or random) case before the azeotropic point and tends to the gradient type for higher CEVE content. The product

$r_1 * r_2 = 0.365$, higher than 0, is closer to zero than to unity. Hence, random copolymers have been formed with a greater tendency for monomeric units to alternate in the copolymer chain. Thus, comonomer units in CEVE/MVE copolymers are incorporated in random fashion and the copolymer sequences have a tendency toward alternation.

* Reactivity of Comonomers

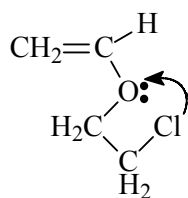
Considering the available information, it appears that reactivity increases in the series: CEVE < MVE < IBVE. The same conclusion was made by Sherrington *et al.* [49] who studied the reactivity of VE monomers at 0°C by adiabatic calorimetric techniques. In case of MVE and CEVE, both exhibit a reactivity one order of magnitude less than the one of IBVE (k_p : rate constant of propagation).

The greatly enhanced reactivities of alkyl VEs arises from resonance delocalization and the contribution of the dipolar canonical structure has the effect of increasing rotational barriers around the R—O—CH= linkage (scheme 3.5).



Scheme 3.5. Resonance delocalization of VEs.

Owen and Sharp [53] established that alkyl VEs exhibit *s-cis/s-trans* conformational equilibria. For MVE the planar *s-cis* form is the dominant form at ambient temperatures even in solutions. Certainly, as confirmed by molecular models, branched alkyl VEs cannot adopt the planar *s-cis* conformation. A major exception is possible in the case of CEVE, which like MVE may adopt such a planar *s-cis* form because of a significant contribution from a favorable *gauche* interaction between the chlorine and oxygen atoms (scheme 3.6). That explains why the reactivity ratios of MVE and CEVE are not so different, and why the one of IBVE is higher.



Scheme 3.6. The planar *s-cis* conformation of CEVE.

3.7. Physical Properties

3.7.1. The Glass Transition Temperature

All copolymers were sticky, viscous materials at room temperature as was expected from the T_g of the homopolymers. The experimental T_g 's of PMVE, PIBVE and PCEVE are respectively $T_{g\text{ PMVE}} = -41^\circ\text{C}$, $T_{g\text{ PIBVE}} = -19^\circ\text{C}$ and $T_{g\text{ CEVE}} = 35^\circ\text{C}$. The T_g of copolymers and homopolymers were determined by differential scanning calorimetry (DSC). Nine samples of copolymers showing different compositions of comonomer 1 and comonomer 2 were analyzed. All the copolymers show a single T_g , which is located at the temperature predicted by the Fox equation [54] for random copolymers. Plots of the T_g 's of the P(MVE-co-CEVE) versus copolymer composition are shown in figure 3.15.

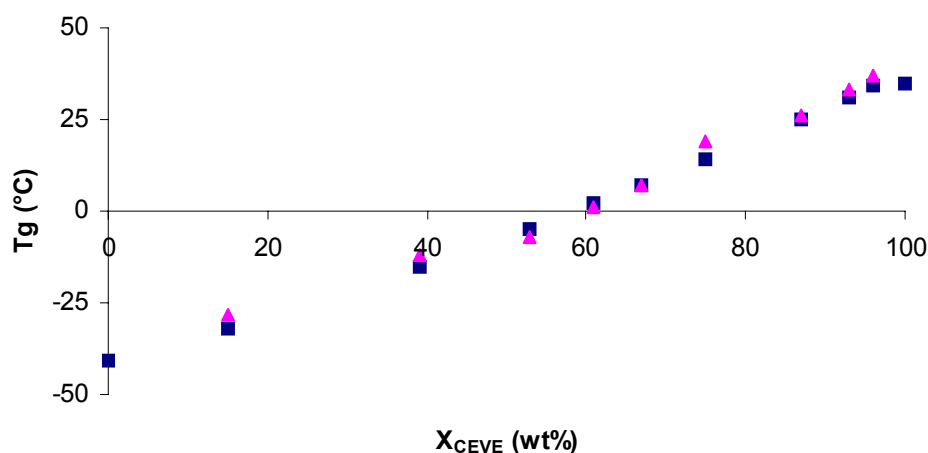


Figure 3.15. Plots of experimental (■) and theoretical T_g (▲) versus copolymer composition (X_{CEVE} = weight fraction of CEVE in the copolymers). The theoretical T_g was determined by the

Fox equation [54]:
$$\frac{1}{T_{g\text{ copolymer}}} = \frac{w_{\text{MVE}}}{T_{g\text{ MVE}}} + \frac{w_{\text{CEVE}}}{T_{g\text{ CEVE}}}$$

3.7.2. Solubility

The compositions of the copolymers are important for their solution properties.

* Solubility of the Homopolymers

The solubility of the homopolymers was tested in different solvents. Table 3.15 shows some solubility properties of the homopolymers. PIBVE and PCEVE are insoluble in polar solvents (water, methanol). PMVE, on the contrary, is soluble in polar solvents (in the range from 0 to 37°C in water). PIBVE, which is more hydrophobic than PCEVE, is soluble in the apolar solvents like cyclohexane or dimethylformamide in contrast to PCEVE.

Table 3.15. Solubilities of the homopolymers (at 20°C) (+: soluble, 0: insoluble, ±: partially soluble)

<i>Solvents</i>	<i>PMVE^a</i>	<i>PIBVE^b</i>	<i>PCEVE^c</i>
Water	+	0	0
Methanol	+	0	0
Ethanol	+	+/-	0
Diethyl ether	+/-	+	0
Acetone	+	+	+
Dimethylformamide	+	+	0
Cyclohexane	0	+	0
Pentane	0	+	0
Dichloromethane	+	+	+
Chloroform	+	+	+
Toluene	+	+	+
Tetrahydrofurane	+	+	+

a) $M_{n,NMR}$ (PMVE) = 3 000 g.mol⁻¹. b) $M_{n,NMR}$ (PIBVE) = 7 000 g.mol⁻¹.

c) $M_{n,NMR}$ (PCEVE) = 4 500 g.mol⁻¹.

Table 3.16. Solubilities of the copolymers (at 20°C) (+: soluble, 0: insoluble, ±: partially soluble)

<i>Solvents</i>	<i>Copolymers I^a</i>	<i>Copolymers II^b</i>	<i>Copolymers III^c</i>	<i>Copolymers IV^d</i>
Water	0	0	0	0
Methanol	+	+	0	0
Ethanol	+	+	0	+/-
Diethyl ether	0	+	+	+
Acetone	+	+	+	+
Dimethylformamide	+	+	0	+
Cyclohexane	0	+	0	+
Pentane	0	+	0	+
Dichloromethane	+	+	+	+
Chloroform	+	+	+	+
Toluene	+	+	+	+
Tetrahydrofurane	+	+	+	+

a) P(MVE-co-CEVE) with molar ratio m/n = 21/79 ($M_{n,NMR}$ = 3 200 g.mol⁻¹) and 91/9 ($M_{n,NMR}$ = 2 000 g.mol⁻¹). b) P(MVE-co-IBVE) with mole ratio m/o = 32/68 ($M_{n,NMR}$ = 4 990 g.mol⁻¹) and 70/30 ($M_{n,NMR}$ = 6 970 g.mol⁻¹). c) P(IBVE-co-CEVE) with molar ratio o/n = 75/25 ($M_{n,NMR}$ = 23 750 g.mol⁻¹). d) P(IBVE-co-CEVE) with molar ratio o/n = 87/13 ($M_{n,NMR}$ = 28 770 g.mol⁻¹).

* Solubility of the Copolymers

The solubility of the copolymers was checked in a variety of solvents. Table 3.16 collects solvents and non-solvents of various copolymers. The copolymers are soluble in all organic solvents but are insoluble in water. Therefore, the increment of CEVE in the copolymer has an influence on

the solubility of P(IBVE-co-CEVE). A copolymer with a high content of IBVE becomes soluble in the apolar solvents. Moreover, it was observed that the P(MVE-co-IBVE) starts to be soluble in water when the IBVE molar fraction is smaller than 10%, and even for P(MVE-co-CEVE) when CEVE molar fraction is smaller than 3%.

3.8. Conclusion

In conclusion, well-defined random copolymers with hydrophilic and hydrophobic units were prepared by living cationic copolymerization using first the DEE/TMSI/ZnI₂ mono-initiating system. This system enabled us to synthesize, in a direct and simple way, well-defined copolymers, which exhibited a narrow molecular mass distribution together with a narrow composition distribution. Secondly, the preparation of the homopolymers of MVE, IBVE and CEVE, and their copolymers (MVE or IBVE with CEVE) with relatively high M_n has been obtained with success via TEOp/TMSI/ZnI₂ as a bi-functional initiating system. In the presence of THA in the polymerization medium, it is possible to synthesize monodisperse P(MVE-co-CEVE) and P(IBVE-co-CEVE) with high M_n (18 000 and 30 000 g.mol⁻¹ respectively), suggesting that the effect of adventitious water largely predominates over other possible side reactions such as transfer reactions. The livingness of the cationic copolymerization has been demonstrated for both initiators.

The monomer reactivity ratios of the monomers were determined from linear and non-linear methods. As expected, the best-fit reactivity ratios were obtained with the non-linear methods, and in both cases with the *terminal* model. The monomer reactivity ratios are $r_{MVE} = 0.82$ and $r_{IBVE} = 1.44$ for P(MVE-co-IBVE), and $r_{MVE} = 0.72$ and $r_{CEVE} = 0.45$ for P(MVE-co-CEVE). In the case of P(IBVE-co-CEVE), the monomer reactivity ratios could not be determined because the reactivity of both monomers is too different. Therefore, the copolymers obtained at high conversion have a moderate gradient-type structure toward strong tendency to alternate for P(MVE-co-IBVE), and a random tendency toward alternation for P(MVE-co-CEVE).

The randomness of the copolymers is also indicated by the correspondence of the Tg's to the one calculated from the Fox equation.

3.9. References

- [1] (a) Mormann W., Ferbitz J., *Macromol. Chem. Phys.*, **2002**, 203, 2616. (b) Thamizharasi S., Gnanasundaram P., Balasubramanian S., *J. Appl. Polym. Sci.*, **2003**, 88, 1817.
- [2] (a) Gatica N., Gargallo L., Radic D., *Polym. Int.*, **1998**, 45, 285. (b) Uyanik N., Erbil C., *Eur. Polym. J.*, **2000**, 36, 2651. (c) Gatica N., Gargallo L., Radic D., *Eur. Polym. J.*, **2002**, 38, 1371. (d) Gatica N., Fernandez N., Opazo E., Alegria S., Gargallo L., Radic D., *Polym. Int.*, **2003**, 52, 1280.

- [3] (a) Eley D.D., Saunders J.S., *J. Chem. Soc.*, **1954**, 1668. (b) Dunphy J.F., Marvel C.S., *J. Polym. Sci.*, **1960**, 46, 542.
- [4] Dunphy J.F., Marvel C.S., *J. Polym. Sci.*, **1960**, 47, 1.
- [5] Shostakovskii M.F., Khomutov A.M., Alimov A.P., *Izv. Akad. Nauk. SSSR, Ser Khim.*, **1954**, 1848.
- [6] Khomutov A.M., Alimov A.P., *Russian Chem. Bull.*, **1967**, 16, 3.
- [7] Fueno T., Okuyama T., Matsumura I., Fukrukawa J., *J. Macro. Sci., Part A: Polym. Chem.*, **2003**, 7, 1447.
- [8] Zhang X., Reyntjens W., Goethals E.G., *Polym. Int.*, **2000**, 49, 277.
- [9] Maeda H., *Macromolecules*, **1995**, 28, 5156.
- [10] (a) Nord F.F., Bier M., Timasheff S.N., *J. Am. Chem. Soc.*, **1951**, 73, 289. (b) Sakurada I., Sakagushi Y., Ito Y., *Kobunshi Kagaku*, **1957**, 14, 41.
- [11] Taylor L.D., Cerankoeski L.D., *J. Polym. Sci.: Polym. Chem. Ed.*, **1975**, 13, 2551.
- [12] Miyazaki H., Kataoka K., *Polymer*, **1996**, 37, 681.
- [13] Okamura H., Morihara Y., Masuda S., Minagawa K., Mori T., Tanaka M., *J. Polym. Sci., Part A: Polym. Chem.*, **2002**, 40, 1945.
- [14] (a) Heymann E., *Trans. Faraday Soc.*, **1935**, 31, 846. (b) Fujishige S., Kubota K., Ando I., *J. Phys. Chem.*, **1989**, 93, 3311.
- [15] Verdonck B., Goethals E.J., Du Prez F.E., *Macromol. Chem. Phys.*, **2003**, 204, 2090.
- [16] (a) Goethals E.J., Reyntjens W., Lievens S., *Macromol. Symp.*, **1998**, 132, 57. (b) Reyntjens W., Jonckheere L., Goethals E., Du Prez F., *Macromol. Symp.*, **2001**, 164, 293.
- [17] Goethals E.J., Reyntjens W., Zhang X., Verdonck B., Loontjens T., *Macromol. Symp.*, **2000**, 157, 93.
- [18] (a) Reyntjens W.G., Jonckheere L.E., Goethals E.J., *Macromol. Rapid. Commun.*, **2002**, 23, 282. (b) Reyntjens W.G., Jonckheere L., Goethals E.J., *J.M.S., Part A: Pure Appl. Chem.*, **2003**, 40, 1. (c) Mpoukouvalas K., Floudas G., Verdonck B., Du Prez F.E., *Phys. Rev.*, **2005**, E72, 011802. (d) Verdonck B., Gohy J.F., Khoussakoun E., Jérôme R., Du Prez F., *Polymer*, **2005**, 46, 9899. (e) Van Durme K., Van Mele B., Bernaerts K.V., Verdonck B., Du Prez F.E., *J. Polym. Sci., Part B: Polym. Phys.*, **2006**, 44, 461. (f) Bernaerts K.V., Fustin C.-A., D'Haese C.B., Gohy J.-F., Martins J.C., Du Prez F.E., *Macromolecules*, **2008**, 41, 2593.
- [19] Forder C., Patrikios C.S., Armes S.P., Billingham N.C., *Macromolecules*, **1996**, 29, 8160.
- [20] (a) Patrikios C.S., Forder C., Armes S.P., Billingham N.C., *J. Polym. Sci., Part A: Polym. Chem.*, **1998**, 36, 2547. (b) Cheol Y., Faust R., *Macromolecules*, **1998**, 31, 2480. (c) Yamauchi K., Hasegawa H., Hashimoto T., Köhler N., Knoll K., *Polymer*, **2002**, 43, 3563. (d) Yun J., Faust R., Szilágyi L.Sz., Kéki S., Zsuga M., *J.M.S., Part A: Pure Appl. Chem.*, **2004**, 41, 613. (e) Schappacher M., Putaux J.L., Lefebvre C., Deffieux A., *J. Am. Chem. Soc.*, **2005**, 127, 2990.
- [21] (a) Patrikios C.S., Forder C., Armes S.P., Billingham N.C., *J. Polym. Sci., Part A: Polym. Chem.*, **1997**, 35, 1181. (b) Bulychev N.A., Arutunov I.A., Zubov V.P., Verdonck B., Goethals E.J., Du Prez F.E., *Macromol. Chem. Phys.*, **2004**, 205, 2457.

- [22] (a) Triveli P., *J. Macromol. Sci. Chem.*, **1980**, A14, 589. (b) Sawamoto M., Ohtoyo O., Higashimura T., Guhrs K.H., Heublein G., *Polym. J.*, **1985**, 17, 929. (c) Tsunogae Y., Majoros I., Kennedy J.P., *J.M.S.-Pure Appl. Chem.*, **1993**, 30, 253. (d) Bevington J.C., Huckerby T.N., Jenkins A.D., *J.M.S.-Pure Appl. Chem.*, **1999**, A36, 1907. (e) Sugihara S., Hashimoto K., Matsumoto Y., Kanaoka S., Aoshima S., *J. Polym. Sci., Part A: Polym. Chem.*, **2003**, 41, 3300. (f) Sugihara S., Kanaoka S., Aoshima S., *Macromolecules*, **2004**, 37, 1711. (g) Zhou Y., Faust R., Richard R., Schwarz W., *Macromolecules*, **2005**, 38, 8183.
- [23] (a) Meirvenne D.V., Haucourt N., Goethals E.J., *Polym. Bull.*, **1990**, 23, 185. (b) Haucourt N.H., Goethals E.J., Schappacher M., Deffieux A., *Makromol. Chem., Rapid. Commun.*, **1992**, 13, 329.
- [24] (a) Bennevault V., Larrue F., Deffieux A., *Macromol. Chem. Phys.*, **1995**, 196, 3075. (b) Bennevault V., Larrue F., Deffieux A., *Macromol. Chem. Phys.*, **1996**, 197, 2603.
- [25] Fineman M., Ross S.D., *J. Polym. Sci.*, **1950**, 5, 259.
- [26] Kelen T., Tüdös F.J., *J. Macromol. Sci. A: Polym. Chem.*, **1975**, 9, 1.
- [27] Tüdös F.J., Kelen T., Földes-Berezsnich T., Turcsányi B.J., *J. Macromol. Sci. Chem.*, **1976**, A10(8), 1513.
- [28] Tidwell P.W., Mortimer G.A., *J. Polym. Sci.*, **1965**, A3, 369.
- [29] (a) Mayo F.R., Lewis F.M., *J. Am. Chem. Soc.*, **1944**, 66, 1594. (b) Mayo F.R., Walling C., *Chem. Rev.*, **1950**, 46, 191. (c) Odian G., "Principles of Polymerization", 4th edition, chap 6-2a, 'Terminal Model; Monomer Reactivity Ratios', pp. 466 – 470, Wiley Interscience, New York, **2003**.
- [30] (a) Merz E., Alfrey jr. T., Goldfinger G., *J. Polym. Sci.*, 1946, 1, 75. (b) Barb W.G., *J. Polym. Sci.*, **1953**, 11, 117. (c) Ham G.E., *J. Polym. Sci., Part A: Polym. Chem.*, **1964**, 2, 2735. (d) Odian G., "Principles of Polymerization", 4th edition, chap 6-5a, 'Kinetic Penultimate Behavior', pp. 513 – 515, Wiley Interscience, New York, **2003**.
- [31] (a) Lowry G.G., *J. Polym. Sci.*, **1960**, 42, 463. (b) Odian G., "Principles of Polymerization", 4th edition, chap 6-5b, 'Depropagation during Copolymerization', pp. 515 – 518, Wiley Interscience, New York, **2003**.
- [32] (a) Seiner J.A., Litt M., *Macromolecules*, **1971**, 4, 308. (b) Odian G., "Principles of Polymerization", 4th edition, chap 6-5c, 'Copolymerization with Complex Participation', pp. 518 – 521, Wiley Interscience, New York, **2003**.
- [33] Haucourt N.H., Goethals E., Schappacher M., Deffieux A., *Makromol. Chem., Rapid Commun.*, **1992**, 13, 329.
- [34] Goethals E., Haucourt N.H., Peng L.B., *Macromol. Symp.*, **1997**, 85, 97.
- [35] Cramail H., Schappacher M., Deffieux A., *Polym. Adv. Tech.*, **1993**, 5, 568.
- [36] (a) Nakamura T., Aoshima S., Higashimura T., *Polym. Bull.*, **1985**, 14, 515. (b) Choi W.O., Sawamoto M., Higashimura T., *Polym. J.*, **1987**, 19, 889.
- [37] Sawamoto M., *Trends Polym. Sci.*, **1993**, 1, 111.
- [38] Matyjaszewski K., Sawamoto M., in 'Cationic Polymerizations mechanisms, Synthesis, and Applications', ed by K. Matyjaszewski, Marcel Dekker, New York, **1996**, p. 265-380.

- [39] Reyntjens W.G.S., Goethals E.J., *Design. Monom. Polym.*, **2001**, 4(2), 195.
- [40] PhD of Reyntjens W.G.S., '*Thermoresponsieve Materialen op Basis van Poly(Vinylethers)*', Ghent University, Belgium, **2001**.
- [41] Bernearts K.V., Du Prez F.E., *Polymer*, **2005**, 46, 8469.
- [42] (a) Minoda M., Sawamoto M., Higashimura T., *Macromolecules*, **1990**, 23, 4889. (b) Liu Q., Konas M., Davis R.M., Riffle J.S., *J. Polym. Sci., Part A: Polym. Chem.*, **1993**, 31, 1709.
- [43] (a) Nuyken O., Rieß G., Loontjens J.A., Van der Linde R., *Macromol. Reports, Part A*, **1995**, 32 (suppl.4), 459. (b) Nuyken O., Ingrish S., *Macromol. Chem. Phys.*, **1998**, 199, 711.
- [44] (a) Bennevault V., Richard G., Deffieux A., *Macromol. Chem. Phys.*, **1997**, 198, 3051. (b) Shappacher M., Deffieux A., *Macromol. Chem. Phys.*, **1997**, 198, 3953. (c) Deffieux A., Schappacher M., *Macromolecules*, **1999**, 32, 1797. (d) Schappacher M., Deffieux A., *Macromolecules*, **2000**, 33, 7371. (e) Muchtar Z., Schappacher M., Deffieux A., *Macromolecules*, **2001**, 34, 7595. (f) Schappacher M., Deffieux A., Putaux J.L., Viville P., Lazzaroni R., *Macromolecules*, **2003**, 36, 5776.
- [45] Van De Velde P., Goethals E.J., Du Prez F., *Polym. Int.*, **2003**, 52, 1589.
- [46] Ohmura T., Sawamoto M., Higashimura T., *Macromolecules*, **1994**, 27, 3714.
- [47] Loontjens T., Derks F., Kleukens E., *Polym. Bull.*, **1992**, 27, 519.
- [48] Lievens S.S., Goethals E.J., *Polym. Int.*, **1996**, 41, 277.
- [49] Ledwith A., Lockett E., Sherrington D.C., *Polymer*, **1975**, 16, 31.
- [50] (a) Jones D.M., Woods N.F., *J. Chem. Soc.*, **1964**, 5400. (b) Ledwith A., Woods H.J., *J. Chem. Soc. (B)*, **1966**, 753.
- [51] Ledwith A., Woods H.J., *J. Chem. Soc. (B)*, **1967**, 973.
- [52] Beginn U., *e-Polymers*, **2005**, no. 073.
- [53] Owen N.L., Sheppard N., *Trans. Faraday Soc.*, **1963**, 634.
- [54] Fox TG., *Bull. Am. Phys. Soc.*, **1956**, 1, 123.

PART II

Design of Novel Thermo-responsive Poly(Methyl Vinyl Ether)-*g*-Poly(Ethylene Oxide) Graft Copolymers via the '*Grafting onto*' Method

Parts of these chapters have been published as articles:

¹Aseyev V., Hietala S., Laukkanen A., Nuopponen M., Confortini O., Du Prez F.E., Tenhu H., *Polymer*, **2005**, *46*, 7118.

²Bulychev N., Confortini O., Kopold P., Arutunov I., Dirnberger K., Schauer T., Du Prez F. E., Zubov V., Eisenbach C. D., *Polymer*, **2007**, *48*, 2636.

³Confortini O., Van Durme K., El Oumarni I., Van Mele B., Du Prez F.E., *Polymer*, submitted, **2009**.

Chapter 4 : Theoretical Aspects of Graft Copolymers	79
4.1. Introduction	79
4.2. Techniques of Grafting.....	80
4.2.1. 'Grafting onto' Methods.....	80
4.2.2. 'Grafting from' Methods.....	81
4.2.3. Graft Copolymers via Macromonomers: 'Grafting through' Methods.....	82
4.3. Factors Influencing the Grafting Procedure.....	83
4.4. Applications.....	85
4.5. References	85
Chapter 5 : Synthesis and Molecular Characterization of Poly(Methyl Vinyl Ether)- <i>g</i> -Poly(Ethylene Oxide) Graft Copolymer	89
5.1. Introduction	89
5.2. Model Reactions.....	91
5.2.1. Analogous Reaction with a Primary Amine	92
5.2.2. Analogous Reaction with Triethylene Glycol (TEG)	93
5.3. Functionalization of PEO with a Terminal Amine	93
5.3.1. Studies of the Functionalization of the Precursor PEO-OH	94
5.3.2. Synthesis of PEO-NH ₂ Side Chains	95
5.4. Synthesis of PMVE- <i>g</i> -PEO via the Grafting onto Method	96
5.4.1. Synthesis	96
5.4.2. Characterization	97
5.4.3. Determination of the Grafting Degree.....	98
5.5. Conclusion	100
5.6. References.....	100
Chapter 6 : Thermo-responsive Properties of PMVE- <i>g</i> -PEO Graft Copolymers	105
6.1. Theory of Stimuli-responsive Micelles	105
6.1.1. Micelles	105
6.1.1.1. Definition.....	105
6.1.1.2. Thermodynamics.....	106
6.1.1.3. Behaviour of the Micelles.....	107
6.1.1.4. Applications of Stimuli-responsive Micelles.....	109
6.1.2. The Theory of the Lower Critical Solution Temperature (LCST).....	110
6.1.2.1. Thermodynamics	111
6.1.2.2. The Phase Diagrams: Type I, II, III.....	112
6.1.2.3. PMVE Phase Diagram.....	113
6.1.2.4. Applications.....	114
6.2. 'Cloud Point' Studies of the Thermo-responsive Random Copolymers.....	115
6.2.1. Introduction	115
6.2.2. Determination of the 'Cloud Point' Temperature of P(MVE- <i>co</i> -IBVE)	116
6.2.3. Influence of the Incorporating CEVE units in PMVE Backbone.....	117
6.2.3.1. UV-VIS Transmission	117
6.2.3.2. Modulated Temperature Differential Scanning Calorimetry (MTDSC).....	119

6.3. Effect of the Temperature on the PMVE-<i>g</i>-PEO	120
6.3.1. Introduction.....	120
6.3.2. UV-VIS Transmission	121
6.3.3. Modulated Temperature Differential Scanning Calorimetry (MTDSC).....	122
6.3.4. High Sensitive-Differential Scanning Calorimetry (HS-DSC)	125
6.3.5. Dynamic Light Scattering (DLS)	128
6.3.5.1. Effect of the Length of PEO.....	128
6.3.5.2. Size Distributions of Hydrodynamic Radius (R_h).....	130
6.3.5.3. Studies on Colloidal Stability.....	131
6.3.6. Surface Tension Measurement	131
6.3.7. Ultrasonic Treatment for Pigment Surface Modification in Pigment Dispersions	132
6.4. Conclusion	133
6.5. References	134

Abstract

Thermo-responsive poly(methyl vinyl ether)-*graft*-poly(ethylene oxide) (PMVE-*g*-PEO) graft copolymers were prepared by a grafting process with a varying content of PEO onto the PMVE backbone. Graft copolymers have been prepared by first generating a statistical poly(methyl vinyl ether-*stat*-2-chloroethyl vinyl ether) P(MVE-*stat*-CEVE) backbone (see **Chapter 5**). In this way, the pendent chlorine groups can be used for the coupling reaction with telechelic PEO, making use of the grafting onto method. In order to investigate the reactivity of the chlorine groups for the grafting process, model reactions were first performed with benzylamine and triethylene glycol (TEG). Finally, PMVE-*g*-PEO copolymers were obtained by substituting the chlorine groups of P(MVE-*stat*-CEVE) with amino-functionalized PEO. The molecular characteristics of the resulting copolymers are discussed, using size exclusion chromatography (SEC), ^1H NMR and elemental analysis (E.A.). The synthesis conditions used gave rise to functionalization degrees varying from 60% to 92%, determined by E.A.

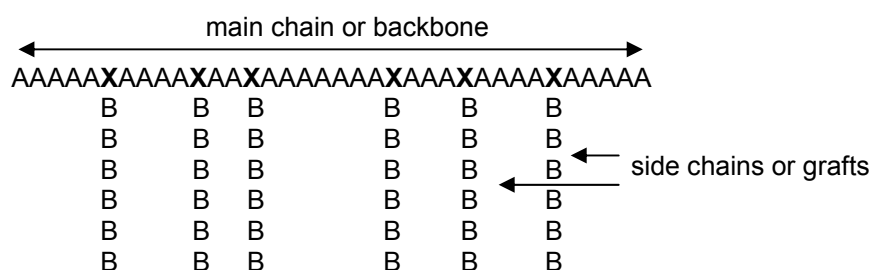
First, the water-solubility of these copolymers was studied by modulated temperature differential scanning calorimetry (MT-DSC) (see **Chapter 6**). The observed LCST phase behaviour is influenced by the copolymerization process: the solubility of the graft copolymer is worse than the PMVE homopolymer. This observation is linked to the immiscibility of the copolymer constituents (PMVE and PEO). Furthermore, in dilute solution, the T_{cp} depends not only on the presence of the chlorine group but also on the grafting degree of PEO. Thus, a combination of DLS and high sensitive microcalorimetry was employed to study PMVE-*g*-PEO in the vicinity of the transition. PMVE-*g*-PEO forms loose aggregates in water at room temperature and undergoes a reversible phase transition upon heating above the T_{cp} between 25 and 39°C, depending on the grafting degree. At temperatures higher than T_{cp} , the polymer main chain collapses and multimolecular aggregates with a hydrophobic PMVE core and a hydrophilic PEO shell are formed. The role of the grafts and the influence of the remaining chlorine groups on the solution properties and colloidal stability have been investigated. The thermal response of the graft copolymers was compared to that of the PMVE homopolymer and P(MVE-*stat*-CEVE).

Chapter 4

Theoretical Aspects of Graft Copolymers

4.1. Introduction

Graft copolymers represent a valuable class of polymeric materials, since a variety of molecular parameter can be varied: i) main and side chain polymer type, ii) DP_n and M_w/M_n of main and side chain, iii) grafting density (average spacing in-between the side chains) and iv) distribution of the grafts (graft uniformity). The branches are usually randomly distributed along the backbone. The simplest case of a graft copolymer can be represented by scheme 4.1 where a sequence of A monomer units is referred to as the main chain or backbone, the sequence B units is the side chain or graft, and X is the unit in the backbone to which the graft is attached.



Scheme 4.1. Structure of graft copolymer.

Graft copolymerization is a common method for modifying polymer properties. Using special polymerization techniques tailor-made graft copolymers can be afforded according to specific needs. These techniques were mainly based on free radical polymerization techniques because of their simplicity. More elaborate techniques were developed later to produce more homogeneous and well characterized graft copolymers. Since the possibilities for producing new monomers at low cost have been diminishing, many scientists and engineers are striving to

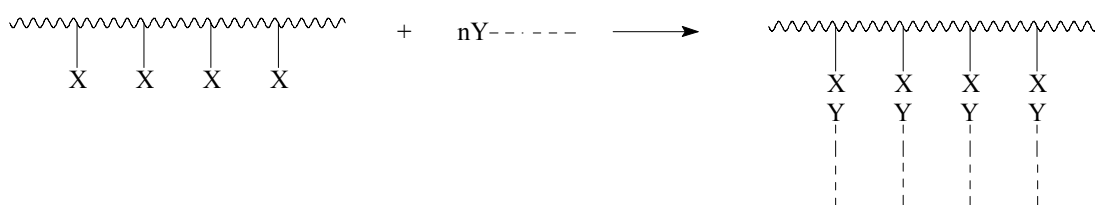
create specialized high performance materials from existing monomers by making copolymers of various compositions and/or architectures [1-2].

4.2. Techniques of Grafting

Graft copolymers are polymers with a linear backbone to which macromolecular side chains are connected. They can be prepared by three different methods: 'grafting onto', 'grafting from' and 'grafting through' copolymerization of macromonomers [1-2].

4.2.1. 'Grafting onto' Methods

'Grafting onto' method is widely used for the preparation of graft copolymers. 'Grafting onto' mechanisms involve the coupling reaction of pre-formed polymers having reactive ends with the backbone bearing functional groups (scheme 4.2).



Scheme 4.2. 'Grafting onto' technique.

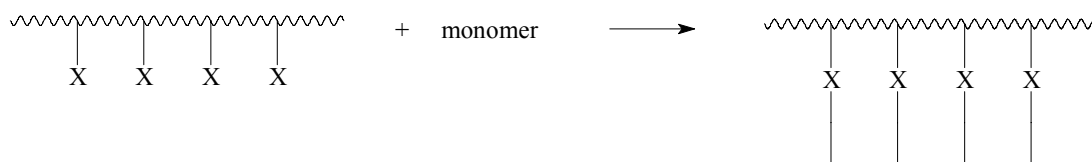
This method provides the advantage that both the backbone and the grafted chains can be characterized separately. If, in addition, the side chains are prepared by anionic polymerization methods, which provide the best control over M_n and M_w/M_n , the resulting graft copolymers have controlled structures and are well defined. The most common case is the reaction of anionic living polymers with backbone electrophilic functionalities such as anhydrides, esters, nitrile, pyridine or benzyl halide groups [3]. A common procedure is the chloromethylation of PS [4] and the subsequent reaction with living polymers. Using this method, Rempp *et al.* prepared polystyrene-*graft*-poly(ethylene oxide) (PS-*g*-PEO) copolymers [5] and Deffieux [6] the polystyrene-*graft*-poly(2-chloroethyl vinyl ether) (PS-*g*-PCEVE).

Several graft copolymers have also been synthesized with PEO side chains [7]. Wesslen and Wesslen prepared amphiphilic comb-shaped copolymers by the polymerization of 2-ethyl-hexyl acrylate with glycidyl methacrylate, followed by transesterification of monomethoxy poly(ethylene glycol) (mPEG) [8]. Derand and Wesslen conjugated mPEG onto the copolymers of styrene and maleic anhydride for preparation of anionic comb-shaped PEG graft copolymers [9]. Twaik *et al.*, Thierry and Skoulios synthesized PEG have grafted copolymers in a similar manner [10]. Jannash *et al.* initiated the grafting polymerization of ethylene oxide on the ionized poly(styrene-*co*-acrylamide) backbone by potassium *t*-butoxide or potassium naphthalene [11].

In the following section (**Chapter 5**), the synthesis of a new graft copolymer, poly(methyl vinyl ether)-*graft*-poly(ethylene oxide) (PMVE-*g*-PEO) will be presented.

4.2.2. 'Grafting from' Methods

The 'grafting from' procedure requires the generation of active sites on the main polymer chain which are capable of initiating the polymerization of a second monomer (scheme 4.3). Based on this definition, the linear precursor polymer can be considered as a multifunctional macromolecular initiator.



Scheme 4.3. 'Grafting from' technique.

Free radicals can be created by several methods such as irradiation of a polymer in the presence of oxygen [12], chain transfer to the backbone [13] or redox reactions [14]. Several commercial products have been produced by these methods because they are simple and rather easy to perform. Several examples of controlled radical grafting have been reported in the literature since few years [15-16]. Polymer chains having labile halogen atoms in combination with various catalysts have been used. Some examples of well-defined graft copolymers utilize the ATRP (see **Chapter 7**) of vinyl monomers from polyethylene (PE). In one example, a commercial copolymer of ethylene with glycidyl methacrylate was used [17]. The epoxy groups were transformed into the α -bromoesters, which initiated ATRP of styrene (St) and (meth)acrylates. In the second example, PE or its copolymer with St was brominated and the generated alkyl bromides initiated the ATRP process, which was catalyzed by CuBr/PMDETA [18]. In a similar way, syndiotactic polystyrene was brominated and grafted with poly(methyl methacrylate) (PMMA), poly(methacrylate) (PMA) and PS [19].

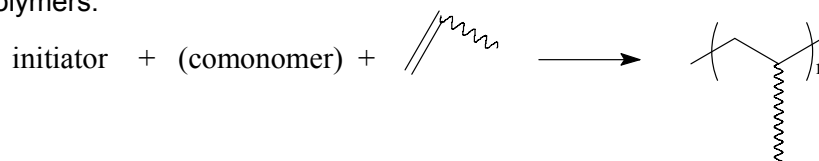
A practical application of amphiphilic graft copolymers has been disclosed in the area of personal care products. Various (meth)acrylates, methacrylic acid (MAA) and *p*-chloromethylstyrene were copolymerized by a conventional free radical copolymerization. *Grafting from* the chloromethylphenyl groups within polysiloxane or PS chains with either MAA, *tert*-butyl acrylate (*t*-BA) or 2-(trimethylsilyloxy)ethyl methacrylate (HEMA-TMS) by ATRP yielded amphiphilic graft copolymers. When HEMA-TMS was used, deprotection was required [20].

Recently, a novel well-defined amphiphilic graft copolymer of PEO as main chain and PMMA as graft chains was successfully prepared by combination of anionic copolymerization with ATRP [21]. The protected glycidol were randomly copolymerized with EO to form the backbone and then deprotected in the acidic conditions. The recovered main chain with multi-pending hydroxyls was esterified with 2-bromoisobutyryl bromide to produce the ATRP macroinitiator to initiate the polymerization of MA.

In our research, ATRP grafting techniques were used for the preparation of poly(methyl vinyl ether)-*graft*-polystyrene (PMVE-*g*-PS) and PMVE-*g*-PMAA graft copolymers in a next session (**Chapter 8**).

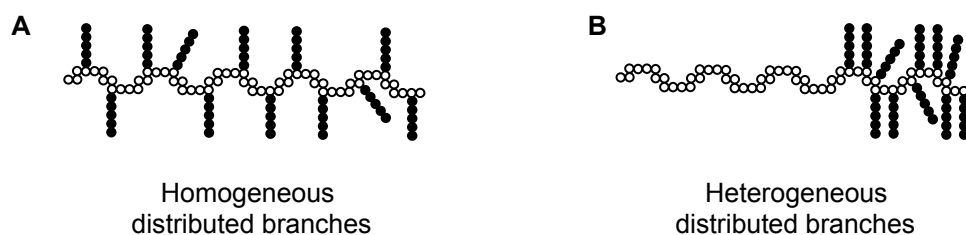
4.2.3. Graft Copolymers via Macromonomers: ‘Grafting Through’ Methods

The ‘*grafting through*’, also referred to as the macromonomer method, is the most applied for the preparation of graft copolymers [16,22]. A macromonomer is an oligomeric or polymeric chain bearing polymerizable end groups (scheme 4.4). Copolymerization with another monomer provides graft copolymers.



Scheme 4.4. ‘Grafting through’ technique.

However, the macromonomer method is still deficient in controlling the spacing of side chains. For example, in scheme 5.5, polymers A and B have the same backbone length, the same branch length, and the same number of branches. Polymer A has homogeneously distributed branch spacing, while polymer B has heterogeneously distributed branch spacing structures.



Scheme 5.5. Graft copolymers A and B with different distributions.

The spacing distribution is determined by the reactivity ratios of the macromonomer and the low molecular weight comonomer. The reactivity ratios, r_A and r_B , are influenced by many factors, especially i) the inherent reactivity of the macromonomer and the comonomer based on their chemical structure, ii) the diffusion or kinetic excluded volume associated with the large size of the macromonomer and iii) propagating comonomer chain due to thermodynamic repulsive interactions [23]. These parameters determine how random the produced graft copolymer will be. A common problem is that the copolymerization is not homogeneous throughout the course of the reaction, since phase separation often occurs in these systems, leading to compositionally heterogeneous products. Müller *et al.* found for a copolymerization of *n*-butyl acrylate (*n*BA) and PMMA macromonomer that this diffusion control effect was reduced by using ATRP (**Chapter 7**) in which the time scale of monomer addition is much slower than in a conventional radical polymerization [24]. Similar results were obtained for PDMS macromonomers, which in ATRP had reactivity ratios much closer to MMA than a conventional process under similar conditions [26]. Another example made by ATRP involved

graft copolymers of PS with N-vinyl-2-pyrrolidone (VP). The method of graft copolymer formation was the copolymerization of VE terminal PS macromonomers with VP by a conventional free radical polymerization. Synthesis of the macromonomers was achieved by the ATRP of St initiated by vinyl chloroacetate.

Several difficulties arising for the characterization of the graft copolymers, in addition to the possible chemical and compositional heterogeneity, make it necessary to use a combination of different characterization methods in order to prove whether the final products are well-defined or not.

4.3. Factors Influencing the Grafting Procedure

In the following sections, several of the many variables that control grafting are presented, including the nature of the backbone, monomer, solvent, initiator, additives, temperature, etc.

** Role of Additives on Grafting*

Grafting yield or the extent of graft copolymerization depends on the presence of additives such as metal ions, acids and inorganic salts. Thus, the reaction between the monomer and the backbone must compete with any reactions between the monomer and additives. Although some additives may enhance the monomer/backbone reaction to increase the grafting efficiency, the reverse will be true if the reaction between the monomer and the additive is dominant.

The role of acid additives is important in some grafting processes [27-28]. However, the nature of acids is important. Among the mineral acids, only sulfuric acid is effective, depending on the nature of the backbone.

The addition of acids and alkali can affect the nature of the backbone, solvent as well the initiator, so that it can influence the grafting.

The enhancement of grafting is also been established by partitioning phenomena in the presence of an inorganic salt (e.g. LiClO₄ or LiNO₃) [29]. Metal salts such as LiClO₄ are more efficient than acids in enhancing photografting due to overall monomer partitioning effect.

Generally, the presence of a metal ion (e.g. Fe²⁺, Cu²⁺) and Mohr's salt preferentially reduces homopolymer formation, thus enhances grafting efficiency [30].

** Nature of the Backbone*

As grafting involves covalent attachment of a monomer to pre-formed polymeric backbone, the nature of the backbone (e.g. physical nature, chemical composition) plays an important role in the process [27,31]. There are various reports regarding the role of chemical composition on grafting [32]. The presence of functional groups in the backbone also influences the grafting [33].

** Effect of Monomer*

As with the nature of the backbone, the reactivity of the monomer is also important in grafting. The reactivity of monomers depends on the various factors, viz. polar and steric nature, swellability of backbone in the presence of the monomers and concentrations of monomers. It is reported that

monomer reactivity ratios for the grafting process are completely different from values observed for conventional solution polymerization [34]. This could be explained by steric considerations [35]. Another reason is that the monomer is susceptible to monomer transfer reaction and tends to terminate the growing grafted chain, resulting in poor grafting efficiency [35] or suppressing grafting [36]. The grafting could depend upon the stability of the radical [37-38], during radiation grafting certain substituents activate monomers whereas others deactivate. In general, the grafting efficiency will depend on the monomer concentration [39]. It is often reported that the grafting efficiency increases with monomer concentration up to a certain limit and then decreases with further increase in the monomer concentration [40]. This behavior may reflect an initial increase of the monomer concentration in close proximity to the backbone. After a certain limit, the increase in monomer concentration accelerates the homopolymerization reaction rather than grafting.

** Effect of Solvent*

In grafting mechanisms, the solvent is the carrier by which monomers are transported to the vicinity of the backbone. The choice of the solvent depends upon several parameters, including the solubility of monomer in solvent [41], the swelling properties of the backbone [42-43], the miscibility of the solvents if more than one is used [43], the generation of free radical in the presence of the solvent [38,44], etc

** Effect of Initiator*

In general, the chemical grafting reactions require an initiator, and its nature, concentrations, solubility as well as function need to be considered. The nature of the initiator has a profound effect on grafting. For example, azo-(bis)-isobutyronitrile (AIBN) exhibits resonance stabilization whereas it is not the case with conventional peroxides [45].

The rate of grafting is dependent on initiator concentration as well as the monomer and the backbone. There are various empirical relationships regarding the dependence of grafting efficiency on the initiator concentration [46]. It is apparent from the observations that once a certain initiator concentration is reached, higher levels of initiator do not increase the conversion of grafted monomer [47].

The solubility of the initiator in the grafting medium is another prime factor. Ideally, the initiator should be fully soluble, so that it can initiate the grafting reaction.

** Effect of Temperature*

The temperature is one of the most important factors that control the kinetics of graft copolymerization. In general, grafting yield increases with increasing temperature, until a limit is attained. One factor in this can be faster monomeric diffusion processes in the backbone increases with increasing temperature, facilitating grafting [40].

4.4. Applications

By controlling the molecular parameters, one can obtain impact resistant materials by combining a hard polymer backbone with soft polymer side chains; thermoplastic elastomers, where a soft polymer backbone is grafted with hard polymer segments; or amphiphilic copolymers for applications as hydrogels, stabilizers, surface-modifying agents, dispersants, emulsifiers and compatibilizers in polymer blends [48]. Moreover, they generally have lower melt viscosities because of their branched structure, which is advantageous for processing. Since graft copolymers have many structural variables (composition, backbone length, branch length, branch spacing, etc.), they have great potential to realize new properties [1-2,49].

4.5. References

- [1] Peleshanko S., Tsukruk V.V., *Prog. Polym. Sci.*, **2008**, 33, 523.
- [2] (a) Tsitsilianis C., in “*Macromolecular Engineering, Precise Synthesis, Materials, Properties, Applications*”, Vol. 2 in ‘*Elements of Macromolecular Structural Control*’, Edited by Matyjaszewski K., Gnanou Y., Leibler L., Wiley-VCH Verlag GmbH & Co. KGaA, Weinheim, Germany, Chap. 4, **2007**. (b) Fukuda T., Tsujii Y., Ohno K., in “*Macromolecular Engineering, Precise Synthesis, Materials, Properties, Applications*”, Vol. 2 in ‘*Elements of Macromolecular Structural Control*’, Edited by Matyjaszewski K., Gnanou Y., Leibler L., Wiley-VCH Verlag GmbH & Co. KGaA, Weinheim, Germany, Chap. 11, **2007**.
- [3] Meng T., Gao X., Zhang J., Li H., Chen X., Sun J., Zhang X., Jing X., *Polymer*, **2009**, 50, 441.
- [4] (a) Altares T. Jr., Wyman D.P., Allen V.R., Meyersen K.J., *J. Polym. Sci., Part A: Polym. Chem.*, **1965**, 3, 4131. (b) Candau F., Rempp P., *Makromol. Chem.*, **1969**, 15, 122. (c) Pepper K.W., Paisley H.M., *J. Chem. Soc.*, **1953**, 4097. (d) Itsuno S., Uchikoshi K., Ito K., *J. Am. Soc.*, **1990**, 112, 8187.
- [5] Candau F., Afchar-Taromi F., Rempp P., *Polymer*, **1977**, 18, 1253.
- [6] (a) Shappacher M., Deffieux A., *Macromol. Chem. Phys.*, **1997**, 198, 3953. (b) Deffieux A., Shappacher M., *Macromolecules*, **1999**, 32, 1797. (c) Shappacher M., Deffieux A., *Macromolecules*, **2000**, 33, 7371. (d) Muchtar M., Shappacher M., Deffieux A., *Macromolecules*, **2001**, 34, 7595. (e) Shappacher M., Deffieux A., Puteaux J.L., Viville P., Lazzaroni R., *Macromolecules*, **2003**, 36, 5776.
- [7] (a) Candau F., Afchar-Taromi, Rempp P., *Polymer*, **1977**, 18, 1253. (b) Berlinova I.V., Amzil A., Tsvetkova S., Panayotov I.M., *J. Polym. Sci., Part A: Polym. Chem.*, **1994**, 32, 1523. (c) Hourdet D., L’Alloret F., Audebert R., *Polymer*, **1994**, 35, 2624. (d) Eckert A.R., Webber S.E., *Macromolecules*, **1996**, 29, 560. (e) Hourdet D., L’Alloret F., Audebert R., *Polymer*, **1997**, 38, 2535. (f) Wang Y., Du Q., Huang J., *Macromol. Rapid Commun.*, **1998**, 19, 247. (g) Xie H.Q., Xie D., *Polym. Sci.*, **1999**, 24, 275. (h) Mihaylova M.D., Krestev V.P., Kresteva M.N., Amzil A., Berlinova I.V., *Eur. Polym. J.*, **2001**, 37, 233. (i) Reutenauer S., Hurtrez G., Dumas P., *Macromolecules*, **2001**, 34, 755. (j) Yin X., Stöver H.D.H., *Macromolecules*, **2002**, 35, 10178. (k) F. Hua, E. Ruckenstein, *Macromolecules*, **2003**, 36, 9971. (l) B. Parrish and T. Emrik, *Macromolecules*, **2004**, 37, 5863.
- [8] Wesslen B., Wesslen K.B., *J. Polym. Sci., Part A: Polym. Chem.*, **1989**, 27, 3915.

- [9] Derand H., Wesslen K.B., *J. Polym. Sci., Part A: Polym. Chem.*, **1995**, 33, 3571.
- [10] (a) Twaik M., Tahan M., Zilkha A., *J. Polym. Sci., Part A: Polym. Chem.*, **1969**, 7, 2469. (b) Thierry A., Skoulios, *Makromol. Chem.*, **1977**, 177, 319.
- [11] Jannash P., Wesslen B., *J. Polym. Sci., Part A: Polym. Chem.*, **1993**, 31, 1519.
- [12] (a) Cooper W., Vaughan G., Miller S., Fielden M., *J. Polym. Sci.*, **1959**, 34, 651. (b) Oster G., Shibata O., *J. Polym. Sci.*, **1957**, 26, 233.
- [13] (a) Brockway C., Moser K., *J. Polym. Sci., Part A: Polym. Chem.*, **1963**, 1025. (b) Maadhah G., Amin M., Usmani A., *Polym. Bull.*, **1985**, 14, 433.
- [14] Franta E., Reibel L., Rempp P., *Polym. Prep.*, **1979**, 20(2), 102.
- [15] (a) Li L.H., Zhu Y., Li B., Gao C.Y., *Langmuir*, **2008**, 24, 13632. (b) Kennedy J.E., Devine D.M., Lyons J.G., Geever L.M., Higginbotham C.L., *J. Mat. Sci.*, **2009**, 44, 889. (c) Gaiolas C., Belgacem M.N., Silva L., Thielemans W., Costa A.P., Nunes M., Silva M.J.S., *J. Colloid. Interf. Sci.*, **2009**, 330, 298.
- [16] Zaichenko A., Mitina N., Shevchuk O., Rayevska K., Lobaz V., Skorokhoda T., Stoika R., *Pure Appl. Chem.*, **2008**, 80, 2309.
- [17] Matyjaszewski K., Teodorescu M., Miller P.J., Peterson M.L., *J. Polym. Sci., Part A: Polym. Chem.*, **2000**, 38, 2440.
- [18] Liu S., Sen A., *Polym. Prepr. (Am. Chem. Soc., Div. Polym. Chem.)*, **2000**, 41, 1573.
- [19] Liu S., Sen A., *Macromolecules*, **2000**, 33, 5106.
- [20] Börner H.G., Duran D., Matyjaszewski K., Da Silva M., Sheiko S.S., *Macromolecules*, **2002**, 35, 3387.
- [21] Li Z., Li P., Huang J., *Polymer*, **2006**, 47, 5791.
- [22] (a) Tomlinson M.R., Genzen J., *Polymer*, **2008**, 49, 4837. (b) Montagne F., Polesel-Maris J., Pugin R., Heinzelmann H., *Langmuir*, **2009**, 25, 983.
- [23] (a) Tsukahara Y., Hayashi N., Jiang X.-L., Yamashita Y., *Polym. J.*, **1989**, 21, 377. (b) Meijs G.F., Rizzardo E., J.M.S., *Makromol. Chem.*, **1990**, C30, 305. (c) Percec V., Wang J.H., *Makromol. Chem., Macromol. Symp.*, **1992**, 54/55, 583.
- [24] Ross S.G., Müller A.H.E., Matyjaszewski K., *Macromolecules*, **1999**, 32, 8331.
- [25] Roos S.G., Müller A.H.E., Matyjaszewski K., *ACS Symp. Ser.*, **2000**, 768, 361.
- [26] Shinoda H., Miller P.J., Matyjaszewski K., *Macromolecules*, **2001**, 34, 3186.
- [27] Chappas W.J., Silverman J., *Radiat. Phys. Chem.*, **1979**, 14, 847.
- [28] (a) Hoffman A.S., *Radiat. Phys. Chem.*, **1979**, 14, 831. (b) El assy N.B., *J. Appl. Polym. Sci.*, **1991**, 42, 885.
- [29] (a) Ang C.H., Garnett J.L., Levol R., Long M.A., *J. Polym. Sci., Part C: Polym. Lett.*, **1983**, 21, 257. (b) Garnett J.L., Jankeiwicz S.V., Long M.A., Sangster D.F., *J. Polym. Sci., Part C: Polym. Lett.*, **1985**, 23, 563.
- [30] Kubota H., Hata Y., *J. Appl. Polym. Sci.*, **1991**, 42, 1029.

- [31] (a) Ibrahim A.A., Nada A.M.A., *Acta Polym.*, **1985**, 36(6), 320. (b) Clark D.C., Baker W.E., Whitney R.A., *J. Appl. Polym. Sci.*, **2000**, 79(1), 96. (c) Ng L-T., Garnett J.L., Zilic E., Nguyen D., *Radiat Phys. Chem.*, **2001**, 62, 89.
- [32] (a) Hornof V., Kokta B.V., Valade J.L., *J. Appl. Polym. Sci.*, **1976**, 20, 1543. (b) Kokta B.V., Valade J.L., Daneault C., *Transactions*, **1981**, 7, TR5-TR10. (c) Tyuganova A.A., Gabraikh L.S., Ulmasove A.A., Tsarevskaya I.T., Khigoyator A.A., *Cell. Chem. Technol.*, **1985**, 19(5), 557.
- [33] (a) Ghosh P., Ghosh T.K., *J. Appl. Polym. Sci.*, **1982**, 18(3), 361. (b) Rao M.H., Rao K.N., *Radiat. Phys. Chem.*, **1985**, 26(6), 669. (c) Meissner H., Meublein G., *Acta Polym.*, **1986**, 37(5), 323. (d) Ghosh P., Bangyopadhyay A.R., *J. Appl. Polym. Sci.*, **1986**, 31(5), 1499. (e) Okieima E.F., Idehem I.K., *J. Macromol. Sci. Chem.*, **1987**, A24(11), 1381. (f) Storey R.F., Dantiki D.S., Goff L.J., *Polym. Mater. Sci. Eng.*, **1988**, 58, 565.
- [34] El-Naggar A.M., Zhody M.H., Sahar S.M., Allan E.A., *Polym. Int.*, **2001**, 50, 1082.
- [35] Misra B.N., Kauer I., Chandel P.S., *Preprints IUPAC MAKROMAINZ*, **1979**, 1, 440.
- [36] Bhattacharya A., Das A., De A., *Ind. J. Chem. Tech.*, **1998**, 5, 135.
- [37] Varma D.S., Narashinan V., *J. Appl. Polym. Sci.*, **1975**, 19, 29.
- [38] Bhattacharya A., Misra B.N., *Prog. Polym. Sci.*, **2004**, 29, 767.
- [39] Kaur I., Misra B.N., Gupta A., Chauhan G.S., *J. Appl. Polym. Sci.*, **1998**, 69, 599.
- [40] Sun T., Xu P., Liu Q., Xue J., Xie W., *Eur. Polym. J.*, **2003**, 39, 189.
- [41] Sanli O., Pulet E., *J. Appl. Polym. Sci.*, **1993**, 47, 1.
- [42] Dili S., Garnett J.L., *J. Appl. Polym. Sci.*, **1967**, 11(6), 859. (a) Yasukawa T., Sasaki Y., Murukami K., *J. Polym. Sci., Part A: Polym. Chem.*, **1973**, 11(10), 2547.
- [43] Bhattacharyya S.N., Maldas D., *J. Polym. Sci., Part A: Polym. Chem.*, **1982**, 20, 939.
- [44] Lee S., Rengarajan R., Parameswara V.R., *J. Appl. Polym. Sci.*, **1990**, 41, 1891.
- [45] Nishioka N., Matsumoto K., Kosai K., *Polymer*, **1983**, 15, 153.
- [46] (a) Bhattacharyya S.N., Maldas D., *Prog. Polym. Sci.*, **1983**, 10, 171. (b) Celik M., Sacak M., *J. Chem.*, **2000**, 24, 269.
- [47] (a) Khali M.I., Rafie M.H., Bendak A., Hebeish A., *Cell. Chem. Technol.*, **1982**, 16(5), 465. (b) Patil D.R., Fanta G.F., *J. Appl. Polym. Sci.*, **1993**, 47, 1765.
- [48] (a) Rempp P.F., Lutz P.J., in 'Comprehensive polymer Science', Allen G., Bevington J.C., Eds., Pergamon Press: Oxford, **1989**, Vol. 6, pp 403. (b) Schultz G.O., Erukhimovich I.Y., *Macromolecules*, **1993**, 26, 276. (c) Pitsikalis M., Pispas S., Mays J.W., Hadjichristidis N., *Adv. Polym. Sci.*, **1998**, 135, 1.
- [49] Bhattacharya A., *Prog. Polym. Sci.*, **2000**, 25, 371.

Chapter 5

Synthesis and Molecular Characterization of Poly(Methyl Vinyl Ether)-*g*-Poly(Ethylene Oxide) Graft Copolymer

5.1. Introduction

The synthesis of thermo-responsive amphiphilic copolymers has attracted much interest in the past decades, since these materials are capable of forming micelles or aggregates in aqueous solution [1]. Among this class of smart materials, graft copolymers were shown to be applicable as surfactants, stabilizers, surface modifiers and compatibilizers in polymer blends [2]. Although recently such graft copolymers have also been quite extensively investigated [2], there is still a strong need in this research field for the design of well-defined graft copolymers in which hydrophilic grafts are attached to a uniform hydrophobic or thermo-responsive backbone.

In this study, PMVE has been chosen as the backbone of the graft copolymers because of its thermo-responsive properties. While PMVE is known to have a LCST about 37°C in water [3] (see further **Chapter 6**), PCEVE is a hydrophobic polymer chain in which the chlorine group can be substituted to form other functional groups. Several substitution reactions were performed with the anions of pyrrolidone [4], succinimide, imidazole and pyrazole [5]. Hashimoto *et al.* [6] used CEVE as a starting material to prepare 2-vinyloxyethyl phtalimide by substitution of the chlorine atom with potassium phtalimide. Out of this monomer, the synthesis of poly(aminoethyl vinyl ether) (PAEVE) was reported by polymerizing 2-vinyloxyethyl phtalimide with HI/I_2 as initiator, followed by hydrazinolysis of the imide functions. In our research group [7], another efficient route for the synthesis of PAEVE was reported, consisting of the synthesis of PCEVE after which the chlorine groups were substituted into phtalimide groups, followed by hydrazinolysis.

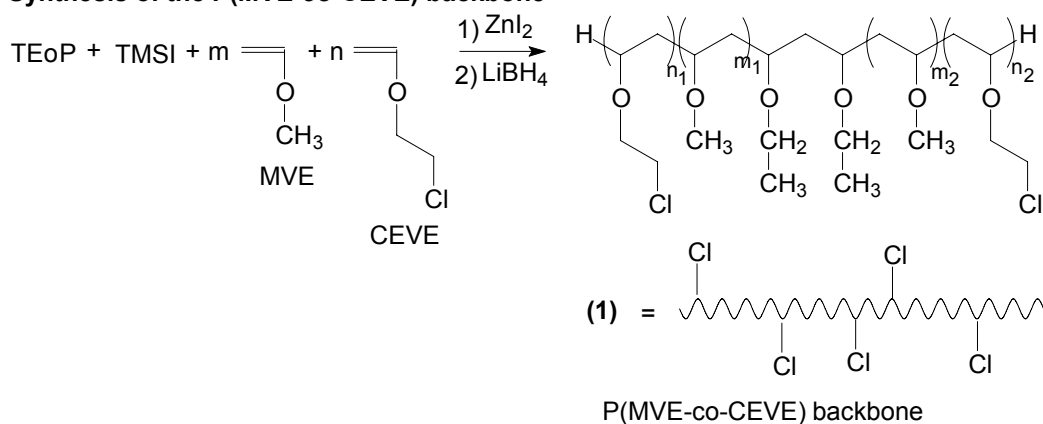
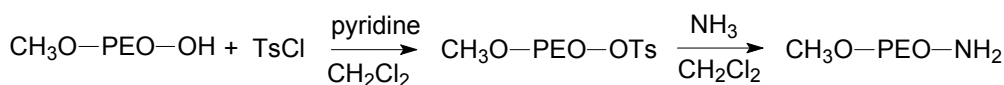
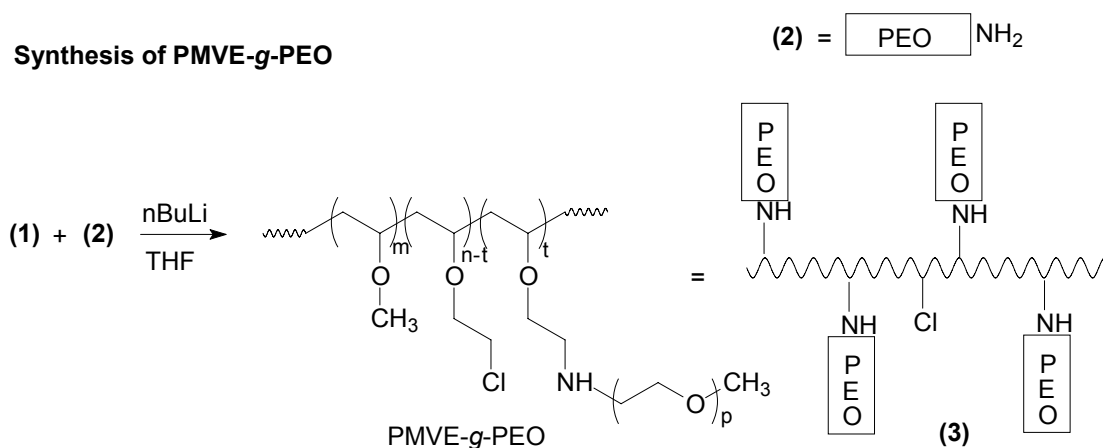
In the previous section (**Chapter 3**), we demonstrated the possibility to copolymerize MVE with CEVE in a living way, where chlorine functional groups are statistically distributed along

the PMVE chain, allowing the introduction of another polymer by a grafting onto process. By the grafting of hydrophilic chains onto PMVE, thermo-responsive graft copolymers with well-defined backbone and side chains will be obtained. Their demixing behavior in water will be compared in the next section (**Chapter 6**).

PEO has often been used as hydrophilic side chain in graft copolymers, owing to its unique physical and biomedical properties [12]. The grafting of PEO onto vinyl polymers containing backbones has been performed by various methods, like carbanionic initiation of PS [8-9,11], alkaline transesterification onto PMMA [13] or poly(ϵ -caprolactone) [14], and radical polymerization of NIPAAm using cerium(IV) redox initiation [15]. Recently, a method was developed by Stöver to attach α -methoxy- ω -hydroxyl-PEO (CH₃-PEO-OH) to copolymer precursors being alternating copolymers of poly(styrene-*alternating*-maleic anhydride) (P(St-*alt*-MA)) and poly((4-*tert*-butylstyrene)-*alternating*-maleic anhydride) (P(*t*BS-*alt*-MA)) [16].

A crucial issue in obtaining well-defined graft copolymers is the quantitative introduction of the branching points, which requires highly selective branching reactions of the peripheral groups. In general, the modification by grafting could be carried out using three synthetic routes: grafting onto (coupling attachment of the side chains onto the main chain), grafting from (direct grafting polymerization of the monomer to form side chains from active points on the backbone), and grafting through (homopolymerization of macromonomers) (see **Chapter 4**). Therefore, in this chapter, we will introduce a relatively simple and effective method to prepare thermo-responsive graft copolymers of interest, generating a series of PMVE-*g*-PEO copolymers. Thus, the pending chlorine groups will act as reactive moieties by substitution along the PMVE backbone, to give a new functionalized graft copolymer carrying PEO side chain via a grafting onto process. The hydroxyl end group of PEO has first been transformed by a primary amine. Preliminary 'model reactions' with benzylamine and triethylene glycol (TEG) instead of PEO have been synthesized with different bases.

The preparation procedure of well-defined PMVE-*g*-PEO copolymers is based on three steps consisting of (1) the synthesis of a statistical P(MVE-*stat*-CEVE) backbone as mentioned in **Chapter 3**, (2) the end-group functionalization of the PEO side chains, and finally (3) the synthesis of the desired PMVE-*g*-PEO copolymers via a grafting onto process. This methodology is illustrated in scheme 5.1, also clarifying the nomenclature of the different compounds used. Only PMVE backbones with a small content of CEVE (< 10 mol-%) were synthesized to keep the thermo-responsiveness of the PMVE.

Synthesis of the P(MVE-co-CEVE) backbone**Functionalization of the PEO side chains****Synthesis of PMVE-g-PEO**

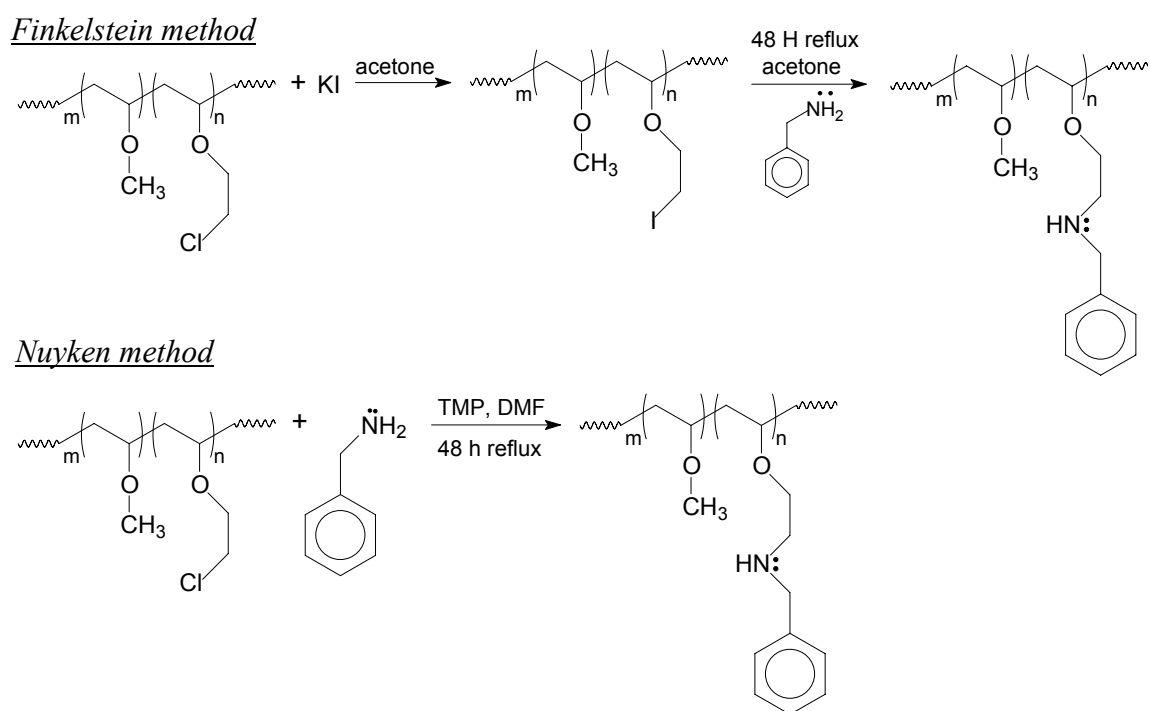
Scheme 5.1. Synthesis of the PMVE-g-PEO graft copolymers in three steps with $m = m_1 + m_2$ and $n = n_1 + n_2$.

5.2. Model Reactions

The direct synthesis of hydroxyl-PEO grafted onto the chlorine groups is not possible because of the relative low leaving capacity of chlorine groups. Indeed, the amino end groups on α -amino- ω -monomethyl ether-poly(ethylene oxide) ($\text{CH}_3\text{-PEO-NH}_2$) are more reactive towards acylating agents than the hydroxyl groups that are present on conventional PEO's [17-18]; hence, the choice of the nucleophilic substitution of the chlorine by a primary amine seems to be more suitable. First, two model reactions were investigated to know if this grafting process could work. A first reaction model was carried out with benzylamine, containing a primary amine group and easily observable (by NMR) phenyl groups. On the other hand, TEG that has a similar structure as the PEO chain, was used for a second model reaction.

5.2.1. Analogous Reaction with a Primary Amine

The first reaction model was made by the substitution of benzylamine in two different ways: the Finkelstein and Nuyken's methods. For the Finkelstein method [19], the iodide, which replaces the chlorine, is interesting because it is a better leaving group than chloride. In the second step, the iodide is substituted by the benzylamine (scheme 5.2). The second reaction model was already used by Nuyken for the nucleophilic substitution of PCEVE homopolymers by the anion pyrrolidone [5], and of poly(isobutyl vinyl ether)-*block*-poly(2-chloroethyl vinyl ether) (PIBVE-*b*-PCEVE) copolymers by the anions of succinimide, imidazole or pyrazole [4]. This reaction takes place in one step with 1,1,5,5-tetramethyl piperidine (TMP) as base in dimethylformamide (DMF) (scheme 5.2).



Scheme 5.2. Model reactions of the substitution of the chlorine pendent group by benzylamine with the Finkelstein and Nuyken's methods.

The ^1H NMR of the resulting product is shown in figure 5.1. The signal between 7.2 – 7.4 ppm, which is absent in the P(MVE-*stat*-CEVE), belongs to the aromatic protons of the benzylamine. The degree of substitution can be calculated by comparing integration of this signal with that of the initiator group *i* at 1.2 ppm (see **Chapter 3**). The calculation revealed that the substitution degree depends on the choice of the method, respectively 60 (Finkelstein) and 81% (Nuyken).

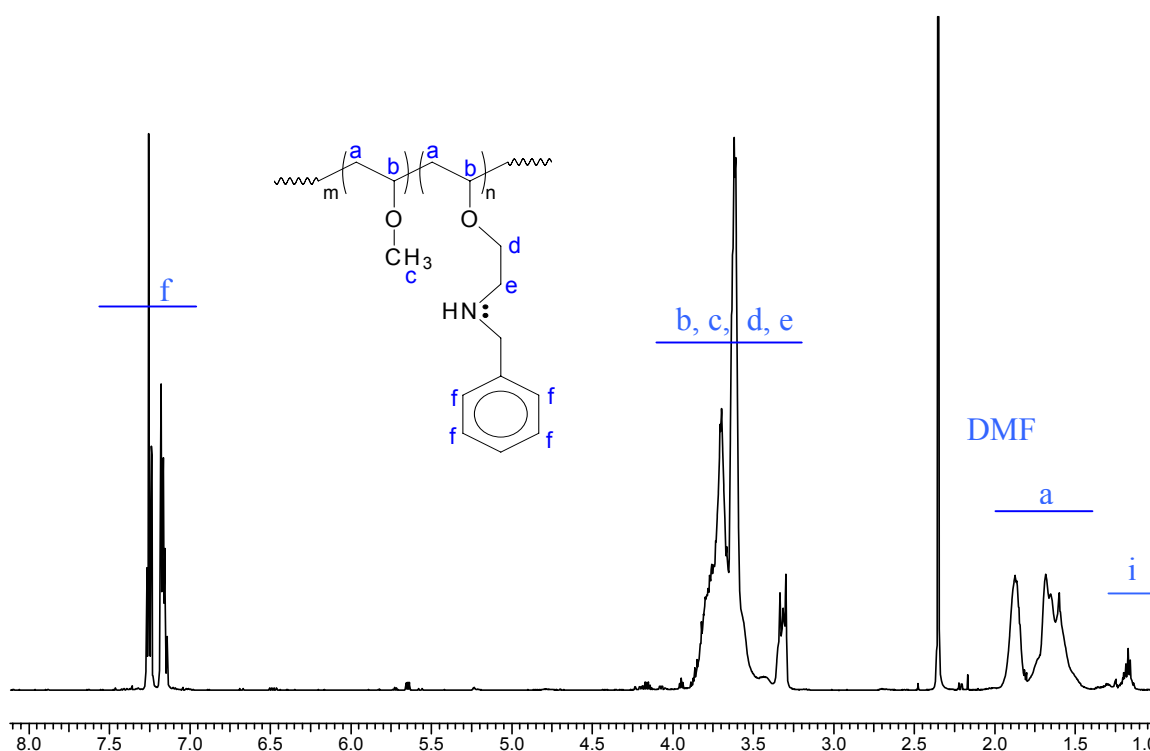


Figure 5.1. ^1H NMR spectrum of the P(MVE-*stat*-CEVE), where the chlorine groups were substituted with benzylamine (in CDCl_3).

Because the nucleophilic substitution is not complete, it should be better to use a stronger base such as *n*-butyl lithium (*n*BuLi) (see below). Moreover, as the solvent DMF is impossible to remove completely and thus interferes with the elemental analysis, THF was chosen for further experiments. Indeed, the results obtained in the presence of THF with *n*BuLi gave better results with respectively 72 (Finkelstein) and 94% (Nuyken) substitution.

5.2.2. Analogous Reaction with Triethylene Glycol (TEG)

The second reaction model was made by the substitution of the chlorine groups by the hydroxyl end group of TEG. Because the nucleophilicity of the hydroxyl is weaker than an amine, *n*BuLi was used. The ^1H NMR of the resulting product is shown in figure 5.2. Comparison with the NMR-spectrum of P(MVE-*stat*-CEVE) shows the characteristic CH_2 signals of TEG at 5.1 ppm from which the substitution of chlorine was calculated. It was found that 98% of chlorine atoms were substituted.

5.3. Functionalization of PEO with a Terminal Amine

PEG was used as a carrier polymer for the attachment, via end groups, of drugs such as penicillin [20], aspirin [21], amphetamine [22], quinidine [23] and atropine [24]. To attach the drugs to PEG, use was made of the terminal hydroxyl groups. These can be reacted with drugs containing suitable groups such as carboxylic ones (esterification). But in order to realize the attachment of drugs having other functional groups there was a need for preparing PEG having

other functional end-groups. Indeed, PEO chains with primary amino groups at the termini are very useful functionalized polymers [17-18].

Also in our research, we found that the functionalization with PEO (molecular weights 2000 and 5000 g.mol⁻¹) was not successful with grafting degrees lower than 60%. Several methods, all of them based on three-step procedures, were therefore developed for converting the terminal hydroxyl groups of PEO into amino groups [17-18,25-27]. For our purpose, because of low yields and non quantitative functionalization, one unpublished two-step procedure with higher yields, earlier developed in our department, was selected for the functionalization of PEO-OH in PEO-NH₂.

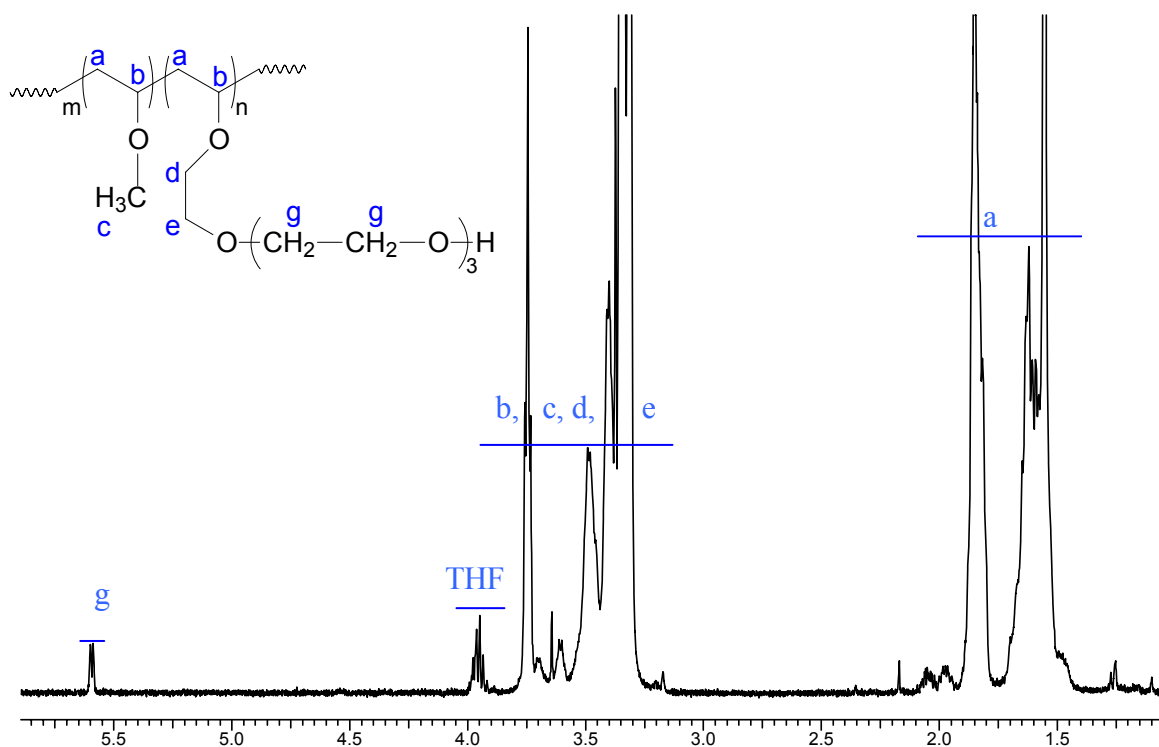
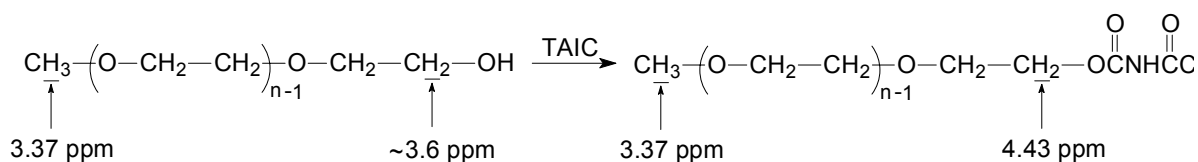


Figure 5.2. ¹H NMR spectrum of the P(MVE-*stat*-CEVE), in which the chlorine groups were substituted by TEG (CDCl₃).

5.3.1. Studies of the Functionalization of the Precursor PEO-OH

For the grafting process, the hydroxyl groups of the semi-telechelic CH₃-PEO-OH have been converted in the more reactive primary amine groups. For this purpose, it is of primary importance that the polymers made are truly semi-telechelic, as the presence of bi-functional PEO would unavoidably lead to the formation of a polymer network. The precursor end-group of both CH₃-PEO-OH with M_w 2000 and 5000 g.mol⁻¹ was analyzed by ¹H-NMR in order to determine its functionality as illustrated in figure 5.3 (A and B). In order to perform such end-group analysis, the monomethyl ether precursor was treated with trichloroacetyl isocyanate (TAIC) (scheme 5.3). This reagent transforms the hydroxyl end-group into a trichloroacetyl urethane end-group, causing a shift of approximately 1 ppm for the methylene protons in the α position of the OH end-group [28].



Scheme 5.3. Reaction of the PEO-OH end-group with TAIC.

Figure 5.3 shows the $^1\text{H-NMR}$ spectrum of a polymer having a molar mass of 2000 g mol^{-1} , which allows differentiating the end-standing methoxy protons (peak a in figure 5.3) from the methylene protons of the polymer chain (peaks d1, d2 and d3). The $[\text{CH}_2(\text{OH})]/[\text{OCH}_3]$ ratio can be determined by integrating the intensity of the methoxy methylene peak a and of the urethane methylene peak d2, respectively. In case of pure monomethyl ether, this ratio should be $2/3$. The observed ratios are, however, much larger, up to 10% for PEO 2000 and up to 25% for PEO 5000, indicating that these polymers contain considerable amounts of bi-functional PEO, which of course may generate undesired reaction products. The same observation was done by others and no purification methods with sufficient yields are available. It should be noted that nowadays monofunctional PEG with higher purities are available.

5.3.2. Synthesis of PEO-NH₂ Side Chains

To obtain the required amino functionalized PEO, the $\text{CH}_3\text{O-PEO-NH}_2$, we followed a more efficient two-step procedure that has already been developed in our department. It consists of a tosylation of the hydroxyl-terminated PEO, followed by a reaction with ammonia (scheme 5.1 (2)). This substitution reaction was carried out for both monomethyl ethers studied (i.e. 2000 and 5000 g mol^{-1}). Note that all reactions have to proceed as quantitatively as possible, because of the inherent difficulties in separating the reacted from the unreacted polymers. For that reason, a large excess of reagents was used. α -tosylate- ω -monomethyl ether poly(ethylene oxide) ($\text{CH}_3\text{O-PEO-OTs}$) was synthesized by reaction of $\text{CH}_3\text{O-PEO-OH}$ with *p*-toluene sulfonyl in dichloromethane (CH_2Cl_2) in the presence of pyridine. Hence, a complete substitution of the terminal hydroxyl groups by tosylate could be achieved.

The obtained $\text{CH}_3\text{O-PEO-OTs}$ was converted into $\text{CH}_3\text{O-PEO-NH}_2$ by stirring a solution of $\text{CH}_3\text{O-PEO-OTs}$ with ammonia (25% in water) at elevated temperature and pressure using a glass autoclave. The nucleophilic substitution efficiency was monitored by $^1\text{H-NMR}$, also shown in figure 5.3 (spectra C and D). These spectra show a complete end-group transformation of $\text{CH}_3\text{O-PEO-OH}$ (spectrum B, peak d2) into $\text{CH}_3\text{O-PEO-OTs}$ (spectrum C, peaks c3 and d3). Finally, the quantitative reaction from $\text{CH}_3\text{O-PEO-OTs}$ to $\text{CH}_3\text{O-PEO-NH}_2$ (spectrum D, peak d4) could also be confirmed. The effectiveness of the nucleophilic substitution was also monitored and confirmed by elementary analysis in the next section.

This $\text{CH}_3\text{O-PEO-NH}_2$ exhibits properties similar to $\text{CH}_3\text{-PEO-OH}$: soluble in CH_2Cl_2 , DMF, water, and insoluble in diethyl ether, cold methanol (MeOH) and ethanol (EtOH).

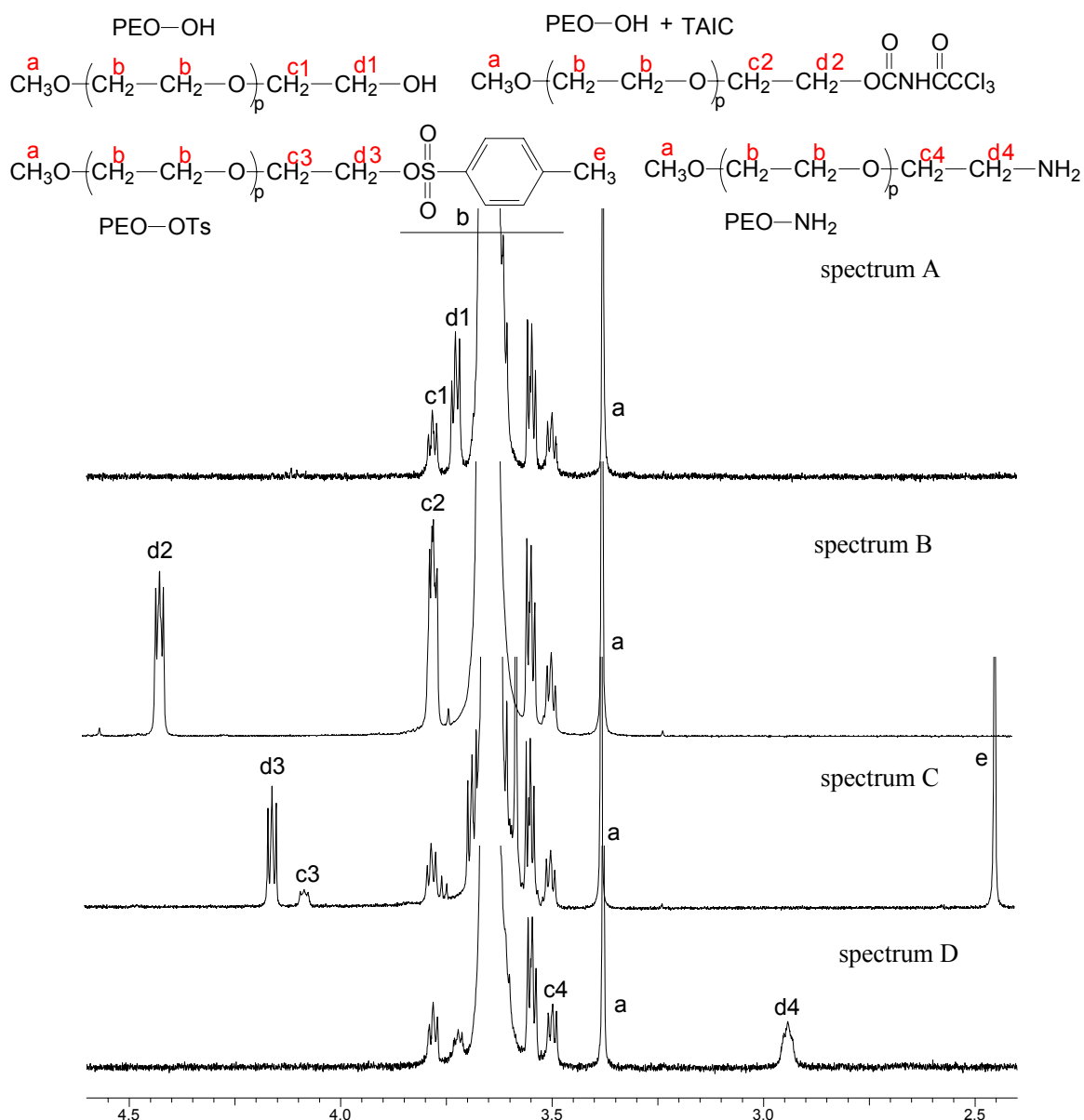


Figure 5.3. $^1\text{H-NMR}$ spectra of PEO ($2\,000\ \text{g}\cdot\text{mol}^{-1}$) with different end-groups in CDCl_3 : (A) $\text{CH}_3\text{O-PEO-OH}$, (B) $\text{CH}_3\text{O-PEO-TAIC}$, (C) $\text{CH}_3\text{O-PEO-OTs}$ and (D) $\text{CH}_3\text{O-PEO-NH}_2$.

5.4. Synthesis of PMVE-*g*-PEO via the Grafting onto Method

5.4.1. Synthesis

Throughout the experiments from the previous section (**Chapter 3**), the composition of the backbones used for the synthesis of the graft copolymers, are summarized in table 5.1. By regulating the feed amount ratio of the two monomers, hence the graft number of the final graft copolymer could be well controlled.

Table 5.1. Overview of the P(MVE-*stat*-CEVE) backbone compositions.

Name	MVE unit	CEVE unit	CEVE (mol-%)	DP _n ^a	M _n (g mol ⁻¹) ¹ H NMR	M _n (g mol ⁻¹) SEC	M _w /M _n ^b
B1	284	5	1.73	289	16 840	32 490	1.17
B2	320	12	3.61	332	19 970	33 940	1.20
B3	303	19	5.90	322	19 620	26 650	1.18

a) DP_n = MVE unit + CEVE unit, the degree of polymerization of P(MVE-*stat*-CEVE) determined by ¹H NMR. b) Calibrated with polystyrene standards.

The graft copolymers were made via a grafting onto process, in which the amino functionalized PEO-chains (scheme 5.1 (2)) are used to substitute the chlorine moieties on the PMVE backbones (scheme 5.1 (1)). The grafting was performed in THF and *n*BuLi. In all cases, the reaction went to completion after three days. Note that the PEO chains were added in excess. Effectively, Stadler [29], and also Rempp [8], in following the grafting onto methodology to prepare polybutadiene-*graft*-poly(ethylene oxide) (PB-*g*-PEO) and PS-*g*-PEO copolymers respectively, demonstrated that the use of an excess of the polymers to be grafted is a necessity. These authors acknowledged that this technique requires a tedious fraction step meant to get rid of unreacted PEO chains and they also conceded that graft copolymers obtained in this way exhibit a fluctuation in composition. Thus, the resulting graft copolymers (scheme 5.1 (3)) have been purified via dialysis (in water) and analyzed by ¹H-NMR and elemental analysis (E.A).

5.4.2. Characterization

As illustrated in figure 5.4, the SEC traces of the backbone, the PEO (2000 g mol⁻¹) and G4 graft copolymers demonstrated, as expected, that the molar mass increased after the grafting process, and exhibit a sharp, symmetrical peak. The peaks b of the backbone and a of the PEO side chain disappeared after the graft copolymerization and a new peak c, corresponding to the resulting graft copolymer, emerged. The non-symmetrical shape of curve c can be explained by the presence of small PEO-fractions that cannot be removed.

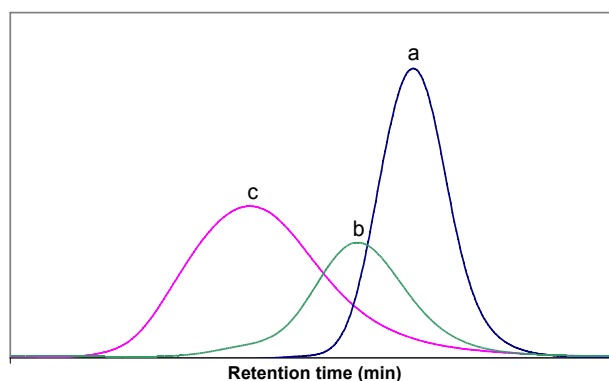


Figure 5.4. SEC chromatograms of the PEO side chains (a), the backbone (b) and the PMVE-*g*-PEO graft copolymer (c).

5.4.3. Determination of the Grafting Degree

As the NMR-signals of PEO, characterized by the methylene protons in the EO units located at 3.5-3.8 ppm, and P(MVE-*stat*-CEVE) at 3.1-3.9 ppm, partially overlap (figure 5.5), the grafting degree t of the graft copolymers $(\text{PMVE})_m(\text{P-Cl})_{1-t}(\text{P-NH-CH}_2\text{-CH}_2(\text{O-CH}_2\text{-CH}_2)_p\text{OCH}_3)_t$ has been determined from experimentally obtained elemental mass fractions, using a mathematical nonlinear least-squares procedure [30-31] reported in **Appendix III**.

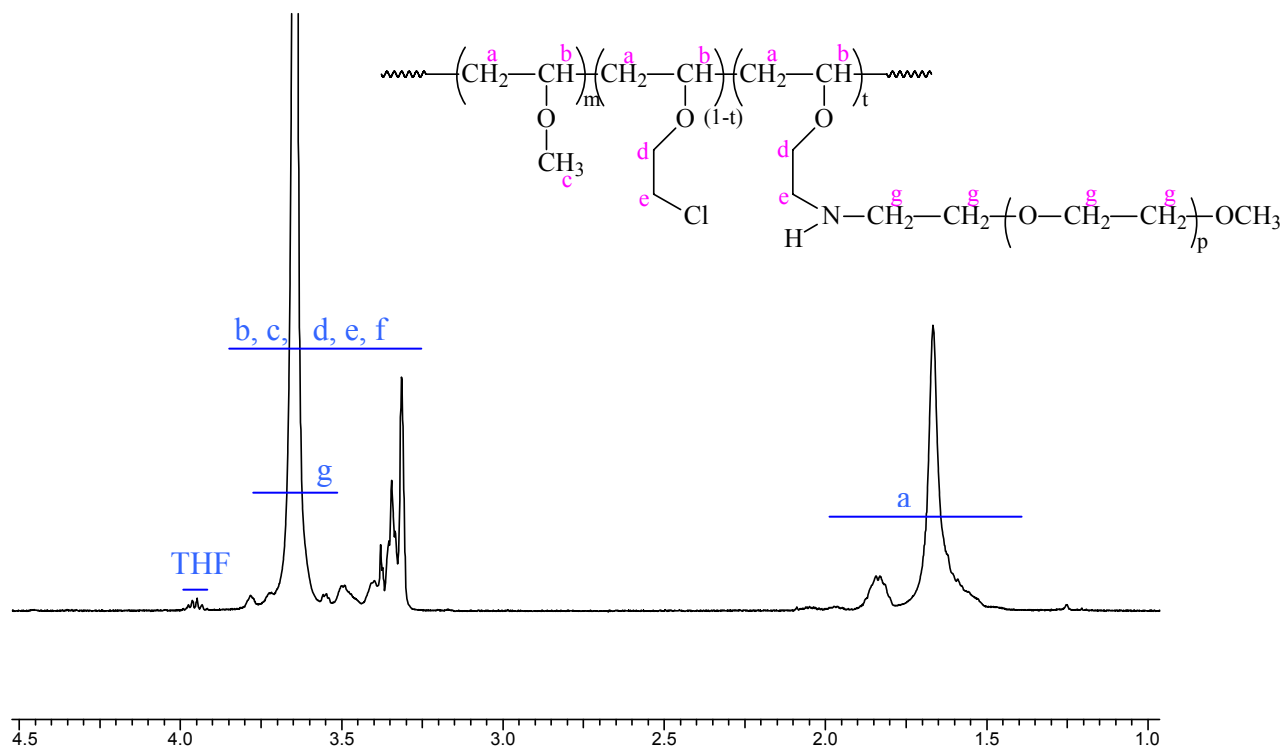


Figure 5.5. ¹H-NMR spectrum of the PMVE-*g*-PEO copolymers in CDCl₃.

E.A. allows detecting the wt-% of C, O, H, and Cl, possibly indicating small amounts of unreacted chlorine groups inside the synthesized graft copolymers. Major attention was paid to the calculation of the grafting degree t using these data, especially because of the results obtained were not always easy to understand. For this, the mathematical analysis provides t as a function of the mass fraction of all elements involved. It reveals that even when the wt-% of all determined elements by E.A. are accurate, the values of t found from the system of equations associated with the considered functionalized polymer can deviate dramatically from the actual ones. From equation eq.11 in **Appendix III**, Willem *et al.* found that a small difference in the value of γ_i results in a rather large confidence on the value obtained for t . Thus, a small uncertainty in the E.A. data results in a huge confidence interval on the value obtained for t . Common use of E.A. results in structural chemistry makes confidence ranges of $\pm 0.3\%$ for C, of $\pm 0.04\%$ for H, of $\pm 0.5\%$ for C and $\pm 0.2\%$ for Cl acceptable. In order to use this method correctly and self-consistently for all compounds, all the graphs should be plotted.

Figure 5.6 shows an example of a simulation of such function for the G4 graft copolymer for the mass fractions of C, O, H and Cl around their expected values and illustrates that

predetermined uncertainty margins on the mass fraction data can lead to very widespread uncertainty margins of the t values, depending on the element used. Moreover, the determination of the t values should be calculated more precisely due to its uncertainties from E.A.. Thus, there is a large error bar on the value of t using the equation for the mass fraction of all elements giving an important change in the value of t . This justifies the use of the statistical non-linear least-squares approach, minimizing the impact of the elements that lead to larger uncertainty margins.

Table 5.2 recapitulated the compositions of the PMVE-*g*-PEO graft copolymers. In general, a certain number of chlorine groups, depending on the reaction conditions and copolymer composition, did not react with PEO-chains. The molecular mass of the graft copolymers was determined from t and the knowledge of the molar mass of the backbone and the side chains.

Table 5.2. Overview of the PMVE-*g*-PEO copolymer compositions.

Sample code	Starting polymer	Number of Cl-groups	PEO				M_n SEC ($g\text{mol}^{-1}$)	M_w/M_n
			M_n	PEO graft	content	t		
			($g\text{mol}^{-1}$)	(E.A.)	(wt-%)	(%)		
G1	B1	5	178	4	4	80	37 060	1.40
G2	B2	12	178	4	3	33	36 210	1.30
G3	B1	5	2000	3	26	60	39 430	1.31
G4	B2	12	2000	11	52	92	44 030	1.25
G5	B3	19	2000	17	63	89	34 740	1.24
G6	B1	5	5000	3	47	60	51 700	1.24
G7	B2	12	5000	5	55	42	52 100	1.22
G8	B3	19	5000	12	75	63	42 920	1.20

As it can be observed, the degree of functionalization t never exceeds 92 mol-%. Even if the t values are determined, the following difficulties need to be pointed out. Only one functionality should be grafted onto the chlorine group. Too large amounts of additional functionalities due to incomplete reactions or side-reactions make the calculation of t from the weight determination questionable. Indeed, using this method, only one equation is available allowing the calculation of only one single functionalization parameter. In this calculation, the amount of PEO was determined, neglecting the formation of cross-linking of PEO. Therefore, SEC/LS measurements were made for a better understanding. Taking into account the number of amines ($nb(N)$) present in the graft copolymers, the value of the functionality F_n can be calculated by the formula:

$$F_n = \frac{M_{w,graft}}{M_{w,backbone} + M_{w,PEO} \times nb(N)}$$

where $M_{w,graft}$, $M_{w,backbone}$ and $M_{w,PEO}$ are respectively the molecular weight of the graft copolymers, the precursor backbone and the PEO side chains. F_n values are recapitulated in table 5.3.

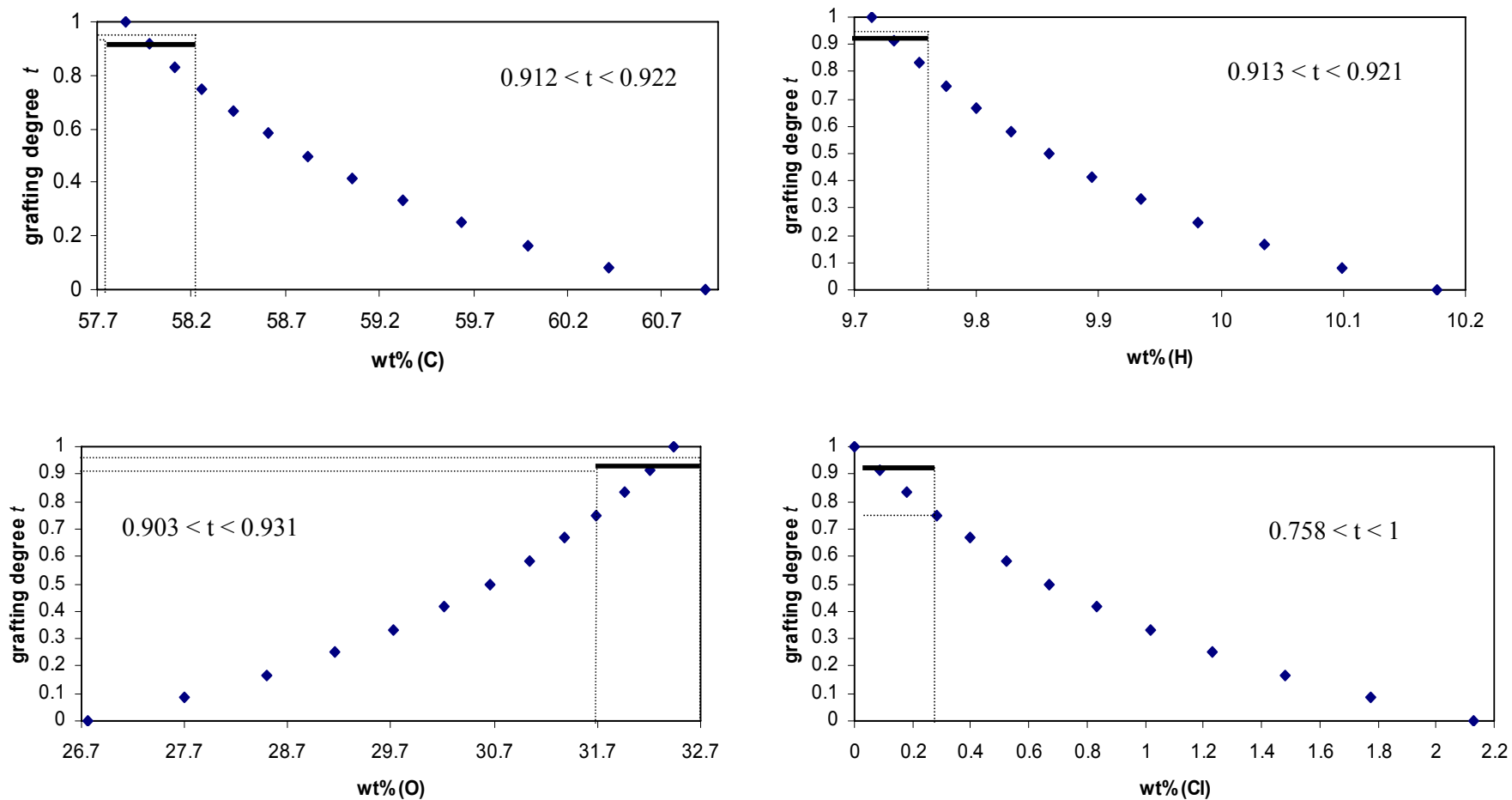


Figure 5.6. Charts of the grafting degree t as a function of the mass fraction of each element in $(\text{PMVE})_m\text{-(P-Cl)}_{1-t}\text{-(P-NH-CH}_2\text{-CH}_2\text{-(O-CH}_2\text{-CH}_2\text{)}_p\text{OCH}_3)_t$. Only the physically possible range of the graphs ($0 \leq t \leq 1$) is displayed; for the mass fraction from elemental analysis the uncertainty margins are given (C \pm 0.3%; H \pm 0.04%; O \pm 0.5%, and Cl \pm 0.2%).

Table 5.3. SEC/LS results of copolymers in THF as eluent.

Name	$M_{w\ SEC} (g.mol^{-1})$	dn/dc	M_w/M_n	$nb (N)$	$F_n \pm 0.05$
B1	19 700	0.056	1.16	/	/
B3	23 960	0.055	1.19	/	/
PEO 2000	2 120	0.060	1.12	/	/
G1	20 400	0.052	1.21	/	/
G2	23 980	0.020	1.40	3	0.92
G3	45 390	0.020	1.27	11	0.96

In all cases, the average molar mass of the backbones and the graft copolymers are narrow ($M_w/M_n < 1.5$). Moreover, in the case of the PMVE-*g*-PEO, the dn/dc values are smaller than their precursors due to the higher hydrophilicity of the grafts, which were absorbed on the column. This is also explained by their higher values of M_w/M_n . So, even if the F_n values are close to 1, few cross-linking polymers are still present in the pure graft copolymers.

All graft copolymers prepared were completely soluble in water and in organic polar solvents, and did not contain any gel. They remained soluble after more than two years of storage.

5.5. Conclusion

The aim of the present study was the synthesis and characterization of well-defined PMVE-based graft copolymers having PEO side chains of predetermined molar mass. First, by making use of model reactions, it was shown that the chlorine groups of the backbone could be substituted by benzylamine and TEG.

In conclusion, starting from CH_3O -PEO- NH_2 , PMVE-*g*-PEO copolymers were obtained with well-defined structure, the grafting degree of which was determined by a statistical non-linear least-squares approach.

5.6. References

- [1] (a) Hadjichristidis N., Pispas S., Floudas G., in 'Block Copolymers: Synthetic Strategies, Physical Properties, and Applications', Wiley-Interscience, 2002. (b) Hamley I., in 'Developments in Block Copolymer Science and Technology', J. Wiley & Sons, New-York, 2004. (c) Dimitrov I., Trzebicka B., Müller A.H.E., Dworak A., Tsvetanov C.B., Prog. Polym. Sci., 2007, 32, 1275.
- [2] (a) Dai L., in 'Intelligent Macromolecules for Smart Devices: From Materials Synthesis to Device Applications', Springer-Verlag: London, 2004. (b) Lequieu W., Shtanko N., Du Prez F.E., J. Membr. Sci., 2005, 256, 64. (c) Lynen F., Heijl J., Du Prez F.E., Brown R., Szucs R., Sandra P., Chromatographia, 2007, 66, 143. (d) Kumar A., Srivastava A., Galaev I.Y., Mattiasson B., Prog.

- Polym. Sci., 2007, 32, 1205. (e) Capadona J.R., Shanmuganathan K., Tyler D.J., Rowan S.J., Weder C., Science, 2008, 319, 1370.
- [3] (a) Schäfer-Soenen H., Moerkerke R., Berghmans H., Koningsveld R., Dušek K., Šolc K., Macromolecules, 1997, 30, 410. (b) Meeussen F., Bauwens Y., Moerkerke R., Nies E., Berghmans H., Polymer, 2000, 41, 3737. (c) Swier S., Van Durme K., Van Mele B., J. Polym. Sci., Part B: Polym. Phys., 2003, 41, 1824. (d) Van Durme K., Bernaerts K.V., Verdonck B., Du Prez F.E., Van Mele B., J. Polym. Sci., Part B: Polym. Phys., 2006, 44, 461. (e) Van Durme K., Loozen E., Nies E., Van Mele B., Macromolecules, 2005, 38, 10234. (f) Van Durme K., Rahier H., Van Mele B., J. Polym. Sci., Part B: Polym. Phys., 2006, submitted.
- [4] Nuyken O., Rieß G., Loontjens J.A., Van der Linde R., J.M.S., Pure Appl. Chem., 1995, A32, 217.
- [5] Nuyken O., Ingrish S., Macromol. Chem. Phys., 1998, 199, 711.
- [6] Hashimoto T., Ibuki H., Sawamoto M., Higashimura T., J. Polym. Sci., Part A: Polym. Chem. Ed., 1988, 26, 3361.
- [7] Van De Velde P., Goethals E.J., Du Prez F., Polym. Int., 2003, 52, 1589.
- [8] Candau F., Afchar-Taromoi F., Rempp P., Polymer, 1977, 18, 1253.
- [9] George M.H., Majid M.A., Barrie J.A., Rezaian I., Polymer, 1987, 28, 1217.
- [10] Piirma I., Lenzotti J.R., Polym. J., 1989, 21, 45.
- [11] (a) Wang Y., Du Q., Huang J., Macromol. Rapid Commun., 1998, 19, 247.
- [12] (a) Rieger J., Dubois P., Jérôme R., Jérôme C., Langmuir, 2006, 22, 7471. (b) Batardo L.A., Iruthayaraj J., Lundin M., Dedinaite A., Vareikis A., Makuska R., van der Wal A., Furo I., Garamus V.M., Claesson P.M., J. Colloid. Interf. Sci., 2007, 312, 21. (c) Van Durme K., Van Assche G., Aseyev V., Raula J., Tenhu H., Van Mele B., Macromolecules, 2007, 40, 3765. (d) Kang S., Asatekin A., Mayes Am., Elimetech M., J. Membr. Sci., 2007, 296, 42. (e) Neugebauer D., Reactive & Funct. Polym., 2008, 68, 535. (f) Mark P.R., Murthy N.S., Weigand S., Breitenkamp K., Kade M., Emrick T., Polymer, 2008, 49, 3116. (g) Bromberg L., J. Control. Release, 2008, 128, 99.
- [13] (a) Twaik M.A., Tahan M., Zilkha A., J. Polym. Sci., Part A: Polym. Chem., 1969, 1, 453. (b) Thierry A., Skoulios A., Makromol. Chem., 1977, 177, 319. (c) Wesslen B., Wesslen K.B., J. Polym. Sci., Part A: Polym. Chem., 1989, 27, 3915. (d) Berlinova I.V., Amzil A., Panayotov I.M., J.M.S., Pure Appl. Chem., 1992, 29, 975. (e) Wesslen B., Wesslen K.B., J. Polym. Sci., Part A: Polym. Chem., 1992, 30, 355.
- [14] Parrish B., Emrik T., Macromolecules, 2004, 38, 4023.
- [15] (a) Topp M.D.C., Dijkstra P.J., Feijen J., Macromolecules, 1997, 30, 8518. (b) Topp M.D.C., Hamse I.M., Dijkstra P.J., Feijen J., ACS Polym. Prepr., 1998, 39, 176. (c) Topp M.D.C., Leunen I.H., Dijkstra P.J., Tauer K., Schellenberg C., Feijen J., Macromolecules, 2000, 33, 4986.
- [16] Yin X., Stöver H.D.H., Macromolecules, 2002, 35, 10178.
- [17] (a) Bückmann A.F., Morr M., Johansson G., Makromol. Chem., 1981, 182, 1379. (b) Einarson M.B., Berg J.C., Langmuir, 1992, 8, 2611.

- [18] Zalipsky S., Gilon C., Zilkha A., E. P. J., 1983, 19(12), 1177.
- [19] (a) Gibson M.S., Bradshaw R.W., *Angew. Chem. Internat. Edit.*, 1968, 7(12), 919. (b) Debenham J., Rodebaugh R., Fraser-Reid B., *Liebigs Ann./Recueil*, 1997, 791. (c) Houllémare D., Outurquin F., Paulmier C., *J. Chem. Soc., Perkin Trans.*, 1997, 1, 1629. (d) Asahara M., Tanaka M., Erabi T., Wada M., *J. Chem. Soc., Dalton Trans.*, 2000, 3493. (e) Ilg K., Werner H., *Chem. Eur. J.*, 2001, 7(21), 4633.
- [20] Ringsdorf H., *J. Polym. Sci. Symp.*, 1975, 51, 135.
- [21] Donaruma L.G., *Progr. Polym. Sci.*, 1975, 4, 1.
- [22] Batz H.G., *Adv. Polym. Sci.*, 1977, 23, 25.
- [23] Zaffaroni A., Bonsen P., *Proc. Internat. Symp. Polym. Drugs*, p.1. Academic Press, New York, 1977.
- [24] Samour C.H., *Chemtech*, 1978, 494.
- [25] (a) Mutter M., *Tetrahedron Letters*, 1978, 31, 2839. (b) Rajasekharan Pillai V.N., Mutter M., Bayer E., Gatfield I., *J. Org. Chem.*, 1980, 45.
- [26] Geckeler K., *Polym. Bull.*, 1979, 1, 427.
- [27] Harris J.M., Struck E.C., Case M.G., Paley M.S., Yalpani M., Van Alstine J.M., Brooks D.E., *J. Polym. Sci., Part A: Polym. Chem.*, 1984, 22, 341.
- [28] Goodlett W., *Anal. Chem.*, 1965, 37, 431.
- [29] Decher H., Stadler R., *Polym. Int.*, 1995, 38, 219.
- [30] (a) Sørensen H.W., in 'Parameter Information', Marcel Dekker Edition, New York, 1980, p 61. (b) Fletcher R., in 'Practical Methods of Optimization', Wiley Edition, New York, 1991. (c) MATLAB Version 5.3, The Mathworks, Inc., Natick, MA, 1999.
- [31] Mercier F.A.G., Biesemans M., Altmann R., Willem R., *Organometallics*, 2001, 20, 58.

Chapter 6

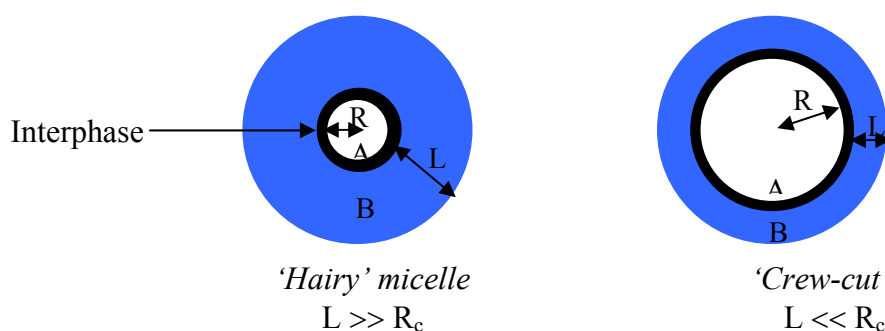
Thermo-responsive Properties of PMVE-*g*-PEO Graft Copolymers

6.1. Theory of Stimuli-responsive Micelles

6.1.1. Micelles

6.1.1.1. Definition

The association of amphiphilic block and graft copolymers, when they are dissolved in a selective solvent (e.g. water), leads to the formation of aggregates often called micelles because in most of their features they resemble those obtained with low- M_n -surfactants [1]. The micellar structure comprises the hydrophobic core, where the insoluble blocks are located, surrounded by a swollen protected corona of soluble blocks. The micelles formed by AB block or A-*g*-B graft copolymers can be classified into two main categories: the *hairy* (or starlike) micelles and the *crew-cut* micelles (scheme 6.1).



Scheme 6.1. Schematic view of AB diblock or A-*g*-B graft copolymer micelles in a selective solvent for the B block. R_c : micellar core radius; L: shell or corona thickness formed by the soluble blocks.

In the former case the insoluble blocks that form the micellar core are short compared to the soluble blocks located in the corona, whereas the opposite ones characterize the second

case. The association of the hydrophobic parts of the block copolymers occurs at a given polymer concentration, often regarded as a critical micelle or aggregation concentration, which greatly depends on the HLB of the polymer. In aqueous solutions of stimulus-responsive, intelligent copolymers, the interaction of one or several parts of the copolymer can be triggered by changes in the surroundings of the parts of the spherical core-shell structures [2-4]. They are switchable amphiphiles in which the solubility properties of each block can be altered by changing the solution pH [5-6], ionic strength [6], temperature [7-12] or by interaction with added substrates [13].

6.1.1.2. Thermodynamics

Micellization in aqueous solutions is caused by the hydrophobic effect driven by an enthalpic process [14]. The negative standard free energy change to transfer 1 mol of amphiphile from the solution to the micellar phase, ΔG_m^0 , is given in terms of the dominant standard enthalpy ΔH_m^0 , and the negative standard entropy ΔS_m^0 of micellization per mol of surfactant as :

$$\Delta G_m^0 = \Delta H_m^0 - T \Delta S_m^0$$

The micellization free energy values are negative, since thermodynamically stable micelles are formed spontaneously. The presence of the hydrophobic moieties in water induces an increase in the degree of structuring of water molecules, owing to cavity formation and causes a significant decrease in the water entropy. When hydrophobic groups aggregate in the aqueous solution to form micelles, the random hydrogen-bonding structure in the water is to large extent restored, and the water entropy increases. This overcomes the loss of entropy due to localization of the hydrophobic groups in the micelles. The entropy contribution usually dominates the micellization process in aqueous surfactant solutions, with the enthalpy playing a minor role. For many nonionic surfactants ΔH_m^0 is positive, indicating that the transfer of unimers from the solution to the micelles is an enthalpically disfavored endothermic process [15-16].

Micellar aggregate formation occurs in dilute solutions of block/graft copolymers in a selective solvent at a fixed temperature above a critical micelle concentration (CMC), which is also called critical association concentration for polymeric micelles. This formation is accompanied by a sharp change in several solution properties (light scattering, viscosity, electrical conductivity, surface tension, solvent power for certain substances, etc.). The free energy of micellization for nonionic surfactants is directly proportional to the logarithm of CMC (when CMC is in mol fraction units) by the following relation [17]: $\Delta G_m^0 = RT \ln(\text{CMC})$

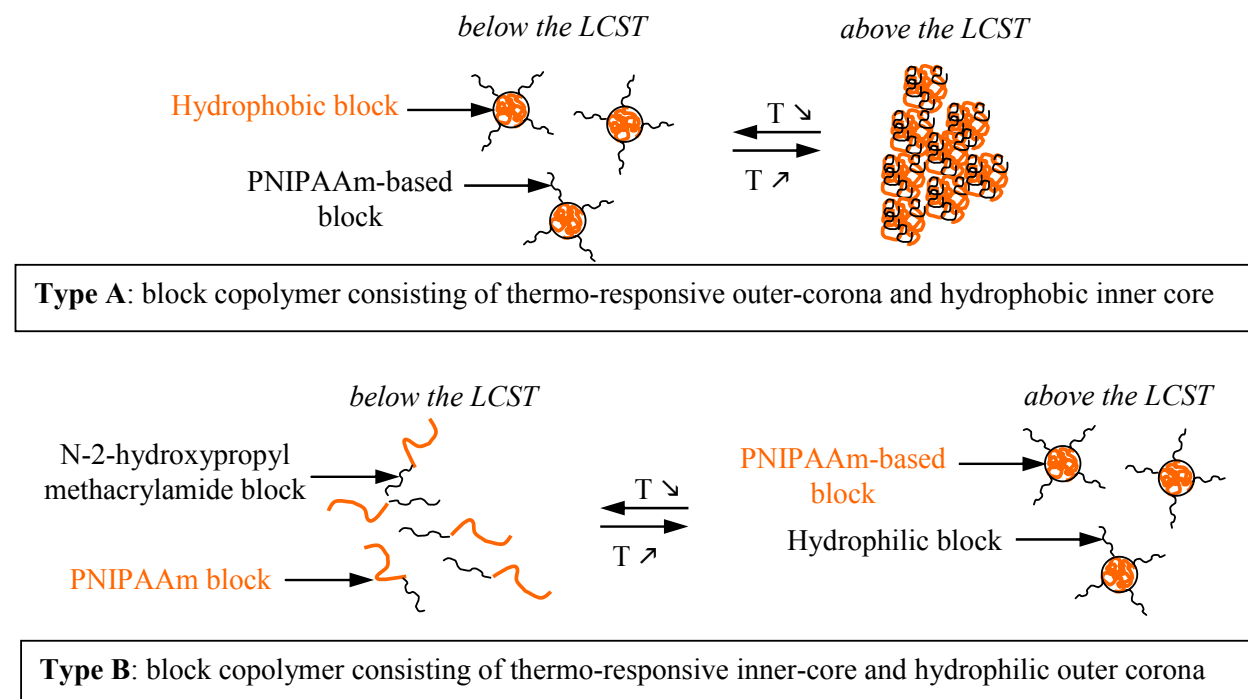
The magnitude of the hydrophobic effect increases with temperatures [15]. ΔG_m^0 becomes more negative, indicating a larger driving force for micellization.

6.1.1.3. Behaviour of the Micelles

During the last decade, stimuli-responsive micelles, as a function of temperature or pH or both, have been studied world-wide, such as by Tenhu [7,18], Armes [19], Okano [20], Webber [21], Kim [22], Aoshima [23], and Gohy and Jérôme [24-25].

Temperature as External Stimulus

Whenever a constitutive block is temperature sensitive, with e.g. a LCST, an appropriate temperature can trigger reversible micellization in water. Two types of micellar structures containing thermo-responsive polymers (e.g. PNIPAAm) can be considered; thermo-sensitive outer corona and thermo-sensitive inner core (scheme 6.2). In the former case, PNIPAAm block has been usually copolymerized with hydrophobic blocks [26]. In the latter case, PNIPAAm segments were combined as a hydrophilic block copolymer [27]. Note that in our work, PMVE was combined on one hand with hydrophilic PEO segments, and on the other hand with hydrophobic PS segments (see scheme A1 in **Introduction**).



Scheme 6.2. Two types of the micellar structure of a block copolymer containing a thermo-responsive polymer segment. Figure taken from [26-27].

An interesting thermo-responsive switching system was developed by Laschewsky [28] from sequential controlled free radical polymerization of non-ionic and zwitterionic monomers. The resulting block copolymers showed one thermo-responsive segment in aqueous solution with one block exhibiting a LCST and the other an upper critical solution temperature (UCST). At intermediate temperatures both blocks were soluble, but an increase or decrease of the temperature provoked the formation of colloidal polar aggregates with one or the other block constituting the core. Kim and coworkers [29] prepared triblock copolymers poly(ethylene oxide)-*block*-poly(lactic-*co*-glycolic acid)-*block*-poly(ethylene oxide) (PEO-*b*-PLGA-*b*-PEO) that formed

micelles in water due to the hydrophobicity of the PLGA block. They demonstrated that the CMC decreased with increasing temperature.

pH as External Stimulus

Block copolymers with one block, which is either a polyacide or a polybase, can self-assemble into micellar structures upon changing pH. The originally ionized block becomes hydrophobic, either by protonation of anionic groups, or deprotonation of cationic groups, whereas the second hydrophilic remains water-soluble.

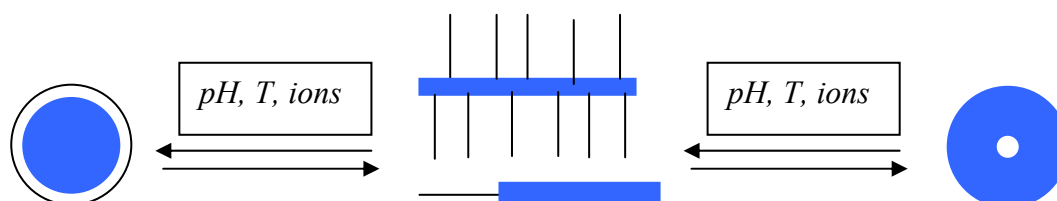
Addition of a base to an acidic aqueous solution of glycopolymers based on cyclic sugar-methacrylate hydrids triggers micellization [30]. An excess of base led to deprotonation of the second block and, consequently, to precipitation of the copolymer. Acidification from pH 8 to 3 of poly(sodium 4-vinylbenzoate)-*block*-poly(ethylene oxide methacrylate) is also efficient in forming micelles in water [31].

Ionic Strength as External Stimulus

Although poly(2-(N-morpholinoethyl)methacrylate) is water soluble at low pH, it precipitates upon addition of electrolytes. Therefore double hydrophilic block copolymers that contain this constitutive block can form micelles by tuning the ionic strength. An example is poly(2-(N-morpholino) ethylmethacrylate)-*block*-poly(diethylaminoethylmethacrylate) (PMEMA-*b*-PDMAEMA) that forms micelles reversibly upon the proper adjustment of pH and salt addition [3]. Micelles with PDMAEMA core can be formed at pH ranging from 4 to 8.5, whereas reverse micelles with a PMEMA core can be prepared at pH 6-6.7 upon addition of Na₂SO₄.

Multi-responsive External Stimuli

Several examples of self-assembled structures with multi-stimuli responsive aptitude have been described in the literature. As a result of changes of temperature, pH and ionic strength, block and graft copolymers can self-assemble into micelles or vesicles (scheme 6.3).



Scheme 6.3. Reversible micellization of diblock and graft copolymer under the influence of external stimuli.

For instance, Armes *et al.* described ‘schizophrenic’ diblock copolymers that form direct and inverse micelles in the same solvent. One example is a more complex zwitterionic diblock of poly(4-(vinylbenzoic acid))-*block*-poly(2-(N-morpholino) ethylmethacrylate) (PVBA-*b*-PMEMA) that can respond to pH, ionic strength and temperature, and form normal as well as inverse micelles [32]. At low pH, they obtained micelles with a 4-vinylbenzoic acid (VBA) core, and at high pH and in the presence of salt, or at high temperatures, micelles with a 2-(N-morpholino)

ethylmethacrylate (MEMA) core. A versatile system as proposed by Nowakowska [33] who synthesized a series of amphiphilic terpolymers based on sodium 2-acrylamido-2-methyl-1-propanesulfonate (AMPS), NIPAAm, and cinnamoyloxyethylmethacrylate (CEMA). The terpolymers were soluble in water, prone to self-assemble into micelles, and sensitive to three stimuli: i) temperature, due to the NIPAAm block that imposed a LCST, ii) UV-light, due to the presence of the CEMA block, and finally iii) ionic strength, that at elevated concentration provoked loss of the temperature-sensitivity. The size of the micelles formed, as indicated by DLS, was found to vary with temperature and UV irradiation.

6.1.1.4. Applications of Stimuli-responsive Micelles

Current and potential application possibilities of copolymer colloidal assemblies are their use as stabilizers, flocculants, nanoreservoir in, among others, controlled delivery of bioactive agents, catalysis, latex agglomeration and stabilization of non-aqueous emulsion.

Solubilization of Active Components in Block Copolymer Micelles: Biomedical Applications

In addition to their applications as biomaterials, such as implants, block copolymers have found since four decades a strong interest in their colloidal form especially as control drug delivery systems [34], as carriers of diagnostic agents and more recently in gene therapy [35].

Adsorption and Surface Modification by Block Copolymer Micelles

Block copolymers, like homopolymers, are known to adsorb on solid surfaces. A great number of experimental and theoretical studies have been published concerning the surface modification by adsorption or chemical attachment of polymer micelles in order to promote specific characteristics, e.g. wetting, dispersibility [36] and stabilization of solid pigment particles in a liquid or in a solid phase, improved biocompatibility, etc.

Dye Stabilization

Recently, our research group has developed a series of amphiphilic PMVE-*b*-PIBVE copolymers, showing remarkable thermo-adjustable surfactant properties [37]. In addition, these polymers are very well suited to create colloidal dispersions of organic pigments, displaying stabilities that can be tuned as a function of temperature [38].

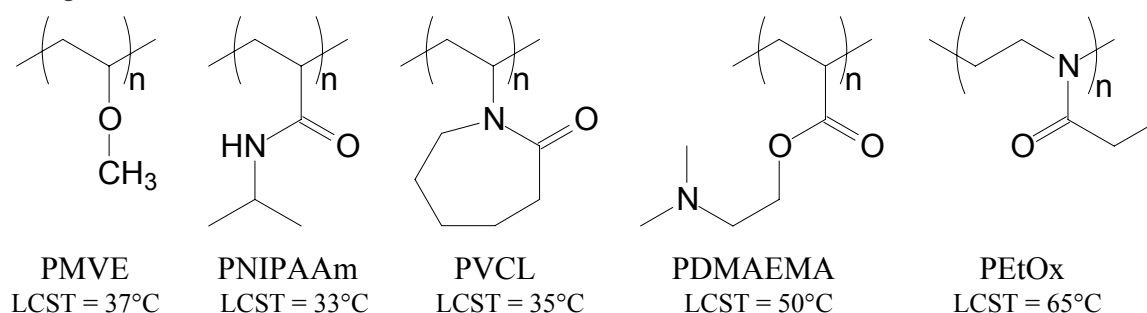
Miscellaneous Applications

The variety of block copolymers which are available, offer different applications as emulsifiers [39-40], as stabilizer in latex technology [39,41-42], as compatibilizers in polymer blends [39,43] and as active component in separation processes [44]. Thus the ability of micelles to solubilize or encapsulate various compounds for biomedical applications [45], can also be employed for purification and separation processes as well as for specific chemical reactions. For example, if removal of oil and organic pollutants in waste water was already achieved with conventional surfactants, the use of block copolymers such as Poloxamers, Pluronics (BASF) or Superonics

(ICI) (PEO-PPO) could significantly improve these processes [44,46]. Ion complexation by block copolymers is not only attracting interest in biomedical applications, but also in catalysis [47], in solar energy-conversion and photoinduced electron transfer processes [48]. Block copolymers are of practical use as viscosity improvers of motor oil, which may be related to association-dissociation of their micelles as a function of temperature [49], and also efficient dispersants and stabilizers for carbon black, a good model for sludge [50]. The platelet structures generated from PEO-PEP diblock copolymers by crystallization of their PEO sequence are efficient pour-point depressing additives for fuel oils [51]. Such platelets are further claimed as efficient stabilizers for polymeric oil-in-oil emulsions of large particle size [52].

6.1.2. The Theory of the Lower Critical Solution Temperature (LCST)

Thermo-responsive polymers have attracted much attention for applications such as drug delivery, membranes and cell culture [53-54]. The LCST is the temperature at which aqueous solutions or hydrogels undergo a transition from a soluble to an insoluble or opaque state or from a swollen hydrogel to a contracted shape as the temperature increases [54-55]. The relative magnitude of the hydrophobic effect increases as the temperature of the aqueous solution is increased [56], and the unfavorable contribution of entropy is enhanced. This may lead to the chain contraction, and eventually to a phase separation if the balance between hydrophobic and hydrophilic groups is appropriate. This type of phase behavior is typical for a large number of non-ionic water soluble polymers [57], such as PNIPAAm [58-59], poly(N-vinyl caprolactam) (PVCL) [60-62], PMVE [25,60-69], PEO (LCST = 95°C) [70], poly(2-ethyl-2-oxazoline) (PEtOx) [71-72] and poly(2-(N,N-dimethylamino) ethylmethacrylate) (PDMAEMA) [72-73]. Scheme 6.4 represents the chemical structures of these polymers that are known to exhibit a LCST-type of demixing behavior.



Scheme 6.4. Structures of thermo-responsive polymers, from left to the right: PMVE, PNIPAAm, PVCL, PDMAEMA and PEtOx.

The large difference in LCST between these materials results from a different HLB in water. Among these polymers, PNIPAAm is definitely the most studied one, because its phase separation in water is very abrupt and completely reversible with temperature [58]. Other polymers of interest are PVCL and PMVE. The former material, in contrast to PNIPAAm, is biocompatible and has therefore attracted much attention in recent years. For that reason the Food and Drug Administration (FDA) has approved this material for biomedical use. In this work,

we will focus on PMVE-system that phase separate at physiological temperatures, as these are promising towards biomedical applications.

6.1.2.1. Thermodynamics

Under certain thermodynamic conditions, a homogeneous polymer solution or mixture can separate into two or more liquid phases that differ in composition. For example, a binary polymer solvent mixture can separate into a dilute and a concentrated phase when the temperature increases. This phenomenon is called temperature-induced phase transition. Figure 6.1 represents a schematic phase diagram of a polydisperse polymer solution having UCST and LCST behavior with the concentration as a function of the temperature, in which UCST and LCST are the maximum and the minimum temperature respectively, in the phase separation curve.

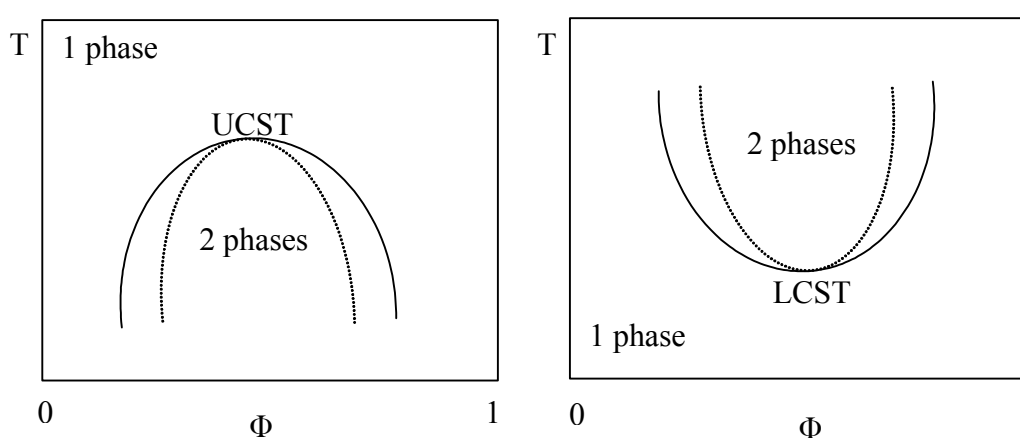


Figure 6.1. Scheme of phase diagram for binary polymer mixtures: spinodal (----) and binodal (—) lines of: UCST-type of phase diagram (left) and LCST-type of phase diagram (right). Figure taken from [69].

In the low temperature region of the diagram the system is stable, which means that the polymer and solvent are compatible in every ratio, leading to one homogeneous concentrated or dilute phase. An increase in temperature will encounter the miscibility gap and induce the formation of two-phase emulsions after some delay which is due to the need for droplets of a new phase to be nucleated. The onset of phase separation is the so-called *cloud point* of the solution and the temperature T_{cp} varies with the concentration resulting in the cloud point curve. At high temperature, the system will spontaneously phase separate by a kinetic mechanism. Approaching the temperature of the metastable region allows the irregular fluctuation regions of the spherical droplets leading to the formation of an emulsion. Another special point in the phase diagram is the *critical point*, where both curves touch each other and share a common tangent as required by thermodynamics. The temperature at which this occurs can either be situated at the lowest temperature where two phases can coexist LCST or at the highest temperature UCST. The latter situation defines a mixture in which miscibility improves by increasing the temperature (figure 6.1 left), while the opposite occurs in the former situation (figure 6.1 right).

The LCST phenomenon has been observed in strongly interacting polar mixtures of small molecules as well as interacting non polar polymer mixtures, especially hydrogen bonding. Even though LCST behavior can be caused by strong interactions or compressibility effects, or a combination of both, the separation is always entropically driven. This can easily be demonstrated via thermodynamics. For compressible mixtures it is convenient to work with the Gibbs free energy according to the second law of thermodynamics [74]: $\Delta G_m = \Delta H_m - T \Delta S_m < 0$

with ΔG_m the Gibbs free energy change upon mixing at constant temperature and pressure, ΔH_m the enthalpy of mixing, ΔS_m the entropy of mixing. Large negative contributions to both ΔH_m and ΔS_m are caused by the ordering of the aqueous solution with the polymer. When the polymer chains are mixed at low temperature, heat is released ($\Delta H_m < 0$) owing to the preferentially favorable attractions. When the temperature reaches the LCST (or T_{cp}), ΔH_m increases and the entropy contribution of ΔG_m will overcome the negative enthalpy solution. Thus, ΔG_m takes a positive value, and the phase separation of the polymer solution begins.

6.1.2.2. The Phase Diagrams: Type I, II, III

Solutions of water-soluble polymers in water can be described by phase diagrams with LCST or UCST [57]. To facilitate the description of the phase-separation phenomenon of aqueous polymer solutions, it is useful to classify them according to the phenomenological analysis of their critical miscibility with water in three types. The three types of phase behavior are schematically illustrated in figure 6.2; they were calculated with the ΔG_m developed by Flory [75], Huggins [76], Staverman and Van Sante [77].

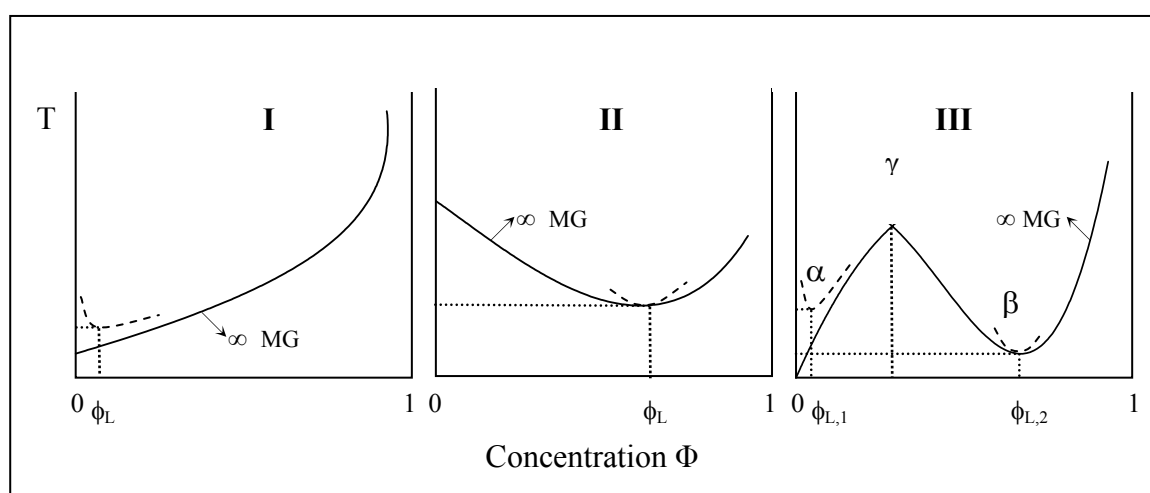


Figure 6.2. Scheme of three types of phase diagram of linear polymers with a LCST-behavior with increase of molecular weight (MG) (the full curve is the equilibrium of the polymer with ∞ MG). Figure taken from [69].

Polymers of Type I follow the classical Flory-Huggins behavior, which means that the LCST of polymers of this type shifts upon increasing the polymer molar mass towards lower

polymer concentrations and lower temperatures (figure 6.2 left). Type I, also called the ‘classical’ demixing behaviour, exhibits the usual Θ behavior and is characterized by a limiting critical concentration, for infinite molar mass, $\Phi_L = 0$ (volume fraction). With Type II, a single off-zero limiting critical concentration, $\Phi_L \neq 0$, occurs at non- Θ -conditions. Type II demixing refers to a miscible gap with a single extremum, the location of which in temperature/concentration space is equally insensitive to molar mass and occurs at a polymer weight fraction around 0.5 (figure 6.2 middle). Type III is characterized by two off-zero limiting critical concentrations and one zero limiting critical concentration (figure 6.2 right). Hence, three different two-phase areas can be distinguished: α , β and γ . The critical point at low polymer concentration again represents the classical Flory-Huggins demixing behavior, while the β -domain displays Type II demixing behavior. Both areas are separated from the γ -domain by a three-phase equilibrium.

According to this classification, the solution properties of these three thermo-responsive polymers, PVCL [78-79], PNIPAAm [80-81] and PMVE [64-67] can be described by different phase diagrams, Type I, Type II and Type III respectively.

6.1.2.3. PMVE Phase Diagram

Aqueous solutions of PMVE are known to cloud in a temperature window ranging from 32 to 40°C, depending on molar mass and concentration [82]. This LCST-behaviour is more complex than can be expected from ‘classical’ theoretical considerations. The phase diagram of PMVE in water, identified by a Type III, is bimodal and the two minima show a different molecular mass dependence [65]. The minimum of lower polymer concentration (5 wt-%) corresponds to Type I behavior, according to the phenomenological classification of Berghmans [65], whereas the one of higher concentration (75 wt-%) is transition of Type II (figure 6.3) and is molar mass independent [64-67,81].

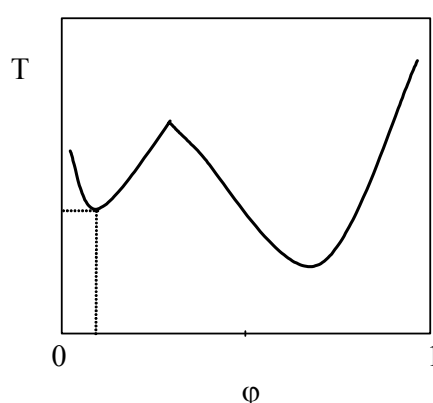


Figure 6.3. Schematic phase diagram for PMVE-water mixture that exhibits two LCST's. Figure taken from [69].

From the structural considerations, it is obvious that in the system PMVE/water, complex formation between the water molecules and the ether functions of the repeating units may be responsible for the non-classical phase behavior. Experimental evidence was already brought by Maeda *et al.* in the 90's [67,83]. The formation of a stable molecular complex with 2.7 molecules

water per chain repeat unit was proposed. At higher overall water content, a higher degree of hydration was suggested with up to five water molecules per repeat unit. Moreover, in 2001, the PMVE/water interactions during the phase transitions were studied by another Maeda with IR spectroscopy [84], and more recently by Van Mele with MTDSC technique [85-87]. This technique provides detailed information on the hydration states of individual functional groups of PMVE below and above the T_{cp} . In solutions below the phase transition, the ether oxygens of the polymer units form hydrogen bonds with water molecules. This enthalpic contribution to the free energy of solution overrides the unfavorable decrease in entropy due to the formation of a layer of organized water around the hydrophobic moieties of the polymer chain. With increasing temperature, from about 33 to 40 °C, the hydrogen bonds between water molecules and the polymer ether oxygens are broken and, at the same time, nonpolar groups are dehydrated. This is accompanied by an endothermic heat effect and a rising opacity of the PMVE/water solution [63-67,84-85,88-89]. These changes in PMVE/water interactions are reflected by changes in the IR bands attributed to the vibration modes of the PMVE backbone bonds and the methoxy groups. Maeda concluded that most of the methyl groups of PMVE are dehydrated above the transition temperature, whereas the ether groups are only partially dehydrated.

In the last decade Spěváček *et al.* used ^1H NMR spectroscopy to investigate changes in the dynamic structure during temperature-induced phase separation in PMVE solutions in a broad range of concentrations ($c = 0.1 - 30$ wt-%) [90]. The phase transition is manifested by line broadening for a major part of PMVE units, indicating the formation of more compact globular-like structures. While for dilute PMVE solutions the transition as detected by NMR is virtually discontinuous for semidilute and concentrated solutions, the transition sets in at lower temperatures and is several Kelvin broad.

6.1.2.4. Applications

The temperature dependent solubility of this type of polymers has fascinated scientists both in academia and industry since the first observations of the thermo-sensitivity of PNIPAAm [91], PVCL [61] and PMVE. Based on controllable change of conformation of a polymer, various smart structures may be created that are sensitive to external stimuli, in this case to temperature.

Thermo-responsive Membranes

For example, a thermally responsive polymer can be cross-linked to form a responsive hydrogel, or a porous surface can be grafted with smart polymers to have controllable porosity and be used as thermally responsive filter unit [92].

Temperature-responsive Chromatography

A new packaging material for High Performance Liquid Chromatography (HPLC) was developed by grafting PNIPAAm onto silica beads. As a result the hydrophilic-hydrophobic nature of the surface can be varied with temperature, which changes the interaction with solutes in the

continuous aqueous phase. At low temperatures, the surface is hydrophilic and the separation selectivity of for example steroids is not that good [93]. However, by increasing the temperature the hydrophobic interaction between PNIPAAm and the steroids is favored, which results in longer retention times for more hydrophobic steroids and a better separation selectivity.

Recently, in our research group, columns were packed with a temperature responsive stationary phase based on PNIPAAm attached to aminopropyl silicagel [94]. The temperature responsive properties of the coupled phase were demonstrated using only water as a mobile phase, whereby an increase in retention is observed with raising temperature. Such temperature responsive stationary phases open perspectives for green chromatography.

Biomedical Applications

Based on the thermo-responsiveness, several applications are proposed in drug delivery, bioseparation, diagnostics, etc [95]. PNIPAAm has been used, for example, in drug targeting for solid tumors with local hyperthermia [94], in thermo-responsive coatings or micelles for controlled release of the drug [96], and as a cell attachment/detachment surface [97]. The use of PVCL and PMVE instead of PNIPAAm is however considered advantageous because of their assumed lower toxicity [98].

Thermo-precipitation Separation

A recognition biomolecule or receptor ligand such as a cell receptor peptide or an antibody is conjugated to an intelligent polymer and used in a precipitation-induced affinity separation process. When mixed with a complex solution, the conjugate will selectively complex its binding partner and then it can be readily and cleanly separated by providing a thermo-stimulus, which causes the polymer-ligand/receptor conjugate/complex to precipitate [99].

At the moment, the number of studies on PMVE is still low, at least compared to those on PNIPAAm and PVCL.

6.2. 'Cloud Point' Studies of the Thermo-responsive Random Copolymers

6.2.1. Introduction

The stimulus that has been most important in these studies is temperature. For this, PMVE has been chosen as the backbone of the graft copolymers because of its thermo-responsive properties. Recently, in our research group, linear and palm-tree block copolymers containing the PMVE as thermo-responsive segment have been explored for emulsion properties and micellization [25,37-38,100]. Similar observations were made for poly(methyl vinyl ether)-*block*-poly(vinyl alcohol) (PMVE-*b*-PVA) where micellization was reported to occur near the T_{cp} of the PMVE homopolymer at 29°C [101]. A more detailed study of poly(methyl vinyl ether)-*block*-

poly(methyl tri(ethylene glycol)vinyl ether) (PMVE-*b*-PMTEGVE) showed that micellization occurred in a limited temperature range only between the T_{cp} 's of homopolymers PMVE and PMTEGVE with the latter having the higher T_{cp} [19]. At temperatures above the T_{cp} 's of both homopolymers, the whole block copolymer became insoluble and precipitation occurred as determined by turbidimetry. Block copolymer T_{cp} s strongly depend on the relative block length of the two blocks and can thus be adjusted between the values for both homopolymers. These thermo-responsive properties in aqueous environment originate from the LCST behaviour of the incorporated PMVE segments [63,66-67,88,102].

The T_{cp} 's of the PMVE statistical copolymers with a small amount of hydrophobic units IBVE or CEVE in aqueous solution, were studied by turbidimetry and modulated temperature differential scanning calorimetry (MTDSC).

6.2.2. Determination of the 'Cloud Point' Temperature of P(MVE-co-IBVE)

The T_{cp} 's were determined for each copolymer using two methods: visually when the solution becomes cloudy and by UV-VIS spectrophotometry. Both methods provided the same T_{cp} values within experimental error range. The T_{cp} 's of the homopolymer and the copolymers with different IBVE ratios are displayed in table 6.1.

Table 6.1. Comparison of the T_{cp} of PMVE and P(MVE-co-IBVE) in water solution as a function of their composition with 0.25 wt-% aqueous solution.

Polymers	M_n NMR (g.mol ⁻¹)	MVE units	T_{cp} (°C)
PMVE ₇₀	4140	70	36
PMVE ₃₀	1820	30	40
P(MVE-co-IBVE) (94/6)	3280	50	10
P(MVE-co-IBVE) (93/7)	3470	52	/

The first observation is that the T_{cp} 's of P(MVE-co-IBVE) are lower than those of PMVE₇₀. This results from the decrease with increasing hydrophobic units in the hydrophilic PMVE. Concordantly, the LCST phenomenon, typical for PMVE, disappears when the copolymer contains more than 7% weight fraction (i.e. 6% molar fraction) of IBVE. It may be concluded that the LCST of PMVE of molecular weight 3000 g.mol⁻¹ is already strongly influenced by the presence of one or two IBVE units in the PMVE-chain. With 6 mol-% of IBVE (i.e. a polymer consisting of 50 MVE units and 3 IBVE units), the cloud point was determined to be 10°C (0.25 wt-% aqueous solution). Moreover, the strong influence of the presence of small fractions of

hydrophobic groups on the LCST-properties was reported earlier by Du Prez, Van Mele and others for PMVE's containing hydrophobic end groups [85,103].

6.2.3. Influence of Incorporating CEVE Units in PMVE Backbone

It was found that the grafting process was not quantitative, causing some chlorine groups to be present in the PMVE backbone (see **Chapter 5**). Because of its hydrophobic character, the remaining CEVE units will most likely affect the thermo-responsive properties of the synthesized graft copolymers. Therefore, we will first evaluate the thermo-responsiveness of P(MVE-*stat*-CEVE) in aqueous solution.

6.2.3.1. UV-VIS Transmission

In order to estimate the effect of PEO-grafting on the LCST phase behaviour of PMVE in water, we should first investigate the water solubility of the backbone material, used to synthesize the graft copolymers. LCST behaviour of the statistical copolymers was tested by preparing a series of 2 mL solutions with varying concentrations, placing them at 4°C in darkness overnight and then determining the T_{cp} by UV-VIS spectrophotometry. The easiest method to determine the T_{cp} of a polymer solution consists of measuring the changes in turbidity as the solution is heated at a constant rate. The temperature of turbidity onset is defined here as the T_{cp} .

An example of such a measurement is given in figure 6.4 for different concentrations of B1. The temperature was changed in the range from ambient temperature up to 50°C, and the copolymer concentrations varied between 1 and 15 mg.mL⁻¹. As can be observed, the turbidity increased sharply as the temperature exceeds this onset value and the transparency changes rather continuous because of the thermo-sensitivity of the copolymers decreased with the concentration.

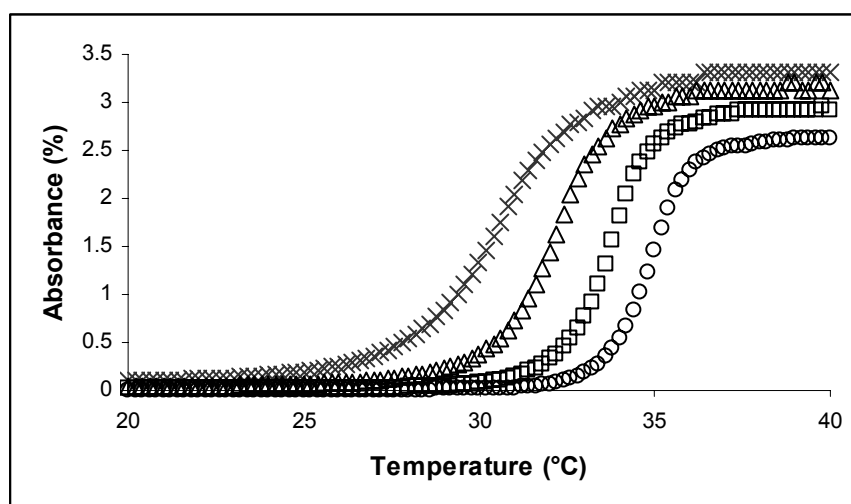


Figure 6.4. UV-VIS measurements as a function of temperature (0.2 °C.min⁻¹) for different concentrations of B1 with 15 mg.mL⁻¹ (x), 10 mg.mL⁻¹ (Δ), 5 mg.mL⁻¹ (□) and 1 mg.mL⁻¹ (○).

At such concentrations ($< 15 \text{ mg}\cdot\text{mL}^{-1}$), the absorbance of the copolymer solutions sharply increased on heating, which reflects the decrease in the solubility of the copolymer resulting in an aggregation process. Above the cloud point, water is a thermodynamically poor solvent and interaction between the repeating units of the polymers is attractive. This results in a macroscopic phase separation of concentrated polymer solutions followed by intermolecular aggregation. No precipitation was observed at higher temperature, but the solution remained cloudy over a long period (two months). For all the samples, an increasing concentration leads to a lower value of the T_{cp} . This is in correspondence to the general accepted LCST principle for dilute solutions: a higher water content leads to more polymer/water interactions, thus more thermal energy is needed to break the water structure and consequently to let the hydrophobic polymer/polymer interactions rule out the polymer/water interactions.

To ascertain the reversibility of the phase transition, polymer solutions heated to 45°C were brought to room temperature at constant cooling rate. The solutions became clear in all cases comparable to the initial solution, and the LCST was the same as the T_{cp} recorded during a heating scan.

In addition, the phase behaviour curve of PMVE homopolymer and P(MVE-*stat*-CEVE) backbones has been plotted in figure 6.5. In this study, the T_{cp} 's are ranged from 27 to 39°C . A remarkable observation is that the T_{cp} of the copolymers is already much affected by a small content of hydrophobic CEVE units. When the molar fraction of CEVE is above 3 mol-% of the total molar number of monomer units, the copolymers are completely insoluble in water. The T_{cp} 's, determined by UV-VIS, were plotted versus the concentration (up to $15 \text{ mg}\cdot\text{mL}^{-1}$) in figure 6.5.

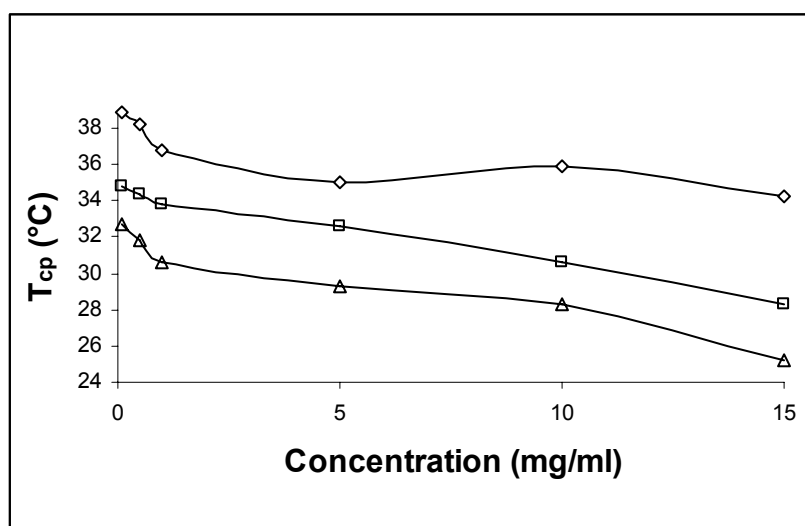


Figure 6.5. Cloud points temperature curves of the homopolymer PMVE₂₀₆ ($12\,000 \text{ g}\cdot\text{mol}^{-1}$) (\diamond), the statistical copolymers B1 (1.73 mol-%CEVE) (\square) and B2 (3.61 mol-%CEVE) (Δ).

It was found that the incorporation of CEVE-groups in the PMVE chain leads to decrease of the T_{cp} (from 35.9 to 33.3°C with 1.73 mol-% CEVE for a $10 \text{ g}\cdot\text{L}^{-1}$ aqueous solution). For that reason, statistical copolymers were synthesized with a small number of chlorine in order to keep

the thermo-responsive properties of the PMVE. The presented results establish that the system P(MVE-*stat*-CEVE)/water behaves like the demixing curve of PMVE with a shift depending on the composition of CEVE present in the copolymers.

6.2.3.2. Modulated Temperature Differential Scanning Calorimetry (MTDSC)

The MTDSC measurements were made by El Ouaamari and Dr. Van Durme with the collaboration of Prof. Van Mele (VUB) in Brussels [104-105]. For the theoretical description of the technique, we refer to the experimental section (**Part IV**).

Figure 6.6 illustrates the influence of incorporating CEVE units on the LCST phase behaviour of PMVE in water. The incorporation of CEVE units clearly lowers the T_{demix} of the PMVE-based polymer, indicating that the hydrophobic CEVE groups partially destroy the hydration structure surrounding the PMVE chains. The observed decrease in T_{demix} becomes more pronounced as the amount of CEVE units increases, independent of the polymer concentration (figure 6.6, compare P(MVE-*stat*-CEVE) with 1.73 mol-% (●) and 3.61 mol-% CEVE (○)). Hence, the initial hydrophilic polymer becomes insoluble in water at room temperature, especially at high polymer concentration, thus limiting the number of potential applications. In addition, it seems that the characteristic bimodal shape of the type III LCST demixing curve is also influenced by the copolymerization with CEVE.

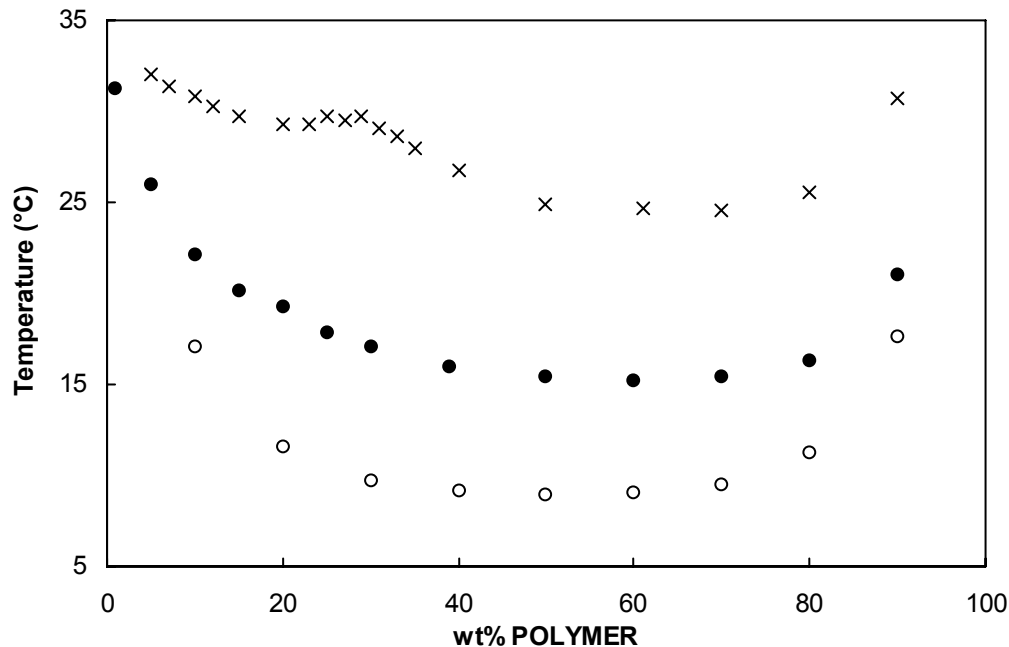


Figure 6.6. LCST demixing curve of PMVE/water (x), P(MVE-*stat*-CEVE) with 1.73 mol-% CEVE/water (●) and with 3.61 mol-% CEVE/water (○). Figure taken from [105].

6.3. Effect of the Temperature on the PMVE-*g*-PEO

6.3.1. Introduction

The most well-known water-soluble polymer is probably PEO, which is discussed in detail e.g. by Kjellander and Florin [106]. Various thermo-responsive copolymers containing PEO grafts have been synthesized and studied widely over the recent years. Copolymers consisting of thermo-responsive PNIPAAm and PEO blocks or grafts are one of the most investigated over the recent years because of their stabilization of dispersions and emulsions [58,107]. Below the T_{cp} of the PNIPAAm block, either poly(ethylene glycol)-*block*-poly(N-isopropylacrylamide) (PEG-*b*-PNIPAAm) or poly(ethylene glycol)-*graft*-poly(N-isopropylacrylamide) (PEG-*g*-PNIPAAm) is highly soluble in aqueous solution, while above the T_{cp} , the thermo-responsive PNIPAAm block precipitates and the copolymer self-assembles into polymeric micelles, which consists of a PNIPAAm core and a hydrophilic shell of PEG [9,108-110]. Tenhu *et al.* studied the aggregation of PEG-*b*-PNIPAAm in water by fluorescence spectroscopy and light scattering [9]; Zhu and Napper studied the gelation of PEG-*b*-PNIPAAm [111]; Wu *et al.* studied the formation of core-shell nanoparticles of PEG-*g*-PNIPAAm through the coil-to-globule transition of the PNIPAAm block [108]; Feijen *et al.* studied the thermosensitive micelle formation of PEG-*b*-PNIPAAm [110].

The properties of thermo-responsive PNIPAAm or PVCL with PEO, block and graft copolymers have recently attracted a lot of attention by Tenhu [7,11-12,108,112-114] and Du Prez [10,62,79,81], because of its intrinsic and technological significance, in particular the temperature-responsive micellization. The interest in these thermo-responsive polymers comes from the fact that their demixing temperature can be tuned closed to body temperature. In contrast to PVCL (Type I) and PNIPAAm (Type II), limited number of studies have been carried out on PMVE containing copolymer structures. To our knowledge, only block and random copolymers based on PMVE have been investigated until now. On the other hand, PMVE-*g*-PEO graft copolymers are of particular interest for reasons of comparison.

By grafting hydrophilic chains of, for instance, PEO on the PMVE backbone, well-defined thermo-responsive graft copolymers are obtained (see **Chapter 5**), the thermal behavior in water of which has to be compared with previously described analogues based on either PVCL [8,10,12,62,114-115] or PNIPAM [7,116-117]. The PMVE-*g*-PEO graft copolymers, dihydrophilic at room temperature and amphiphilic above the T_{cp} , should exhibit interesting thermo-responsive aggregational behaviour at their T_{cp} , which depends on the polymer concentration, such as for the aqueous solutions of PMVE homopolymer, and on the number of PEO side chains.

The influence of the number and length of the PEO grafts, as well as of the presence of the unreacted chlorine-group on the T_{cp} of graft copolymers and on the formation of the micelle-

like aggregates was examined. The thermo-responsiveness of the PMVE-*g*-PEO copolymers and the miscibility between PMVE and PEO were studied by MTDSC for a large range of concentrations. Also a new method, namely high sensitive-differential scanning calorimetry (HS-DSC or microcalorimetry) was used to study the influence of hydrophilic grafts on the temperature-induced phase separation of PMVE. Generally, this technique is used for biomolecular interactions with proteins. But since a few years, this technique was also applied on investigations on polymers solutions. Few groups that are active in this field are the groups from Winnik in Montreal [118] and Tenhu in Helsinki [7,12,112,119]. Moreover, DLS has been proven to be a powerful technique to investigate the particle size and the shape of polymers in water as a function of temperature.

6.3.2. UV-VIS Transmission

The LCST behaviour of the graft copolymers was determined in the same way as the backbone. Likewise, the reversibility of the phase transition behaviour was observed after heating and cooling. In this study, the T_{cp} is ranging from 21 to 36°C. The T_{cp} of the graft copolymers differs slightly from the homopolymers because of the presence of the PEO side chains. T_{cp} 's for different concentrations of the water-soluble PMVE-*g*-PEO graft copolymers are displayed as a function of the concentration for different PEO content in the graft copolymers in figure 6.7 and 6.8.

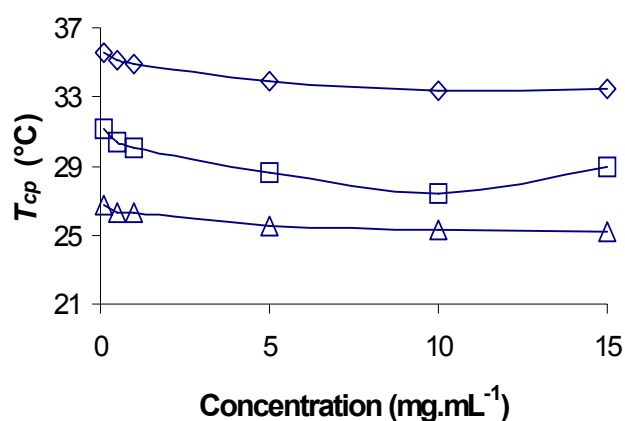


Figure 6.7. Cloud points temperature curves of the graft copolymer G6 (3 PEO, 47 wt-%) (\diamond), G7 (5 PEO, 55 wt-%) (\square) and G8 (12 PEO, 75 wt-%) (Δ) with PEO 5000 g.mol^{-1} .

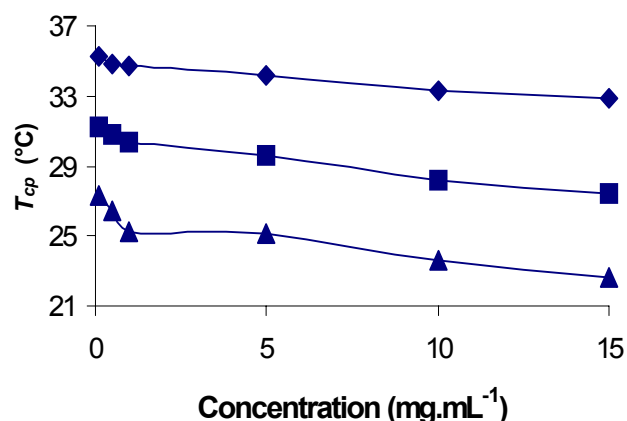


Figure 6.8. Cloud points temperature curves of the graft copolymer G3 (3 PEO, 26 wt-%) (\diamond), G4 (12 PEO, 52 wt-%) (\blacksquare) and G5 (17 PEO, 63 wt-%) (\blacktriangle) with PEO 2000 g.mol^{-1} .

First, the effect of the PEO chain length was investigated. Both graft copolymers present the same number of chlorine (2) and the same distribution of the side chains (3 PEO chains), corresponding respectively to G3 and G6. Only the length of PEO differs with 2000 and 5000 g.mol^{-1} . For the same concentration, the T_{cp} 's are similar, so no significant effect of the length of the PEO chains was observed.

The influence of the distribution of the side chains attracted more attention. From figure 6.7 and 6.8, it is observed that the T_{cp} of the graft copolymer decreased as a function of the solution concentration as already expected from the behaviour of the homopolymer and the statistical copolymers. The figures also indicate that the T_{cp} decreases for higher amounts of hydrophilic PEO relative to the PMVE backbone. This is opposite to the conventional accepted idea for random copolymers, stating that the incorporation of a hydrophilic comonomer raises the T_{cp} , whereas a hydrophobic comonomer leads to lower T_{cp} values [120]. One can suppose that, because there are still chlorine groups present in the graft copolymers, they should influence the T_{cp} of the graft copolymers by their hydrophobic nature. In fact, it is not the case. Regarding G3, G4 and G5 in figure 6.8, where the number of PEO chains is between 3 and 17, the T_{cp} 's decreased with the number of hydrophilic PEO chains, even if the number of remaining chlorines is only 1 or 2. These results may be explained by the competition between PEO and PMVE for water molecules. Also for AB-block copolymers based on PNIPAAm and PEO, a decreasing T_{cp} was observed with increasing amount of PEO [121]. The authors proposed that the PEO-segments increased the hydrophobic interactions (the hydrogen bonds are broken) during phase separation and stabilize the dehydrated PNIPAAm-segments. This phenomenon was also observed by Verbrugghe in the PVCL-*g*-PEO graft copolymers [10,115]. Therefore, the hydrophobic PMVE-interactions dominate from lower temperatures. This effect increases with the PEO content as observed from the series G3-G4-G5 (figure 6.8) and G6-G7-G8 (figure 6.7).

Because of the limited accuracy of UV-vis transmission to determine T_{cp} for different concentrations, the MTDSC technique was used to determine the phase diagram of the PMVE-*g*-PEO in the whole range of the polymer solution. This study was investigated by Dr. Van Durme in collaboration with the research group of Prof. Van Mele (VUB) in Brussels.

6.3.3. Modulated Temperature Differential Scanning Calorimetry (MTDSC)

Measurement

** Thermo-responsive Properties of Aqueous PMVE-*g*-PEO Solutions*

Three PMVE-*g*-PEO graft copolymers were introduced into water to reach concentrations between 20/80 and 90/10 polymer/water solution. In this section, the effect of PEO-grafting on the thermo-responsive properties will be described. Figure 6.9 illustrates that the improved water solubility relates to the amount of PEO attached, i.e. it becomes more significant when increasing the PEO molar mass (left, compare \circ with \bullet) or when the number of PEO-grafts increases (compare left with right). Figure 6.9 (right) shows that the LCST of the graft copolymer (G4, 11 PEO-chains) increases compared to the random copolymer. On the other hand, a much higher increase could be expected taking into account the hydrophilic nature of PEO. In fact, this can be ascribed to the phase behavior between PEO and PMVE, as will be explained in the next section.

This behavior is in contrast to graft copolymer systems of PEO with PNIPAAm and PVCL [117,79], as a result of different demixing kinetics (see below).

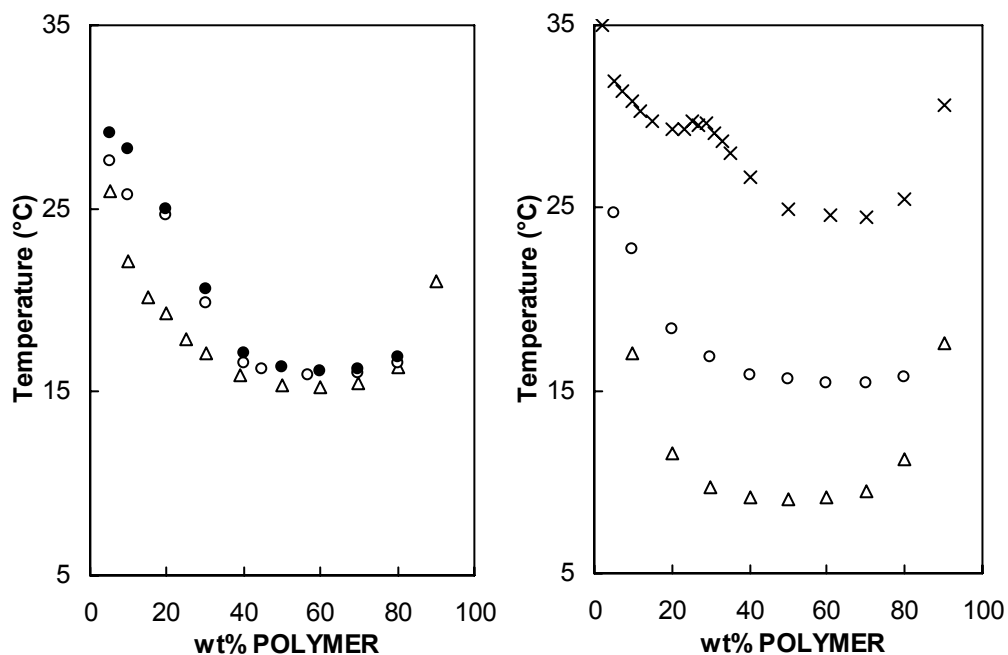


Figure 6.9. LCST demixing curve of: (left) P(MVE-*stat*-CEVE), 1.73 mol-% CEVE/water (Δ), G1 (\circ) and G3 (\bullet); (right) PMVE ($M_w = 20\,000\text{ g}\cdot\text{mol}^{-1}$) (\times), P(MVE-*stat*-CEVE), 3.61 mol-% CEVE/water (Δ) and G4 (\circ). Figure taken from [105].

* *Quasi-isothermal demixing/remixing: phase separation kinetics*

The phase separation kinetics of an aqueous polymer solution can be evaluated in more detail via quasi-isothermal MTDSC experiments [79,81,117]. By doing so, at temperatures above T_{demix} , c_p^{app} becomes time-dependent until a final excess contribution is attained, illustrated in Figure 6.10 for a 40/60 G4/water mixture. Note that similar results were obtained for both other compositions and other PMVE-*g*-PEO graft copolymers. The observed evolution with time (which typically lasts up to 5000 min) reflects the ongoing interphase development (i.e. morphological changes) within the phase separating polymer solution, which apparently is hardly influenced by the incorporation of PEO-grafts, unlike what was observed for both PVCL and PNIPAM where the final excess contribution was immediately attained at each temperature within the demixing region [79,117]. These inconsistencies between PMVE and other amphiphilic polymers is most-likely linked to the (im)miscibility of the polymer constituents, which will therefore be evaluated in following section.

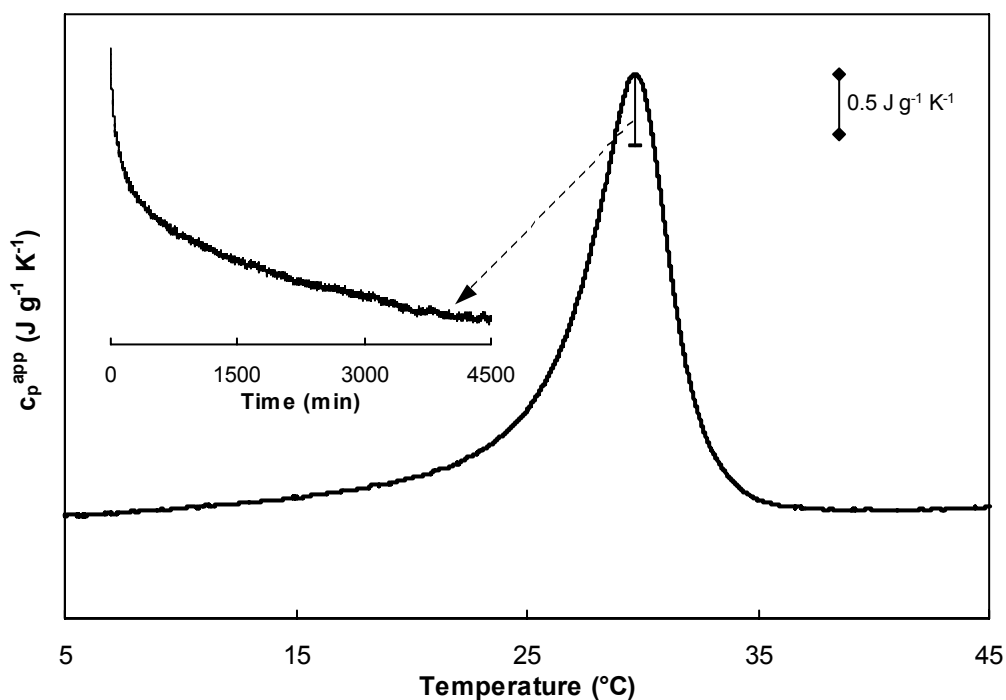


Figure 6.10. Overlay of c_p^{app} during non-isothermal heating and quasi-isothermal demixing at 29.33°C (starting from a homogeneous mixture at 5°C heated at 0.2°C·min⁻¹ to the quasi-isothermal condition) for 40/60 G4/water. Time-evolution is given by the vertical line and the inset, – denotes final value of c_p^{excess} . Figure taken from [105].

** Miscibility Behaviour of PMVE with PEG/PEO of Different Molecular Mass*

It was shown that PEO influences the phase behavior of PMVE in water, although in a different manner as was observed for other amphiphilic polymers [79,117], possibly linked to the (im)miscibility of PEO with the polymer backbone. In order to prove this assumption we will now investigate the miscibility of PMVE with PEO of different molar mass. Figure 6.11 shows the evolution of c_p^{app} for PMVE/TEG blends spanning the entire concentration range.

Each blend exhibits two distinct T_g 's (nearly equal to those of the pure PEG and PMVE), independent of its composition. Hence, despite the similar chemical structure of both structures, PMVE and TEG appear to be immiscible in the temperature range studied. Although the miscibility of the constituents is not likely to improve when increasing the polymer molar mass, we also examined blends containing PEO of higher molar mass (up to 2000 g·mol⁻¹), as these were used during the synthesis of the graft copolymers. Most blends, especially those with a high amount of PEO, again display two glass transition temperatures (not shown). Moreover, these kinds of blends exhibit crystallization of PEO upon (slow) cooling, inevitably causing crystallization induced phase separation. The observed crystallization process is not influenced by the amount of PMVE present in the blend, again suggesting immiscibility of both polymers. Consequently, one observes the melting of PEO in the subsequent heating.

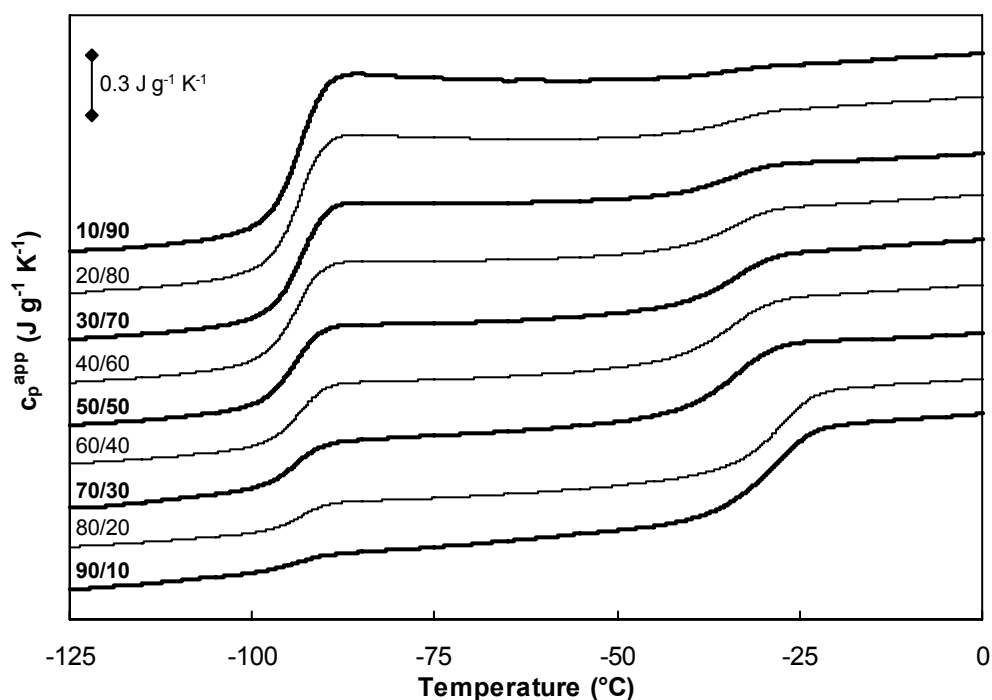


Figure 6.11. c_p^{app} during non-isothermal heating of different PMVE/TEG blend compositions. Curves are shifted vertically for clarity. Figure taken from [105].

6.3.4. High Sensitive-Differential Scanning Calorimetry (HS-DSC)

The phase behaviour of the aqueous polymer solutions of PMVE, P(MVE-*stat*-CEVE) backbones and PMVE-*g*-PEO graft copolymers were also studied by microcalorimetry (table 6.2, figure 6.12) in collaboration with Dr. Laukkanen and Prof. Tenhu from the university of Helsinki. The differences in the graft copolymers may be detected by studying calorimetrically the collapse of the PMVE backbone. In water PMVE is surrounded by highly organized water molecules that dissociate with increasing temperature to free water molecules due to enhanced hydrophobic interactions of the PMVE segments [67,84,85-86,122-123]. The dissociation of the water clusters is an endothermic process and can be detected by microcalorimetric measurements.

The changes with temperature of the partial excess heat capacity C_p of aqueous solutions of several copolymer samples (5 g.L^{-1}) are presented in figure 6.12. The copolymers show interesting differences in their thermal behaviour.

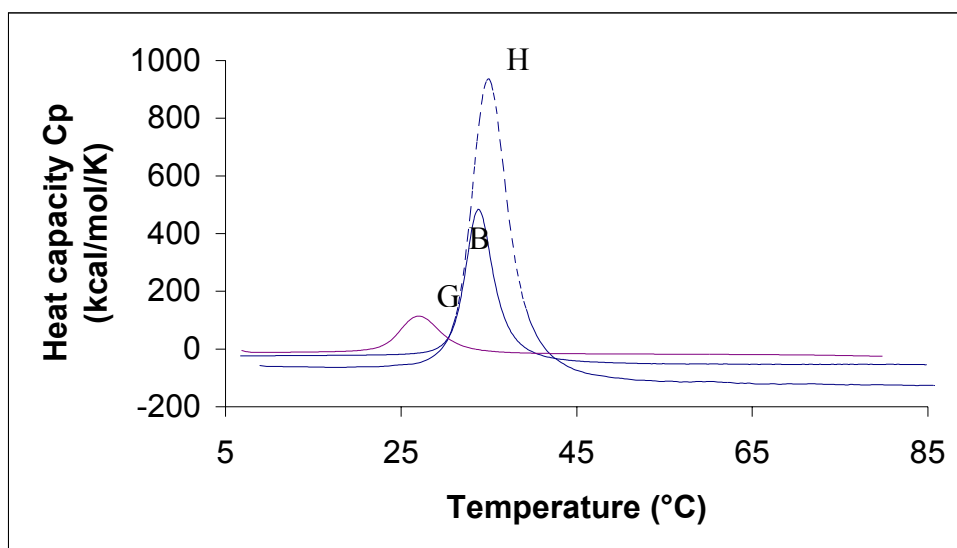


Figure 6.12. Microcalorimetric endotherms for aqueous solutions of PMVE 12 000 homopolymer (H), the backbone B1 (B) and the graft G5 (G). Cp is expressed per $\text{J}\cdot\text{mol}^{-1}\cdot\text{K}^{-1}$ (per gram) of dry polymer. The polymer concentration is in all cases $5\text{ g}\cdot\text{L}^{-1}$ and the heat rate is $90^\circ\text{C}/\text{h}$.

All thermograms, shown in figure 6.12, are endothermic, narrow, and symmetric, with a sharp increase in heat capacity Cp on the low temperature side (onset of the transition, T_{onset}) and a continuous decrease of Cp for temperatures higher than a maximum temperature T_{peak} . The sharp endothermic peak of Cp is followed by a well-defined plateau. The difference between the heat capacities of the coil and the globular states can be measured as the difference between Cp(T) curves extrapolated from both sides of the transition (i.e. from the coil and the globular states) to its middle point at T_{peak} . It is clearly seen in this figure that the heat capacity of copolymers at high temperature is smaller than that at low temperatures, thus a negative change in heat capacity due to the transition can be detected. For PMVE, the value of ΔCp was $-74\text{ J}\cdot\text{mol}^{-1}\cdot\text{K}^{-1}$.

Spartly observation was also detected for cooling scans from 100 to 10 °C, although the sign of ΔCp was opposite. A similar negative change in Cp has also been observed for PVCL ($\Delta\text{Cp} -70\text{ J}\cdot\text{mol}^{-1}\cdot\text{K}^{-1}$) [10] and for PNIPAAm ($\Delta\text{Cp} -63\text{ J}\cdot\text{mol}^{-1}\cdot\text{K}^{-1}$) [122-123]. This negative heat capacity change was explained by the dehydration of MVE units during the coil-to-globule transition. A similar lowering of the heat capacity can also be detected for low molar mass surfactants during micelle formation [124] and for protein refolding [125], as well as for phase transitions of various pluronic-type block copolymers [126]. Such a negative heat capacity change during the phase transition may be taken as an indication of diminished interaction between water molecules and polymer chains. Correspondingly, the present decrease of Cp(T) reflects the collapse of the polymer upon heating.

From plots of the partial heat capacity of copolymer solutions versus temperature, one can extract three thermodynamic parameters: T_{onset} , T_{peak} and ΔH , the enthalpy of the transition.

The values of T_{onset} and T_{peak} follow the same trends as the values of T_{cp} . Table 6.2 shows the difference between the T_{cp} 's of the graft copolymers derived from the PMVE-*stat*-CEVE.

Table 6.2. Summary of microcalorimetry DSC results in H₂O with 5.00 g.L⁻¹ concentration. The heating rate is 90°C/h and the enthalpy is given in kilojoules per mol MVE repeating units.

Sample	PEO wt-%	T_{onset} (°C)	T_{peak} (°C)	ΔH (kJ mol ⁻¹)
PMVE 12000	/	31.2	37.5	5.00
B1	/	25.7	33.9	1.83
B2	/	23.9	32.8	1.87
G1 TEG	4	24.3	34.5	0.79
G3 2000	26	28.0	35.0	0.03
G4 2000	52	23.1	31.0	0.59
G5 2000	63	17.4	27.1	0.69
G6 5000	47	27.7	34.6	0.17
G8 5000	75	17.0	27.7	0.47

The peak temperatures of the collapse were 31.0°C and 27.1°C for G4 and G5, respectively. The difference in T_{cp} is of the same order of magnitude as was observed by UV-spectrophotometry. The T_{cp} of the graft copolymers prepared from PMVE-*stat*-CEVE with high PEO contents are shifted to ~ 28°C while PMVE-*stat*-CEVE has a T_{cp} at ~ 34°C, so we can conclude that the presence of PEO decreases the T_{cp} of the graft copolymers. For that reason, the effect of the grafting degree was studied.

The enthalpy of transition, as well, exhibits a significant dependence on the PEO grafting degree. The effect of the number of PEO chains on the T_{cp} and on the corresponding enthalpy change is clearly seen in figure 6.13.

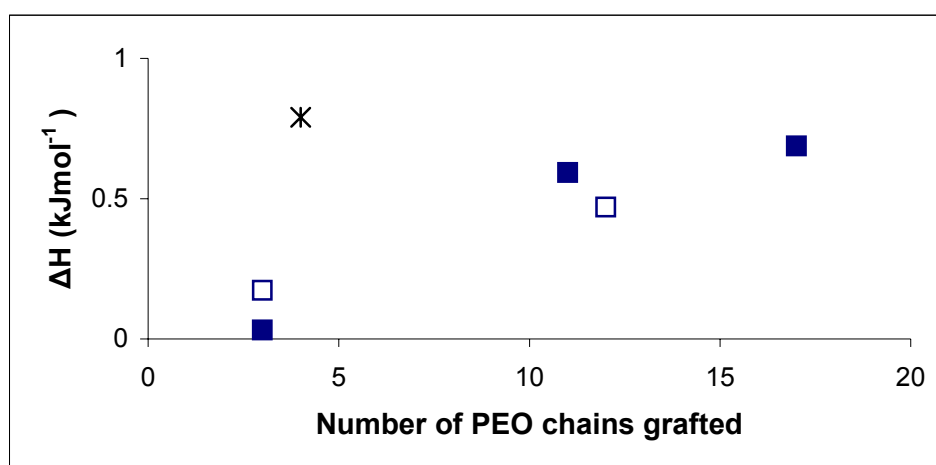


Figure 6.13. Dependence of the heat of transition on the mass fraction of PEO in PMVE-*g*-PEO with PEO 2000 (■), PEO 5000 (□) and TEG(*). Enthalpy is given in kilojoules per mol MVE repeating units.

In figure 6.13, the heats of transition of PMVE-*g*-PEO, obtained from the thermograms in figure 6.12, are shown as a function of the number of the PEO grafts. From this, it becomes clear that the heat of transition results from the PMVE segment as the enthalpy change is almost constant regardless of the degree of grafting. However, the average ΔH ($\text{kJ}\cdot\text{mol}^{-1}$) is smaller than those reported for homopolymer PMVE and the statistical copolymers P(MVE-*stat*-CEVE). This could be explained by the fact that PMVE is less surrounded by water because of the presence of chlorine groups and PEO grafts (see earlier).

6.3.5. Dynamic Light Scattering (DLS)

6.3.5.1. Effect of the Length of PEO

A temperature scan of the apparent hydrodynamic radius R_h and the intensity of light I of the three graft copolymers were conducted by DLS (see **PART IV.: Experimental Part**). As expected from the thermo-responsiveness of PMVE, the solution behaviour of PMVE-*g*-PEO copolymers differs below and above T_{cp} and discussed separately. The apparent R_h and I scattered from the aqueous polymer solutions with a constant concentration ($1.0 \text{ g}\cdot\text{L}^{-1}$) are plotted versus temperature in figure 6.14 for different grafting degree of PEO. For all the samples, the light scattered intensity increases significantly at T_{cp} and stabilizes above this temperature. This means that no precipitation occurred above the T_{cp} . This is also confirmed by the high R_h values, which do not decrease after the T_{cp} . The colloidal stability will be discussed later.

Moreover, the temperature dependant behaviour of polymers with varying PEO amount ($M_{n \text{ PEO}} = 5\,000 \text{ g}\cdot\text{mol}^{-1}$) is plotted in figure 6.14. The amount of PEO has indeed an influence on the T_{cp} . I scatters at lower temperature when the number of PEO side chains increases, in other words the more PEO side chains are present in the graft copolymers, the less they are soluble in water. This conclusion is in agreement with the one obtained from the previous techniques.

DLS was used to study the aggregation behaviour of the graft copolymers in water as a function of temperature, and was compared to the homopolymer and the backbone. The results are recapitulated in table 6.3.

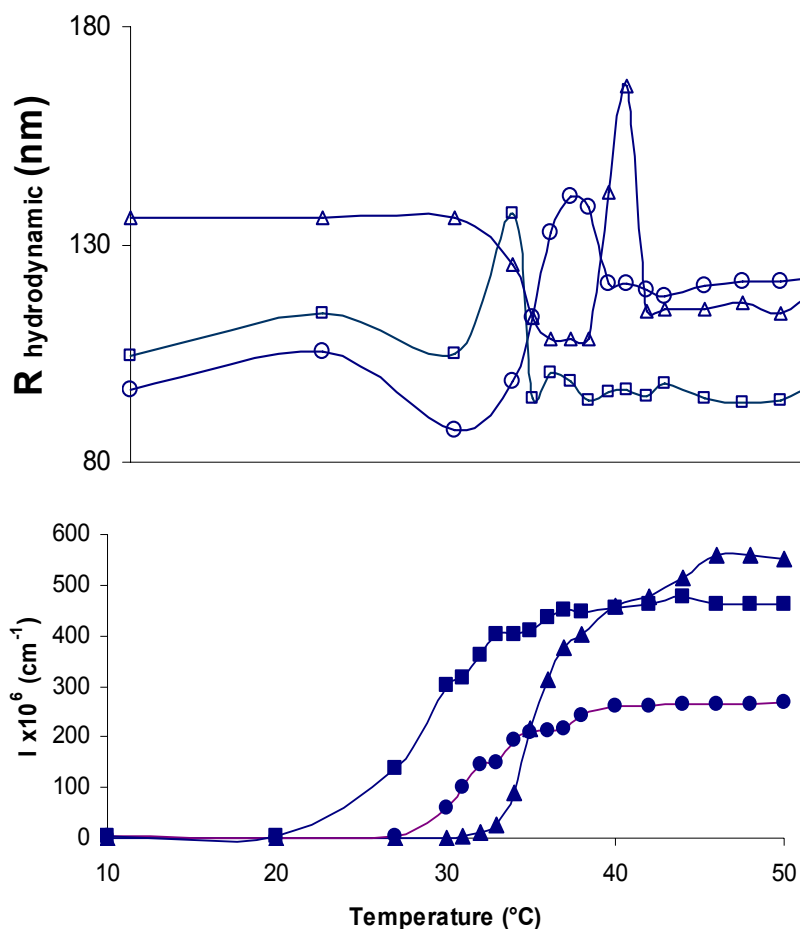


Figure 6.14. Temperature dependencies of apparent hydrodynamic radius R_h (open symbols) and intensity of scattered light I (filled symbols) obtained at 90° scattering angle. Data collected for equilibrium heated G6 (3 PEO) (Δ , \blacktriangle), G7 (5 PEO) (\circ , \bullet) and G8 (12 PEO) (\square , \blacksquare) with 1.00 g.L^{-1} copolymer concentration.

Table 6.3. Results of the size distribution of hydrodynamic radius on the PMVE 12 000, the backbone B1 and the graft copolymers with 1.0 g.L^{-1} concentration at different temperatures.

Sample Code	T_{cp} (DLS)	R_h at 20°C (nm)	R_h at T_{peak} (nm)	R_h at 50°C (nm)
PMVE 12000	39	110	225	150
B1	35	125	146	114
G1	34	113	149	101
G3	35	114	176	131
G6	36	136	166	124
G7	33	106	141	126
G8	30	114	137	103

For all polymers, a R_h of about 115 nm was measured at room temperature due to interchain interactions or microscopic phase separation. At T_{cp} , an increase in R_h was found, due

to the increase of the size of the interchain aggregates. Further heating of the solutions leads to the formation of stable aggregates, which shrink with increasing temperature (see below).

When the number of PEO side chains increased, I decreased, which confirms the hypotheses made by Ikeda [121] and Verbrugghe [10,115] (see before). As was already observed previously with other techniques (see **6.3.2. UV-VIS transmission** and **6.3.4. HS-DSC**), the length of the PEO chains does not really affect the T_{cp} of the graft copolymers (G3 and G6) for the same number of chlorine groups and the same number of PEO side chains. Moreover, for PMVE-*g*-PEO (G6, G7 and G8) in aqueous solutions, a decrease of T_{cp} s was found with increasing PEO graft content (table 6.3). This was expected, again because of the competition between PEO and PMVE to interact with water and their immiscibility.

The change of R_h can be divided into three stages: 1) when temperature increases from 20 to 32°C, water progressively becomes a poor solvent for the PMVE chain backbone, resulting in a slight decrease of R_h ; 2) in the range ~32-34°C, the PMVE chain backbone undergoes the intrachain 'coil-to-globule' transition so that R_h rapidly increases; and 3) at temperatures higher than 34°C, the PMVE chain backbone is already in its fully collapsed state, so that a further increase of temperature has little effect on R_h .

6.3.5.2. Size Distributions of Hydrodynamic Radius (R_h)

The size distributions of R_h can be observed in figure 6.15.

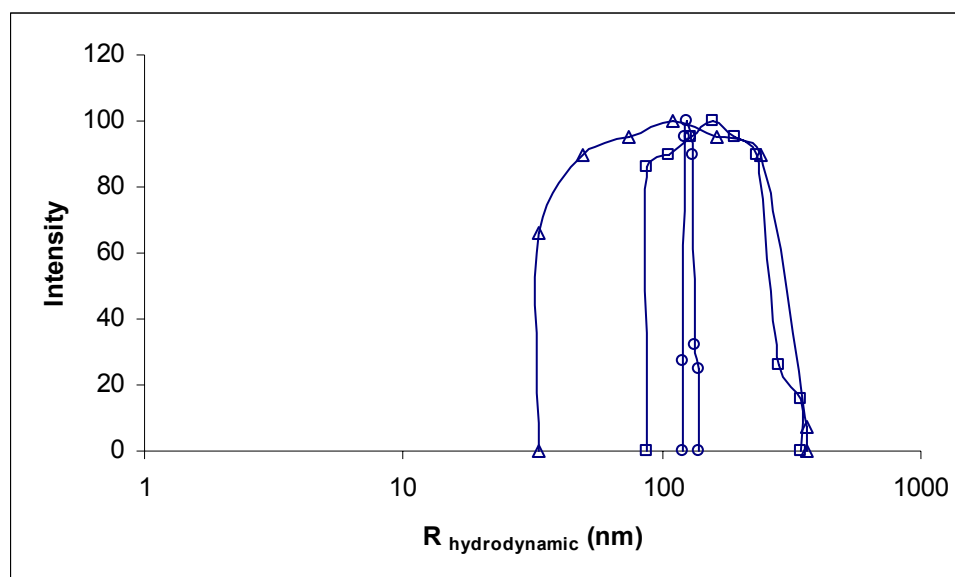
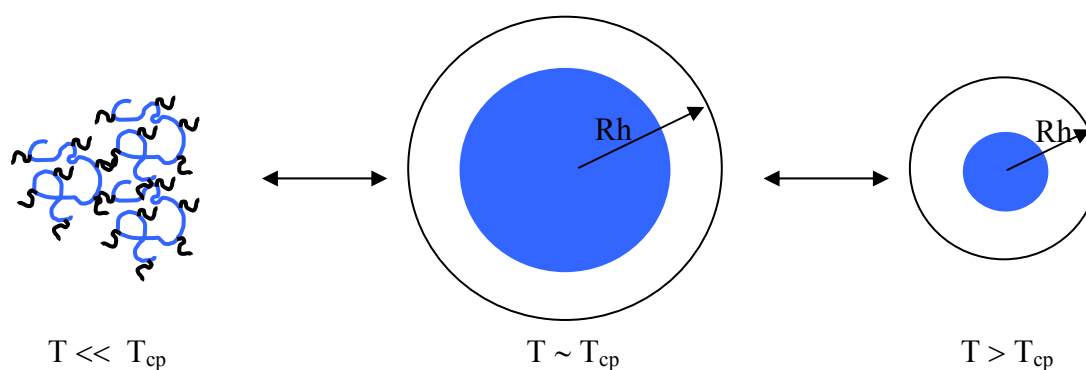


Figure 6.15. Size distribution of R_h displayed by intensity I obtained for G3 for selected temperatures above (\circ), at T_{peak} (\square) and below (Δ) the T_{cp} with 1.00 g.L⁻¹ concentration.

According to this, the particle size is constant below the LCST and upon heating above $T > 45$ °C, but differs at the T_{cp} . Below the T_{cp} , even if the particle size is constant (table 6.3), the size distribution is broad and the high R_h values refer to aggregate formation (figure 6.15). This could be explained by the specific PMVE behaviour. Arndt [127] and Tenhu [123] have concluded that PMVE does not exist as isolated chains in water, but forms stable mesoglobules ($R_h = 200$ -

220 nm). Even if the R_h values increase at the T_{cp} , the size distribution of R_h is still broad and a slight variation could be observed. Above the T_{cp} , the size distribution of the copolymers becomes narrow. Thus, we can conclude that the graft copolymers follow the same trends as the PMVE chains in aqueous solution. These swelling and shrinking aggregates below and above the T_{cp} are represented in scheme 6.5.



Scheme 6.5. Formation of an aggregate and the dependence of its average hydrodynamic radius R_h on temperature. Model describing the steps for the formation of an aggregate and its shrinking upon slow heating from 20°C to 35°C and to 50°C.

6.3.5.3. Studies on Colloidal Stability

In order to study the colloidal stability of the copolymers, the behaviour of I was observed from figure 6.14 in aqueous solutions from the polymer concentration range of 0.02 to 1.00 g.L⁻¹ at 50°C (above T_{cp}). Above the T_{cp} , the solutions are cloudy, which can be seen by the increase of I. The high turbidity at elevated temperatures was caused by colloidal particles formed by the aggregates PMVE-*g*-PEO. The distribution of R_h of the aggregates is monomodal and narrow (figure 6.15). The particles were remarkably stable against further aggregation and no precipitation was detected for several weeks. Although the aggregates are large enough to be observed visually, they do not precipitate. After leaving the aqueous solutions at 50 °C during two years, a precipitation was observed after two months for the concentration higher than 0.5 g.L⁻¹ but they did not precipitate for lower polymer concentration.

6.3.6. Surface Tension Measurement

It was shown in the previous section by DLS measurements that below the T_{cp} , even at low concentration (1 g.L⁻¹), no micelles but stable aggregates are formed. So, it would be interesting to know at which concentration the aggregates start to be formed. Surface tension measurements were made to determine the critical aggregate concentration (CAC) (see figure 6.16).

As it can be seen in figure 6.16, the surface tension decreases when micelles or single chains are present in aqueous solution. When the surface tension is stabilized, which can be defined as the start of the plateau, aggregates are formed. According to this figure, CAC is

determined at $0.00026 \text{ mg.mL}^{-1}$. Because of this low value, we could wonder if this value is a good one according to the loss of accuracy of the apparatus at such low concentrations. The same observations were also done above the T_{cp} (45°C).

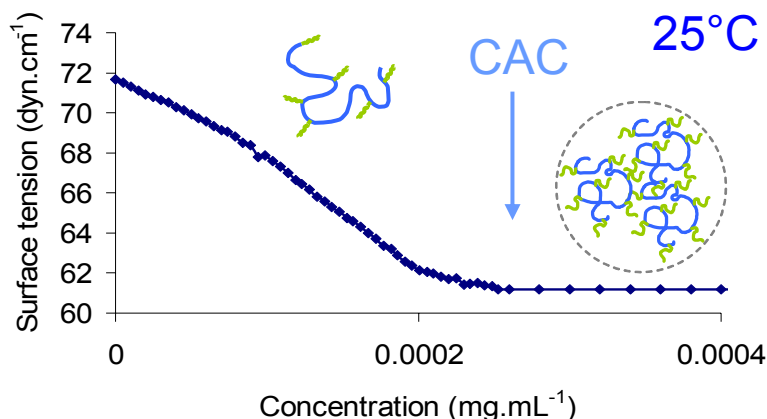


Figure 6.16. Surface Tension measurement of PMVE-g-PEO in water at 25°C .

6.3.7. Ultrasonic Treatment for Pigment Surface Modification in Pigment Dispersions

The process of surface modification of hydrophobic organic pigments (copper phthalocyanine (CuPc) as well as a hydrophilic inorganic pigment (titanium dioxide (TiO_2)) in aqueous dispersions by employing tailor-made thermo-responsive PMVE-*g*-PEO, and the colloidal stability have been studied as a function of temperature. The pigment surface modification is achieved by conventional adsorption and by thermoprecipitation. The effect of mechanical treatment of the pigment dispersion by ultrasonic power alone or in combination with the LCST property was investigated by Nicolaï Bulychev in the University of Stuttgart in Germany in collaboration with Professor Eisenbach [128]. The course of the pigment surface coating process was followed by the Electrokinetic Sonic Amplitude (ESA) method (not further explained, outside the scope of this thesis).

It was found that ultrasonic treatment together with LCST thermoprecipitation is a promising method for the surface modification of pigments with regard to dispersion stability. It was shown that, depending on the temperature, those graft copolymers can be adsorbed on both hydrophilic and hydrophobic pigment surfaces. Below the LCST, all grafts are hydrophilic and thus act as efficient stabilizers of TiO_2 aqueous dispersions. Above the LCST, a fast coagulation occurs. A subsequent cooling below the LCST in combination with ultrasonic action allows to redisperse the system. In the case of CuPc aqueous dispersions, reverse stabilization behavior is observed: above the LCST, all grafts copolymers act as stabilizers of CuPc aqueous dispersions, while fast coagulation is observed below LCST. ESA measurements proved the absence of

adsorption below the LCST; however above the LCST, PMVE-*g*-PEO is able to adsorb on the CuPc surface in aqueous dispersions.

This allows for the use of these PMVE graft copolymers as *universal smart surfactants* for surface modification of both polar inorganic and non-polar organic pigments and for temperature-controlled interaction.

6.4. Conclusion

It was found that phase separation of PMVE copolymers in aqueous solution depends on the structure of the second monomer (IBVE or CEVE) and the composition of the copolymer. In graft copolymers, where hydrophilic and hydrophobic groups are not randomly located, well-defined self-organized structures are formed. However, in statistical copolymers the tendency of self-organization would be considerably reduced, especially when the segregation tendency of both groups is not very large. The presence of a small content of hydrophobic PCEVE and PIBVE in the random copolymers influences the solubility of the PMVE. P(IBVE-*co*-MVE) is only water-soluble if the IBVE content is 7 mol-% or lower. Moreover, the T_{cp} of PMVE decreases very much until 10°C when only 6 mol-% IBVE units are present in the copolymer. Also, in the case of P(MVE-*stat*-CEVE) where CEVE is less hydrophobic than IBVE, the incorporation of CEVE units clearly lowers the T_{cp} of the PMVE up to a complete loss of the water-solubility for copolymers with CEVE content higher than 3 mol-%.

PMVE-*g*-PEO aqueous solutions were evaluated for their thermo-responsive behaviour. The influence of polymer concentration, the presence of chlorine groups, the grafting degree and the length of the PEO side chains was monitored by UV-spectrophotometry, microcalorimetry and MTDSC measurements of the solutions as a function of temperature. All the copolymers share a number of characteristics when dissolved in water: they undergo a reversible heat-induced phase transition when brought to a temperature beyond a critical value. This temperature, detectable by changes in the absorbance of the solution, or more accurately measured by DSC, depends on the number and the distribution of the PEO grafts. PEO grafts form a hydrophilic shell stabilising the hydrophobic PMVE and some PEO in the core. DLS shows that the graft copolymers tend to form well-defined polymeric aggregates but never micelles below and above T_{cp} . Moreover, the grafting degree has no effect on the particle size. Furthermore, the water solubility of the PMVE-*g*-PEO was much improved with the incorporation of PEO side chains. Both PMVE and PEO were found to be immiscible in water, which results in a 'phase-separated' water-soluble polymer.

Polymeric aggregates are well investigated transport systems for drugs, and the combination with thermo-responsivity is now being explored for 'intelligent' drug delivery systems. Besides, it has been demonstrated that PMVE-*g*-PEO could be used as smart surfactants for surface modification of both polar inorganic and non-polar organic pigments.

6.5. References

- [1] (a) Price C., in 'Developments in Block Copolymers 1', 'Colloidal Properties of Block Copolymers', edited by Goodman I., London: Applied Science, **1982**, pp. 39-79. (b) Kim S., Park K.M., Ko J.Y., Kwon I.C., Cho H.G., Kang D., Yu I.T., Kim K., Na K., *Colloid Surf. B, Biointerface.*, **2008**, *63*, 55.
- [2] (a) Martin T.J., Prochazka K., Munk P., Webber S.E., *Macromolecules*, **1996**, *29*, 6071. (b) Sedlak M., Antonietti M., Cölfen H., *Macromol. Chem. Phys.*, **1998**, *199*, 247. (c) Thunemann A.F., Beyermann J., Kukulka H., *Macromolecules*, **2000**, *33*, 5906. (d) Qi L.M., Cölfen H., Antonietti M., *Angew. Chem. Int. Ed. Engl.*, **2000**, *39*, 604. (e) Gohy J.F., Varshney S.K., Jérôme R., *Macromolecules*, **2001**, *34*, 3361. (f) Zhu P.W., *J. Mater. Sci. Mater. Med.*, **2004**, *15*, 567.
- [3] Bütün V., Billingham N.C., Armes S.P., *J. Am. Chem. Soc.*, **1998**, *120*, 11818.
- [4] (a) Musyanovych A., Landfester K., in "Macromolecular Engineering, Precise Synthesis, Materials, Properties, Applications", Vol. 2 in 'Elements of Macromolecular Structural Control', Edited by Matyjaszewski K., Gnanou Y., Leibler L., Wiley-VCH Verlag GmbH & Co. KGaA, Weinheim, Germany, Chap. 13, **2007**. (b) Wu C.Z., Xie Y., *J. Nanosci. Nanotech.*, **2008**, *8*, 6208. (c) Comini E., Barotto C., Faglia G., Ferroni M., Vomiero A., Sberveglieri G., *Prog. Polym. Sci.*, **2009**, *54*, 1.
- [5] Bütün V., Billingham N.C., Armes S.P., *Chem. Commun.*, **1997**, *7*, 671.
- [6] Mathur A., Dreschner B., Scranton A., Klier J., *Nature*, **1998**, *392*, 367.
- [7] (a) Virtanen J., Baron C., Tenhu H., *Macromolecules*, **2000**, *33*, 336. (b) Virtanen J., Tenhu H., *Macromolecules*, **2000**, *33*, 5970. (c) Virtanen J., Lemmetyinen H., Tenhu H., *Polymer*, **2001**, *42*, 9487.
- [8] (a) Virtanen J., Tenhu H., *J. Polym. Sci., Part A: Polym. Chem.*, **2001**, *39*, 3716. (b) Laukkanen A., Wiedmer S.K., Varjo S., Riekkola M.L., Tenhu H., *Colloid. Polym. Sci.*, **2002**, *280*, 65. (c) Virtanen J., in 'Self-assembling of Thermally Responsive Block and Graft Copolymers in Aqueous Solutions', **2002**. Academic dissertation. Yliopistopaino, University of Helsinki. <http://ethesis.helsinki.fi/julkaisut/mat/kemia/vk/virtanen>. (d) Zhang W., Shi L., Wu K., An T., *Macromolecules*, **2005**, *38*, 5743. (e) Motokawa R., Morishita K., Koizumi S., Nakahira T., Annaka M., *Macromolecules*, **2005**, *38*, 5748.
- [9] Virtanen J., Holoppa S., Lemmetyinen H., Tenhu H., *Macromolecules*, **2002**, *35*, 4763.
- [10] Verbrugghe S., Laukkanen A., Aseyev V., Tenhu H., Du Prez F., *Polymer*, **2003**, *44*, 6807.
- [11] Laukkanen A., Winnik F.M., Tenhu H., *Macromolecules*, **2005**, *38*, 2439.
- [12] (a) Laukkanen A., Valtola L., Winnik F.M., Tenhu H., *Polymer*, **2005**, *46*, 7055. (b) Laukkanen A., in 'Thermally Responsive Polymers Based on N-vinylcaprolactam and an Amphiphilic Macromonomer', **2005**. Academic dissertation. Yliopistopaino, University of Helsinki. <http://ethesis.helsinki.fi/julkaisut/mat/kemia/vk/laukkanen>.
- [13] (a) Dash P., Toncheva V., Schacht E., Seymour L., *J. Control. Rel.*, **1997**, *48*, 269. (b) Harada A., Kataoka K., *J. Am. Chem. Soc.*, **1999**, *121*, 9241. (c) Bronish T., Nehls A., Eisenberg

- A., Kabanov V., Kabanov A., *Colloids Surf. B, Biointerface*, **1999**, *16*, 243. (d) Nishiyama N., Yokoyama M., Aoyagi T., Okano T., Sakurai Y., Kataoka K., *Langmuir*, **1999**, *15*, 377.
- [14] (a) Tanford C., *J. Phys. Chem.*, **1974**, *78*, 2469. (b) Tanford C., in *'The Hydrophobic Effect: Formation of Micelles and Biological Membranes'*, 2nd ed.; J. Wiley & Sons, New York, **1980**. (c) Hamad E., Qutubuddin, *Macromolecules*, **1990**, *23*, 4185.
- [15] Alexandridis P., Nivaggioli T., Hatton T.A., *Langmuir*, **1995**, *11*, 1468.
- [16] (a) Alexandridis P., Holzwarth J.F., Hatton T.A., *Macromolecules*, **1994**, *27*, 2414. (b) Sulthana S.B., Bhat S.G.T., Rakshit A.K., *Colloid Surf. A, Physicochem. Eng. Aspects*, **1996**, *111*, 57. (c) Sulthana S.B., Bhat S.G.T., Rakshit A.K., *Langmuir*, **1997**, *13*, 4562.
- [17] (a) Attwood D., Florence A.T., in *'Surface Systems: Their Chemistry, Pharmacy and Biology'*, Chapman and Hall, London, **1983**. (b) Hunter R.J., in *'Foundations of Colloid Science'*, Oxford University Press, New York, **1987**, Vol. 1. (c) Sandoval R.W., Williams D.E., Kim J., Roth C.B., Torkelson J.M., *J. Polym. Sci. Part B: Polym. Phys.*, **2008**, *46*, 2672.
- [18] Standman S., Zarembo A., Darinskii M., Lauritnaki P., Butcher S.J., Vuorimaa E., Lemmetyinen H. Tenhu H., *Macromolecules*, **2008**, *41*, 8855.
- [19] (a) Vamvakaki M., Billingham N.C., Armes S.P., *Macromolecules*, **1999**, *32*, 2088. (b) Liu S.L., Billingham N.C., Armes S.P., *Angew. Chem. Int. Ed. Engl.*, **2001**, *40*, 2328. (c) Lee A.S., Bütün V., Vamvakaki M., Armes S.P., Polpe J.A., Gast A.P., *Macromolecules*, **2002**, *35*, 8540. (d) Zhu Z.Y., Xu J., Zhon Y.M., Jiang X.Z., Armes S.P., Liu S.Y., *Macromolecules*, **2007**, *40*, 6393. (e) Sakai K., Vamvakaki M., Smith E.G., Wanless E.J., Armes S.P., Biggs S., *J. Colloid Interface Sci.*, **2008**, *317*, 383. (f) Lidardi M., Craparo E.F., Giammona G., Armes S.P., Tang Y., Lewis A.L., *Macromol. Biosci.*, **2008**, *8*, 615. (g) Shen L., Duz J.Z., Armes S.P., Liu S.Y., *Langmuir*, **2008**, *24*, 10019.
- [20] (a) Kohori F., Sakai K., Aoyagi T., Yokoyama M., Sakurai Y., Okano T., *J. Control. Rel.*, **1998**, *55*, 87. (b) Shibanuma T., Aoki T., Sanui K., Ogata N., Kikuchi A., Sakurai Y., Okano T., *Macromolecules*, **2000**, *33*, 444. (c) Nakayama M., Okano T., Miyazaki T., Kohori F., Sakai K., Yokoyama M., *J. Control. Rel.*, **2006**, *115*, 46. (d) Nakayama M., Chung J.E., Miyazaki T., Yokoyama M., Sakai K., Okano T., *React. & Funct. Polym.*, **2007**, *67*, 1398. (e) Nakayama M., Okano T., *Macromolecules*, **2008**, *41*, 504. (f) Akimoto J., Nakayama M., Sakai K., Okano T., *J. Polym. Sci. Part A: Polym. Chem.*, **2008**, *46*, 7127.
- [21] (a) Martin T.J., Prochazka K., Munk P., Webber S.E., *Macromolecules*, **1996**, *29*, 6071. (b) Simmons C., Webber S.E., Zhulina E.B., *Macromolecules*, **2001**, *34*, 5053. (c) Hahn J., Webber S.E., *Langmuir*, **2004**, *20*, 1489.
- [22] (a) Jeong B., Bae Y.H., Lee D.S., Kim S.W., *Nature*, **1997**, *388*, 860. (b) Jeong B., Bae Y.H., Lee D.S., Shon J., Kim S.W., *J. Polym. Sci., Part A: Polym. Chem.*, **1999**, *37*, 751. (c) Park S.Y., Han B.R., Na K.M., Han D.K., Kim S.W., *Macromolecules*, **2003**, *36*, 4115. (d) Jeong J.H., Kim S.H., Kim S.W., Park T.G., *J. Nanosci. Nanotech.*, **2006**, *6*, 2790. (e) Kim S.H., Jeong J.H., Mok H., Lee S.H., Kim S.W., Park T.G., *Biotech. Prog.*, **2007**, *23*, 232. (f) Kim S.W., Kim J.Y., Huh K.M., Acharya G., Park K., *J. Control. Rel.*, **2008**, *132*, 222.

- [23] (a) Okabe S., Sugihara S., Aoshima S., Shibayama M., *Macromolecules*, **2003**, *36*, 4099. (b) Sugihara S., Kanaoka S., Aoshima S., *J. Polym. Sci. Part A: Polym. Chem.*, **2004**, *42*, 2601. (c) *Macromolecules*, **2005**, *38*, 1919. (d) Okabe S., Seno K., Kanaoka S., Aoshima S., Shibayama M., *Macromolecules*, **2006**, *39*, 1592; (e) *Polymer*, **2006**, *47*, 7572.
- [24] (a) Gohy J.-F., Creutz S., Garcia M., Mahltig B., Stamm M., Jérôme R., *Macromolecules*, **2000**, *33*, 6378. (b) Gohy J.-F., Willet N., Varshney S.K., Zhang J.-X., Jérôme R., *e-polymers*, **2002**, no. 035. (c) Gohy J.-F., Lohmeijer B.G., Varshney S.K., Déchamps B., Leroy E., Boileau S., Schubert U.S., *Macromolecules*, **2002**, *35*, 9748. (d) Lei L., Gohy J.-F., Willet N., Zhang J.-X., Varshney S.K., Jérôme R., *Macromolecules*, **2004**, *37*, 1089. (e) De Cupere V.M., Gohy J.-F., Jérôme R., Rouxhet P.G., *J. Colloid Interface Sci.*, **2004**, *271*, 60. (f) Van Butsele K., Sibret P., Fustin C.-A., Gohy J.-F., Passirani S., Benoit J.P., Jérôme R., Jérôme C., *J. Colloid Interface Sci.*, **2009**, *323*, 235.
- [25] Verdonck B., Gohy J.-F., Khouzakoun E., Jérôme R., Du Prez F.E., *Polymer*, **2005**, *46*, 9899.
- [26] (a) Cammas-Marion S., Okano T., Kataoka K., *Colloids Surf., B, Biointerface*, **1999**, *16*, 207. (b) Kim I.S., Jeong Y.I., Cho C.S., Kim S.H., *Int. J. Pharm.*, **2000**, *205*, 165.
- [27] Konak C., Oupicky D., Chytrý V., Ulbrich K., *Macromolecules*, **2000**, *33*, 5318.
- [28] Arotçaréna M., Heise B., Ishaya S., Laschewsky A., *J. Am. Chem. Soc.*, **2002**, *124*, 3787.
- [29] Jeong B., Bae Y.H., Kim S.W., *Colloids Surf. B, Biointerface*, **1999**, *16*, 185.
- [30] Narain R., Armes S.P., *Macromolecules*, **2003**, *36*, 4675.
- [31] Wang X.S., Jackson R.A., Armes S.P., *Macromolecules*, **2000**, *33*, 255.
- [32] Liu S., Armes S.P., *Langmuir*, **2003**, *19*, 4432.
- [33] Szczubiałka K., Nowakowska, *Polymer*, **2003**, *44*, 5269.
- [34] Allen C., Maysinger D., Eisenberg A., *Colloids Surf. B, Biointerface*, **1999**, *16*, 3.
- [35] (a) Bronich T.K., Nehls A., Eisenberg A., Kabanov V.A., Kabanov A.V., *Colloids Surf. B, Biointerface*, **1999**, *12*, 2153. (b) Caputto A., Betti M., Altavilla G., Bonaccorsi A., Boarini C., Marchisio M., Butto S., Sparnacci K., Laus M., Tondelli L., Ensoli B., *Vaccine*, **2002**, *20*, 2303.
- [36] Webber S.E., *J. Phys. Chem. B*, **1998**, *102*, 2618.
- [37] Verdonck B., Goethals E.J., Du Prez F., *Macromol. Chem. Phys.*, **2003**, *204*, 2090.
- [38] Bulychev N., Arutunov I., Verdonck B., Zhang T., Goethals E., Du Prez F.E., *Macromol. Chem. Phys.*, **2004**, *205*, 2457.
- [39] Riess G., Hurtrez G., Bahadur P., in *'Block Copolymers'*, 2nd ed., in *'Encyclopedia of Polymer Science and Engineering'*, New York: Wiley, **1985**, Vol. 2, P. 324-434.
- [40] Pons R., in *'Polymeric Surfactants as Emulsion Stabilizers'*, In: Alexandridis P., Lindman B., editors, in *'Amphiphilic Block Copolymers: Self Assembly and Applications'*, Amsterdam: Elsevier, **2000**, p. 409-422.
- [41] Riess G., Dumas Ph., Hurtrez G., in *'Block Copolymer Micelles and Assemblies'*, MML series 5, London: Citrus Books, **2002**, p. 69-110.

- [42] (a) Piirma I., in *'Polymeric Surfactants'*, Surfactant science series 42, New York: Marcel Dekker, **1992**, p. 1-285. (b) Gerst M., Schuch H., Urban D., in *'Amphiphilic Block Copolymers as Surfactants in Emulsion Polymerization'*, In: Glass J.E. editor, in *'Associative Polymers in Aqueous Media'*, ACS symposium series 765, **2000**, p. 37-51.
- [43] Hamley I.W., in *'The Physics of Block Copolymers'*, In: Hamley I.W. editor, Oxford Science Publication, **1998**, chap. 3 and 4, p. 131-265.
- [44] Svenson M., Johansson H.O., Tjerneld F., in *'Application of Amphiphilic Block Copolymers in Separations'*, In: Alexandridis P., Lindman B. editors, in *'Amphiphilic Block Copolymers: Self Assembly and Applications'*, Amsterdam: Elsevier, **2000**, p. 377-408.
- [45] Chen G.H., Hoffman, *Nature*, **1995**, 373, 49.
- [46] (a) Xie H.Q., Guo J.S., *Angew. Makromol. Chem.*, **1996**, 238, 41. (b) and *Angew. Makromol. Chem.*, **1999**, 264, 82.
- [47] Sulman E., Bodrova Y., Matveeva V., Semagina N., Cerveny L., Kurtc V., Bronstein L., Platonova O., Valetsky P., *Appl. Catal. A: Gen.*, **1999**, 176, 75.
- [48] Hou S., Chan W.K., *Macromol. Rapid Commun.*, **1999**, 20, 440.
- [49] Price C., in *'Colloidal Properties of Block Copolymers'*, In: Goodman I. editor, in *'Developments in Block Copolymers 1'*, London: Applied Science, **1982**, p. 39-79.
- [50] Fillod E., in *'Synthesis and Characterization of (meth)acrylic Block Copolymers Containing a Polar Sequence; Colloidal Properties Inorganic Medium'*, PhD Thesis, University of Haute Alsace, France, **1997**.
- [51] Fetters L., *ACS Polymer Prepr. (Div. Polym. Chem.)*, **1999**, 40(2), 972.
- [52] (a) Crepeau C., Hoerner P., Riess G., in *'Stable Emulsions, their Preparation Process and their Applications'*, French Patent Application 9,803,234, 17/03/1998 to Hutchinson. (b) De Smet S.C., Demeester J., Hennink W.E., *Pharm. Res.*, **2000**, 17, 113.
- [53] (a) Allcock H.R., in *'Biodegradable Polymers as Drug Delivery Systems'*, Langer R., Chasin M., Eds.; Marcel Dekker, New York, **1990**. (b) De Rossi D., Kajiwara K., Osaka Y., Yamauchi A., in *'Polymer Gels: Fundamental and Biomedical Applications'*, Eds., Plenum Press, New York, **1991**. (c) Stayton P.S., Shimoboli T., Long C., Chilkoti A., Chen S.H., Harris J.M., Hoffman A.S., *Nature*, **1995**, 378, 472. (d) Kumar A., Srivastava A., Galaev I.Y., Mattiasson B., *Prog. Polym. Sci.*, **2007**, 32, 1205. (e) Dimitrov I.; Trzebickar B., Müller A.H.E., Dworak A., Tsvetanov C.B., *Prog. Polym. Sci.*, **2007**, 32, 1275. (f) Labuschagne P.W., Germishuizen W.A., Verryn S.M.C., Moolmann F.S., *E.P.J.*, **2008**, 44, 2146. (g) Capadona J.R., Shanmuganathan K., Tyler D.J., Rowan S.J., Weder C., *Science*, **2008**, 319, 1370.
- [54] Couto D.S., Hong Z.K., Mano J.F., *Acta Biomater.*, **2009**, 5, 115.
- [55] Shi J., Liu L.H., Liu X.P., Sun X.M., Cao S.K., *Polym. Adv. Tech.*, **2008**, 19, 1467.
- [56] Widom B., Bhimalapuram B., Koga K., *Phys. Chem. Phys.*, **2003**, 5, 3085.
- [57] Molyneux P., in *'Water-solubles Synthetic Polymers: Properties and Behavior'*, CRC Press, Inc.: Boca Raton, Washington DC, **1985**, p. 11.
- [58] Schild G.H., *Prog. Polym. Sci.*, **1992**, 17, 163.

- [59] (a) Heskins M., Guillet J.E., *J. Macromol. Sci. Chem.*, **1968**, 2, 41. (b) Platé N.A., Lebedeva T.L., Valuev L.I., *Polym. J.*, **1999**, 31, 21. (c) Loos W., Du Prez F., *Macromol. Symp.*, **2004**, 210, 483.
- [60] Kirsh Y.E., in 'Water-soluble Poly-N-vinylamides', Chichester: John Wiley & Sons, **1998**.
- [61] Solomon O.F., Corciovei M., Ciută I., Boghina C., *J. Appl. Polym. Sci.*, **1968**, 12, 1835.
- [62] (a) Verbrugghe S., Bernearts K., Du Prez F., *Macromol. Chem. Phys.*, **2003**, 204, 1217.
- [63] Horne R.A., Almeida J.P., Day A.F., Yu N.T., *J. Colloid Interface Sci.*, **1971**, 35, 77.
- [64] (a) Schäfer-Soenen H., Morekerke R., Berghmans H., Koningsveld R., Dušek K., Šolc K., *Macromolecules*, **1997**, 30, 410. (b) Swier S., Van Durme K., Van Mele B., *J. Polym. Sci., Part B: Polym. Phys.*, **2003**, 41, 1824.
- [65] Morekerke R., Meeussen F., Berghmans H., Koningsveld R., Mondelares W., Schacht E., Dušek K., Šolc K., *Macromolecules*, **1998**, 31, 2223.
- [66] Meeussen F., Bauwens R., Moerkerke R., Nies E., Berghmans H., *Polymer*, **2000**, 41, 3737.
- [67] Maeda H., *J. Polym. Sci., Part B: Polym. Phys.*, **1994**, 32, 91.
- [68] (a) Šolc K., Dušek K., Koningsveld R., Berghmans H., *Collect. Czech. Chem. Commun.*, **1995**, 60, 1661. (b) Moerkerke R., Koningsveld R., Berghmans H., Dušek K., Šolc K., *Macromolecules*, **1995**, 28, 1103. (c) Zhang J., Teng X., Zhou D., Shen D., *Polym. Bull.*, **2002**, 48, 277.
- [69] Verdonck Beatrice, in 'Ontwikkeling van Thermo-responsive Polymeersurfactanten op basis van Poly(methylvinylether)', PhD thesis, Ghent University, Belgium, **2004**.
- [70] (a) Saeki S., Kuwahara N., Nakata M., Kaneko M., *Polymer*, **1976**, 71, 685. [73] Malcolm G.N., Rowlinson J.S., *Trans. Faraday Soc.*, **1957**, 53, 921.
- [71] Christova D., Velichkova R., Loos W., Goethals E., Du Prez F., *Polymer*, **2003**, 44, 2255.
- [72] Christova D., Velichkova R., Goethals E., Du Prez F., *Polymer*, **2003**, 44, 2255.
- [73] (a) Cho S.H., Jhon M.S., Yuk S., Lee H.B., *J. Polym. Sci., Part B: Polym. Phys.*, **1997**, 35, 595. (b) Cho S.H., Jhon M.S., Yuk S., *E.P.J.*, **1999**, 35, 1841. (c) Chen Y.M., *Rad. Phys. Chem.*, **2001**, 61, 65. (d) Heijl J.M.D. and Du Prez, *Polymer*, **2004**, 45, 6771.
- [74] (a) MacKnight W.J., Karasz F.E., in 'Comprehensive Polymer Science: the Synthesis, Characterization, Reactions & Applications of Polymers', Eds. Sir Allen G. FRS, Bevington J.C., New York, Pergamon Press, **1989**, Vol. 1, Chap. 4. (b) Radush H.J., Tung N.T., Wohlfarth C., *Angew. Makromol. Chem.*, **1996**, 235, 175.
- [75] (a) Flory P.J., *J. Chem. Phys.*, **1941**, 9, 660. (b) Flory P.J., *J. Chem. Phys.*, **1942**, 10, 51. (c) Flory P.J., in 'Principles of Polymer Chemistry', Cornell University Press, **1953**, Chap. XIII.
- [76] (a) Huggins M.L., *J. Chem. Phys.*, **1941**, 9, 440. (b) Huggins M.L., *Ann. N. Y. Acad. Sci.*, **1942**, 43, 1.
- [77] (a) Staverman A.J., Van Santen J.H., *Recl. Trav. Chim. Pays-Bas*, **1941**, 60, 76. (b) Staverman A.J., Van Santen J.H., *Recl. Trav. Chim. Pays-Bas*, **1941**, 60, 640.
- [78] Meeussen F., Nies E., Verbrugghe S., Goethals E., Du Prez F., Berghmans H., *Polymer*, **2000**, 41, 8597.

- [79] Van Durme K., Verbrugghe S., Du Prez F., Van Mele B., *Macromolecules*, **2004**, 37, 1054.
- [80] Afroze F., Nies E., Berghmans H., *J. Mol. Struct.*, **2000**, 554, 55.
- [81] Van Durme K., Van Assche G., Van Mele B., *Macromolecules*, **2004**, 37, 9596.
- [82] Nishi T., Kwei K., *Polymer*, **1975**, 16, 285.
- [83] Maeda H., *Macromolecules*, **1998**, 28, 5256.
- [84] Maeda Y., *Langmuir*, **2001**, 17, 1737.
- [85] Van Durme K., Bernaerts K.V., Verdonck B., Du Prez F.E., Van Mele B., *J. Polym. Sci., Part B: Polym. Phys.*, **2006**, 44, 461.
- [86] Pyda M., Van Durme K., Wunderlich B., Van Mele B., *J. Polym. Sci., Part B: Polym. Phys.*, **2005**, 43, 2141.
- [87] (a) Loozen E., Van Durme K., Nies E., Van Mele B., Berghmans H., *Polymer*, **2006**, 47, 7034. (b) Van Durme K., Van Assche G., Nies E., Van Mele B., *J. Phys. Chem.*, **2007**, 111, 1288.
- [88] Van Durme K., Loozen E., Nies E., Van Mele B., *Macromolecules*, **2005**, 38, 10234.
- [89] Yang Y., Zeng F., Xie X., Tong Z., Liu X., *Polym. J.*, **2001**, 33, 399.
- [90] (a) Spěváček J., Hanyková L., Ilavský M., *Macromol. Symp.*, **2001**, 166, 231. (b) Hanyková L., Spěváček J., Ilavský M., *Polymer*, **2001**, 42, 8607. (c) Spěváček J., Hanyková L., *Macromol. Symp.*, **2003**, 203, 229.
- [91] Heskins M., Guillet J.E., *Macromol. Sci. Chem.*, **1968**, A2, 1441.
- [92] Shtanko N.I., Kabanov V.Y., Apel P.Y., Yoshida M., Vilenskii A.I., *J. Membrane Sci.*, **2000**, 179, 155.
- [93] (a) Kanazawa H., Sunamoto T., Ayano E., Matsushima Y., Kibuchi A., Okano T., *Anal. Sci.*, **2002**, 18, 45. (b) Kibuchi A., Okano T., *Macromol. Symp.*, **2004**, 205, 217.
- [94] Lynen F., Heijl J.M.D., Du Prez F.E., Brown R., Szucs R., Sandra P., *Chromatographia*, **2007**, 66, 143.
- [95] (a) Byeongmoon J., Gutowska A., *Trends Biotech.*, **2002**, 20, 305. (b) Hoffman A.S., Stayton P.S., *Macromol. Symp.*, **2004**, 207, 139. (c) Piskin E., *Int. J. Pharm.*, **2004**, 277, 105.
- [96] (a) Meyer D.E., Shin B.C., Kong G.A., Dewhirst M.W., Chilkoti A., *J. Control. Rel.*, **2001**, 74, 213. (b) Chilkoti A., Dreher M.R., Meyer D.E., Raucher D., *Adv. Drug Delivery Rev.*, **2002**, 54, 613.
- [97] (a) Okano T., Yamada N., Okuhara M., Sakai H., Sakurai Y., *Biomaterials*, **1995**, 16, 297. (b) Ebara M., Yamato M., Aoyagi T., Kikuchi A., Sakai K., Okano T., *Biomacromolecules*, **2004**, 5, 505.
- [98] Vihola H., Laukkanen A., Vatola L., Tenhu H., Hirvonen J., *Biomaterials*, **2005**, 26, 3055.
- [99] Chen J.P., Hoffman A.S., *Biomaterials*, **1990**, 11, 631.
- [100] Bernaerts K.V., Fustin C.-A., Bomal d'Haese C., Gohy J.-F., Martins J.C., Du Prez F.E., *Macromolecules*, **2008**, 41, 2593.
- [101] Forder C., Patrikios C.S., Billingham N.C., Armes S.P., *Chem. Commun.*, **1996**, 883.
- [102] Spěváček J., Hanyková L., Starovoytova L., *Macromolecules*, **2004**, 37, 7710.

- [103] Patrikios C.S., Forder C., Armes S.P., Billingham N.C., *J. Polym. Sci. Part A Polym. Chem.*, **1998**, *36*, 2547.
- [104] Ismail El Ouaamari, in 'Miscibility and thermo-responsive behaviour of water-soluble polymers', Master's thesis, in Free Brussels University (VUB) in Brussels, Belgium, **2005**.
- [105] Confortini O., Van Durme K., El Oumarri I., Van Mele B., Du Prez F.E., *Polymer*, **2009**, submitted.
- [106] Kjellander R., Florin E., *J. Chem. Soc., Faraday Trans. I.*, **1981**, *77*, 2053.
- [107] (a) Kubota K., Fujishige S., Ando I., *J. Phys. Chem.*, **1990**, *94*, 5154. (b) Wu C., Zhou S., *Macromolecules*, **1995**, *28*, 5388. (c) Wu C., Qiu X.P., *Phys. Rev. Lett.*, **1998**, *80*, 620. (d) Jankova K., Chen X., Kops J., Batsberg W., *Macromolecules*, **1998**, *31*, 538. (e) Ulrich K.E., Cannizzaro S.M., Langer R.S., Shakesheff K.M., *Chem. Rev.*, **1999**, *99*, 3181. (f) Bromberg L.E., Ron E.S., *Adv. Drug Delivery Rev.*, **1998**, *31*, 197. (g) Zhang W., Shi L., Wu K., An Y., *Macromolecules*, **2005**, *38*, 5743.
- [108] Qiu X., Wu C., *Macromolecules*, **1997**, *30*, 7921.
- [109] Liang D., Zhou S., Song L., Zaitsev V.S., Chu B., *Macromolecules*, **1999**, *32*, 6326.
- [110] Topp M.D.C., Dijkstra P.J., Talsma H., Feijen J., *Macromolecules*, **1997**, *30*, 8518.
- [111] Zhu P.W., Napper D.H., *Macromolecules*, **1999**, *32*, 2068; and *Langmuir*, **2000**, *16*, 8543.
- [112] Laukkanen A., Valtola L., Winnik F.M., Tenhu H., *Macromolecules*, **2004**, *37*, 2268.
- [113] (a) Kjøniksen A.-L., Nyström B., Tenhu H., *Colloids Surf. A: Physicochem. Aspects*, **2003**, *28*, 75. (b) Galant C., Kjøniksen A.-L., Knudsen K.D., Helgesen G., Lund R., Laukkanen A., Tenhu H., Nyström B., *Langmuir*, **2005**, *21*, 8010. (c) Shuan J., Nuopponen M., Jiang H., Viitalen T., Kauppinen E., Konturi K., Tenhu H., *Macromolecules*, **2005**, *38*, 2918.
- [114] Kjøniksen A.-L., Laukkanen A., Galant C., Knudsen K.D., Tenhu H., Nyström B., *Macromolecules*, **2005**, *38*, 948.
- [115] (a) Verbrugge Sam, in 'Ontwikkeling van Intelligente Polymeerarchitecturen bestaande uit Poly(N-vinylcaprolactam)', PhD thesis, Ghent University, Belgium, **2003**. (b) Yanul N.A., Kirsh Y.E., Verbrugge S., Goethals E.J., Du Prez F.E., *Macromol. Chem. Phys.*, **2001**, *202*, 1700..
- [116] Shuan J., Nuopponen M., Jiang H., Viitala T., Kauppinen E., Konturi K., Tenhu H., *Macromolecules*, **2005**, *38*, 2918.
- [117] Van Durme K., Van Assche G., Aseyev V., Raula J., Tenhu H., Van Mele B., *Macromolecules*, **2007**, *40*, 3765.
- [118] (a) Principi T., Goh E.C.C., Liu R.C., Winnik F.M., *Macromolecules*, **2000**, *33*, 2958. (b) Poncet-Legrand C., Winnik F.M., *Polym. J.*, **2001**, *33*(3), 277. (c) Kujawa P., Winnik F.M., *Macromolecules*, **2001**, *34*, 4130. (d) Kujawa P., Goh E.C.C., Calvet D., Winnik F.M., *Macromolecules*, **2001**, *34*, 6387. (e) Diab C., Akiyama Y., Kataoka K., Winnik F.M., *Macromolecules*, **2004**, *37*, 2556. (f) Kujawa P., Segui F., Shaban S., Diab C., Okada Y., Tanaka F., Winnik F.M., *Macromolecules*, **2006**, *39*, 341.
- [119] (a) Nuopponen M., Ojala J., Tenhu H., *Polymer*, **2004**, *45*, 3643. (b) Shuan J., Chen J., Nuopponen M., Tenhu H., *Langmuir*, **2004**, *20*, 4671. (c) Vihola H., Laukkanen A., Valtola L.,

Tenhu H., Hirvonen J., *Biomaterials*, **2005**, 26, 3055. (d) Burova T.V., Grinberg N.V., Grinberg V.Y., Kalinina E.V., Lozinsky V.I., Aseyev V.O., Holappa S., Tenhu H., Khokhlov A.R., *Macromolecules*, **2005**, 38, 1292.

[120] Feil H., Bae Y.H., Feijen J., Kim S.W., *Macromolecules*, **1993**, 26, 2496.

[121] Maeda Y., Taniguchi N., Ikeda I., *Macromol. Rapid Commun.*, **2001**, 22, 1390.

[122] Aseyev V.O., Tenhu H., Winnik F.M., *Adv. Polym. Sci.*, **2006**, 196, 1.

[123] Aseyev V., Hietala S., Laukkanen A., Confortini O., Du Prez F.E., Tenhu H., *Polymer*, **2005**, 46, 7118.

[124] Kwak J.C.T., in *'Polymer-surfactants Systems'*, Surfactant Science Series, vol. 77, New York: Dekker, **1998**.

[125] Privalov P.L., Griko Y.V., Venyaminov S.Y., Kutysenko V.P., *J. Mol. Biol.*, **1986**, 190, 487.

[126] Breezer A.E., Loh W., Mitchell J.C., Royall P.G., Smith D.O., Tute M.S., Armstrong J.K., Chowdhry B.Z., Leharne S.A., Eagland D., Crowther N.J., *Langmuir*, **1994**, 10, 4001.

[127] (a) Arndt K.F., Schmidt T., Menge H., *Macromol. Symp.*, **2001**, 164, 313. (b) Arndt K.F., Schmidt T., Reichelt R., *Polymer*, **2001**, 42, 6785.

[128] Bulychev N., Confortini O., Kopold P., Arutunov I., Dirnberger K., Schauer T., Du Prez F.E., Zubov V., Eisenbach C.D., *Polymer*, **2007**, 48, 2636.

PART III

**Well-defined Stimuli-responsive
Graft Copolymer Structures by Combination
of the "*Grafting From*" Method and ATRP**

Chapter 7 : Theory of Controlled Radical Polymerizations 147

7.1. Introduction	147
7.2. Controlled Radical Polymerization (CRP).....	148
7.2.1. Mechanism.....	148
7.2.2. Characteristics of Controlled Polymerization Processes.....	149
7.2.3. The Different Controlled Radical Polymerizations.....	150
7.3. Atom Transfer Radical Polymerization (ATRP).....	152
7.3.1. Polymerization Mechanism.....	152
7.3.2. Role of the Reactants in ATRP.....	153
7.3.3. Kinetics.....	155
7.3.4. Graft Copolymers.....	157
7.4. General Features and Future Perspectives of CRP.....	157
7.5. References	158

Chapter 8 : Synthesis of Poly(Methyl Vinyl Ether) based Graft Copolymers via 'Grafting From' Method 161

8.1. Introduction	161
8.2. Homopolymerizations of St and tBMA via ATRP.....	163
8.2.1. Synthesis with a Copper Catalyst	164
8.2.1.1. Homopolymerization of PtBMA.....	164
8.2.1.2. Homopolymerization of Styrene.....	169
8.2.2. Synthesis with a Nickel Catalyst	172
8.2.2.1. Pseudo-Living Polymerization of St with NiBr ₂ (PPh ₃) ₂	172
8.2.2.2. Homopolymerization of tBMA.....	177
8.2.3. Conclusion	177
8.3. Synthesis of the Graft Copolymers	178
8.3.1. First Step: Synthesis of the Macroinitiator	178
8.3.2. Second Step: Synthesis of PMVE- <i>g</i> -PS and PMVE- <i>g</i> -PtBMA.....	180
8.3.2.1. Mechanism.....	180
8.3.2.2. Synthesis of PMVE- <i>g</i> -PS with Copper Catalyst	181
8.3.2.3. Synthesis of PMVE- <i>g</i> -PS with Nickel Catalyst	183
8.3.2.4. Synthesis of PMVE- <i>g</i> -PtBMA as Precursor of PMVE- <i>g</i> -PMAA	186
8.4. Conclusion	187
8.5. References.....	188

Chapter 9 : Properties of Thermo-responsive PMVE-*g*-PS Graft Copolymer 191

9.1. Introduction	191
9.2. The Thermo-responsive Properties of PMVE- <i>g</i> -PS.....	192
9.2.1. Phase Diagram by Modulated Temperature Differential Scanning Calorimetry (MTDSC)	193
9.2.2. Determination of the "Cloud Point" Temperature of Diluted Solutions.....	195
9.2.3. Microcalorimetry.....	195

9.2.4. Dynamic Light Scattering (DLS).....	196
9.2.4.1. Dependence of the Heating Rate.....	196
9.2.4.2. DLS-measurement at Room Temperature.....	197
9.2.4.3. Effect of the Heating.....	198
9.2.5. Atomic Force Microscope (AFM).....	203
9.3. Conclusion.....	204
9.4. References.....	205

Abstract

Smart copolymers with thermo-and/or pH-responsive properties were prepared by grafting polystyrene (PS) or poly(methacrylic acid) (PMAA) of different molecular weights from the thermo-responsive PMVE. First homopolymerizations of styrene, and also of *tert*-butyl methacrylate (*t*BMA), which is the protected monomer of methacrylic acid (MAA), were investigated with a new ATRP-initiator, 2,2,2-tribromoethanol (TBE), and two catalyst systems: $\text{NiBr}_2(\text{PPh}_3)_3$ and PMDETA/CuBr. From the results of these homopolymerizations, macromolecular graft copolymers with a statistical side chain spacing along the PMVE backbone have been synthesized by the 'grafting from' approach. For this, a macroinitiator was prepared by transforming the statistical P(MVE-*stat*-CEVE) copolymers into PMVE-*g*-TBE by the nucleophilic substitution of the chlorine groups.

From this macroinitiator, PMVE-*g*-PS, and also PMVE-*g*-*t*BMA graft copolymers were synthesized by ATRP (see **Chapter 8**). In the case of PMVE-*g*-*t*BMA conditions to control the grafting process could not be found, thus the synthesis of PMVE-*g*-PMAA was not further investigated. For PMVE-*g*-PS, $\text{NiBr}_2(\text{PPh}_3)_3$ was found to be the best catalyst system, resulting in narrow polydispersity index and longer side chains.

MTDSC was applied to study the influence of the presence of PS grafts on the solubility behavior of PMVE backbone in water (see **Chapter 9**). The presence of PS grafts diminishes the solubility of PMVE until a complete immiscibility occurs in water at room temperature. The phase diagram showed that the LCST of PMVE disappears. These graft copolymers were used to prepare aqueous aggregates. The morphological characterization of the aggregates was performed by DLS and atomic force microscopy (AFM). The larger structures were the result of micelle-like aggregates.

Besides, the thermo-responsiveness of the novel PMVE-*g*-PS graft copolymers was compared to those of the conventional aqueous PMVE solutions. The behavior of aggregates of PMVE-*g*-PS resembles the one of the mesoglobules of the PMVE homopolymer. Large aggregates collapses upon heating, whereas collapse occurred slowly within a broad temperature range in the case of micelle like structures. However, with microcalorimetry the collapse of the PMVE chain was observed to take place in all samples, suggesting that the shells of the micellar particles are crowded in a way that hinders the compression of the PMVE backbone.

Chapter 7

Theory of Controlled Radical Polymerizations

7.1. Introduction

Radical polymerization is industrially the most widespread method to produce materials such as plastics, rubbers and fibers [1]. The advantages of radical polymerizations over ionic polymerizations are numerous: a large variety of vinyl monomers have been polymerized or copolymerized and the reaction conditions require only the absence of oxygen. The major drawbacks of free radical polymerization are related to the lack of control over the polymer structure.

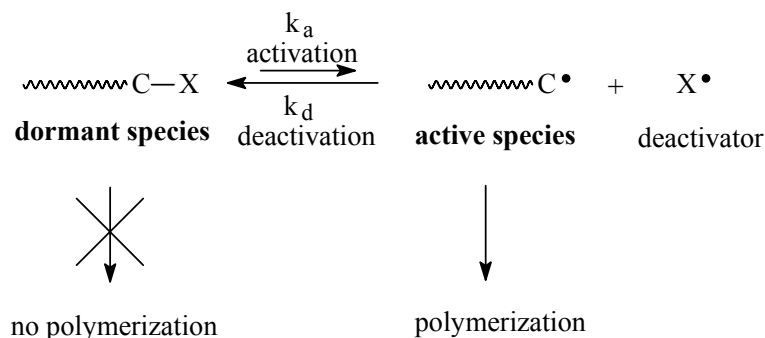
The development of ionic polymerization methods allowed for the preparation of well-defined polymers with controlled chain end functionalities and the synthesis of well-defined block and graft copolymers [2]. However, these polymerizations have to be carried out with nearly complete exclusion of moisture and often at very low temperatures. Moreover, only a limited number of monomers can be used, and the presence of functionalities in the monomers can cause undesirable side reactions.

More than a decade ago, a relatively new method to synthesize well-defined polymers, called Controlled Radical Polymerization (CRP) [3-5], was developed by several groups. There are now several procedures for controlling the radical polymerization, and corporations are introducing products based on CRP into numerous high-value markets [6]. One of the most successful methods is atom transfer radical polymerization (ATRP), introduced by Matyjaszewski and Sawamoto in 1995 [4-7]. As the ATRP-process will be used in this research, it will be presented in detail in this chapter.

7.2. Controlled Radical Polymerization (CRP)

7.2.1. Mechanism

A Controlled Radical Polymerization (CRP) is a polymerization based on an equilibrium between growing 'active species', growing polymer chain with an active radical at the end, and a 'dormant species' [5,8]. A deactivator reacts with growing chains to deactivate them, forming dormant species which prevent from termination reaction as shown in scheme 7.1.



Scheme 7.1. Mechanism of activation-deactivation for CRP.

Radicals formed during the initiation in CRP are present in the reaction mixture during several hours, while in free radical polymerization, the lifetime of a radical is very short, in the order of a second during which the initiation, propagation and termination take place. The initiation step of a CRP has to be very fast compared to the propagation step so that all the radicals are formed at the same time, and thus the propagation of the polymer chains can occur simultaneously.

Propagating species are produced by an activation process (with rate constant k_a in which the radical is being formed). The active species are deactivated reversibly (with a deactivation rate constant k_d) by the deactivator X. Only active species can polymerize with propagation rate constant k_p .

Because of the equilibrium between active and dormant species, the concentration of the radicals (active species) during the polymerization is very low, leading to a slow propagation and the reduction of the termination or transfer reactions. The dynamic equilibrium between the active and dormant chains influences the concentration of the radicals and thus the speed of the reaction. The more the equilibrium is shifted to the left (dormant species), the more the reaction is controlled [3-4]. Every polymer chain grows over a long period of time repeating activation/deactivation cycle. The time interval between each cycle is typically in the range of 0.1 to 10 ms.

7.2.2. Characteristics of Controlled Polymerization Processes

A radical polymerization is considered to be controlled if it is conform to certain criteria, for which the evolutions during the polymerization are shown in figure 7.1.

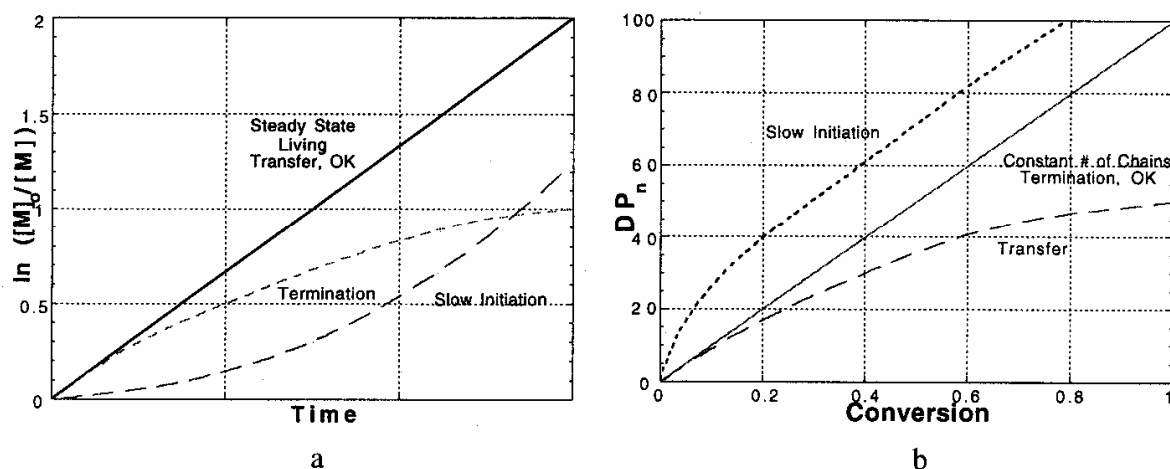


Figure 7.1. Influence of slow initiation step, termination and transfer on (a) kinetic plot and on (b) molecular weight. Figures taken from ref [4].

CRP differs from free radical polymerization by [3-4,7,9]:

✓ *Internal first-order kinetics with respect to monomer*

The evolution of $\ln[M]_0/[M]$ as a function of time has to be linear, if the reaction is of first order, proportional to the monomer concentration $[M]$ (eq. 7.1) (figure 7.1a). This provides that initiation is fast. Equation (7.2) of the propagation rate (R_p) shows that if R_p is first-order with respect to monomer concentration $[M]$, the propagation rate constant k_p is constant throughout the reaction, and hence the termination reactions are neglected.

$$\ln \frac{[M]_0}{[M]} = k_p' \cdot t \quad \text{eq. 7.1, with } k_p' = [P_n] [M]$$

$$R_p = -\frac{d[M]}{dt} = k_p \cdot [P_n] [M] \quad \text{eq. 7.2}$$

An accelerating plot is due to a slow initiation, and a decelerating plot is due to termination reactions.

✓ *Linear growth of DP_n with conversion*

Fast initiation, at least as fast as propagation, gives control over M_n (the DP_n is defined by the ratio of concentrations of the consumed monomer to the introduced initiator $DP_n = \Delta[M]/[I]_0$). The evolution of the M_n as a function of conversion has to be linear (figure 7.1b). A higher M_n than expected is obtained if the initiation step is not efficient or if some combination occurs. On the contrary, a lower M_n can be the result of transfer reactions (scheme 7.1).

✓ *Narrow M_w/M_n*

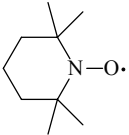
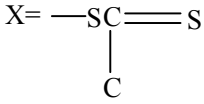
The M_w/M_n decreases with the conversion for systems with a slow initiation step and a slow exchange between dormant chain and active chains.

7.2.3. The Different Controlled Radical Polymerizations

Currently, three methods appear to be most efficient and can be successfully applied to a large number of monomers: stable free radical polymerization (SFRP), best represented by nitroxide mediated polymerization (NMP), reversible addition-fragmentation chain transfer (RAFT), and metal catalyzed atom transfer radical polymerization (ATRP) along with other degenerative transfer processes.

All CRP techniques mentioned before use an agent that reacts with growing chains to 'deactivate' them, and so preventing termination reactions. The main difference between the polymerization techniques is the nature of the deactivator X (scheme 7.2), apart from other specific reactants. For NMP, RAFT and ATRP, the deactivating species X are given in table 7.1. In ATRP, the radical at the active polymer chain end is trapped by an halogen [6].

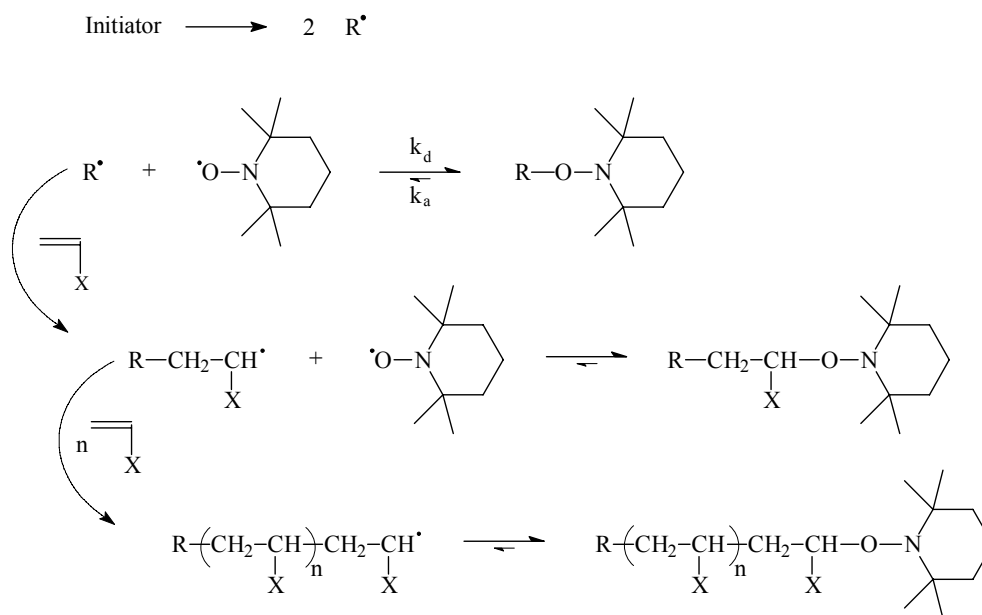
Table 7.1. Deactivators used in CRP.

<i>CRP technique</i>	<i>NMP</i>	<i>RAFT</i>	<i>ATRP</i>
	Nitroxides	Dithioesters	Halogen metal ions
Deactivator X	$X = $  TEMPO	$X = $ 	$X = \text{Br, Cl} + \text{metal}$ (Cu ^I Br/2L, etc)

Nitroxide Mediated Polymerization (NMP) [4,10]

In this process, which is similar to ATRP, control is introduced by the use of a nitroxide. The polymerization process is a dissociation-combination mechanism where R-X is thermally or photochemically dissociated into R^{*}, the growing chain polymer, and X^{*}, the nitroxide. This is the initiation step.

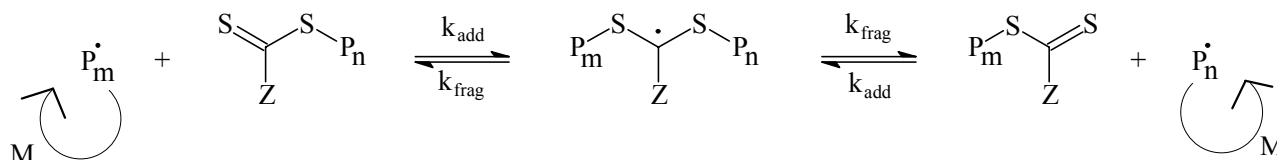
X^{*} is a stable radical that can only react with R^{*} to form a dormant species (alkoxyamine). X^{*} radicals should not react between themselves, and should not initiate propagation. R^{*} induces propagation by adding a monomer and the dissociation-combination process takes place until the end of the polymerization (scheme 7.2).



Scheme 7.2. Reaction of polymerization using TEMPO.

Reversible Addition Fragmentation Transfer (RAFT) [4,11-12]

This process makes use of a dithioester compound [12] to obtain a dynamic equilibrium between the dormant and the active species. The dithioester (table 7.1) undergoes a fragmentation to form an active radical P_i^\bullet ($i = m$ or n) and a dormant species (scheme 7.3). After addition of monomer, addition occurs again, and the cycle can be repeated.



Scheme 7.3. Reaction of polymerization by RAFT process.

This technique can be used to polymerize all kinds of vinyl monomers such as styrenes, (meth)acrylates including acrylic acid and vinyl acetate which are not polymerizable by ATRP. Thioesters are revealed to be good transfer agents [13]. Some problems of RAFT are related to the dithioesters themselves. They are not commercially available and the resulting polymers are sometimes coloured. Furthermore, dithioesters and their reaction can give rise to unpleasant odour.

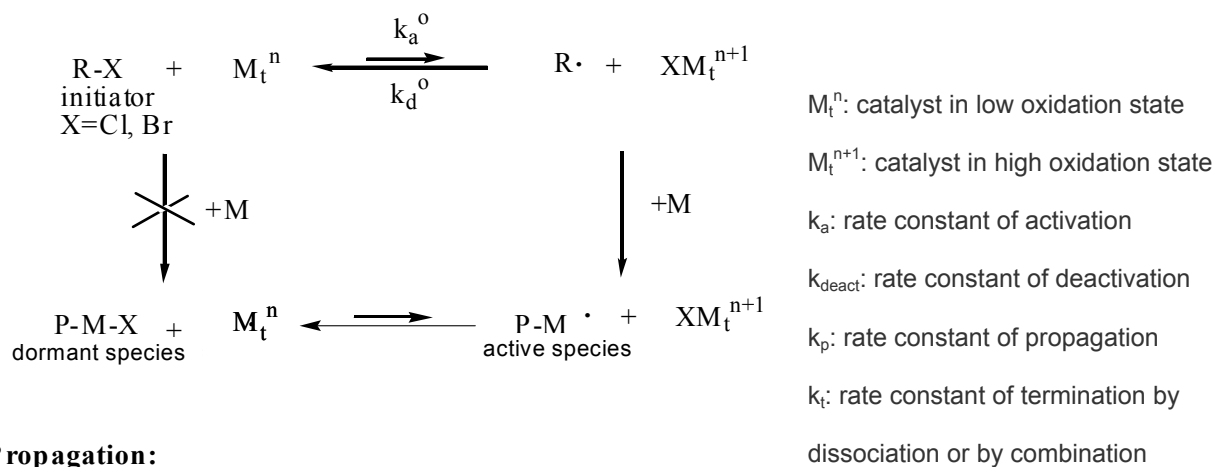
Atom Transfer Radical Polymerization (ATRP) [3-5,7]

As our research was focused on ATRP, its mechanism will be presented in more detail in the following section.

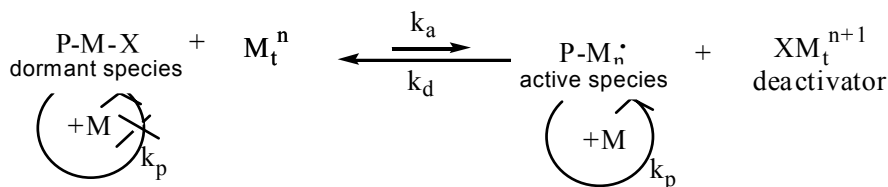
7.3. Atom Transfer Radical Polymerization (ATRP)

7.3.1. Polymerization Mechanism

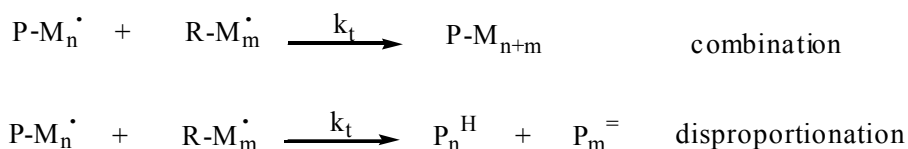
Initiation:



Propagation:



Termination:



Scheme 7.4. Mechanism of ATRP.

Because the key step in controlling the polymerization is atom (or group) transfer between growing chains and the catalyst, this process was called ATRP. In this mechanism, the active radical $\text{R}\cdot$ is formed by a transfer of the halide group X to a transition metal complex M_t^n . This radical can initiate the propagation of the monomer and form the propagating species $\text{P-M}\cdot$, the 'active species' (scheme 7.4).

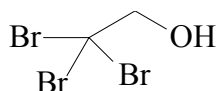
ATRP is a catalytic process: the rate of polymerization depends on the concentration of the transition metal in its lower oxidation rate. It is one of the principal advantages of this method. The control over the polymerization depends on the equilibrium between the active and the dormant species. The active species reacts with the metal halide complex to form the 'dormant species' P-M-X . This is in fact a redox reaction.

7.3.2. Role of the Reactants in ATRP

All the ATRP systems consist of an initiator, a transition metal complex with a ligand and a monomer. The control over the polymerization process depends on the equilibrium between the active and the dormant species. In the following, each component of the ATRP system will be discussed in more detail.

* *Initiator*

Two parameters are important for a successful ATRP initiating system: 1) initiation should be fast in comparison with propagation; 2) the probability of side reactions should be minimized. The amount of the initiator determines the final M_n of the polymer at full monomer conversion. The initiator is generally an alkyl halide RX whose structure is analogous to the polymer. Its main role is to generate growing chains. The radical formed on the terminal structure is secondary or tertiary, dependent on the terminal structure of the polymer. For example, a secondary initiator will normally be used to polymerize acrylates, while a tertiary one will be used to polymerize methacrylates. The halide group must rapidly and selectively migrate between the growing chains and the transition metal. Chloride and bromide have been shown to be the best halides for this exchange. The bromide forms a weaker bond than the chloride, which permit to have faster initiation and propagation steps. Fluorine is bound too strongly to the growing chain, and although iodine is a good leaving group for acrylate polymerizations, it is involved in side reactions in styrene polymerization. In this work, tribromoethanol (TBE) and derived products have been used as the initiator (scheme 7.5).



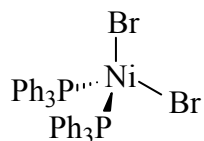
Scheme 7.5. Tribromoethanol (TBE).

* *Catalyst*

The catalyst is a transition metal that is complexed by one or more ligands in order to obtain an optimal control of the polymerization; it does not need to be used in one to one ratio with the initiator but can be used in smaller quantities. There are several prerequisites for an efficient transition metal catalyst: 1) the metal center must have at least two readily accessible oxidation states separated by one electron; 2) the metal center should have reasonable affinity towards a halogen; 3) the coordination sphere around the metal should be expandable upon oxidation to selectively accommodate a (pseudo)-halogen; 4) the ligand should complex the metal relatively strongly.

The catalyst is usually a copper (I) halide system. Cu (I) complexes are mostly used for the polymerization of styrenes, (meth)acrylates, acrylonitriles and dienes since they have been shown to be the most efficient catalysts. Also, various polydentate imine/amine ligands are used to solubilise the catalyst, as discussed below.

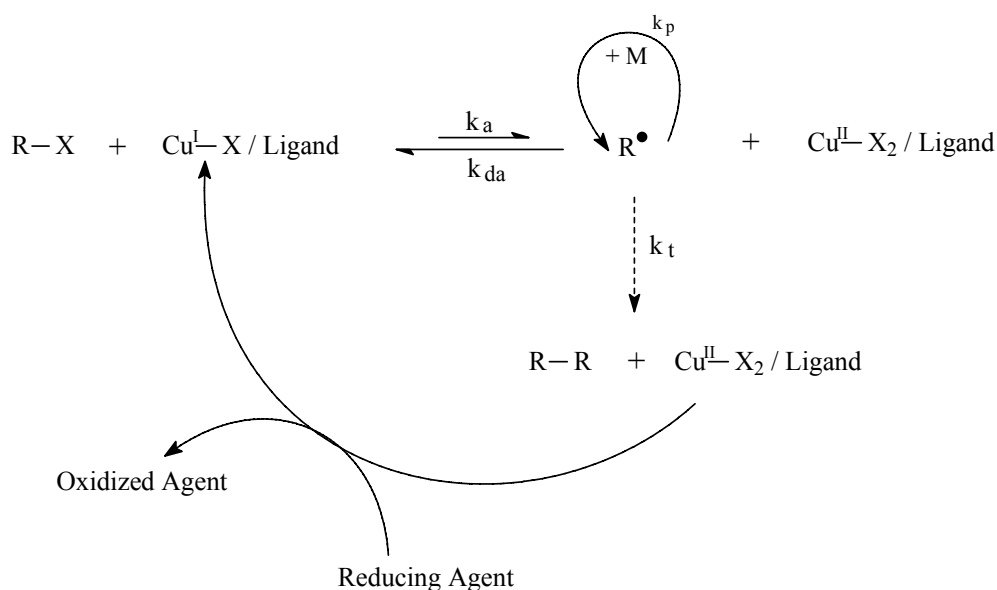
Moreover, a lot of others metals like Ni, Pd, Ru, Re... have been used. In this work, nickel (II) bis(triphenylphosphine) dibromide ($\text{NiBr}_2(\text{PPh}_3)_2$) (scheme 7.6) was used. The particularity of this catalyst is to provide ATRP in the absence of any Lewis acid additive or ligand.



Scheme 7.6. Nickel (II) bis(triphenylphosphine) dibromide ($\text{NiBr}_2(\text{PPh}_3)_2$).

At the end of the polymerization, the catalyst system introduces a halide end group to the polymer chains. The attractive flexible initiation with RX /transition metal catalyst is often overcompensated by the difficulties of catalyst removal from the polymer. Therefore, its industrial application is unlikely as long the toxic and coloured catalysts can not be removed from the polymers properly.

After our research, processes with ppm amounts of copper have also been developed where the activators are regenerated by electron transfer (ARGET) ATRP. This method provides a continuous controlled polymerization with a significant reduction of the amount of copper based catalyst complex (down to ~ 10 ppm) due to a constant regeneration of the Cu(I) activator species by environmentally acceptable reducing agents, which compensate for any loss of Cu(I) by termination (scheme 7.7) [16]. In this way, higher M_w polymers were synthesized [14-15].

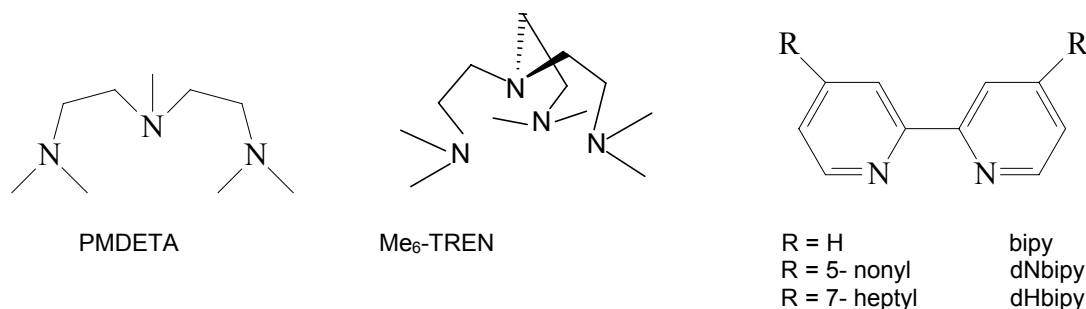


Scheme 7.7. Proposed Mechanism for Activators Regenerated by Electron Transfer for ATRP (ARGET ATRP).

*** Ligand**

The role of the ligand is to solubilize the catalyst and to react in the redox reaction by forming a complex with the metal. The ligands influence the equilibrium between the active and the dormant species: the lower the redox potential of the Cu /ligand is, the more the equilibrium shifts from dormant species to active species, leading to more radicals in the system. Ligands may also facilitate the removal and recycling of the catalyst.

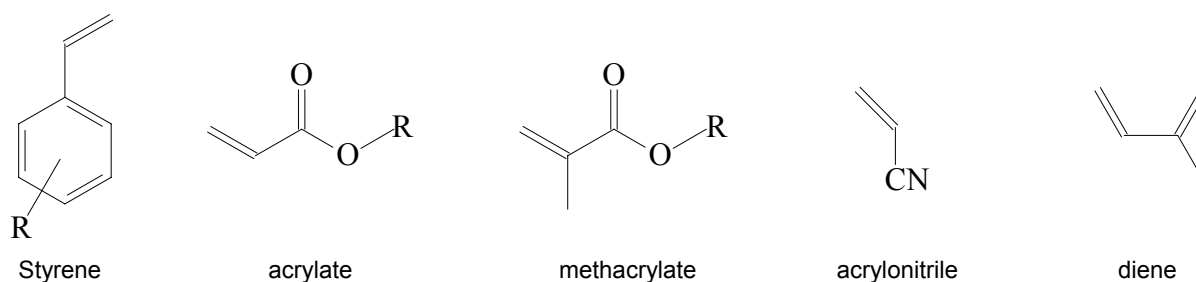
The most common ligands are 2,2'-bipyridine (bipy) and derivatives, N,N,N',N'',N'''-pentamethyldiethylenetriamine (PMDETA) and N,N,N',N'',N'''-hexamethyl-tris (2 aminomethyl) amine (Me₆TREN) (scheme 7.8).



Scheme 7.8. Typical ligands for Cu-based ATRP.

* Monomer

By ATRP many kinds of vinyl monomers can be used such as styrenes, (meth)acrylates, acrylonitriles, acrylamides and dienes (scheme 7.9).



Scheme 7.9. Examples of monomers used in ATRP.

However, ATRP is not able to polymerize (meth)acrylic acid because of the sensitivity of the catalyst system to the acid functionalities. For example, CuBr₂ quickly reacts with the monomer to generate Cu(acrylate)₂, an efficient radical scavenger. To overcome these complications, protective derivatives of the acids can be used in the polymerization. This work will focus on styrene on one hand, and methacrylate on the other hand, specifically *tert*-butyl methacrylate in order to form methacrylic acid.

The advantage of ATRP compared to the other techniques is that it permits to polymerize a large variety of vinylic monomer in a large range of temperatures. The reaction can also be performed in bulk, solution, dispersion or emulsion. It allows easy control of chain topology, composition and functionality.

7.3.3. Kinetics

According to scheme 7.4, the kinetics of ATRP are discussed here using an homogeneous catalyst system. First, initiation should be fast, providing a constant concentration of growing polymer chains; secondly, because of the persistent radical effect (PRE), termination becomes insignificant and the speed of activation and deactivation can be written as follow:

$$R_{act} = k_{act} [I]_0 [Mt^n] \quad \text{eq. 7.3}$$

$$R_{deact} = k_{deact} [P^*] [X - Mt^{n+1}] \quad \text{eq. 7.4}$$

with $[I]_0$ = concentration of initiator

$[P^*]$ = concentration of polymer radical

$[Mt^n]$ = concentration of catalyst at low oxidation state

$[X-Mt^{n+1}]$ = concentration of oxidized metal complexes as persistent radicals

The rate of the polymerization is also influenced by the ratio of concentrations of the activator to deactivator, although this may change during polymerization. The rate law for ATRP can be derived as follows:

$$R_p = \frac{-d[M]}{dt} = k_p [M] [P^*] = k_p K_{eq} [M] [I]_0 \times \frac{[Mt^n]}{[X - Mt^{n+1}]} \quad \text{eq. 7.5}$$

with $K_{eq} = \frac{k_{act}}{k_{deact}}$, the magnitude equilibrium constant determining the polymerization rate

k_{act} = rate constant of activation

k_{deact} = rate constant of deactivation

k_p = rate constant of propagation

Results from kinetic studies of ATRP indicate that the rate of polymerization is first-order with respect to monomer, initiator and metal complex concentrations. These observations are all consistent with the derived rate law (eq. 7.5). The kinetically optimal ratio of ligand to copper in the polymerization of both St and MA was determined to be 2/1. Below this ratio, the polymerization rate was usually slower, and above this polymerization rate remained constant. It should be noted that the optimum ratio can vary with regard to changes in the monomer, counter anion, ligand, temperature and other factors [16].

The precise kinetic law for the deactivator ($X-Mt^{n+1}$) is more complex due to the spontaneous generation of Mt^{n+1} via the PRE [17]. In the atom transfer step, a reactive organic radical is generated along with a stable Mt^{n+1} species that can be regarded as a persistent metallo-radical. If the initial concentration of deactivator Mt^{n+1} in the polymerization is not sufficiently large to ensure a fast rate of deactivation ($k_{deact}[Mt^{n+1}]$), then coupling of the organic radicals will occur, leading to an increase in the Mt^{n+1} concentration. Radical termination occurs rapidly until a sufficient amount of deactivator Mt^{n+1} is formed and the radical concentration becomes low enough. Under such conditions, the rate at which radicals combine ($k_t[R^1]^2$) will become much slower than the rate at which radicals react with the metal complex ($k_{deact}[R^1][Mt^{n+1}]$) in a deactivation process and a controlled/living polymerization will proceed. Typically, a small fraction (~5%) of the total growing polymer chains will be terminated during the early stage of the polymerization, but the majority of the chains (> 90%) will continue to grow

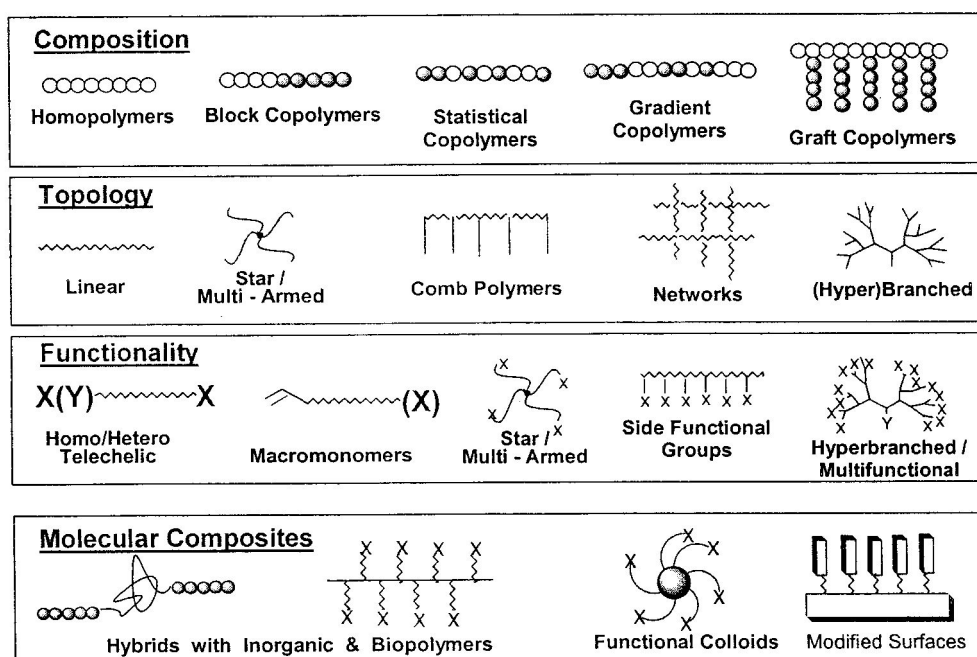
successfully. If a small amount of the deactivator (~10 mol-%) is added initially to the polymerization, then the proportion of terminated chains can be greatly reduced [18].

7.3.4. Graft Copolymers

Because of the control over M_n and functionality, ATRP has allowed for the synthesis of numerous materials with many novel topologies. With the exception of linear polymers, architectural differences lie in branched structures with regard to the number of branches and their relative placement in the macromolecules. However, these changes in composition may provide dramatic differences in their properties. The following examples serve as starting points for our next study (**Chapter 8**) that will concentrate on the synthesis of graft copolymers. Two methods, *grafting from* and *grafting through*, have been used in conjunction with ATRP in the design of graft copolymers and underscore the versatility of this controlled radical polymerization technique to synthesize a variety of copolymers. Some examples are already described in **Chapter 4.2**. In our case, the chlorine groups of PMVE backbone will be substituted by TBE to create a macroinitiator (**Chapter 8**). In that way, poly(*tert*-butyl methacrylate) (PtBMA), precursor of the PMAA, and in a second stage, PS, were grafted from the backbone via ATRP.

7.4. General Features and Future Perspectives of CRP

Not only can linear polymers be synthesized with a high degree of control, but CRP also allows the polymer chemist to vary architecture of the polymer chains by relatively simple means, controlled compositions and functionalities. Thus, a variety of novel polymer materials with predetermined composition, topology and functionality, as illustrated in scheme 7.10, can be created.



Scheme 7.10. Schematic representation of controlled topologies, compositions, functionalities and molecular composites prepared by ATRP. Figure taken from ref [4].

There are so many interesting structures to be prepared that this technique should find commercial use and many new industrial applications in the very near future. It is possible to design novel surfactants, dispersants, lubricants, adhesives, gels, coatings, and many other materials which can only be prepared by controlled/living radical polymerization.

7.5. References

- [1] Moad G., Salomon D.H., in *'The Chemistry of Free Radical Polymerization'*, Oxford: Pergamon, **1995**.
- [2] (a) Hsieh H.L., Quirk R.P., in *'Anionic Polymerization: Principles and Practical Applications'*, New York: Marcel Dekker, **1996**. (b) Matyjaszewski K., Ed., in *'Cationic Polymerizations: Mechanisms, Synthesis and Applications'*, New York: Marcel Dekker, **1996**. (c) Kennedy J.P., Jacob S., *Acc. Chem. Res.*, **1998**, *31*, 835.
- [3] (a) Buback M., Herk A.M., in *'Radical Polymerization: Kinetics and Mechanism'*, Ed. WILEY-VCH Verlag GmbH, **2007**. (b) Matyjaszewski K., Braunecker W.A., in *"Macromolecular Engineering, Precise Synthesis, Materials, Properties, Applications"*, Vol. 1 in *'Synthetic Techniques'*, Edited by Matyjaszewski K., Gnanou Y., Leibber L., Wiley-VCH Verlag GmbH & Co. KGaA, Weinheim, Germany, Chap. 5, **2007**.
- [4] Matyjaszewski K., Ed., Washington, DC: American Chemical Society, (a) in *'Controlled Radical Polymerization'*, **1998**. (b) in *'Controlled/Living Radical Polymerization'*, **2000**. (c) in *'Advances in Controlled/Living Radical Polymerization'*, **2003**. (d) in *'Controlled/Living Radical Polymerization, From Synthesis to Materials'*, **2006**.
- [5] Kamigaito M., Ando T., Sawamoto M., *Chem. Rev.*, **2001**, *101*, 3689.
- [6] (a) Matheson R.R., in *'The Knowledge Foundation Meeting'*, Boston, **2000**. (b) Auschra C., Eckstein E., Knischka R., Pirrung F., Harbers P., *Eur. Coatings J.*, **2004**, *6*, 26. (c) Nakagawa Y., *Polym. Mat. Sci. Eng.*, **2004**, *45*, 109. (d) Muehlebach A., *Polym. Mat. Sci. Eng.*, **2004**, *90*, 180. (e) Coca S., Woodworth B.E., *Polym. Mat. Sci. Eng.*, **2004**, *90*, 182. (f) Ruy D.Y., Shin Y., Drockenmuller E., Hawker C.J., Russell T.P., *Science*, **2005**, *308*, 236. (g) Matyjaszewski K., Spanswick J., *Materials today*, March **2005**, 26.
- [7] (a) Coessens V., Pintauer T., Matyjaszewski K., *Prog. Polym. Sci.*, **2001**, *26*, 337. (b) Qiu J., Charleux B., Matyjaszewski K., *Prog. Polym. Sci.*, **2001**, *26*, 2083. (c) Matyjaszewski K., Xia J., *Chem. Rev.*, **2001**, *101*, 2921. (d) Goto A., Fukuda T., *Prog. Polym. Sci.*, **2004**, *29*, 329.
- [8] (a) Wang J.S., Matyjaszewski K., *J. Am. Chem. Soc.*, **1995**, *117*, 5614. (b) Matyjaszewski K., Xia J., *Chem. Rev.*, **2001**, *101*, 2921.
- [9] Matyjaszewski K., Davis T.P., in *'Handbook of Radical Polymerization'*, Ed. Wiley-Interscience: Hoboken, NJ, **2002**.
- [10] (a) Malmström E., Miller R.D., Hawker C.J., *Tetrahedron*, **1997**, *53*, 15225. (b) Matyjaszewski K., Woodworth B., Zhang X., Gaynor S.G., Metzner Z., *Macromolecules*, **1998**, *31*, 5955. (c) Fukuda T., Goto A., Ghno K., *Macromol. Rapid Commun.*, **2000**, *21*, 151.

- [11] Chiefari J., Chong Y.K.B., Ercole F., Kristina J., Jeffrey J., Le T.P.T., Mayadunne R.T.A., Meijs G.F., Moad C.L., Moad G., Rizzardo E., Thang S.H., *Macromolecules*, **1998**, *31*, 5559.
- [12] (a) Moad G., Chiefari J., Chong Y.K., Kristina J., Mayadunne R.T.A., Postma A., Rizzardo E., Thang S.H., *Polym. Int.*, **2000**, *49*, 993. (b) Monteiro M.J., Sjöberg M., Van der Vlist J., Göttgens M., *J. Polym. Sci., Part A: Polym. Chem.*, **2000**, *38*, 4206. (c) Uzulina I., Kanagasabapathy S., Claverie J., *Macromol. Symp.*, **2000**, *150*, 33. (d) Goto A., Sato K., Tsujii Y., Fukuda T., Moad G., Rizzardo E., Thang S.H., *Macromolecules*, **2001**, *34*, 402. (e) Monteiro M.J., de Barbeyrac J., *Macromolecules*, **2001**, *34*, 4416.
- [13] (a) Mayadunne R.T.A., Rizzardo E., Chiefari J., Kristina J., Moad G., Postma A., Thang S.H., *Macromolecules*, **2000**, *33*, 243. (b) Charmot D., Corpart P., Adam H., Zard S.Z., Biadatti T., Bouhadir G., *Macromol. Symp.*, **2000**, *150*, 23. (c) Destarac M., Charmot D., Franck X., Zard S.Z., *Macromol. Rapid Commun.*, **2000**, *21*, 1035.
- [14] Jabubowski W., Min K., Matyjaszewski K., *Macromolecules*, **2006**, *39*, 39.
- [15] Matyjaszewski K., Jabubowski W., Min K., Tang W., Huang J., Braunecker W.A., Tsarevsky N.V., *Proc. Natl. Acad. Sci. USA*, **2006**, *103*, 15309.
- [16] (a) Percec V., Barboiu B., Neumann A., Ronda A., *Macromolecules*, **1996**, *29*, 3665. (b) Wang J.-L., Grimaud T., Matyjaszewski K., *Macromolecules*, **1997**, *30*, 6507. (c) Levy A.T., Olmstead M.M., Patten T.E., *Inorg. Chem.*, **2000**, *39*, 1628.
- [17] (a) Matyjaszewski K., Patten T.E., Xia J., *J. Am. Chem. Soc.*, **1997**, *119*, 674. (b) Fisher H., *J. Polym. Sci., Part A: Polym. Chem.*, **1999**, *37*, 1885. (c) Shipp D.A., Matyjaszewski K., *Macromolecules*, **2000**, *33*, 1553.
- [18] (a) Matyjaszewski K., Coca S., Gaynor S.G., Greszta D., Patten T.E., Wang J.S., Xia J., *WO Pat. 9718247, U.S. Pat. 5,807,937*. (b) Kajiwara A., Matyjaszewski K., Kamachi M., *Macromolecules*, **1998**, *31*, 595.

Chapter 8

Synthesis of Poly(Methyl Vinyl Ether) based Graft Copolymers via the 'Grafting From' Method

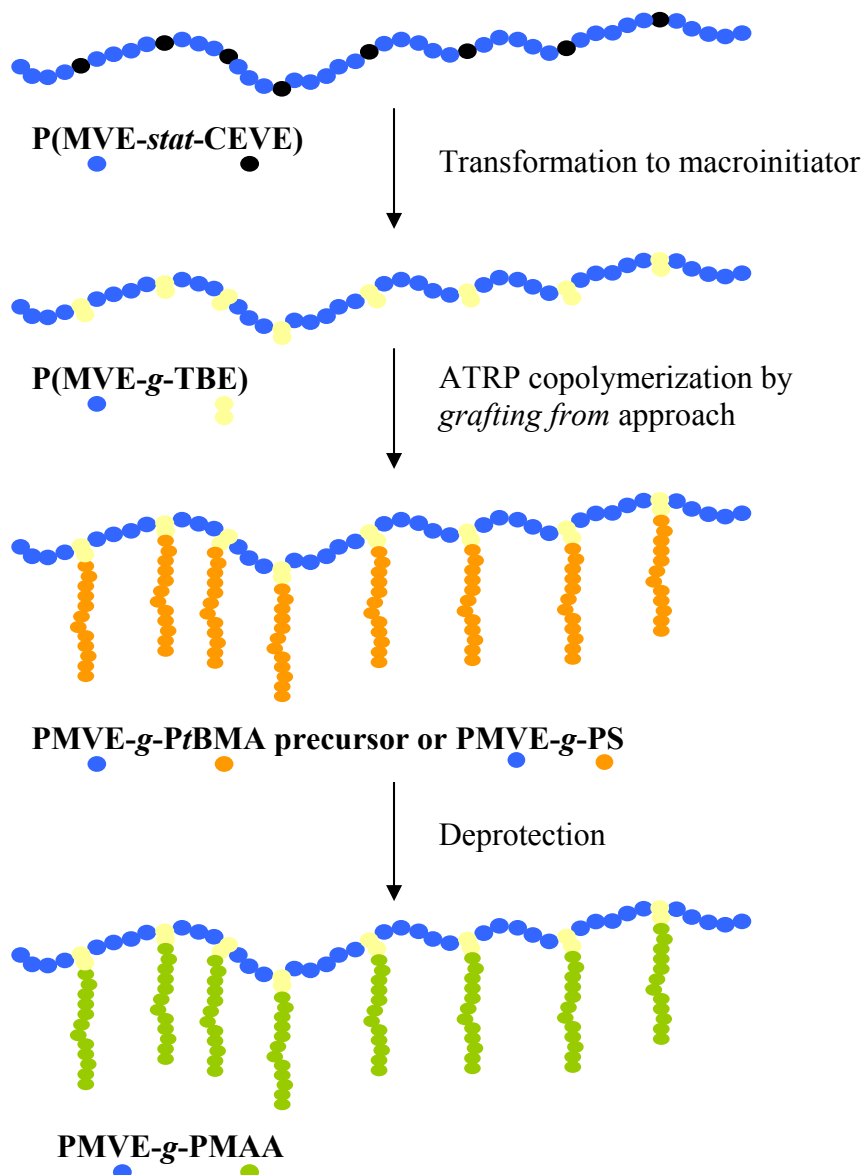
8.1. Introduction

Among the methods of polymer modifications, grafting is one of the promising methods. In principle, graft copolymerization is an attractive method to impart a variety of functional groups to a polymer [1]. Until recently, new types of radical techniques have become available for the preparation of well-defined polymers. One of the most important types of controlled/'living' radical polymerizations is ATRP [1-3] (see **Chapter 7**) that has been used to prepare graft copolymers by both *grafting through* and *grafting from* methods (see **Chapter 4**).

To make graft copolymers with specific properties, the structures must be controlled. For this reason, the *grafting from* method is one of the useful ways to design and get well-defined graft copolymers. This approach uses a macroinitiator that carries initiation groups to start a polymerization reaction of a monomer. The synthesis of the macroinitiator allows the control of the main chain parameters (DP_n , M_w/M_n) as well as the pre-determination of side chain density and side chain distribution. The main difficulty in this approach is to ensure a uniform propagation of the side chains and furthermore to suppress chain coupling reactions. Hence, ATRP has been applied in the synthesis of several well-defined graft copolymers in which a polymer possessing ATRP-active halide atoms as side groups is used as a macroinitiator in the ATRP of a second monomer[4].

In the last decade, various *grafting from* copolymers with chlorine pendant groups have been synthesized by ATRP [5-7]. For example, graft copolymers of poly(methyl methacrylate) (PMMA) [5] or polystyrene (PS) [6] backbones with respectively poly(2-methyl-2-oxazoline) (PMeOXA) and poly(ethyl methacrylate) (PEMA) as branches were synthesized starting from some chloromethyl styrene groups present in the backbone by ATRP.

In this chapter, the synthesis of graft copolymers composed of hydrophobic PS or pH-responsive PMAA as side chains, *grafted from* a thermo-responsive PMVE backbone, will be described. Chlorine pendant groups resulting from the CEVE-units in the P(MVE-*stat*-CEVE) (see **Chapter 3**) were used as starting points for the synthesis of a macroinitiator for ATRP. For this purpose, chlorine groups have been substituted by 2,2,2-tribromoethanol (TBE) as ATRP initiator (see scheme 8.1).



Scheme 8.1. Strategy for the synthesis of PMVE-*g*-PMAA and PMVE-*g*-PS graft copolymers.

In a next step, poly(*tert*-butyl methacrylate) (PtBMA) side chains, precursor of PMAA, and PS were *grafted from* the PMVE backbone *via* ATRP. Indeed, ATRP is commonly not able to polymerize acidic monomers, such as AA or MAA due to a side reaction of the monomer with the metal complex and quaternization of the nitrogen ligands [8]. One strategy to overcome these complications is the ATRP synthesis of protected derivatives of the acidic monomers such as *tert*-butyl (meth)acrylates [3], benzyl (meth)acrylates [9-10] and 1-ethoxyethyl acrylate [11], followed

by hydrolysis [9], debenzoylation [12] or thermolysis [13], respectively. In first instance, the ATRP technique was developed with TBE as initiator for the polymerizations of *t*BMA and St with CuBr/PMDETA as metal/ligand catalyst. In an alternative approach, we have investigated a new supported catalytic system based on nickel dibromide triphenyl phosphine ($\text{NiBr}_2(\text{PPh}_3)_2$), which does not require the addition of any complexes to give controlled ATRP. The combination of ATRP and LCP would permit us to control the structure of the graft copolymers: molecular weight, narrow polydispersity and length of the graft copolymers.

To find a suitable catalyst system for the synthesis of graft copolymers with St and MAA via ATRP, we initially investigated the influence of the catalyst system (Cu- and Ni-based catalysts) on the homopolymerization of St and *t*BMA.

8.2. Homopolymerizations of St and *t*BMA via ATRP

In ATRP, the choice of initiator is important to obtain good control over the polymerization. Polyhalogenated compounds of the general formula R-CX_3 , where X stands for halogen and R can be hydrogen, halogen or various organic substituents, were tested, in which at least one of the halogen atoms can be released and generate a primary radical capable of initiation of polymerization.

These compounds are mostly commercially available, inexpensive and can be simply purified by common methods like distillation. In the case of polychloroalkanes, their reactivity increases with increasing number of chlorine atoms per molecule. Because of their moderate reactivity, very few examples of initiation by mono- [14] and dichloro compounds [15] can be found in the literature.

Destarac *et al.* studied ATRP of St [16] from both the kinetic and mechanistic point of view, initiated with various polychloroalkane-type initiators of the general formula RCCl_3 such as methyl trichloroacetate, 1,1,1-trichloro-2,2,2-trifluoroethane, 1,1,1-trichlorononane or 2,2,2-trichloroethyl pivalate, and catalyzed with CuCl in the presence of bipy ligand. It was found that all the compounds used are active initiators in ATRP of St. However, the type R group affects the rate of polymerization.

Since few years, Masař *et al.* [17] synthesized a novel type of bifunctional ATRP initiator with two trichloromethyl groups as the active sites by reaction of an aromatic diisocyanate first, but also *tert*-butyl acrylate (*t*BuA) with 2,2,2-trichloroethanol (TCE). Only few research groups [11,17-19] used TCE initiator successfully to synthesize block copolymers of methacrylates and acrylates for ATRP.

Matyjaszewski and co-workers [18] were the first to report the polymerization of MMA by ATRP using the CuCl/bipy catalyst system with TCE initiator. Recently, Klumperman *et al.* [19] reported the synthesis of AB and BA block copolymers of MMA and *t*BMA utilizing TCE with CuCl/HMTETA as catalyst system. Moreover, in our laboratory, Du Prez *et al.* [11] synthesized

poly((1-ethoxyethyl methacrylate) (PEEMA) and poly(1-ethoxyethyl acrylate) (PEEA) by ATRP with TCE, directly resulting in PAA and PMAA by thermolysis.

In examination of the atom transfer radical process, TCE containing the required primary alcohol for the substitution of the chlorine groups of CEVE, and an initiating functionality for ATRP, could have been used. However, tribromoethanol (TBE) was selected as our initial functional initiator, not only for its commercial availability and relatively low cost, but particularly for the presence of bromide end groups, which are more suitable to determine the number of initiating site compared to the chlorine groups of CEVE that are still present on the backbone.

Initially, the efficiency of TBE to initiate the controlled free radical polymerization of vinyl monomers was investigated by Jérôme [17,20-22], Wooley [23] and Shimada [24]. Jérôme *et al.* [25] reported the synthesis of ABA triblock copolymers of methyl methacrylate (MMA) and BA using the homogeneous $\text{NiBr}_2(\text{PPh}_3)_2$ ATRP polymerization of MMA with a bromide end-functionalized poly(*n*-butyl acrylate) (*n*PBA) macroinitiator with TBE initiator. Under standard conditions [20], using CuBr/bipy as the metal complex, the homopolymerization of St with TBE was shown to be a living process. Similarly, the homopolymerization of MMA using TBE and $\text{NiBr}_2(\text{PPh}_3)_2$ as metal catalysts was observed to be a living process [22].

According to these literature data, ATRP syntheses of St and *t*BMA with TBE initiator were investigated first with CuBr/PMDETA catalyst system and secondly with $\text{NiBr}_2(\text{PPh}_3)_2$ metal catalyst.

8.2.1. Synthesis with a Copper Catalyst

8.2.1.1. Homopolymerization of *t*BMA

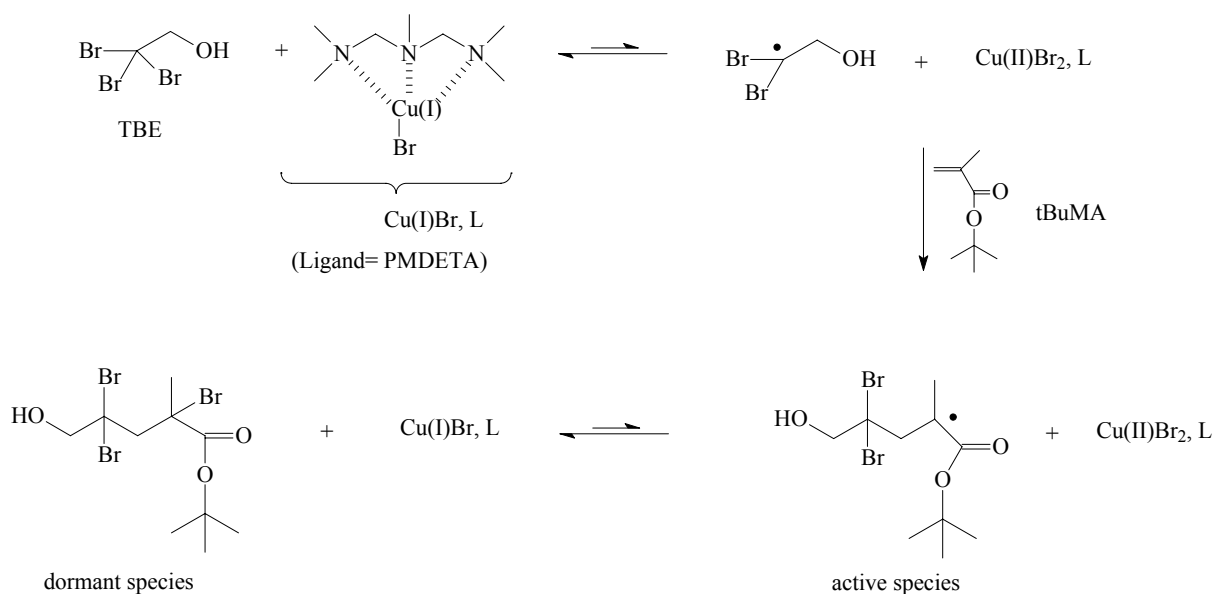
The overall rate of polymerization and level of control during the polymerization are influenced by several variables, such as initiator, catalyst, solvent, ligand, type of transferring halogen (X), and external variables such as temperature [26]. The choice of the appropriate initiator/CuX (X = Cl, Br) system is a key parameter, when polymerizing monomers such as *t*BMA to reduce the termination process (second order with respect to the concentration of radicals) and to establish the dynamic equilibrium between the dormant and active species [27]. Previously, Destarac *et al.* [16] showed that the use of TCE resulted in a fast and nearly quantitative initiation of MMA with a CuCl/bipy catalyst system. Although three chloride atoms are present per molecule, it is suggested in the literature that only one atom is viable for initiation [16]. In this work, PMDETA was selected because (a) this catalyst gave the best results for polymerization of *t*BMA with TCE and CuBr metal (85% conversion) [19], (b) easily available, (c) cost-effective and (d) the catalyst complex can be easily separated from the polymer [28]. As the backbone is viscous and sticky, it seems to be better to carry out the grafting reaction in solution with a large

amount of solvent (instead of bulk), in order to obtain a homogenous mixture with the backbone, the initiator TBE and the monomer.

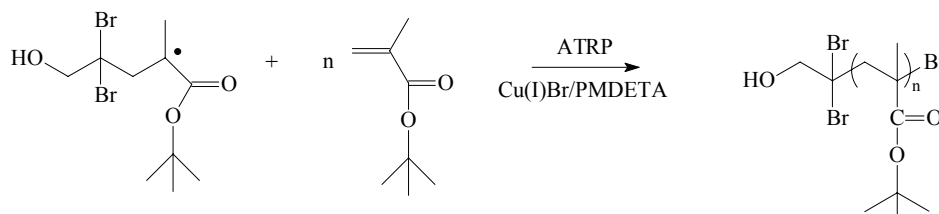
** Mechanism*

The ATRP mechanism of the homopolymerization is shown in the following scheme 8.2. The active radical (propagating species) is formed by the transfer of a bromide group from the initiator TBE to the metal complex CuBr(I)/PMDETA. This active radical initiates the propagation step.

• Initiation



• Propagation



Scheme 8.2. Mechanism of the homopolymerization of tBMA via ATRP.

** Experimental Conditions*

In order to determine the best parameters for the homopolymerization of tBMA with TBE, a series of experiments were carried out. Our ATRP formulations are based on the one originally described by Klumperman [19]. As was already mentioned in the previous paper of Klumperman [19], the efficiency of PtBMA ATRP polymerization was tested in a combination with CuBr/PMDETA complex with TCE as initiator in toluene and methyl ethyl ketone (MEK) respectively at 90°C. Solvents, temperature and concentration of the reactants were varied to optimize polymerization conditions (see table 8.1 and 8.2). As can be seen in table 8.1 (entry 1 and 2), although M_w/M_n is narrow, only polymer traces are observed. Conversions, which are very low, do not correspond to the expected one, meaning that TCE is a better initiator than TBE in these conditions.

Table 8.1. Results of the homopolymerization of *t*BMA in different solvents ($V_{tBMA}/V_{solvent} = 1/1$ (50 vol-%)) with $[tBMA]_0/[TBE]_0/[CuBr]_0/[PMDETA]_0 = 50/1/1/1$ and $M_{n,theoretical} = 7\,100\text{ g}\cdot\text{mol}^{-1}$.

entry	solvent	T (°C)	reaction time ^a (min)	conversion (%) ^b	M_n^c (g·mol ⁻¹)	M_w/M_n^c
1	toluene	90	165	6	620	1.14
2	MEK	90	15	16	1 230	1.06
3	<i>n</i> -butyl acetate	90	45	8	860	1.62
4	acetone	50	17	14	1 100	1.02
5	ethyl acetate	70	45	18	1 320	1.18
6	THF	60	60	42	3 180	1.13

a) time at which the conversion remains stable. b) Determined by GC. c) Determined by SEC with polystyrene standards.

In order to improve these results, ATRP reactions were investigated with other solvents, first with 'green' solvents such as *n*-butyl acetate (*n*BuAc) and ethyl acetate, but also with THF and acetone that are known to be good solvents to dissolve the PMVE backbone. Moreover, polymerization of *t*BMA was already carried out in acetone [19] and in THF [29]. Polymerization in *n*BuAc resulted in uncontrolled polymerization with high M_w/M_n (table 8.1, entry 3). Because these reactions were carried out at 90°C (entry 1, 2 and 3), one can suppose that the reaction temperature is too high to control the polymerization, and thus termination reactions occurred. So, polymerizations at lower temperature were investigated in other solvents (table 8.1 entry 4, 5 and 6). Comparing the reactions in different solvents, the conversion in the presence of acetone and ethyl acetate is very low showing the bad efficiency of the catalytic system in these solvents.

At 60°C, in the presence of THF, the polymerization is distinctly the best, reaching 42% monomer conversion within 1 hour and leading to a product with a narrow M_w/M_n (= 1.13) (table 8.1 entry 6). According to these results, it seems that the high reaction temperature has a strong impact on the controlled polymerization, meaning that TBE is more sensitive to the temperature than TCE. To improve the last results (table 8.1 entry 4, 5 and 6), a new set of experiments have been done at higher concentrations (25 vol-% solvent, see table 8.2). This concentration is still sufficient to keep the macroinitiator dissolved.

Table 8.2. Results of the homopolymerization of *t*BMA in different solvents ($V_{tBMA}/V_{solvent} = 3/1$ (25 vol-%)) with $[tBMA]_0/[TBE]_0/[CuBr]_0/[PMDETA]_0 = 50/1/1/1$ and $M_{n,theoretical} = 7\,100\text{ g}\cdot\text{mol}^{-1}$.

entry	solvent	T (°C)	reaction time ^a (min)	conversion (%) ^b	M_n^c (g·mol ⁻¹)	M_w/M_n^c
1	acetone	50	60	46	3 400	1.17
2	ethyl acetate	70	30	62	4 530	1.16
3	THF	60	45	61	4 440	1.17

a) time at which the conversion remains stable. b) Determined by GC. c) Determined by SEC with polystyrene standards.

Interestingly enough, in all cases, higher conversions were obtained with narrower M_w/M_n (< 1.2), which indicates a better controlled polymerization than in less concentrated solution. When polymerized in 25 vol-% ethyl acetate and THF (table 8.2 entry 2 and 3), *t*BMA conversion reaches about 61% within 30 and 45 min respectively, giving a polymer with the highest conversions and the highest M_n values.

According to these results, TBE seems to be a good initiator for the polymerization of *t*BMA but looks more sensitive to the temperature, the concentration and the choice of the solvent than TCE. After this initial study, kinetics of these three last reactions was studied to know if these polymerizations could be controlled.

* Kinetics

A kinetic run was made in order to know if the polymerization reaction is controlled or not and if the evolution of the M_n is in good agreement with the expected value. For a controlled polymerization, the following criteria have to be fulfilled: linearity of (i) $\ln([M]_0/[M])$ as a function of time and of (ii) M_n as a function of conversion have to be linear, (iii) and a narrow M_w/M_n (see **Chapter 7**).

A typical semilogarithmic kinetic plot of the homopolymerization of *t*BMA in different solvents, as studied by GC, is shown in figure 8.1. Additionally, the conversion versus M_n and M_w/M_n plots in figure 8.2 shows that all polymerizations are controlled processes until a certain conversion. In all cases, the M_n increases during polymerization, and M_w/M_n is narrow (< 1.2).

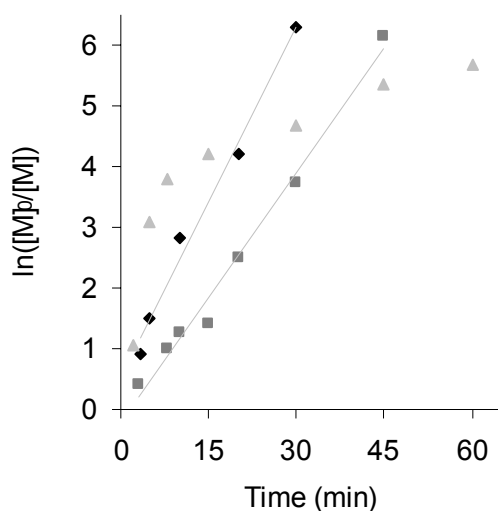


Figure 8.1. Comparison of the kinetics plots for *t*BMA polymerization in different solvents, with (◆) in ethyl acetate at 70°C, (■) in THF at 60°C and (▲) in acetone at 50°C.

Conditions:

$$[tBMA]_0/[TBE]_0/[CuBr]_0/[PMDETA]_0 = 50/1/1/1 \text{ in 25-vol\% solvent.}$$

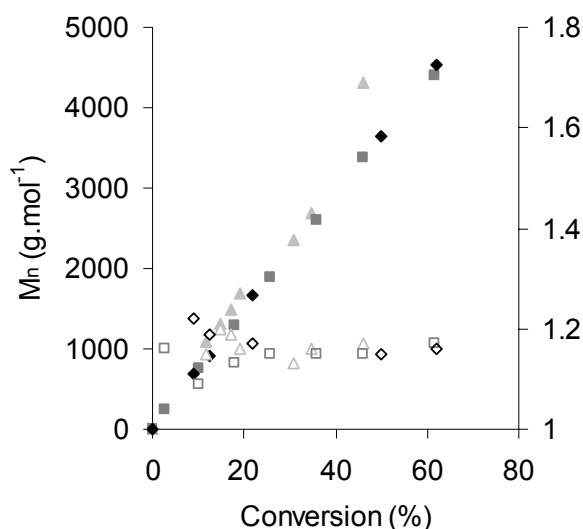


Figure 8.2. Evolution of M_n SEC and M_w/M_n with conversion in the ATRP of *t*BMA polymerized in different solvents, with (◆, ◇) in ethyl acetate at 70°C, in (■, □) in THF at 60°C and (▲, △) in acetone at 50°C.

Conditions:

$$[tBMA]_0/[TBE]_0/[CuBr]_0/[PMDETA]_0 = 50/1/1/1 \text{ in 25-vol\% solvent. Open symbols relate to } M_w/M_n \text{ and the filled ones to } M_n \text{ SEC.}$$

In the presence of acetone, the kinetic study of the polymerization shows that the $\ln ([M]_0/[M])$ versus time plot exhibits a downward curvature after 10 min (figure 8.1) indicating termination of the process. Also, the molecular weight of the polymer does not increase at conversions higher than 36% (figure 8.2). Thus, the polymerization is ill-controlled under these conditions.

On the other hand, the *t*BMA polymerizations in ethyl acetate and in THF results are comparable. The first-order kinetic plot of the $\ln ([M]_0/[M])$ versus time is linear up to 61% conversion, indicating that a constant number of growing polymer chains is present (figure 8.1). Beyond this conversion, termination reactions proceed. Their M_n s increased linearly with conversion, and the M_w/M_n decreased progressively with conversion with a final value of less than 1.2 (figure 8.2). The ATRP polymerization of *t*BMA in ethyl acetate and in THF is quite similar. The only difference is that the polymerization in ethyl acetate is faster than in THF.

* End-group Analysis

The use of TBE as initiator allowed us to analyze the terminal structure of the polymers by ^1H NMR spectroscopy (figure 8.3). The *Pt*BMA end groups have been analyzed by ^1H NMR spectroscopy, and the observations are in line with the previous study of PMMA by Sawamoto *et al.* [30]. Besides the large absorptions of the repeating units of *t*BMA (a, b and c), there are characteristic signals originating from the α -halocarbonyl compounds as initiators at 4.68 ppm (peak i). The methylene protons of the ω -end group of unit of *t*BMA (peak a'') and the ω -end group methyl protons of the *tert*-butyl ester group (peak b') were seen at 1.34 ppm. The terminal α -end group was identified as the dibromide by the presence of the small peaks (i and a') attributed to the terminal protons adjacent to the halogen. These results indicate that this ATRP polymerization proceeds via activation of the C-Br bond, originating from the initiator, by the CuBr/PMDETA catalyst system.

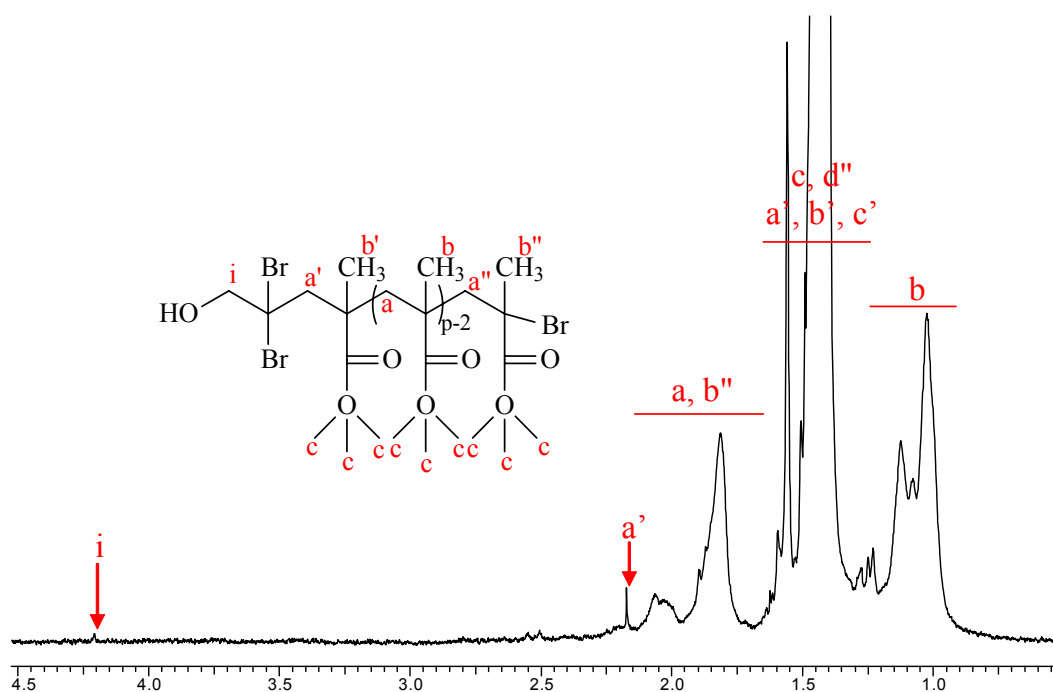


Figure 8.3. ^1H NMR spectrum of *Pt*BMA in CDCl_3 .

After that, DP_n (which corresponds to the *t*BMA unit number p) and M_n of P*t*BMA were calculated from the ^1H NMR spectrum. DP_n could be calculated from the integration of the tert-butyl group (peak c) of P*t*BMA and the one of the initiator (peak i), which gives the following equation:

$$DP_n = p = (I_c / 9) \times (2 / I_i)$$

The calculation of DP_n permits to determine the M_n of the polymer by the following equation:

$$M_n = M_{\text{TBE}} + M_{\text{tBMA}} \times p = 282.7 + 142.2 \times p$$

As shown in table 8.3, the M_n obtained from the peak intensity ratio $(I_c / 9) \times (2 / I_i)$ [M_n NMR] was 4540 $\text{g}\cdot\text{mol}^{-1}$, which was not in very good agreement with that obtained from SEC [M_n SEC = 5 400 $\text{g}\cdot\text{mol}^{-1}$] calibrated against PS standards.

Table 8.3. DP_n and M_n calculated by ^1H NMR and SEC.

DP_n NMR	M_n NMR ($\text{g}\cdot\text{mol}^{-1}$)	M_n SEC ($\text{g}\cdot\text{mol}^{-1}$)
49	7 240	8 250
30	4 540	5 400
31	4 680	5 590
23	3 550	4 600

8.2.1.2. Homopolymerization of Styrene

A huge number of studies have been performed, dealing with ATRP polymerization of St with a wide spectrum of initiating systems. Matyjaszewski *et al.* have polymerized St in a controlled way by ATRP catalyzed by a copper complex CuBr/bipy with TCE as initiator [31]. For our experiments, PS was synthesized by a similar strategy but with TBE as initiator.

* Kinetics

Figure 8.4 compares the plot of $\ln([M]_0/[M])$ versus time for St polymerization initiated at two different temperatures, 90 and 110°C, while keeping the monomer/initiator and catalyst/Br molar ratios comparable. At 110°C, polymerization is four times faster than at 90°C, and conversion is also higher. However, in figure 8.5, the M_w/M_n (< 1.3) is lower at 90°C, indicating a better control than at 110°C. In both cases, the molecular parameters of PS, including the chain polydispersity ($M_w/M_n < 1.4$), are well controlled until a certain conversion. Slower kinetics indicates that either the propagation rate constant is smaller or the equilibrium is more displaced toward the dormant species (see **Chapter 7**).

At high St conversion, a shoulder is observed on the SEC chromatograms on the high M_n side. Although the molecular weight of the chains associated remains constant, the polydispersity index increases, which suggests the occurrence of transfer reactions and autopolymerization. These transfer reactions have also been detected by Matyjaszewski *et al.* for other copper catalysts.

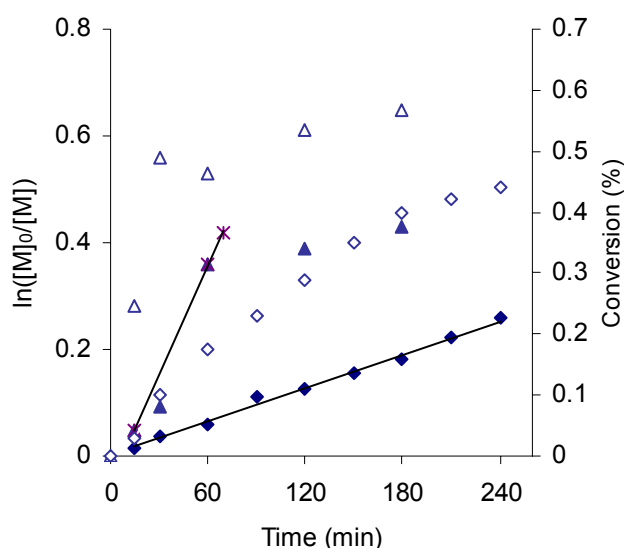


Figure 8.4. Kinetic plots for St polymerization in toluene at 90 and 110°C, with (◆) $\ln([M]_0/[M])$ at 90°C, (▲) $\ln([M]_0/[M])$ at 110°C, (◇) conversion at 90°C and (△) conversion at 110°C. Conditions: $[St]_0/[TBE]_0/[CuBr]_0/[PMDETA]_0 = 50/1/1/1$ in 25 vol-% toluene.

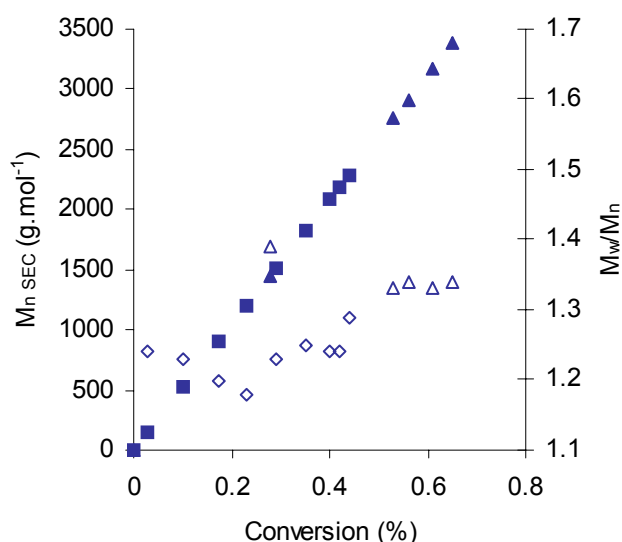


Figure 8.5. Conversion dependence of $M_{n,SEC}$ and M_w/M_n for St polymerization in toluene at 90 and 110°C, with (◆) $M_{n,SEC}$ at 90°C, (▲) $M_{n,SEC}$ at 110°C, (◇) M_w/M_n at 90°C and (△) M_w/M_n at 110°C. Conditions: $[St]_0/[TBE]_0/[CuBr]_0/[PMDETA]_0 = 50/1/1/1$ in 25 vol-% toluene.

* Effect of the Initiator/Catalyst Molar Ratio

Until recently, the major drawback of ATRP is the large amount of catalyst, which is usually required to promote the polymerization control [32]. After the completion of this thesis, new developments with ppm-amounts of copper have been described (see **Chapter 7**).

Experiments were thus carried out by varying the ratio of the initial concentrations of TBE to CuBr, while the ratio of monomer to TBE was kept constant ($[St]_0/[TBE]_0 = 50$). In table 8.4, the initiator/catalyst molar ratio has been decreased from 1.0 to 0.5, which results in a slower initiation efficiency and a longer reaction. Moreover, the $M_{n,SEC}$ increased whereas the conversion was smaller. The decrease in the initiation efficiency f ($f = M_{n,calc} / M_{n,SEC}$) might be attributed to more frequent termination reactions during the early stage of the polymerization, thus before the persistent radical effect is effective and allows for self-regulation of the radical polymerization [16].

Table 8.4. Effect of the initiator/catalyst molar ratio (Conditions: $T = 110^\circ\text{C}$, solvent = 25 Vol-% toluene, $[M]_0/[TBE]_0 = 50/1$).

$[TBE]_0/[CuBr]_0/[PMDETA]_0$	Time (min)	Conv (%)	$M_{n,SEC}^a$ (g.mol ⁻¹)	M_w/M_n^a	f^b
1/1/1	60	56	2 920	1.23	0.96
1/0.75/0.75	195	43	2 830	1.35	0.76
1/0.5/0.5	240	34	3 620	1.51	0.47

a) using PS standards. b) $f = M_{n,calc} / M_{n,SEC}$

* End-group Analysis

The terminal structure of the polymers obtained with CuBr/PMDETA was then analyzed by ^1H NMR. Both α - and ω -end groups of a PS sample were characterized by ^1H NMR spectroscopy as demonstrated in figure 8.6.

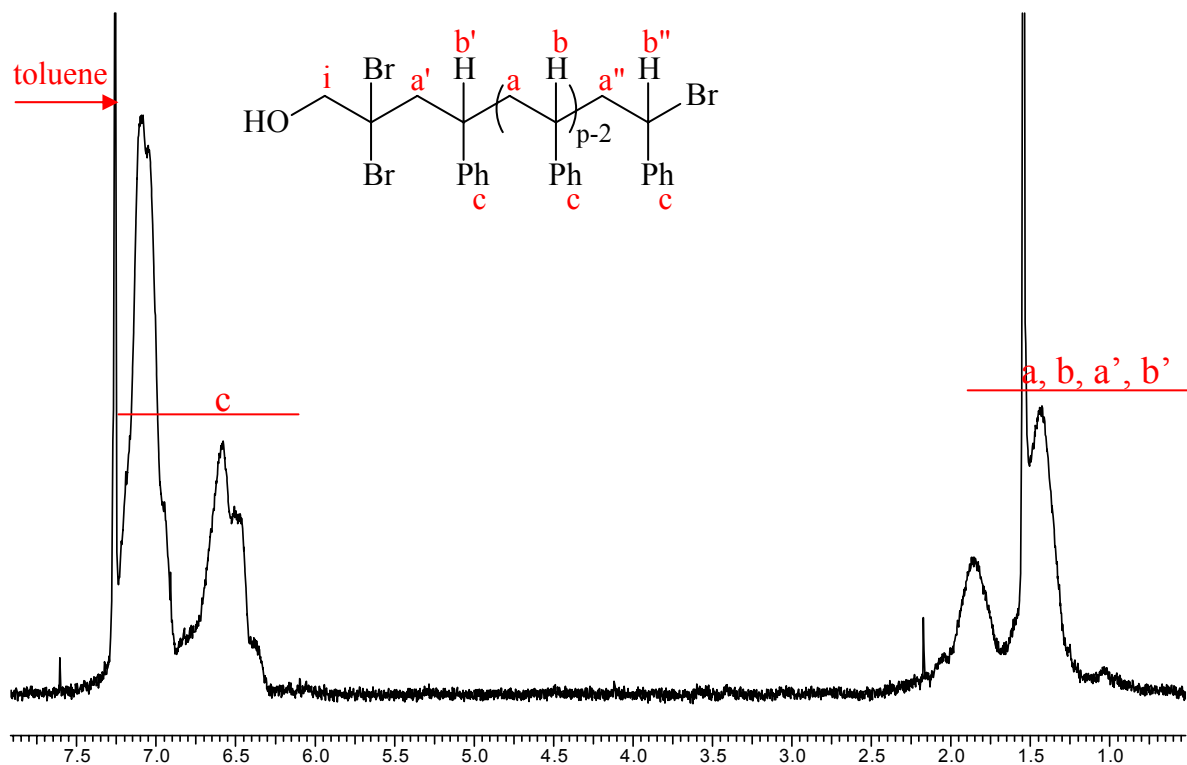


Figure 8.6. ^1H NMR spectrum of PS with $M_{n, \text{NMR}} = 3600 \text{ g.mol}^{-1}$ in CDCl_3 .

Besides signals at δ 1.05-2.45 ppm (a and b) and δ 6.30-7.30 ppm (c) ascribed to the repeating monomer unit, characteristic resonances originating from the initiator and catalyst moieties are visible at δ 4.45 ppm (i) and δ 4.8 ppm (b''), respectively. Significantly, the ^1H NMR spectrum of PS showed a minor resonance at 4.24 ppm (a'') which can be attributed to the methylene protons of the tribromoethoxy end group. Integration of these signals and comparison with the methylene resonance of styrene between 1.05 and 2.45 ppm resulted in a M_n of 2500 g.mol^{-1} , which is essentially the same as that determined from theory and confirms that TBE is an efficient initiator for controlled polymerization of St and leads to materials with a single tribromoethyl chain end. Additionally, the integral ratio of the two signals of the methylene protons of $\text{HO-CH}_2\text{-CBr}_2\text{-CH}_2$ (i, a'') with the terminal methylene (b'') adjacent to the Br atom is 2.2/1, demonstrating that the chain transfer reaction of TBE is negligible. So, it can be concluded that the $\text{HO-CH}_2\text{-CBr}_2$ group and Br atom reside at α - and ω -end of the polymer respectively.

These results suggest that TBE is an efficient initiator for controlled ATRP of St and tBMA, which is in agreement with recent work on the use of polyhalogenated initiators, such as CCl_4 , in ATRP [33]. The research toward higher molecular weight polymers of St and tBMA is described in the next part. For that reason, polymerizations with another metal catalyst, $\text{NiBr}_2(\text{PPh}_3)_2$, have been done.

8.2.2. Synthesis with a Nickel Catalyst

In typical ATRP, an alkyl halide and transition-metal compound complexed by an appropriate ligand in its lower oxidation state are used in the initiating system. Nickel, a late transition metal, differs from copper. Due to its preference to oxidative addition and reductive elimination by a two-electron transfer reaction instead of a one-electron redox addition process, there have only been a limited number of examples about nickel-catalyzed Kharash reactions.

Few documents are reported on nickel-based ATRP. Teyssié *et al.* [34] first introduced the homogeneous $[\text{Ni}(\text{o},\text{o}'(\text{CH}_2\text{NMe}_2)_2\text{C}_6\text{H}_3)\text{Br}]$ catalyst to the controlled polymerization of MMA and *n*BMA (*n*-butyl methacrylate). $\text{NiBr}_2(\text{Pn-Bu}_3)_2$ or $\text{NiBr}_2(\text{PPh}_3)_2$ complexes induced living radical polymerization of MMA in the presence of an aluminium additive [30,35]. Jérôme *et al.* [36] reported on the controlled radical polymerization of MMA, *n*BA (*n*-butyl acrylate) and the synthesis of poly(methyl methacrylate)-*block*-poly(*n*-butyl methacrylate)-*block*-poly(methyl methacrylate) (PMMA-*b*-*n*BMA-*b*-PMMA) triblock copolymer with a difunctional initiator catalyzed by $\text{NiBr}_2(\text{PPh}_3)_2$. Sawamoto *et al.* [37] gave examples of zerovalent nickel complex, $\text{Ni}(\text{PPh}_3)_4$, in controlling MMA polymerization with additives [38]. Without a radical initiator, $\text{NiBr}_2(\text{Pn-Bu}_3)_2$ catalyzed air- induced polymerization of phenethyl methacrylate in a living process through an unknown mechanism [39]. ATRP of side-group siloxane containing monomer mediated by $\text{NiBr}_2(\text{PPh}_3)_2$ was reported recently [40].

However, so far, there are few reports concerning nickel complexes used for controlled radical polymerization of St [30,41] and none about *t*BMA. Nickel-mediated ATRP was used here for ATRP of St and *t*BMA, catalyzed by a $\text{NiBr}_2(\text{PPh}_3)_2$ complex in the absence of Lewis acid. This knowledge will be used in a next step for the construction of graft copolymer structures based on the same complex.

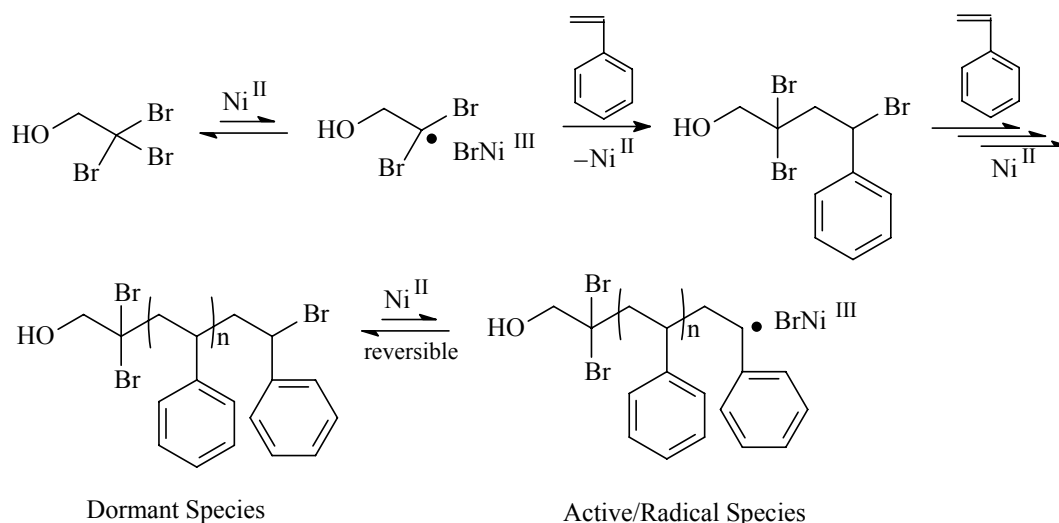
8.2.2.1. Pseudo-Living Polymerization of St with $\text{NiBr}_2(\text{PPh}_3)_2$

* Mechanism

The mechanism of the homopolymerization of St via ATRP with $\text{NiBr}_2(\text{PPh}_3)_2$ as metal catalyst is described in scheme 8.3. The Ni(II)-mediated controlled polymerization most likely proceeds via the reversible and homolytic cleavage of the carbon-bromine terminal group that originates from the organic bromides, where the cleavage involves a redox reaction between Ni(II) and Ni(III) species. Such a reversible redox reaction is due to the wide variety of possible oxidation states of nickel (0 – IV) [42]. Furthermore, the equilibrium is shifted to the dormant state because nickel favors the divalent (+2) state over the trivalent (+3) state. This process is followed by the radical addition of $\text{HO-CH}_2\text{-Br}_2\bullet$ to St, after which the Ni(III) species is reduced to the original Ni(II) complex to give the $\text{HO-CH}_2\text{-Br}_2\text{-St}$ adduct with a terminal C-Br bond. This keeps the concentration of the radical species (the growing end) low enough to suppress the side reactions between propagation radical species. The

polymerization proceeds via repetitive addition of St to the radical species, reversibly generated from the covalent species with the C-Br terminal.

Note that $\text{NiBr}_2(\text{PPh}_3)_2$ is a single-component system, which acts as a catalyst without ligand, whereas a nitrogen-based ligand is required to complex copper ions in the other systems.



Scheme 8.3. Synthesis of St with TBE as initiator and $\text{NiBr}_2(\text{PPh}_3)_2$ as metal catalyst via ATRP.

* Effect of Temperature

St was polymerized in bulk at different temperatures (without any activator as a Lewis acid). Comparison experiments were carried out to estimate the catalytic activity of $\text{NiBr}_2(\text{PPh}_3)_2$ with TBE as the initiator in the radical polymerization of St, and the results are summarized in tables 8.5 and 8.6. Note that because of the slow thermal decomposition of the $\text{NiBr}_2(\text{PPh}_3)_2$ complex as mentioned by Sawamoto [30], this could be avoided (or at least reduced) by increasing the monomer concentration, thus decreasing the reaction time compared to the catalyst decomposition. For that reason, experiments were made at high monomer concentration: $[\text{St}]_0/[\text{TBE}]_0/[\text{Ni}]_0 = 250/1/0.5$.

The results in table 8.5 and figures 8.7 and 8.8 prompted us to examine in detail the effect of the temperatures on the polymerization of St.

The rate of polymerization decreased with temperature, more specifically at 90°C the conversion reached 85% in 20 hours whereas those at 105 and 120°C needed 1 and 8 hours respectively to reach a lower conversion. As expected, the reaction is faster at high temperature but not controlled anymore. In all cases, in the beginning of the reaction, a first-order kinetics is observed with a narrow M_w/M_n , although they became broader with increasing time and at higher temperatures.

Table 8.5. ATRP homopolymerization of St in bulk with $[St]_0/[TBE]_0/[Ni]_0 = 250/1/0.5$ at different temperatures.

entry	T (°C)	time (hour)	Conversion ^a (%)	$M_{n\text{ calc}}^a$ (g.mol ⁻¹)	$M_{n\text{ SEC}}^b$ (g.mol ⁻¹)	M_w/M_n^b	f^c
1	120	8.25	4.8	1 480	1 300	1.90	1.13
2	105	13	30.5	7 910	7 950	1.45	0.99
3	90	20	85.4	21 630	21 250	1.16	1.02

a) determined by GC. b) determined by SEC using PS standards. c) $f = M_{n\text{ calc}} / M_{n\text{ SEC}}$

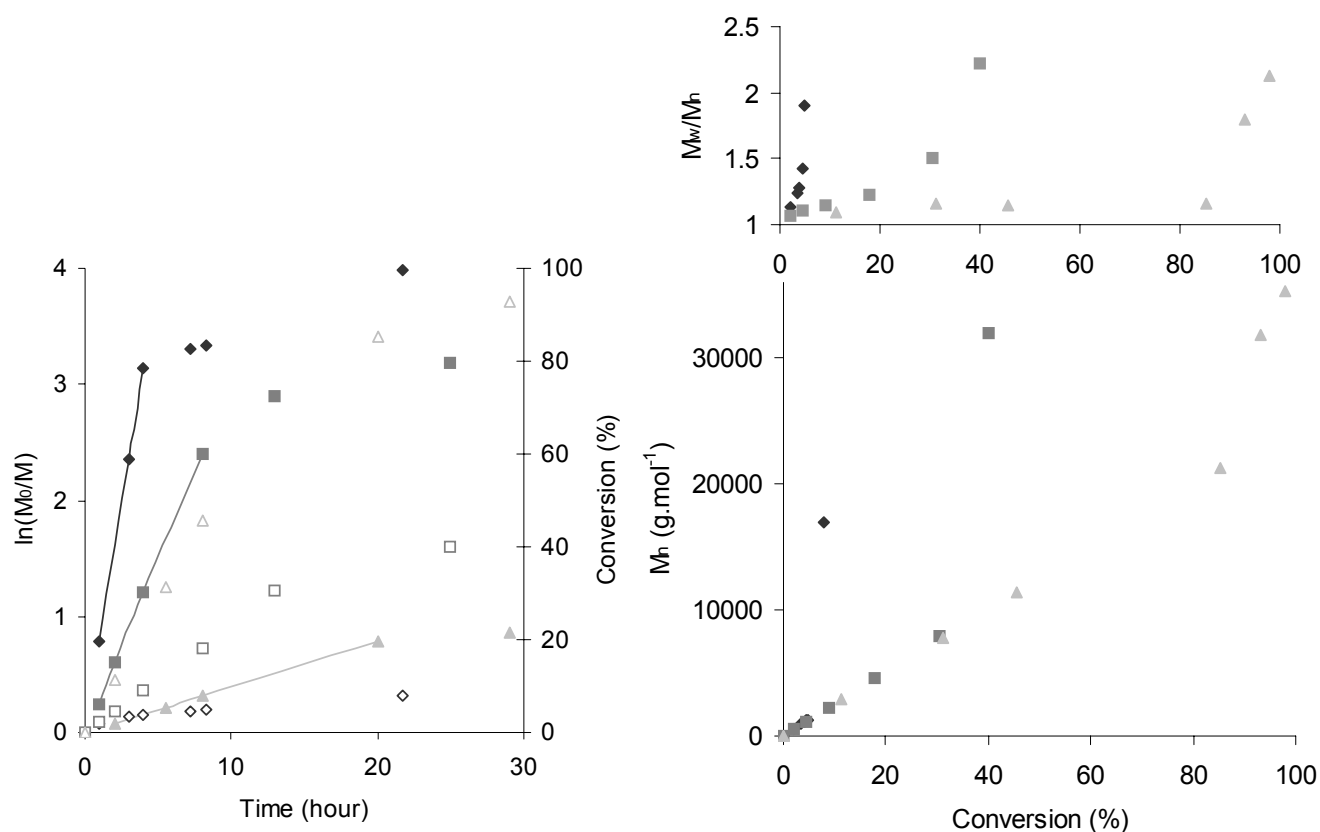


Figure 8.7. Kinetics plots for St polymerization in bulk at different temperatures with $\ln([M]_0/[M])$ (filled symbols) and conversion (opened symbols): (◆, ◇) at 120°C, (■, □) at 105°C and (▲, △) at 90°C.

Conditions: $[St]_0/[TBE]_0/[Ni(II)]_0 = 250/1/0.5$.

Figure 8.8. Conversion dependence of $M_{n\text{ SEC}}$ and M_w/M_n for St polymerization in bulk with (▲) at 90, (■) at 105°C and (◆) at 120°C.

Conditions: $[St]_0/[TBE]_0/[Ni(II)]_0 = 250/1/0.5$.

The polymerization of St with TBE initiator at high temperature (120 and 105°C) shows a fast and controlled initiation, but slowed down in a few hours, resulting in ill-controlled polymers of low M_n and wide M_w/M_n (see figures 8.7 and 8.8) due to its thermal decomposition. Effectively, Sawamoto has reported [30,36] that this $NiBr_2(PPh_3)_2$ metal catalyst appears not to be stable and soluble enough in organic solvents, and some decomposition has been noted in prolonged use at relatively high temperatures, thus considerably retarding the polymerization. To overcome these disadvantages, polymerization was done at lower temperature.

Decreasing the temperature to 90°C resulted in a better control of polymerization. The linear time dependence of $\ln([M]_0/[M])$ (figure 8.7) is consistent with a controlled polymerization that is first-order in monomer. Although the origin for the short introduction period is not clear yet, it might be related to the formation of the actual initiating species as a result of an interaction between the catalyst and the initiator [43]. An alternative explanation might be found by Matyjaszewski *et al.* [44]. The dependence of molecular weight and polydispersity on the St conversion is illustrated in figure 8.8. The linear dependence observed for M_n is in agreement with a controlled process with a constant number of growing chains. However, a slight broadening of the polydispersity is observed beyond 70% conversion. The dramatic increase of viscosity of the polymerization medium at high conversion is expected to change the rate of exchange between active and dormant species and accordingly increase the polydispersity.

From the experimental $M_{n, SEC}$ compared to the calculated one $M_{n, calc}$ ($M_{n, calc} = [St]_0/[TBE]_0 \times M_w$ monomer \times conversion), f close to unity has been calculated (table 8.5), which is much better compared to the value reported by Sawamoto *et al.* [30] for PMMA ($f = 0.75$). Sawamoto concluded that increasing the MMA concentration is a way to preserve the polymerization control although no Lewis acid activator is used anymore. In our case, these results indicate that this ATRP polymerization proceeds via activation of the C-Br bond originated from the initiator by the Ni catalyst system.

* Effect of Concentration of Ni

Generally, ATRP catalysts are used in near stoichiometric amounts relative to the activated bromide. Paradoxically according to Sawamoto research, better controlled polymerization is obtained with lower Ni catalyst concentration [30]. A series of experiments was carried out, where the concentration of Ni catalyst was varied from 0.5 to 0.2 according to one mole of TBE (see table 8.6).

Table 8.6. ATRP homopolymerization of St in bulk at 90°C with $[St]_0/[TBE]_0 = 250/1$ with different concentrations of $NiBr_2(PPh_3)_2$.

entry	$[TBE]_0/[Ni]_0$	time (hour)	Conversion ^a (%)	M_n (g.mol ⁻¹) ^b	M_w/M_n ^b
1	1/0.5	20	85	21 250	1.16
2	1/0.2	26	94	24 300	1.07

a) determined by GC. b) determined by SEC using PS standards.

In both cases, the M_w/M_n of the polymers is unimodal and narrow, and the conversion reached 85 and 94% (table 8.6). Comparing the effect of different ratios of $[TBE]_0/[Ni]_0$, it is obvious that diminishing the concentration of Ni lowered the value of M_w/M_n and resulted in high conversions (94%). Actually, the decrease of the catalyst concentration, which increases the polymerization time and narrows the polydispersity of the products, was also observed by Sawamoto [45]. This suggests that $NiBr_2(PPh_3)_2$ interacts with the bromide initiator to render part of TBE ineffective as the initiating species during the early stage polymerization. In other words, part of TBE does not serve as initiator. This work is

currently in progress by Sawamoto. Moreover, the equilibrium is shifted to the dormant state because nickel favors the divalent (+2) state over the trivalent (+3) state. This keeps the concentration of radical species low enough to suppress the side reactions between propagation radical species themselves like radical coupling and/or disproportionation.

* Kinetics

In figure 8.9, the linear plot of $\ln([M]_0/[M])$ versus reaction time through the origin indicated that the polymerization was first-order without induction time and that the concentration of active centers remained constant throughout the reaction. Under these conditions, the polymerization occurred smoothly, and monomer conversion reached 94% in 26 hours. In figure 8.10, the M_n increased in direct proportion to monomer conversion up to 24 300 $\text{g}\cdot\text{mol}^{-1}$ with narrow M_w/M_n ($M_w/M_n = 1.07$). This confirmed us the possibility to prepare higher M_n PS with the $\text{NiBr}_2(\text{PPh}_3)_2$ metal catalyst system at lower concentration.

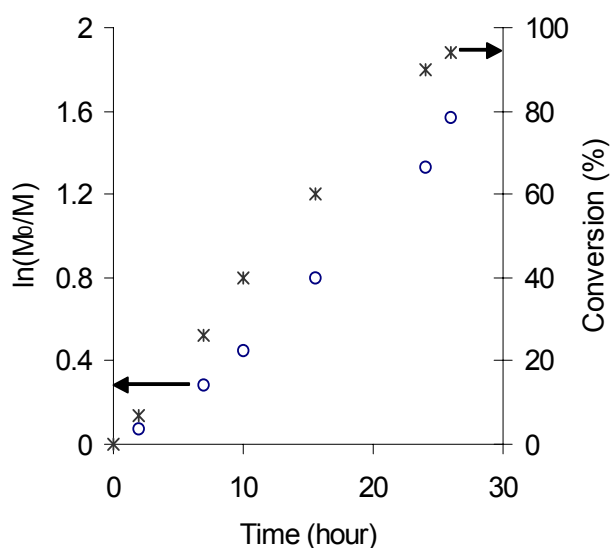


Figure 8.9. Kinetics plots for St polymerization in bulk at 90°C with (o) $\ln([M]_0/[M])$ and (*) conversion.

Conditions: $[\text{St}]_0/[\text{TBE}]_0/[\text{Ni}]_0 = 250/1/0.2$.

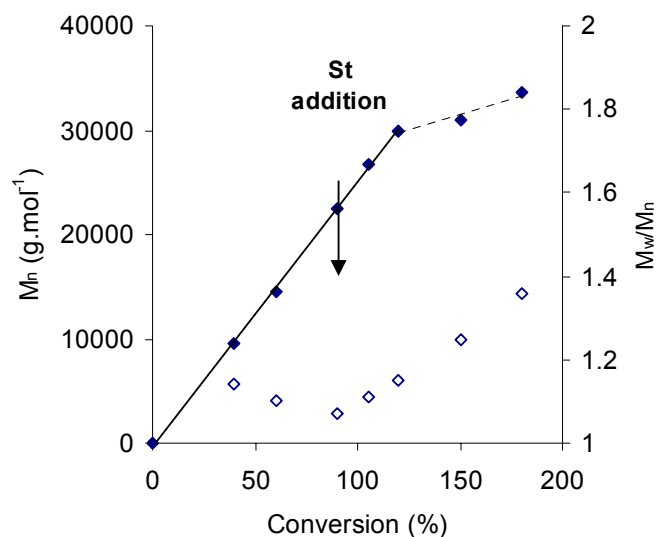


Figure 8.10. (◆) M_n and (◇) M_w/M_n as function of conversion of PS obtained in monomer-addition experiment with $[\text{TBE}]_0/[\text{Ni}]_0 = 1/0.2$ in bulk at 90°C.

$[\text{St}]_0/[\text{St}]_{\text{add}}/[\text{TBE}]_0 = 250/250/1$.

* Pseudo-living Polymerization and Narrow M_w/M_n

To investigate the living nature of the polymerization with $[\text{TBE}]_0/[\text{Ni}]_0 = 1/0.2$, a fresh feed of St was added to the reaction mixture at 90°C when most of the initial St was consumed (> 90% conversion in 25 hours). After the addition, a smooth second-phase polymerization took place, and conversion reached 120% (30% consumption of the added St) in additional 8h30 (figure 8.10). Until 120% conversion, M_n increased in direct proportion to monomer conversion, and M_w/M_n remained narrow and shifted to higher M_n . After this time, the second-phase polymerization was considerably slower due to the loss of the complex by thermal decomposition (dashed line in figure 8.10). This non-living process was already observed by Sawamoto for the homopolymerization of MMA with CCl_3Br as

initiator in toluene at 80°C and was ascribed to the thermal instability of the Ni catalyst [35]. Such kind of results is referred to as pseudo-living polymerizations.

8.2.2.2. Homopolymerization of *t*BMA

In contrast to the variety of transition metal complexes that induced living polymerization of MMA, no examples have been reported, to the best of our knowledge, about the radical homopolymerization of *t*BMA via activation of carbon-halogen bonds with the use of Ni metal catalysts. We attempted to employ the NiBr₂(PPh₃)₂-based initiating system with TBE for homopolymerizations of *t*BMA.

However, this metal catalyst does not initiate polymerization as shown in table 8.7. At different temperatures and in different solvents varying the concentration of Ni, conversions are low after 25 hours and polymers have ill-controlled M_n and broad M_w/M_n.

Table 8.7. ATRP of *t*BMA initiated by TBE with NiBr₂(PPh₃)₂ as metal catalyst. [tBMA]₀/[TBE]₀/[Ni]₀ = 200/1/1).

entry	solvent	T (°C)	reaction time (h)	Conversion ^a (%)	M _{n calc} ^b (g.mol ⁻¹)	M _w /M _n ^c
1	bulk	90	20	4	1 180	1.27
2	bulk	75	20	3	1 020	1.05
3	25vol-% acetone	50	25	4	1 230	1.28
4	25vol-% ethyl acetate	70	25	7	2 120	1.48
5	25vol-% THF	60	25	7	1 960	1.60

a) determined by GC. b) M_{n calc} = ([tBMA]₀/[TBE]₀) * monomer conversion * M_{w initiator}. c) determined by SEC using PS standards.

These results could be explained by the insolubility of NiBr₂(PPh₃)₂ with the *t*BMA monomer, in contrast to St. Thus, in what follows only the Cu/ligand catalyst system will be further employed for the synthesis of PtBMA-containing graft copolymers.

8.2.3. Conclusion

The opportunity now exists to combine these results into a novel synthetic strategy for the synthesis of a wide variety of graft copolymers from a readily available backbone using TBE as ATRP initiator. Table 8.8 recapitulates the homopolymerization results.

In all cases, TBE was found to be a good initiator for both homopolymerizations of *t*BMA and St, but the results diverge with the choice of catalyst. For the homopolymerization of *t*BMA, only CuBr/PMDETA catalyst is able to supply a controlled polymerization, whereas NiBr₂(PPh₃)₂, because of its insolubility with the monomer, does not. Thus far, the ATRP polymerization of St with TBE initiator can be successfully carried out, catalyzed by two different transition metal compounds, CuBr₂ and NiBr₂(PPh₃)₂. The polymers obtained are functionalized by α- group and ω-bromide atom, which can be used to initiate a normal ATRP process by addition of a second monomer.

Table 8.8 M_n characteristics of homopolymers prepared by ATRP.

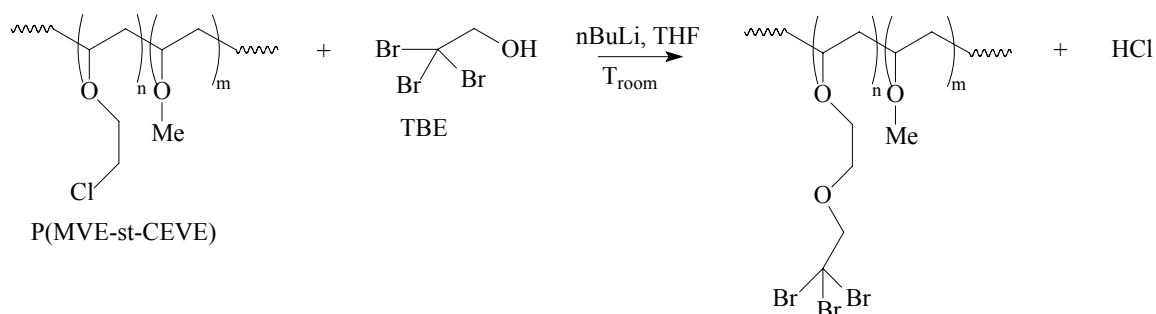
Monomer	Metal catalyst	$M_{n, SEC}$ (g.mol ⁻¹)	$M_{n, calc}$ (g.mol ⁻¹)	M_w/M_n
tBMA	CuBr/PMDETA	5 400	4 540	1.16
tBMA	NiBr ₂ (PPh ₃) ₂	/	/	/
styrene	CuBr/PMDETA	3 040	2 920	1.35
styrene	NiBr ₂ (PPh ₃) ₂	25 310	24 300	1.07

8.3. Synthesis of the Graft Copolymers

The goal of this work was to synthesize PMVE-*g*-PS and PMVE-*g*-PMAA graft copolymers. The generally applicable approach for the preparation of these graft copolymers involves two steps. The first step is the LCP synthesis of the backbone, as already described previously in **Chapter 3**, which results in a linear statistical copolymer with MVE and CEVE units, with a small amount of CEVE to keep the thermo-responsiveness of PMVE. To control the syntheses of PMVE-*g*-PS and PMVE-*g*-PMAA by the grafting from method via ATRP, the PMVE backbone is turned into a macroinitiator, which is obtained by the nucleophilic substitution of the chlorine groups, resulting into PMVE-*g*-TBE. This macroinitiator permits St and tBMA to be grafted from the backbone via ATRP. Then, PMVE-*g*-PMAA is obtained by the deprotection of the PtBMA side chains. The way of this synthesis is described in scheme 8.1.

8.3.1. First Step: Synthesis of the Macroinitiator

To investigate the compatibility of the PMVE backbone with the conditions necessary for the ATRP of tBMA and St, an appropriate macroinitiator was synthesized. TBE with a hydroxyl end group on one hand, for the substitution of chlorine pendent groups, and a tertiary bromide end group for ATRP reaction on the other hand, is highly desirable in the synthesis of the macroinitiator (Scheme 8.4).

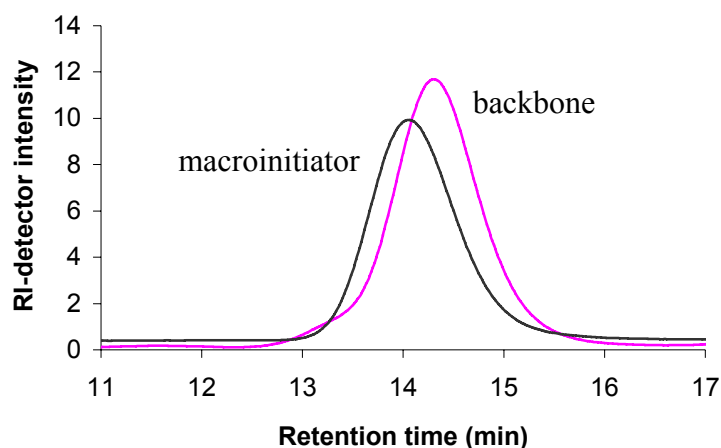
**Scheme 8.4.** Synthesis of the macroinitiator.

Throughout the experiments described in **Chapter 3**, the composition of the backbones used for the synthesis of the macroinitiator as precursor of graft copolymers, are summarized in table 8.9. By regulating the feed amount ratio of the two monomers, hence the number of the initiating site from the macroinitiator as well as the graft number the final graft copolymers could be well controlled.

Table 8.9. Overview of the P(MVE-*stat*-CEVE) backbone compositions.

Name	MVE ^a unit	CEVE ^a unit	CEVE ^a (mol-%)	DP _n ^a	M _n ^{1H NMR} (g mol ⁻¹)	M _n ^{SEC} (g mol ⁻¹)	M _w /M _n ^b
B4	336	4	1.78	340	19 940	32 490	1.18
B5	296	10	3.32	306	18 360	31 080	1.16
B6	270	11	6.96	281	16 840	29 530	1.17

The macroinitiators were prepared by a nucleophilic substitution of chlorine groups from the CEVE units of the PMVE backbone by an excess of TBE. As for the synthesis of PMVE-*g*-PEO (see **Chapter 5**), the pendant chlorine groups on the PMVE backbone were substituted by the hydroxyl end group of TBE with the help of a strong base, *n*BuLi. The products were characterized by ¹H NMR and SEC. Figure 8.11 presents the SEC traces of the starting materials and isolated product.

**Figure 8.11.** SEC traces of the P(MVE-*stat*-CEVE) backbone and the synthesized PMVE-*g*-TBE macroinitiator.

The macroinitiator trace shifted entirely to higher molecular weight. No significant shoulder can be observed, suggesting negligible contributions of side reactions. Transformation can be confirmed by ¹H NMR spectroscopy (see figure 8.12) as well as by E.A. (see table 8.10). The ¹H NMR spectrum shows the presence of the characteristic peak of the CH₂ protons (peak f) near the three bromine groups of TBE, which demonstrates that the reaction proceeded.

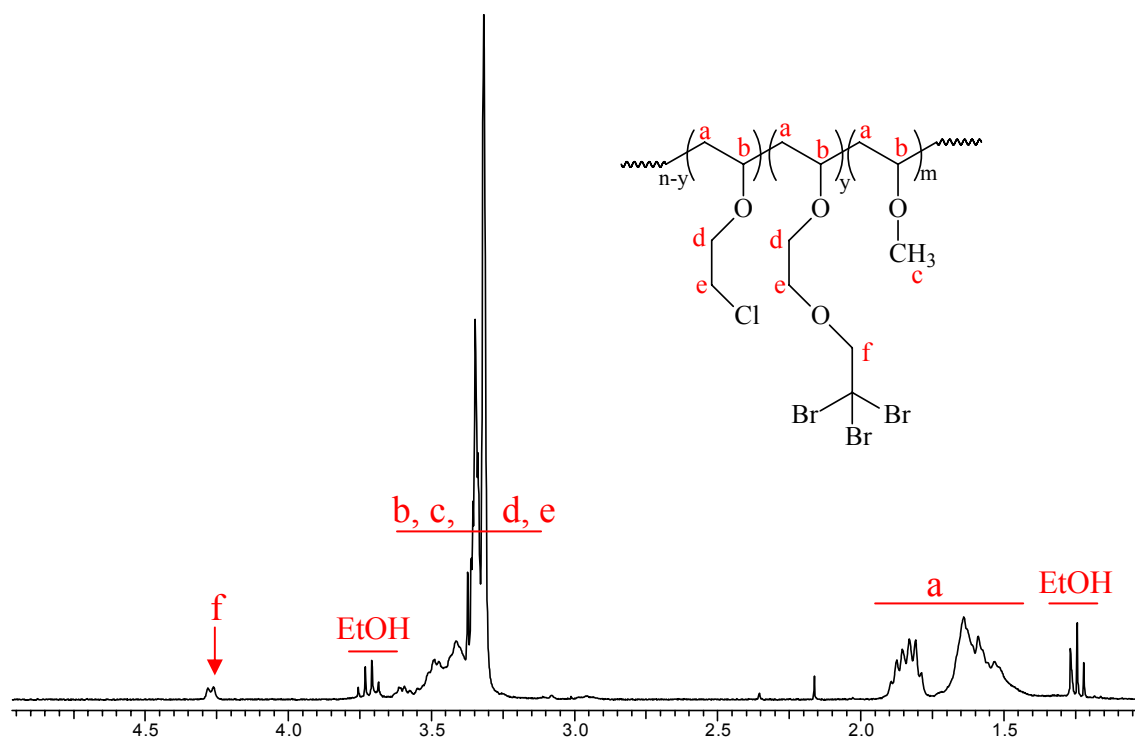


Figure 8.12. ^1H NMR spectrum of the macroinitiator in CDCl_3 .

Table 8.10 summarizes the results of the macroinitiator syntheses.

Table 8.10. Results of the nucleophilic substitution of the backbone precursor and the synthesized macroinitiator, determined from E.A.

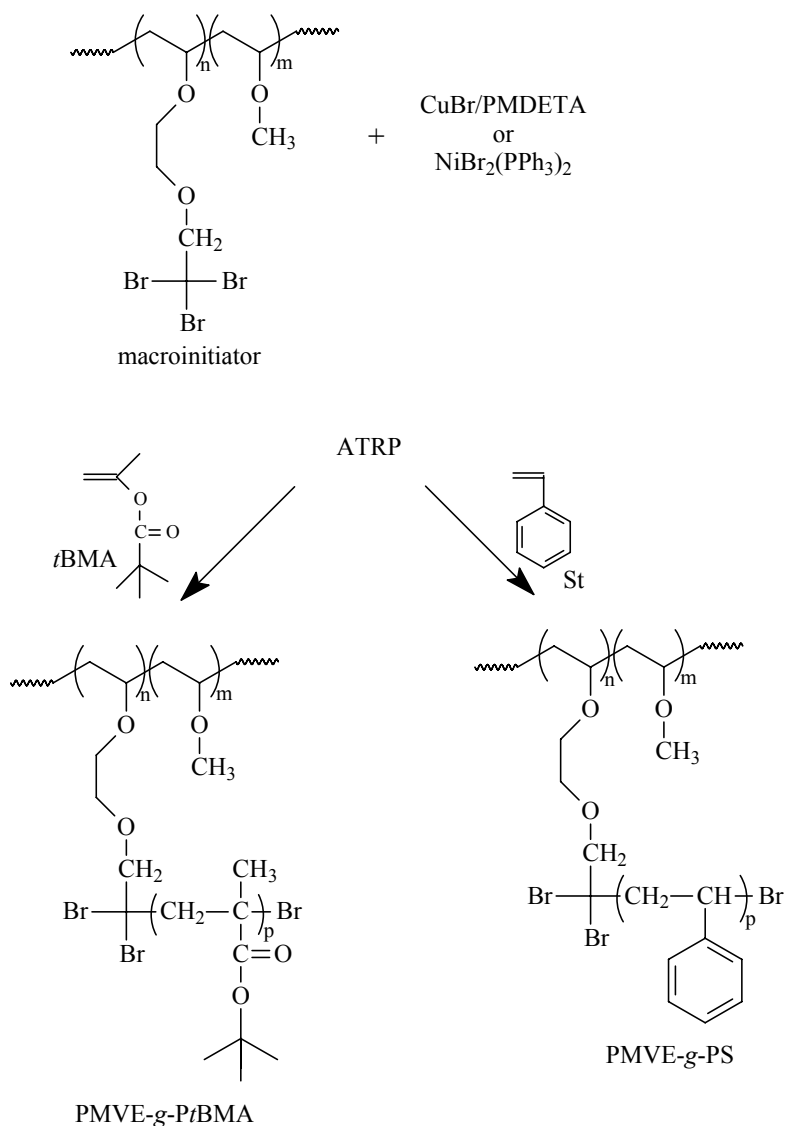
Number of CEVE unit in the backbone	Number of Cl substituted	Nucleophilic substitution %	M_n backbone ($\text{g}\cdot\text{mol}^{-1}$)	M_n macroinitiator ($\text{g}\cdot\text{mol}^{-1}$)	M_w/M_n
4	4	100	19 940	20 930	1.16
10	8	80	18 360	20 330	1.19
11	9	80	16 840	19 060	1.15

In all cases, the polydispersity remained narrow, and the M_n increased with the number of TBE grafted onto the precursor. As can be seen most of the chlorine groups were substituted by TBE.

8.3.2. Second Step: Synthesis of PMVE-*g*-PS and PMVE-*g*-PtBMA

8.3.2.1. Mechanism

PMVE-*g*-PtBMA and PMVE-*g*-PS grafts copolymer, with TBE as initiating groups, were synthesized by ATRP with the same procedure as the homopolymers (see previous section) (Scheme 8.5).



Scheme 8.5. Synthesis of PMVE graft copolymers with PMVE-*g*-TBE macroinitiator via ATRP.

8.3.2.2. Synthesis of PMVE-*g*-PS with Copper Catalyst

PS side chains were first polymerized with CuBr/PMDETA catalyst system at 90°C via ATRP in 25 vol-% toluene solution, as was determined in the previous section as the best parameters for the St homopolymerization. The resulting M_n and M_w/M_n are summarized in table 8.11. Note that the graft copolymerizations in this section were made from the macroinitiator of B6.

Table 8.11. Graft copolymerization of PMVE-*g*-PS at 90°C, with the initial conditions, M_n NMR macroinitiator = 19 060 g.mol⁻¹ with 9 TBE and $[\text{St}]_0/[\text{TBE}]_0/[\text{CuBr}]_0/[\text{PMDETA}]_0 = 225/1/1/1$ ($DP_{n, \text{theor}}/\text{PS chain} = 25$).

solvent	conversion (%)	time (min)	DP_n^a/chain	$M_n^{\text{NMR}^a}$ (g.mol ⁻¹)	$M_n^{\text{SEC}^b}$ (g.mol ⁻¹)	M_w/M_n^b
25 vol-% toluene	13	7	3	21 870	28 720	1.52
50 vol-% toluene	20	10	5	23 750	26 980	1.15

a) determined by ¹H NMR. b) determined by SEC with PS standards

While the copolymerization with 25 vol-% is not controlled, higher conversion and lower M_w/M_n are obtained for more diluted conditions (50% solvent). Because of the high viscosity of PMVE, a diluted solution permits a better increment of St from the backbone.

Reactions were monitored over time to determine whether the M_n was a linear function of conversion and whether the polymerizations exhibit first-order kinetics with respect to monomer over the course of the reaction (figures 8.13 and 8.14).

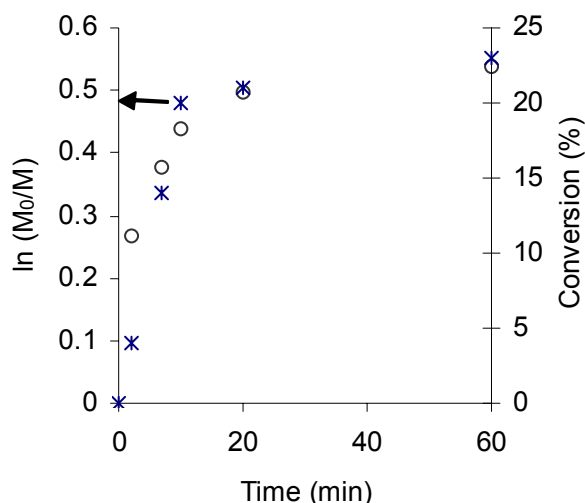


Figure 8.13. Plots of conversion and $\ln([M]_0/[M])$ versus time for PMVE-*g*-PS copolymerization in 50 vol-% toluene at 90°C with (o) $\ln([M]_0/[M])$ and (*) conversion. Conditions: $[St]_0/[TBE]_0/[CuBr]_0/[PMDETA]_0=225/1/1$ (DP_n/PS chain = 25).

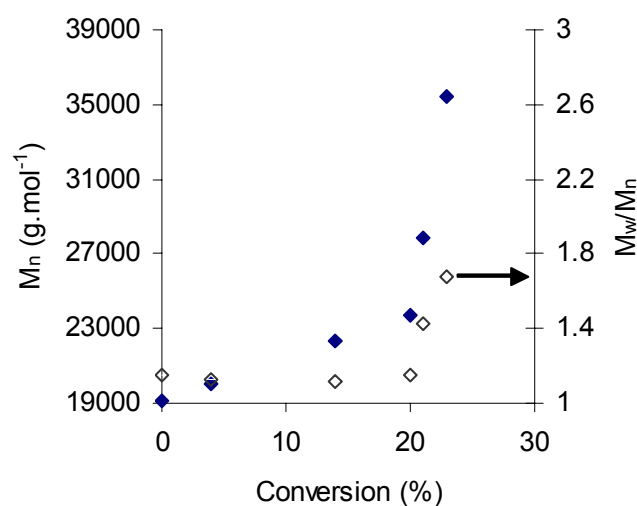


Figure 8.14. (◆) M_n and (◇) M_w/M_n as function of conversion of PMVE-*g*-PS obtained in monomer-addition experiment. Conditions: $[St]_0/[TBE]_0/[CuBr]_0/[PMDETA]_0=225/1/1$ (DP_n/PS chain = 25).

M_w/M_n was typically narrow for low conversions (> 20%) and broader at higher conversions with the emergence of a high molecular weight shoulder in SEC traces. Although higher molecular weights could be obtained, broader M_w/M_n s were observed, presumably due to graft-graft coupling at higher conversion. We can deduce that a certain degree of disproportion or radical coupling of initiators is likely occurring. This is supported by the fact that the molecular weight increased whereas no more monomer conversion is observed, and secondly by an increase of the viscosity in the polymer mixture. From all these observations, it can be concluded that the graft copolymerization is poorly controlled with the initiator catalyst CuBr/PMDETA.

Recently, Müller *et al.* reported the synthesis of well-defined hyperbranched copolymers via ATRP with CuBr/PMDETA as initiator system at 60°C in ethyl acetate [46]. However, the system had several drawbacks, including limited molecular weights and extremely low rate. Hence, these drawbacks were resolved by the use of $NiBr_2(PPh_3)_2$ as metal catalyst to prepare well-defined, monodisperse and highly hyperbranched polymers [47]. Indeed, the control of M_n and M_w/M_n in ATRP with CuBr/PMDETA is poor, due to radical coupling and chain transfer reactions of the growing radical species. Hence, the possibility of using CuBr/PMDETA system for the synthesis of highly branched

PMVE-*g*-PS was ruled out. In this regard, since few years, the use of Ni metal catalyst provided considerable control in the polymerization of star block and hyperbranched copolymers of MMA.

Therefore, we extended our synthetic approach to the preparation of PMVE-*g*-PS using ATRP polymerization techniques with a Ni catalyst system.

8.3.2.3. Synthesis of PMVE-*g*-PS with Nickel Catalyst

According to the conditions of the homopolymerization of St in the previous session, the nickel-mediated radical graft polymerization was carried out first at 90°C in bulk as shown in table 8.12. Note that the graft copolymerizations in this section were made from the macroinitiator of B5.

Table 8.12. Graft copolymerization of PMVE-*g*-PS with the initial conditions, M_n NMR macroinitiator = 20330 g.mol⁻¹ with 8 TBE and $[St]_0/[TBE]_0/[Ni(II)]_0 = 200/1/0.2$ ($DP_{n, theor}/PS$ chain = 25).

solvent (vol-%)	T (°C)	conversion (%)	time (min)	DP _n /chain ^a	M _n NMR ^a (g.mol ⁻¹)	M _n SEC ^b (g.mol ⁻¹)	M _w /M _n ^b
bulk	90	38	30	10	28 690	40 990	1.91
50 % toluene	90	38	90	9	27 860	40 970	1.52
50 % THF	75	90	90	23	39 570	49 460	1.18
50 % ethyl acetate	60	32	120	8	27 020	39 740	1.12

a) determined by ¹H NMR. b) determined by SEC with PS standards.

Upon completion of the bulk polymerization and because of broad polydispersity ($M_w/M_n = 1.91$), the polymer was dissolved in a 50 vol-% solvent. The composition of the mixture also requires a solvent such as THF or ethyl acetate to facilitate miscibility of the macroinitiator. The Ni catalyst has shown to be active under mild conditions in both organic solvents (see previous section).

On the basis of this result, the solution polymerization of PMVE-*g*-PS graft copolymers was conducted using three different solution systems at different temperatures. These results are summarized in table 8.12. When the polymerization was done using 50 vol-% toluene at 90°C, the conversion reached 38% (as determined by GC) but with lower M_w/M_n , even if it still remains broad. Thus, the addition of solvent in the system decreases the viscosity of the reaction mixture and aims to lower M_w/M_n .

For the polymerization in THF at 75°C, in contrast to the polymerization in ethyl acetate, almost full conversion (90%) was reached after 90 min, and the M_n was 39 570 g.mol⁻¹ corresponding to $DP_n /chain = 23$, which is almost the same as the theoretical value ($DP_{n theor} /chain = 25$), and the M_w/M_n was narrow (1.18). Therefore the kinetics of this reaction was studied (see figures 8.15 and 8.16).

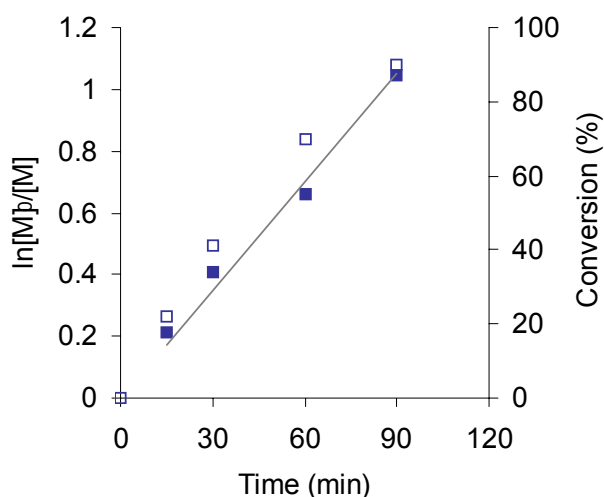


Figure 8.15. Kinetics plots for St graft copolymerization in 50 vol-% THF at 75°C with (■) $\ln ([M]_0/[M])$ and (□) conversion (%). Conditions: $[St]_0/[TBE]_0/[Ni(II)]_0 = 200/1/0.2$.

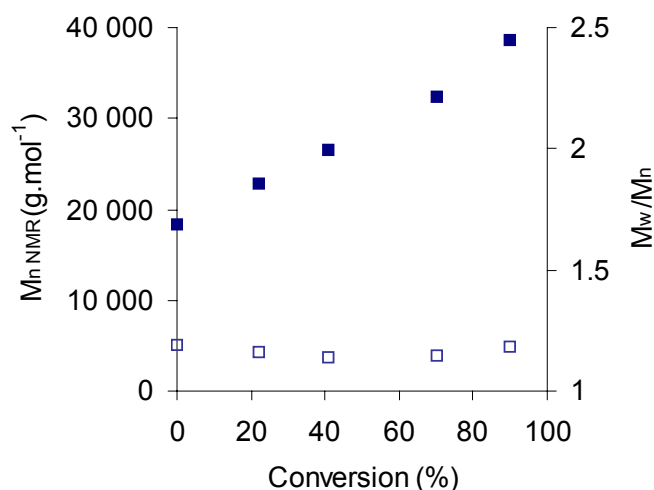


Figure 8.16. Conversion dependence of M_n NMR and M_w/M_n for St graft copolymerization in 50 vol-% THF at 75°C, with (■) M_n NMR and (□) M_w/M_n . Conditions: $[St]_0/[TBE]_0/[Ni(II)]_0 = 200/1/0.2$.

As expected, the first-order kinetic plot of the polymerization in THF in figure 8.15, and the M_n as function of conversion in figure 8.16, both show the linear behaviour. Thus, the grafting ratio increased with reaction time and linearly with conversion with a negligible contribution of transfer and terminations.

Figure 8.17 shows the SEC traces of graft copolymers and the chain extended macroinitiator. The clear shift of the SEC peak of the macroinitiator to shorter retention times and the absence of a tail or shoulder at higher retention times show that the efficiency of the macroinitiator is high and confirms that the grafting process of PS chains proceeded in a controlled fashion.

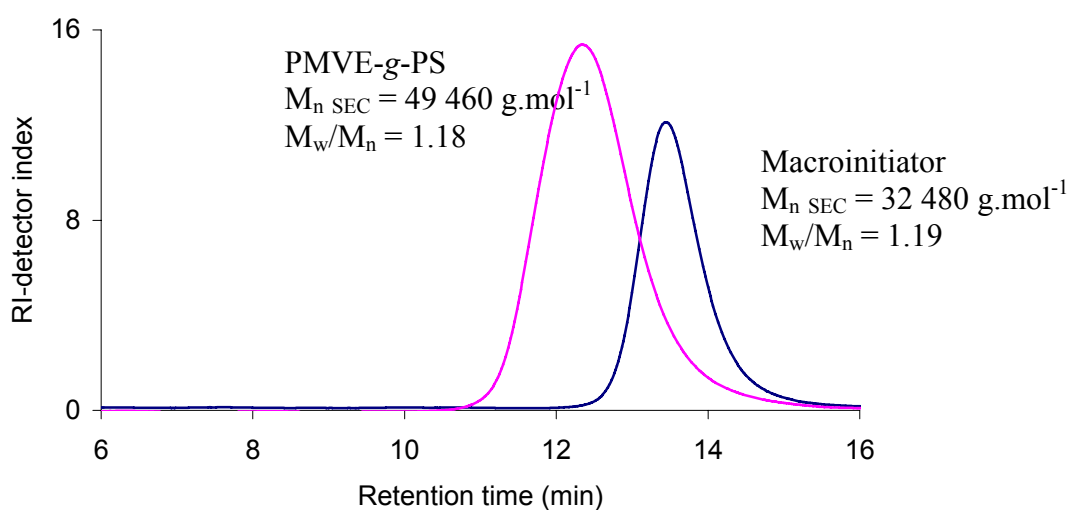


Figure 8.17. SEC traces of macroinitiator (M_n SEC = 32 480 $g \cdot mol^{-1}$, $M_w/M_n = 1.19$, with 8 initiating sites) and graft copolymer ($M_n = 49 460$ $g \cdot mol^{-1}$, $M_w/M_n = 1.18$, with 8 grafts). $[St]_0/[PMVE-Br]_0/[Ni]_0 = 200/1/0.2$, in 50 vol-% THF at 75°C.

The polymerization was stopped before 100% conversion of monomer to avoid side reactions, which could lead to high M_w/M_n . The graft copolymers were purified, dried, and analyzed by ^1H NMR to verify incorporation of the St monomer. Figure 8.18 shows a typical ^1H NMR spectrum of PMVE-*g*-PS. The assignment of each proton shows that the ^1H NMR spectrum is consistent with the expected copolymer structure. By taking the area ratio of the phenyl PS protons to the PMVE protons, we were able to estimate the weight percentage of PS (PS wt-%) in the copolymer and the degree of polymerization of grafted PS chains ($\text{DP}_{n \text{ PS chain}}$) on the PMVE chain backbone. The NMR results are listed in tables 8.13 and 8.14.

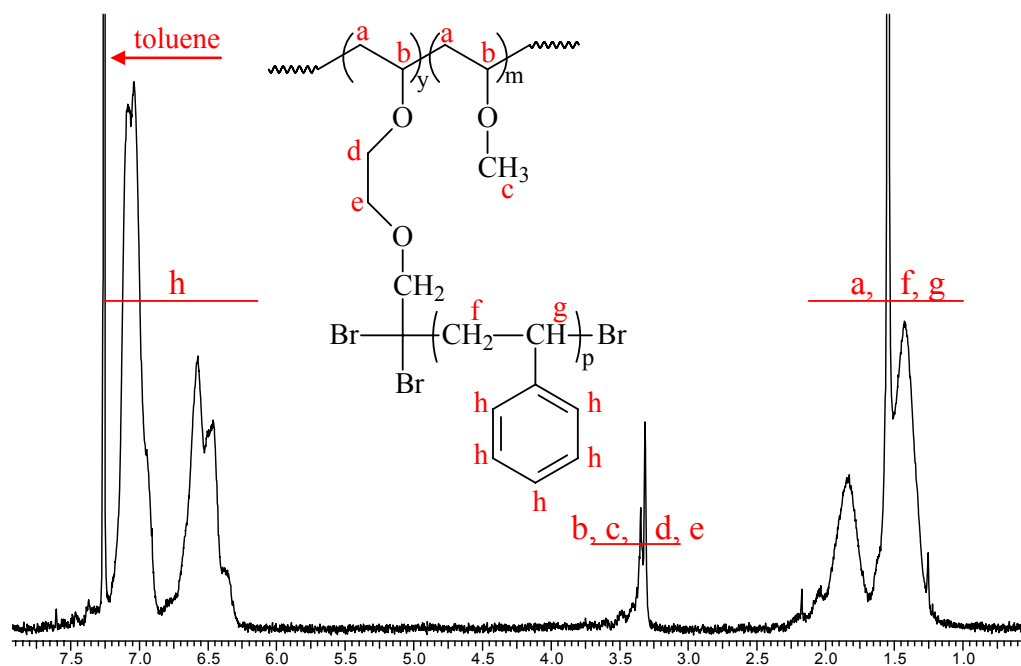


Figure 8.18. ^1H NMR spectrum of PMVE-*g*-PS in CDCl_3 .

In all cases, these graft copolymers have the same length of the backbone and same distribution of the PS grafts over the PMVE chain. Integration of the peak areas was used to generate the data shown in tables 8.13 and 8.14.

Table 8.13. Results of the PMVE-*g*-PS data from ^1H NMR and SEC.

Macroinitiator	PMVE- <i>g</i> -PS	DP_n PS/chain	$M_n \text{ NMR (g}\cdot\text{mol}^{-1})$	$M_n \text{ SEC (g}\cdot\text{mol}^{-1})$	M_w/M_n
B4	GPS1	24	30 970	38 710	1.19
B4	GPS3	76	52 710	58 570	1.25
B5	GPS2	23	39 570	49 460	1.18
B5	GPS4	71	80 550	89 500	1.27

Table 8.14. Results of the GPS2 data from ^1H NMR and SEC.

time (min)	conversion (%)	M_n NMR ($\text{g}\cdot\text{mol}^{-1}$)	M_n SEC ($\text{g}\cdot\text{mol}^{-1}$)	f^a
0	0	20 330	32 480	0.63
15	22	22 760	33 470	0.68
30	41	26 560	37 940	0.70
60	70	32 360	42 580	0.76
90	90	39 570	49 460	0.80

$$a) f = M_n \text{ NMR} / M_n \text{ SEC}$$

Moreover, the M_n of PMVE-*g*-PS, as determined by SEC using PS standards, was $49\,460 \text{ g}\cdot\text{mol}^{-1}$, which is different to the one determined by NMR ($M_{n \text{ NMR}} = 39\,570 \text{ g}\cdot\text{mol}^{-1}$). This could be explained by the difference of the hydrodynamic volume of PMVE (see **Chapter 3**). The fact that the f value gets closer to the unity could be explained by the affinity of the PS side chains with PS standards.

The efficiency of the catalyst system and the nature of the ligand used to complex metal ions were found to play an important role in the determination of the activity, molecular weights, M_n and length of side chains. For a successful PMVE-*g*-PS via ATRP, a sufficient proportion of dormant species should be maintained throughout the polymerization to keep a low concentration of monomeric and polymeric radicals. In our copolymerization system, the difference in the reactivity between the catalyst systems CuBr/PMDETA and $\text{NiBr}_2(\text{PPh}_3)_2$ is basically related to the equilibrium between the active and dormant species in the system. As the equilibrium is faster in the case of $\text{NiBr}_2(\text{PPh}_3)_3$ catalyst system, it permits a better control of graft copolymerizations than with CuBr/PMDETA catalyst system.

8.3.2.4. Synthesis of PMVE-*g*-P*t*BMA as Precursor of PMVE-*g*-PMAA

In order to graft PMAA side chains from the macroinitiator via ATRP, P*t*BMA had to be used as precursor of PMAA because of the possible side reactions between the catalyst system and acidic functionalities (see before). Copolymerizations with *t*BMA were performed with the same conditions as for the homopolymerization (see previous section) to obtain PMVE-*g*-P*t*BMA graft copolymers with a range of molecular weights (table 8.15). Note that B6 was used as the macroinitiator in this case.

First, graft copolymerizations were made in 25-vol% solvent as for the homopolymerization. As can be seen, graft copolymerization in ethyl acetate resulted in uncontrolled polymerization with broad M_w/M_n (> 2) and low conversion (15%). In THF, despite the narrow M_w/M_n (< 1.2), the low conversion indicates a too fast initiation. One can suppose that terminations or transfer reactions occurred because of the high viscosity of the macroinitiator, as for the graft copolymerizations of PMVE-*g*-PS (see previous section). So, graft copolymerizations in diluted solutions were investigated. Comparing the reactions, the broad M_w/M_n 's in the presence of ethyl acetate show the bad efficiency of this solvent. Increasing the solvent concentration results in broader M_w/M_n in both cases, indicating an uncontrolled process.

Table 8.15. Graft copolymerization of PMVE-*g*-P*t*BMA with the initial conditions, M_n NMR macroinitiator = 19 060 g.mol⁻¹ with 9 TBE and [tBMA]₀/[TBE]₀/[CuBr]₀/[PMDETA]₀ = 225/1/1/1 (DP_r/PS chain = 25).

solvent (vol-%)	T (°C)	conversion (%)	time (min)	DP _n ^a PtBMA/chain	M _n NMR ^a (g.mol ⁻¹)	M _n SEC ^b (g.mol ⁻¹)	M _w /M _n ^b
25 % THF	60	15	45	4	22 820	36 810	1.16
25 % ethyl acetate	70	15	30	4	22 820	39 240	2.32
50 % THF	60	9	60	2	20 940	33 780	1.54
50 % ethyl acetate	70	23	45	6	24 710	43 860	2.49

a) determined by ¹H NMR. b) determined by SEC with PS standards.

Also the kinetics (not shown) confirmed that the synthesis of PMVE-*g*-P*t*BMA with the CuBr/PMDETA catalyst system was not successful, most probably caused by the heterogeneous catalyst conditions due to the low solubility of Cu^{II} species in the reaction mixture. As further attempts did not lead to the design of better controlled graft structures based on PMVE and P*t*BMA, the research toward bi-responsive graft copolymer structures was stopped at this stage. In the next chapter, we will focus on the thermo-responsive properties of the PS-containing structures.

8.4. Conclusion

In conclusion, we have first demonstrated that CuBr/PMDETA can be used as a metal catalyst for the controlled polymerization of *t*BMA and St whereas NiBr₂(PPh₃)₂ was found to be able to polymerize styrene only. In the case of the use of CuBr/PMDETA as catalyst system, low molecular weights were obtained because of transfer reaction occurring during the polymerization. Much higher molecular weights could be reached for the Ni-based system. Other benefit effects were that no activator, such as a Lewis acid, is required anymore and that the catalyst/initiator molar ratio can be decreased down to 0.2, although the polymerization rate and the initiation efficiency remain controlled.

Based on these results, a macroinitiator was synthesized in a first step by substituting the chlorine groups of the backbone by TBE. Both CuBr/PMDETA ATRP and nickel-mediated ATRP were applied to the controlled graft polymerization of PS from a PMVE backbone. While good conditions for the synthesis of PMVE-*g*-P*t*BMA graft copolymers could not be found, tribromo initiating groups were found to be compatible with the reaction conditions for the ATRP of St, only with a nickel metal catalyst, and PMVE-*g*-PS graft copolymers with controlled M_n and narrow M_w/M_n were obtained. This strategy allowed for the design of novel well-defined, thermo-responsive graft copolymers to be readily prepared in a minimum number of steps under synthetically non-demanding conditions. In the next chapter, the research on the thermo-properties of the PMVE-*g*-PS is described.

8.5. References

- [1] (a) Tsitsilianis C., in *“Macromolecular Engineering, Precise Synthesis, Materials, Properties, Applications”*, Vol. 2 in *‘Elements of Macromolecular Structural Control’*, Edited by Matyjaszewski K., Gnanou Y., Leibler L., Wiley-VCH Verlag GmbH & Co. KGaA, Weinheim, Germany, Chap. 4, **2007**; and Fukuda T., Tsujii Y., Ohno K., chap. 11. (b) Peleshanko S., Tsukruk V.V., *Prog. Polym. Sci.*, **2008**, 33, 523.
- [2] Matyjaszewski K., Braunecker W.A., in *“Macromolecular Engineering, Precise Synthesis, Materials, Properties, Applications”*, Vol. 1 in *‘Synthetic Techniques’*, Edited by Matyjaszewski K., Gnanou Y., Leibler L., Wiley-VCH Verlag GmbH & Co. KGaA, Weinheim, Germany, Chap. 5, **2007**. [3] (a) Patten T.E., Matyjaszewski K., *Adv. Mater.*, **1998**, 10, 901. (b) Ashford E.J., Naldi V., O’Dell R., Billingham N.C., Armes S.P., *Chem. Commun.*, **1999**, 14, 1285.
- [4] (a) Yamamoto S., Ejaz M., Tsujii Y., Matsumoto M., Fukuda T., *Macromolecules*, **2000**, 33, 5608. (b) Yamamoto S., Ejaz M., Tsujii Y., Matsumoto M., Fukuda T., *Macromolecules*, **2000**, 33, 5608. (c) Yamamoto S., Ejaz M., Tsujii Y., Matsumoto M., Fukuda T., *Macromolecules*, **2000**, 33, 5995. (d) Zhao B., Brittain W.J., Zhou W., Cheng S.Z.D., *Macromolecules*, **2000**, 33, 1837. (e) Kong X., Kawai T., Abe J., Iyoda T., *Macromolecules*, **2001**, 34, 1837.
- [5] Rueda-Sánchez J., Galloso M.C., *Macromol. Rapid Commun.*, **2001**, 22, 859.
- [6] Coşkun M., Temüz M.M., *J. Polym. Sci., Part A: Polym. Chem.*, **2003**, 41, 668.
- [7] (a) Santos C.G., Parker J., Jones R.G., Holder S.J., *Polym. Int.*, **2002**, 51, 1107. (b) Ning F., Jiang M., Mu M., Duan H., Xie J., *J. Polym. Sci., Part A: Polym. Chem.*, **2002**, 40, 1253. (c) Masař B., Janata M., Vlček P., Polická P., Toman L., Kurková D., *J. Appl. Polym. Sci.*, **2002**, 86, 2930. (d) Bicak N., Ozlem M., *J. Polym. Sci., Part A: Polym. Chem.*, **2003**, 41, 3457. (e) Kazwierski K., Hurduc N., Sauvet G., Chojnowski J., *J. Polym. Sci., Part A: Polym. Chem.*, **2004**, 42, 1682. (f) Sugizaki T., Kashio M., Kimura A., Yamamoto S.I., Moriya O., *J. Polym. Sci., Part A: Polym. Chem.*, **2004**, 42, 4212. (g) Zou J. Cao C., Dong J.Y., Hu Y., Chung T.C., *Macromol. Rapid Commun.*, **2004**, 25, 1797. (h) Cao C., Zou J., Dong J.Y., Hu Y., Chung T.C., *J. Polym. Sci., Part A: Polym. Chem.*, **2005**, 43, 429. (i) Li C., Shi Y., Fu Z., *Polym. Int.*, **2006**, 55, 25.
- [8] Hawker C.J., Malmstrom E.E., Frechet J.M.J., Leduc M.R., Grubbs R.B., Barclay G.G., in *‘Controlled Radical Polymerizations’*, American Chemical Society: Washington DC, **1998**, Vol. 685.
- [9] Davis K.A., Charleux B., Matyjaszewski K., *J. Polym. Sci., Part A: Polym. Chem.*, **2000**, 38, 2274.
- [10] (a) Haddleton D.M., Crossman M.C., Dana B.H., Duncalf D.J., Hering A.M., Kukulj D., Shooter A.J., *Macromolecules*, **1999**, 32, 2110.
- [11] Van Camp W., Du Prez F.E., Bon S.A.F., *Macromolecules*, **2004**, 37, 6673.
- [12] Bütün V., Vamvakaki M., Billingham N.C., Armes S.P., *Polymer*, **2000**, 41, 3173.
- [13] Hoogenboom R., Schubert U., Van Camp W., Du Prez F., *Macromolecules*, **2005**, 38, 7653.
- [14] (a) Julia M., Le Thuillier G., Saussine L., *J. Organomet. Chem.*, **1979**, 177, 211. (b) Mitani M., Kato I., Koyama K., *J. Am. Chem. Soc.*, **1983**, 105, 6719.
- [15] (a) Murai S., Tsutsumi S., *J. Org. Chem.*, **1966**, 31, 3000. (b) Matsumoto H., Nikaido T., Nagai Y., *J. Org. Chem.*, **1976**, 41, 396.

- [16] Destarac M., Bessiere J.M., Boutevin B., *J. Polym. Sci., Part A: Polym. Chem.*, **1998**, *36*, 2933.
- [17] (a) Toman L., Janata M., Spěváček J., Masař B., Vlček P., Polická P., *Polym. Prepr. (Am. Chem. Soc., Div. Polym. Chem.)*, **2002**, *43*, 18. (b) Malinowska A., Vlček P., Kříž J., Toman L., Látalová P., Janata M., Masař B., *Polymer*, **2005**, *46*, 5.
- [18] Destarac M., Matyjaszewski K., Boutevin B., *Macromol. Chem. Phys.*, **2000**, *201*, 265.
- [19] Karanam S., Goossens H., Klumperman B., Lemstra P., *Macromolecules*, **2003**, *36*, (a) 3051-3060 and (b) 8304-8311.
- [20] Hawker C.J., Hedrick J.L., Malmström E.E., Trollsås M., Mecerreyes D., Moineau G., Dubois Ph., Jérôme R., *Macromolecules*, **1998**, *31*, 213.
- [21] Moineau G., Minet M., Dubois Ph., Teyssié Ph., Senniger T., Jérôme R., *Macromolecules*, **1999**, *32*, 27.
- [22] Granel C., Moineau G., Lecomte Ph., Dubois Ph., Jérôme R., Teyssié P., *Polym. Prepr.*, **1997**, *38*, 450.
- [23] Wooley K.L., *J. Polym. Sci., Part A: Polym. Chem.*, **2000**, *38*, 1397.
- [24] Yamamoto K., Miwa Y., Tanaka H., Sakaguchi M., Shimada S., *J. Polym. Sci., Part A: Polym. Chem.*, **2002**, *40*, 3350.
- [25] Moineau G., Minet M., Teyssié Ph., Jérôme R., *Macromolecules*, **1999**, *32*, 8277.
- [26] (a) Matyjaszewski K., Xia J., *Chem. Rev.*, **2001**, *101*, 2921. (b) Kamigaito M., Ando T., Sawamoto M., *Chem. Rev.*, **2001**, *101*, 3039.
- [27] Matyjaszewski K., Wang J., Grimaud T., Shipp D.A., *Macromolecules*, **1998**, *31*, 1527.
- [28] Kroll R., Eschbaumer C., Schubert U.S., Buchmeister M.R., Wurst K., *Macromol. Chem. Phys.*, **2001**, *202*, 645.
- [29] (a) Wang X.S., Luo N., Ying S.K., *Polymer*, **1999**, *40*, 4515. (b) Zheng G., Stöver H.D.H., *Macromolecules*, **2002**, *35*, 7612.
- [30] Uegaki H., Kotani Y., Kamigaito M., Sawamoto M., *Macromolecules*, **1997**, *30*, 2249.
- [31] Wang J.S., Matyjaszewski K., *J. Am. Chem. Soc.*, **1995**, *117*, 5614.
- [32] Matyjaszewski K., Coca S., Gaynor S.G., Wei M., Woodworth B.E., *Macromolecules*, **1997**, *30*, 7348.
- [33] Ando T., Kato M., Kamigaito M., Sawamoto M., *Macromolecules*, **1996**, *29*, 1070.
- [34] Granel C., Dubois Ph., Jérôme R., Teyssié Ph., *Macromolecules*, **1996**, *29*, 8576.
- [35] Uegaki H., Kotani Y., Kamigaito M., Sawamoto M., *Macromolecules*, **1998**, *31*, 6756.
- [36] (a) Moineau G., Minet M., Dubois Ph., Teyssié Ph., Senniger T., Jérôme R., *Macromolecules*, **1999**, *32*, 27. (b) Moineau G., Minet M., Teyssié Ph., Jérôme R., *Macromolecules*, **1999**, *32*, 8277. (c) Moineau G., Minet M., Teyssié Ph., Jérôme R., *Macromol. Chem. Phys.*, **2000**, *201*, 1108.
- [37] Uegaki H., Kamigaito M., Sawamoto M., *J. Polym. Sci., Part A: Polym. Chem.*, **1999**, *37*, 3003.
- [38] Johnson R.M., Corbin P.S., Ng C., Fraser C.L., *Macromolecules*, **2000**, *33*, 7404.
- [39] Acar A.E., Yağcı M.B., Mathias L.J., *Macromolecules*, **2000**, *33*, 7700.

- [40] Youngblood J.P., McCarthy T.J., *Polym. Prepr. (Am. Chem. Soc., Div. Polym. Chem.)*, **2000**, 41(2), 1554.
- [41] (a) Moineau G., Minet M., Dubois Ph., Teyssié Ph., Senninger T., Jérôme R., *Macromolecules*, **1999**, 32, 27. (b) Li P., Qiu K.Y., *J. Polym. Sci., Part A: Polym. Chem.*, **2001**, 39, 4001. (c) Li P., Qiu K.Y., *Polymer*, **2002**, 43, 3019. (d) Qin D.Q., Qin S.H., Qiu K.Y., *Acta Polym. Sin.*, **2002**, 1, 108.
- [42] Ozawa F., in 'Synthesis of Organometallic Compounds', Komiyama S., Ed.; Wiley: Chichester, **1997**, Chapter 12, p. 248.
- [43] Van de Kuil L.A., Grove D.M., Gossage R.A., Zwikker J.W., Jenneskens L.W., Drenth W., Van Koten G., *Organometallics*, **1997**, 16, 4985.
- [44] Matyjaszewski K., Coca S., Gaynor S.G., Wei M., Woodworth B.E., *Macromolecules*, **1998**, 31, 5967.
- [45] Ando T., Kamigaito M., Sawamoto M., *Macromolecules*, **1997**, 30, 4507.
- [46] Muthukrishnan S., Jutz G., André X., Mori H., Müller A.H.E., *Macromolecules*, **2005**, 38, 9.
- [47] Muthukrishnan S., Mori H., Müller A.H.E., *Macromolecules*, **2005**, 38, 3108.

Chapter 9

Properties of Thermo-responsive PMVE-*g*-PS Graft Copolymer

9.1. Introduction

Since the past 20 years, extensive attention has been paid to block and graft amphiphilic copolymers for their capability to form stable aggregates with a core-shell structure in solution [1]. For example, an amphiphilic copolymer consisting of a hydrophobic chain backbone grafted with a number of hydrophilic branches can form stable colloidal particles in water through a one-step precipitation or solvent exchange [2]. It has been shown that a very slow addition of THF or DMF solution containing individual amphiphilic copolymer chains into a large quantity of water or directly dialyzed against water can lead to stable colloidal nanoparticles with the aggregated hydrophobic backbone chains as a hydrophobic corona shell [3]. The nanoparticle size is normally in the range 10-500 nm, depending on the formation conditions and the copolymer structure. Another interesting point is that such colloidal particles were narrowly distributed, even though the copolymer chains used were polydisperse [4].

Usually, amphiphilic copolymers behave as single chains in aqueous solution like classical polymers or polyelectrolytes, whereas its aggregation, similar to that of amphiphilic copolymers, can occur under the influence of given external stimuli, mainly temperature, pH, ionic strength changes, or complexation [5]. Polystyrene-*block*-poly(acrylic acid) (PS-*b*-PAA) and polystyrene-*block*-poly(methacrylic acid) (PS-*b*-PMAA) are representative examples of well-defined amphiphilic block copolymers commonly studied in water [6]. Eisenberg *et al.* showed that the micellar morphology of PS-*b*-PAA copolymers could be changed from spheres to rods, to vesicles and even to more complexes structures, such as multiple micellar morphologies, by changing the copolymer's composition, the ionic strength, and the conditions for micellization.

PMVE is known to have a LCST in water [7] (see also **Chapter 6**). It is therefore expected that block and graft copolymers consisting of PMVE backbone and hydrophobic PS side chains

would possess temperature-dependent surfactant properties. PMVE/PS block copolymer structures have already been investigated by Deffieux *et al.* [8-9]. They report the topology, the organization and the aqueous solution properties of dendigrfts with a PS core and PS-*b*-PMVE diblock as external branches [8-9]. Since PS and PMVE blocks are incompatible in solution, they tend to self-organize intramolecularly, within the macromolecule, to form segregated subdomains yielding original morphologies such as the recently observed grapelike organization [8]. Such specific spatial arrangement in nanometer size domains can be explained by the capacity of macromolecular blocks constituting a branch (PS and PMVE) to get in contact and associate with the blocks of the same nature in neighbouring branches, within the dendigrft macromolecule. Their capacity to self-assemble and the subdomain size will depend on their relative proximity, block length, and limited degree of freedom, since each block copolymer branch is linked at one end to the dendigrft backbone. Another example of thermo-responsive aggregation, investigated by Dr. Bernaerts in the PCR-group, has been illustrated for block copolymers poly(methyl vinyl ether)-*block*-polystyrene (PMVE-*b*-PS) [10].

In this chapter, we focus our attention on the micelle formation and phase behavior of the aqueous solution of the corresponding graft copolymers (PMVE-*g*-PS) for which we expected a different phase behaviour. The micelle core consists of aggregated PS grafts that are surrounded by a corona region containing PMVE chains. In the present work, the LCST demixing behaviour of PMVE of well-defined molar mass, bearing different PS graft content, was investigated by MTDSC (collaboration with prof. B. Van Mele, VUB), and in dilute conditions by UV-VIS transmission, microcalorimetry and DLS (collaboration with prof. H. Tenhu, Helsinki). The phase behaviour of PMVE-*g*-PS was evaluated and compared with its precursor, the PMVE homopolymer. The objective is to obtain a detailed picture of the competition between intrachain behaviour and interchain association in the process of a better understanding of the self-assembly of amphiphilic copolymers. Moreover, the LCST behaviour of PMVE-*g*-PS was also compared to those of PMVE-*b*-PS.

9.2. The Thermo-responsive Properties of PMVE-*g*-PS

Since PS is a hydrophobic polymer and PMVE is hydrophilic, water is a good solvent for PMVE (at low temperature) but poor for PS. If the molecular weight of PS increased (e.g. GPS3 and GPS4 in table 9.1), these PMVE-*g*-PS copolymers became progressively immiscible in water. Similarly, Dr. Bernaerts, who synthesized PMVE-*b*-PS, has found that PMVE₃₂-*b*-PS₂₅ block copolymer (corresponding to 62 wt-% PS) is not soluble anymore in water, whereas that was not the case for PMVE₃₂-*b*-PS₅ block copolymer (corresponding to 26 wt-% PS) [10].

In order to study the properties of PMVE-*g*-PS in water, we therefore decided to focus on the graft copolymer structures with low PS content, e.g. GPS1 and GPS2 samples in table 9.1. The investigated graft copolymers and main characteristics are presented in table 9.1. In order to

compare the effect of the PS grafts on the thermo-responsiveness of PMVE backbone, the two samples, containing different number of PS grafts, were investigated.

Table 9.1. Characteristics of PMVE-*g*-PS.

Name PMVE- <i>g</i> - PS	M_n initiator ($\text{g}\cdot\text{mol}^{-1}$)	M_n one PS graft ($\text{g}\cdot\text{mol}^{-1}$)	number of PS graft	M_n graft copol ($\text{g}\cdot\text{mol}^{-1}$) ^a	wt-% PS ^a	M_w/M_n ^b	Solubility in water ^c
GPS1	20 930	2 510	4	30 970	32	1.16	+
GPS2	20 330	2 400	8	49 460	49	1.18	+
GPS3	20 930	7 950	4	58 570	60	1.25	-
GPS4	20 330	7 530	8	89 500	75	1.27	-

a) determined by ^1H NMR. b) determined by SEC with PS as standards in CDCl_3 . c) +: soluble in water, -: insoluble in water.

9.2.1. Phase Diagram by Modulated Temperature Differential Scanning Calorimetry (MTDSC)

MTDSC has been used to determine a state diagram over the entire composition range for different PMVE-*g*-PS. For the principles of the technique, we refer to the experimental section (see **PART IV**). This part results from a collaboration with Dr. Zhao, Dr. Van Assche and Prof. Van Mele from the VUB in Brussels. A publication of this work is in preparation [11] and only a summary is given here to highlight the most important facts.

* Demixing-remixing behaviour in aqueous solution

The demixing and remixing kinetics in aqueous solutions of PMVE-*g*-PS, GPS1 and GPS2, has been studied by means of MTDSC in both non-isothermal and quasi-isothermal modes. The remixing in the solutions of GPS1 is found to be almost as fast as the demixing, which is completely different from that in the solutions of linear PMVE and PMVE-*g*-PEO/water system (see **Chapter 6**). However, the remixing in the solutions of GPS2 is much slower than the demixing, which is quite similar to that in the solutions of linear PMVE.

The quasi-isothermal measurements show that the solutions of GPS1 are always time-independent for the temperatures both outside and in the phase transition region, while the solutions of GPS2 have time-dependence in the transition region. The decrease of c_p^{app} during the quasi-isothermal remixing in the solutions of GPS2 might be due to macroscopic phase separation, by which large domains of polymer-rich phase and water-rich phase are formed.

* Phase diagrams

The thermal transitions have been brought together to construct a state diagram, including the demixing threshold temperature $T_{\text{demix}}^{\text{threshold}}$ (heating) over a full range of PMVE-*g*-PS wt-% (figure 9.1).

Increasing the temperature of a homogeneous PMVE-*g*-PS/water solution induces phase separation. By the measurement of the T_{cp} 's for different compositions, the $T_{demix}^{threshold}$ curve can be constructed (figure 9.1). It has been known that the moisture absorbed by PMVE/PS homopolymer blends considerably lowers the phase-separation temperature [12]. On the other hand, it was shown for other systems that the introduction of a hydrophobic polymer segment into a thermoresponsive water-polymer system can result in an increase of its temperature of phase separation and inversely [13-15]. Few years ago, it was reported by our research group, for PVCL-*g*-PTHF/water system in which PTHF is a hydrophobic polymer, the T_{cp} 's increase with the amount of PTHF because the PTHF microdomains prevent the globular aggregation until higher temperatures [13].

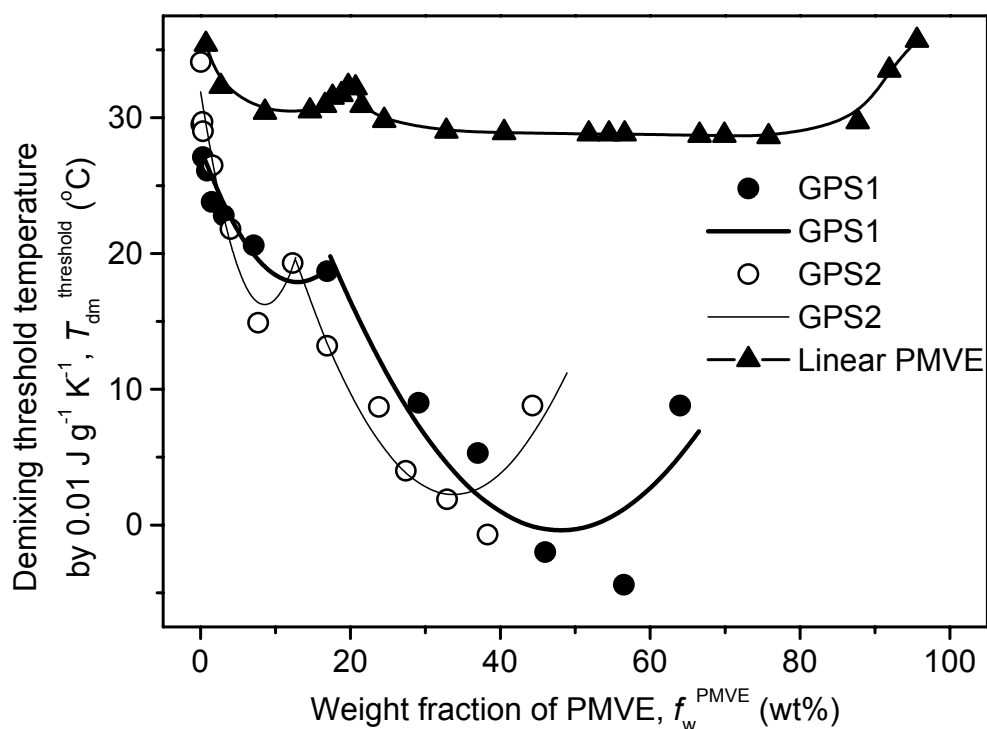


Figure 9.1. Phase diagram of GPS1 with (●) $T_{demix}^{threshold}$, of GPS2 with (○) $T_{demix}^{threshold}$, and of linear PMVE ($M_w = 20\,000\text{ g}\cdot\text{mol}^{-1}$) (▲) $T_{demix}^{threshold}$. Figure taken from ref. [11].

In general, GPS1 and GPS2 follow the type III LCST phase behaviour such as PMVE homopolymer with two LCST's. It becomes clear from Figure 9.1 that the incorporation of PS grafts markedly changes the phase separation process of PMVE in water. Addition of PS grafts on the PMVE decreases $T_{demix}^{threshold}$ compared to the pure PMVE [16]. In comparison to the phase diagram of linear PMVE ($M_w = 20\,000\text{ g}\cdot\text{mol}^{-1}$), at any PMVE-*g*-PS wt-%, the $T_{demix}^{threshold}$'s of the graft copolymers significantly shift to lower values. [11]. This decrease might be ascribed to the presence of bromide groups in the PS chains coming from the TBE initiator. Effectively, it was shown in our research group that the presence of only one bromide end group to PMVE dramatically decreases the T_{cp} of PMVE to 17°C [16].

PMVE-*g*-PS aqueous solutions were also studied with other techniques such as microcalorimetry and dynamic light scattering (DLS).

9.2.2. Determination of the “Cloud point” of Diluted Solutions

First, T_{cp} of the graft copolymers, which is related to the aggregation of the copolymers in water, was determined by different techniques: UV-Vis spectrophotometry, microcalorimetry and DLS. The results are recapitulated in table 9.2.

Table 9.2. T_{onset} , T_{demix} and T_{peak} ($^{\circ}\text{C}$) values of GPS1 and GPS2 by turbidimetry, microcalorimetry and DLS.

C mg/mL	UV-VIS		microcalorimetry				DLS			
	GPS1	GPS2	GPS1		GPS2		GPS1		GPS2	
	T_{onset}		T_{onset}	T_{demix}	T_{onset}	T_{demix}	T_{onset}	T_{peak}	T_{onset}	T_{peak}
10							30	35		
5							30	35		
1	32	24	19.2	33.7	17.2	31.7	31	37	29	35
0.5	33	25	21.2	34.0	20.1	32.5	31	37	29	35
0.1	33	28	23.3	34.4	21.7	32.7	31	37	29	35
0.05	34	30	24.1	35.1	23.9	33.6	31	37		

Table 9.2 shows that the measured T_{cp} 's with UV-VIS and DLS are similar, whereas they are higher than those obtained with microcalorimetry. The T_{onset} values from HS-DSC measurements correspond to an earlier detection and a shift of about 10°C . This difference could mean that HS-DSC shows dehydration of the polymer, whereas optical methods are sensitive to the formation of intermolecular aggregates. Another explanation might be that heat effects related to changing PMVE-*g*-PS/water interactions with temperature occur before phase separation [17-18], leading to a deviation in the baseline of the reversing heat flow signal. An indication for such an effect can also be found in PMVE solutions, when MTDSC measurements are compared to DLS measurements [19].

9.2.3. Microcalorimetry

Concerning the high sensitivity DSC measurements (for background: see **PART IV**), some thermograms of PMVE, GPS1 and GPS2 are shown in figure 9.2. All three samples (**a**, **b** and **c**) showed ΔH values within the same range (around $2\text{-}5\text{ kJ}\cdot\text{mol}^{-1}$ PMVE), even though the enthalpy change was somewhat smaller for PMVE-*g*-PS copolymers compared to PMVE. Polymer **a** showed a T_{onset} and a T_{demix} that are typical for pure PMVE, whereas the other two polymers **b** and **c**, much more hydrophobic, started to dehydrate at lower temperatures. Thus, hydrophobic groups lowered the maximum temperature of the dehydration of the PMVE corona, as it is expected. Also, the temperature range of the PMVE collapse broadened as the size of the hydrophobic part increased in the aggregate core. The dehydration took place over a temperature range of $\sim 17\text{-}45^{\circ}\text{C}$. It has been shown earlier that PMVE dehydrates slowly due to the stable

structures of the micellar particles [20]. The same could also be concluded for PMVE-*g*-PS copolymers. This phenomenon will be studied in more detail by DLS in the next section.

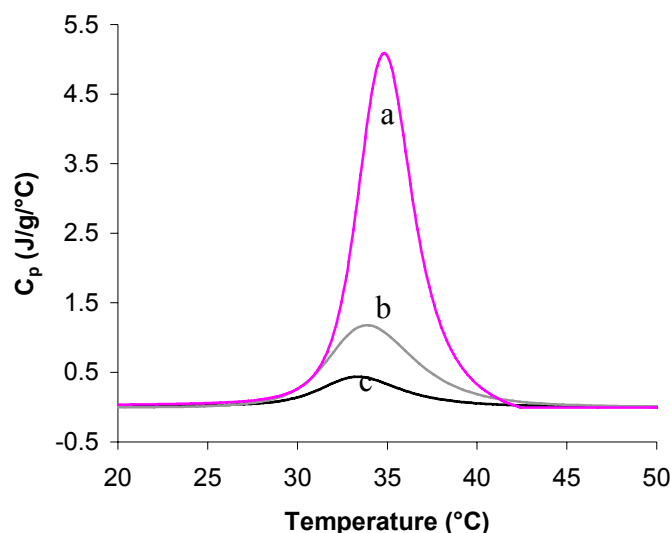


Figure 9.2. PMVE 12 000 (a), GPS1 (b) and GPS2 (c) at 1 mg.mL⁻¹.

9.2.4. Dynamic Light Scattering (DLS)

Previous DLS studies revealed that the CONTIN routine was an appropriate tool for the analysis of DLS data, to characterize dilute aqueous mixtures of, for instance, PNIPAA-*b*-PS [21]. DLS was used to monitor the coil-to-globule transition for PMVE single chains [20]. The driving force for this coil-to-globule transition is associated with the temperature-dependent molecular interaction, mainly hydrogen bonding and hydrophobic association. First of all, because PS is hydrophobic, micelle formation with the hydrophobic core of PS and hydrophilic PMVE corona should be expected. DLS was used to determine the size of such particles.

9.2.4.1. Dependence of the Heating Rate

Figure 9.3 shows the heating rate dependence of the apparent hydrodynamic radius R_h for GPS1 and GPS2 in water at 10 mg.mL⁻¹: ‘the slow heating’ represents the step-by-step increase of temperature at each degree, while ‘the fast heating’ means an increase of temperature in steps of 5°C. It shows that the formation of nanoparticles by means of the slow and the fast heating process results in similar R_h values. The only difference observed is at the T_{cp} . The size of the aggregates formed at this temperature during the slow heating is systematically larger than that formed in the fast heating process. This can be attributed to the competition between the intrachain ‘coil-to-globule’ transition and the interchain aggregation. In the fast heating process, micellar particles have less time to aggregate with each other before they are collapsed and stabilized by the PMVE corona above 45°C. For all the next studies, only the slow heating rate was used.

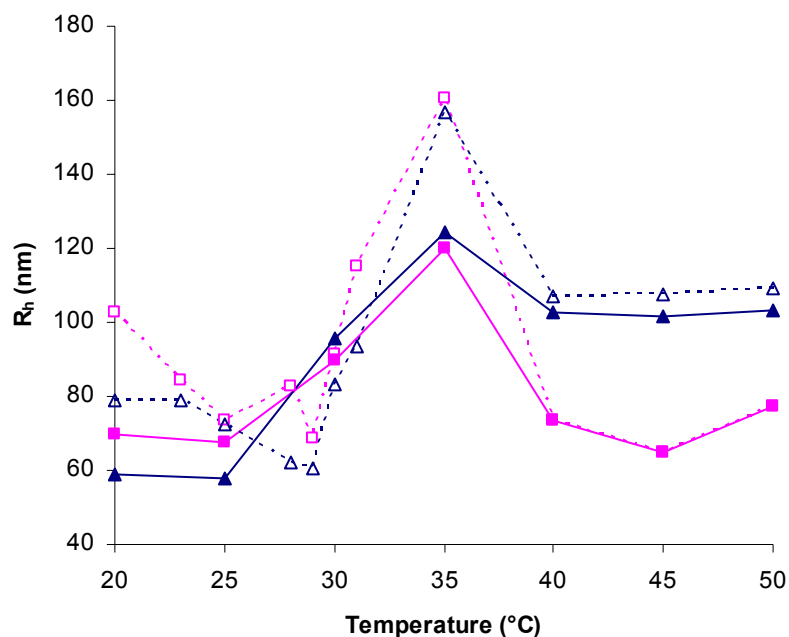


Figure 9.3. Heating-rate dependence of the hydrodynamic radius R_h of GPS1 (\triangle \blacktriangle) and GPS2 (\square \blacksquare) graft copolymers in water at $10 \text{ mg}\cdot\text{mL}^{-1}$, where ‘the fast speed’ means 5°C between two measurements (closed symbols), and ‘the slow speed’ 1°C between two measurements (open symbols).

9.2.4.2. DLS-measurements at Room Temperature

* Effect of concentration on R_h

The effect of the polymer concentration on the size of the aggregates was investigated at different angles (40 to 150°) at room temperature. Figure 9.4 shows the hydrodynamic radius R_h at different concentrations in the range between 0.01 and $10 \text{ mg}\cdot\text{mL}^{-1}$.

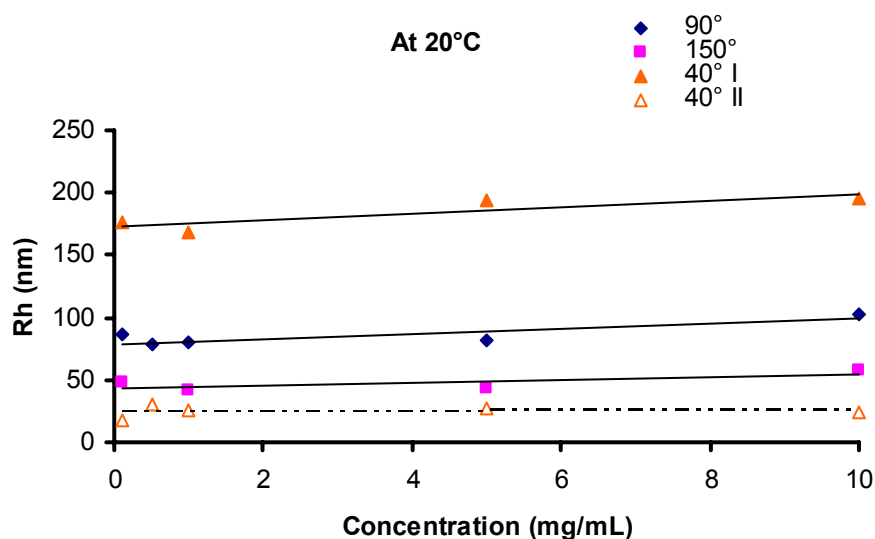


Figure 9.4. Plot of R_h of GPS1 between 0.01 and $10 \text{ mg}\cdot\text{mL}^{-1}$ as function of polymer concentration at 20°C with angular dependence: at 150° (\blacksquare), at 90° (\blacklozenge), at 40° (\blacktriangle , population I of aggregates, and \triangle , population II of micelles).

The PMVE-*g*-PS graft copolymers exhibit very similar characteristics and behaviour (almost same size and aggregates formation) in the whole angle range examined at room temperature. Because a slight dependence of concentration was observed, the study of the aggregate formation of the graft copolymers was focused at low concentrations (up to $0.5 \text{ mg}\cdot\text{mL}^{-1}$) in the next stage. Besides, at 40° , where the resolution for large scatterers is better than at 90° , two populations are observed. The small-size population was attributed to individual micelles while the large one was attributed to aggregates. These aggregates could result from the clustering of several micelles (see below).

9.2.4.3. Effect of the Heating

* Effect of temperature on the intensity and on R_h

The R_h and the intensity of light scattering I are plotted against temperature for the graft copolymers, in figure 9.5, for a concentration of $0.1 \text{ mg}\cdot\text{mL}^{-1}$. Heating of a PMVE-*g*-PS aqueous solution results in a sharp increase in the light scattered intensity I at the T_{cp} that depends on both PS content and the concentration.

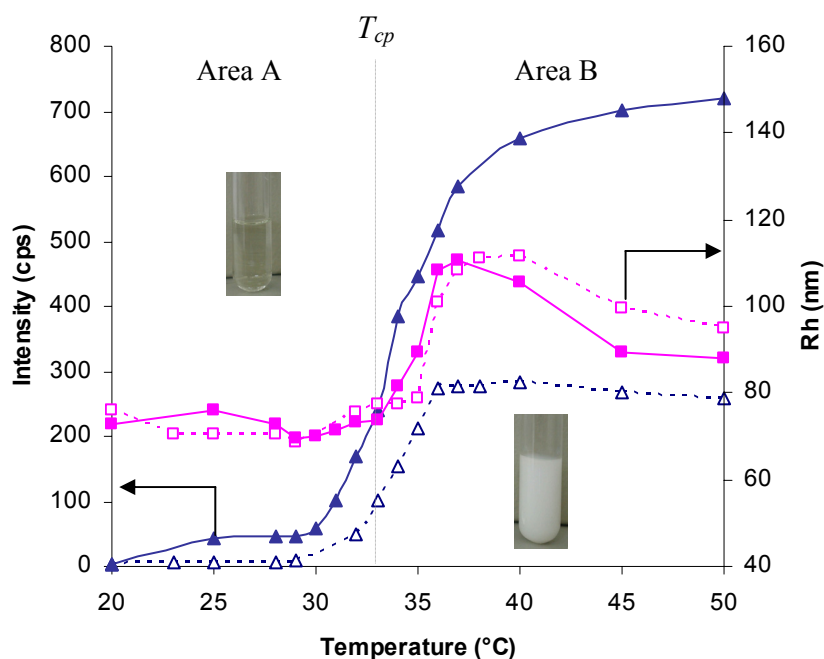


Figure 9.5. Variation of the hydrodynamic radius R_h (squares) and the intensity (triangles) of GPS1 (open symbols) and GPS2 (closed symbols) graft copolymers in water at $0.1 \text{ mg}\cdot\text{mL}^{-1}$ as a function of temperature (5 min between two measurements).

A strong influence of temperature is observed in the aqueous solution for both graft copolymers. A small decrease of the R_h at temperatures ranging from 20 to 30°C is first observed. This can be related to a volume concentration of the PMVE shell associated to its solubility decrease when temperature increases. This phenomenon is followed at 34°C by a rapid increase of the apparent hydrodynamic radius (R_h from 80 nm and more) and size distribution broadening of the objects, suggesting aggregation between graft copolymers. This is in agreement with the LCST properties

brought by the PMVE shell to the graft copolymers [9,22-23]. At T_{cp} , the size of aggregates increases as a result of intermolecular association. Additionally, the increase in the intensity of scattered light is ascribed to the increase of molar mass of the aggregates and to a decrease of the thermodynamic quality of the solvent.

Multimolecular micelle-like aggregates formed above $\sim 35^\circ\text{C}$ show colloidal stability against further precipitation. Once formed, they shrink upon further heating. Their size remains constant above 45°C . Colloidal stability has earlier been observed for PMVE homopolymer and was explained in terms of a viscoelastic effect [20]. Thus at elevated temperature, particles are dehydrated and therefore dense.

For the graft copolymers, PS grafts further decrease the mobility of the PMVE chains similar to what has been proposed earlier for PNIPAAm-*b*-PS [21]. Moreover, the reversibility of the LCST processes reported for linear homo- and PMVE [22-23] copolymers with PS blocks is also observed with the graft copolymers.

The R_h values of both graft copolymers at different concentrations are recapitulated in table 9.3. In all cases, R_h increases at the T_{cp} and decreases above T_{cp} , confirming first the intermolecular association and then the collapse of the micellar particles. Moreover, because of the high R_h values, we could conclude that aggregates are formed instead of unimolecular micelles, even at such diluted concentrations. On the other hand, R_h values below T_{cp} are lower than above T_{cp} , which indicates the aggregation behaviour of the micelles at elevated temperature and no precipitation. Additionally, R_h values are similar for all investigated concentrations and PS content.

Table 9.3. R_h values of GPS1 and GPS2 at different temperatures.

C	0.5 mg.mL ⁻¹			0.1 mg.mL ⁻¹			0.05 mg.mL ⁻¹		
	T < T_{cp}	T_{cp}	T > T_{cp}	T < T_{cp}	T_{cp}	T > T_{cp}	T < T_{cp}	T_{cp}	T > T_{cp}
R_h GPS1									
(nm)	78	102	87	86	102	94	75	117	80
R_h GPS2									
(nm)	88	114	103	73	106	88	76	90	88

** Dependence of the concentration*

One interesting point is to determine the critical aggregate concentration (CAC) in order to know at which concentration the aggregates start to be formed. Selected DLS data are shown in figures 9.6 and 9.7. In the first graph (figure 9.6), the intensity of light scattering was plotted as a function of concentration at different temperatures.

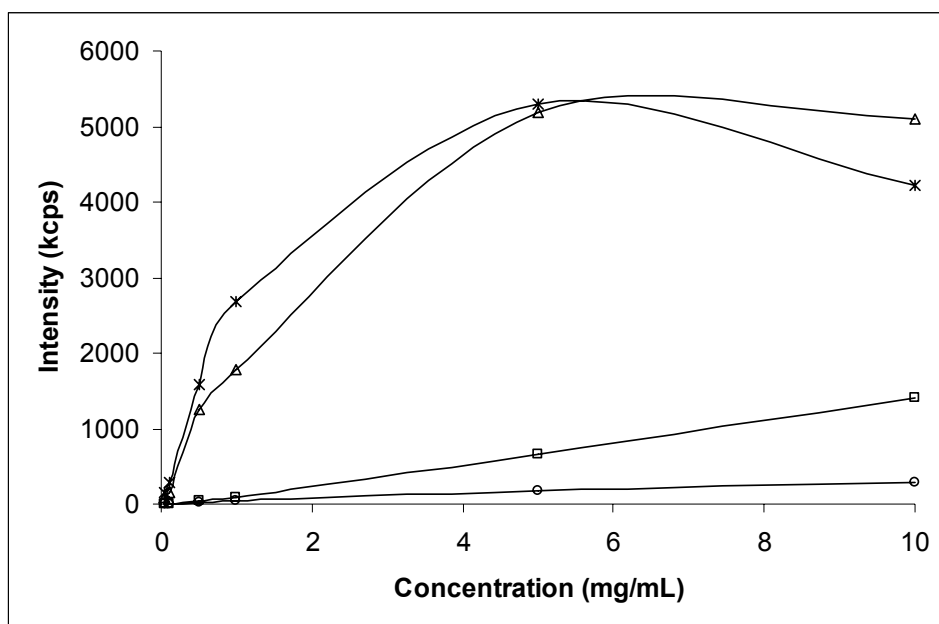


Figure 9.6. Variation of the intensity of light scattering of GPS1 graft copolymers in water at any concentration ($\text{mg}\cdot\text{mL}^{-1}$) as a function of temperature: at 25°C (○), at 30°C (□), at 40°C (△), at 45°C (*).

The absence of a plateau at lowest concentration indicated that no CAC is present, meaning that aggregates are formed at any concentration. What is more, below the T_{cp} , at any concentration, the intensity increases linearly with concentration. Above the T_{cp} ($T > 35^\circ\text{C}$), for higher concentration, the intensity decreases, which means precipitation is starting. At high temperature (above T_{cp}), the mechanism of the colloidal stability above T_{demix} resembles that of the mesoglobules formed by the PMVE homopolymer [20].

This is confirmed by the second graph (figure 9.7). Above the T_{cp} , the intensity remains constant but for concentrated solution (above $5 \text{ mg}\cdot\text{mL}^{-1}$), the intensity starts to decrease slowly.

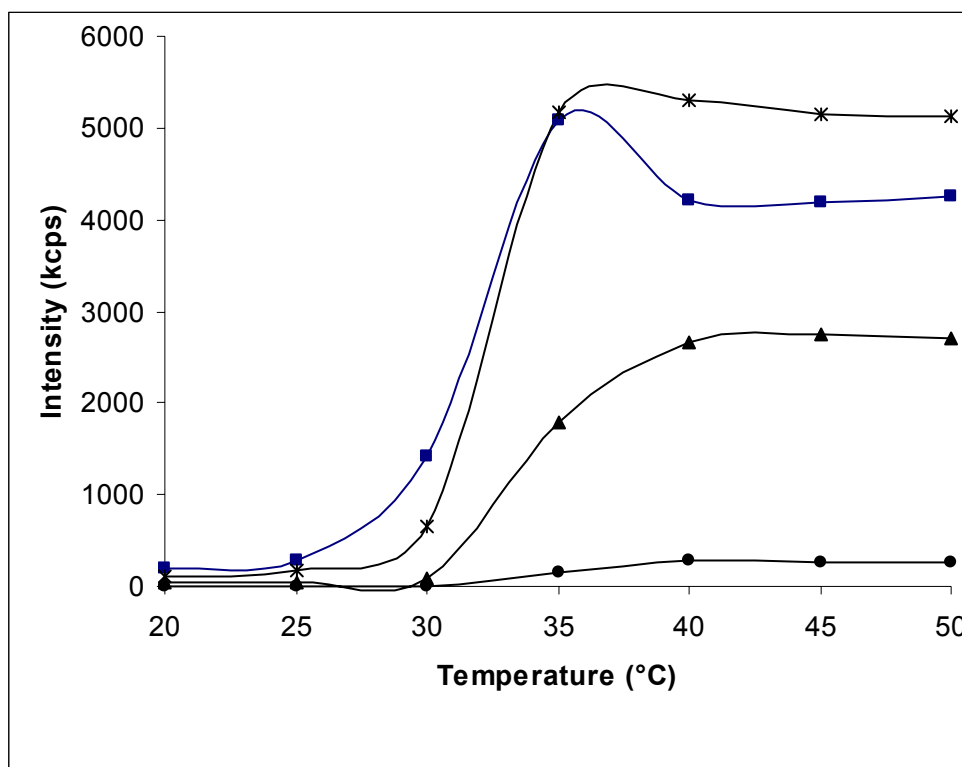


Figure 9.7. Variation of the intensity I of GPS1 graft copolymers in water at different temperature ($^{\circ}\text{C}$) as a function of concentration (mg.mL^{-1}): at 0.01 mg.mL^{-1} (●), at 1 mg.mL^{-1} (▲), at 5 mg.mL^{-1} (■), at 10 mg.mL^{-1} (*).

** Size distribution and R_h observations*

DLS measurements performed at various angles (40 to 150°) indicate the presence of heterogeneous population for GPS1 and GPS2. Because the same phenomena were observed for GPS1 and GPS2 at different concentration, only the sample of GPS1 at 0.5 mg.mL^{-1} is shown in figure 9.8.

Below the T_{cp} , at 90° , R_h distribution is very broad. Moreover, R_h distribution at 90° covers the R_h values at 150° and 40° . This means that the size distribution of aggregates is broad in water solution. As indicated by their hydrodynamic radius and broad size distribution in solution at 90° , the graft copolymers (figure 9.8) behave as aggregates. According to figure 9.4, formation of the intermolecular aggregates is confirmed at 40° , by the presence of two populations (aggregates (population I) + unimolecular micelles (population II)), where the resolution for large scatterers is better than at 90° .

As can be seen in figure 9.8, the R_h changed with temperature. Above the T_{cp} , the signals of the intensity of scattered light are still observed, so at the first point of view, no precipitation occurred. Besides, the highest R_h values have disappeared at 90° and 40° , which proved that only larger particles have precipitated, which is in agreement with figures 9.6 and 9.7.

As for the population of micelles with small R_h , the signal at 40° and 90° disappear after heating. This could be explained by the enhanced stickiness of the individual polymer chains, which promote multichain association and formation of clusters or aggregates. Moreover, the decrease of the R_h above the T_{cp} confirms the shrink phenomenon due to the hydrophobic character of

PMVE. Thus, the R_h values, which correspond to the largest aggregates, disappear above the T_{cp} showing the increase of the intramolecular interaction between aggregates. This can be explained by the internal contraction of PMVE corona.

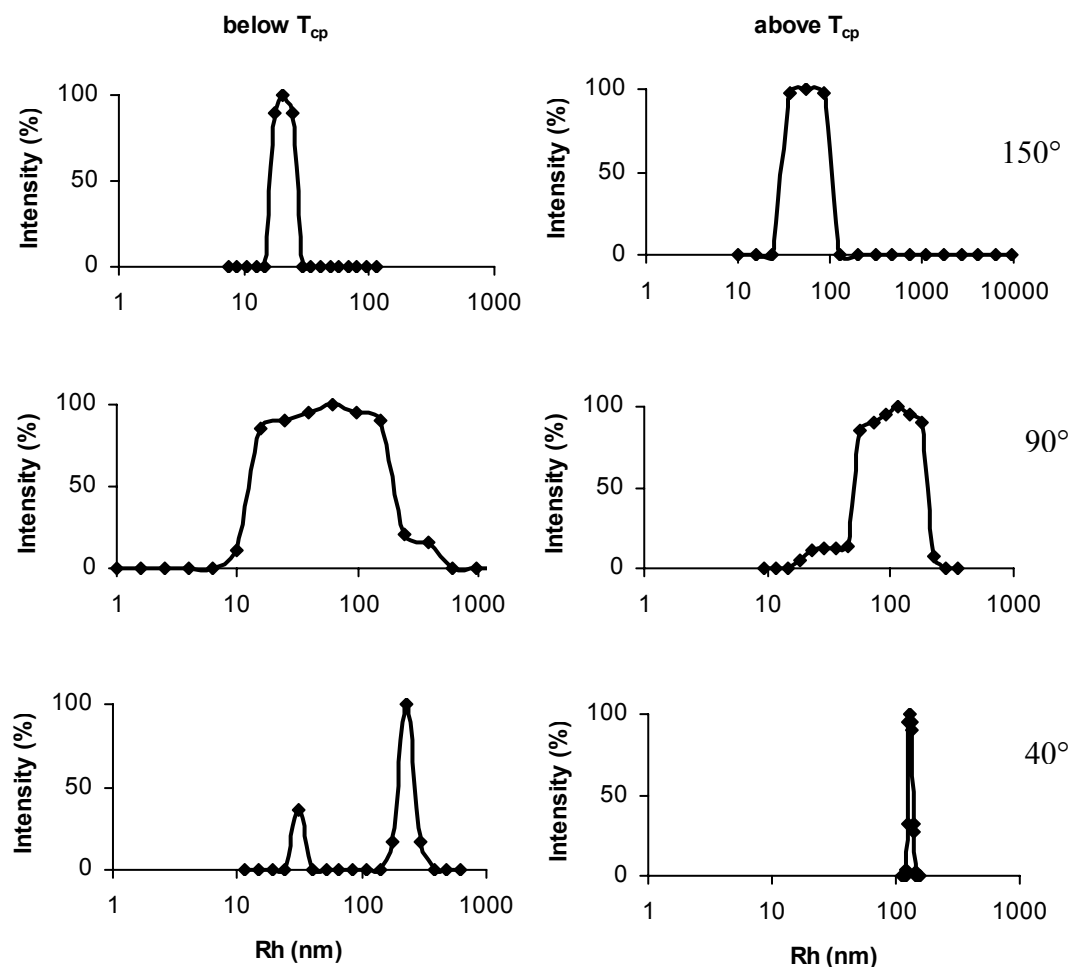


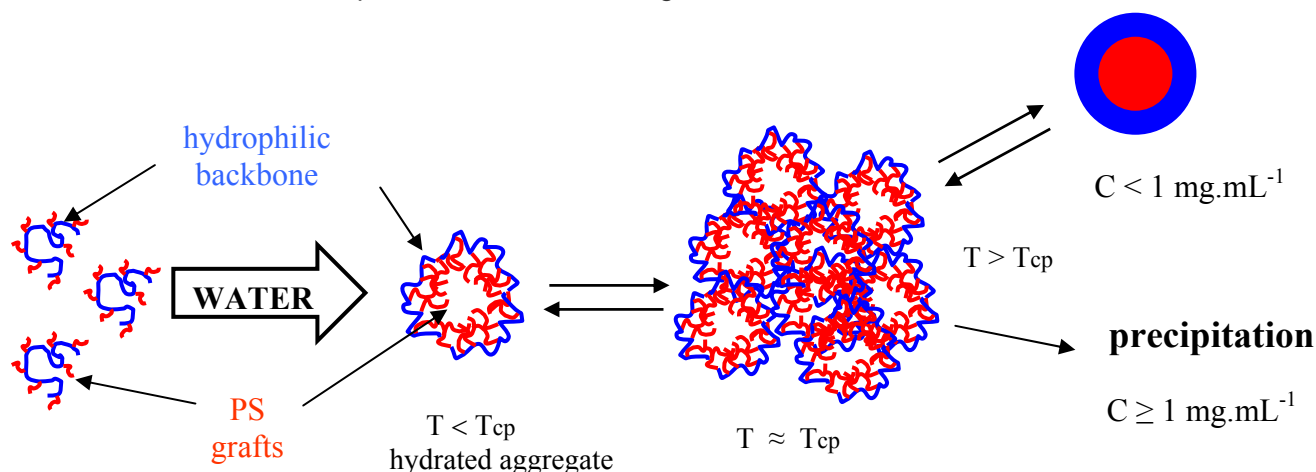
Figure 9.8. Distributions of the hydrodynamic radius R_h of GPS1 obtained at different angles below and above T_{cp} for a concentration $0.5 \text{ mg}\cdot\text{mL}^{-1}$.

Although the PMVE-*g*-PS graft copolymers exhibit a much more compact aggregate above T_{cp} , thanks to the PMVE shell they collapse together because of the intramolecular interactions, as indicated in figure 9.7. Also, the characteristic features of the PMVE-*g*-PS aggregates seem to be significantly different from those of PNIPAAm-*b*-PS [21]. Indeed, Tenhu and coworkers reported that PNIPAAm-*b*-PS block copolymers formed only isolated micelles with D_h in the 15-30 nm. Aggregates were, however, observed for polymers with higher molecular weights or containing a higher PS weight fraction. In some cases, these aggregates could be suppressed whenever the micelles were prepared via a dialysis method [24].

It has been shown that PMVE dehydrates slowly due to the stable structures of the micellar particles [20]. For the same reason, the dehydration does not necessarily lead to a huge change in the particle size. This may be rationalized by concluding that GPS1, which has the lowest PS content, do not disturb the formation of a micellar particle with a hydrophobic core. GPS1 and

GPS2 form mesoglobules with dimensions of the same order of magnitude as the dimensions of the fully stretched macromolecules. The same conclusion was made in the case of PNIPAAm-*b*-PS and PNIPAAm-*b*-P*t*BMA [21].

In general, we could conclude from the complete study, that only large particles precipitate above T_{cp} and particularly for higher concentration ($C \geq 1 \text{ mg.mL}^{-1}$), but the smallest particles remain stable in water, and a shrink phenomenon is observed due to the hydrophobic character of PMVE. This could be represented in the following scheme 9.1:



Scheme 9.1. Micellar particles behaviour of PMVE-*g*-PS in water solution at different temperatures.

9.2.5. Atomic Force Microscope (AFM)

The morphology of the micelle-like aggregates was then examined by AFM. The aggregates formed by PMVE-*g*-PS sample are shown in figure 9.9. Polydisperse spherical aggregates are clearly seen in these samples but they are poorly contrasted. The diameter of these micelle-like aggregates is in the range of 20-500 nm and therefore in agreement with the DLS results. Large aggregates have been occasionally observed, as shown in figure 9.9. The large aggregates revealed a cluster morphology. However, no information about their internal structure could be deduced so far.

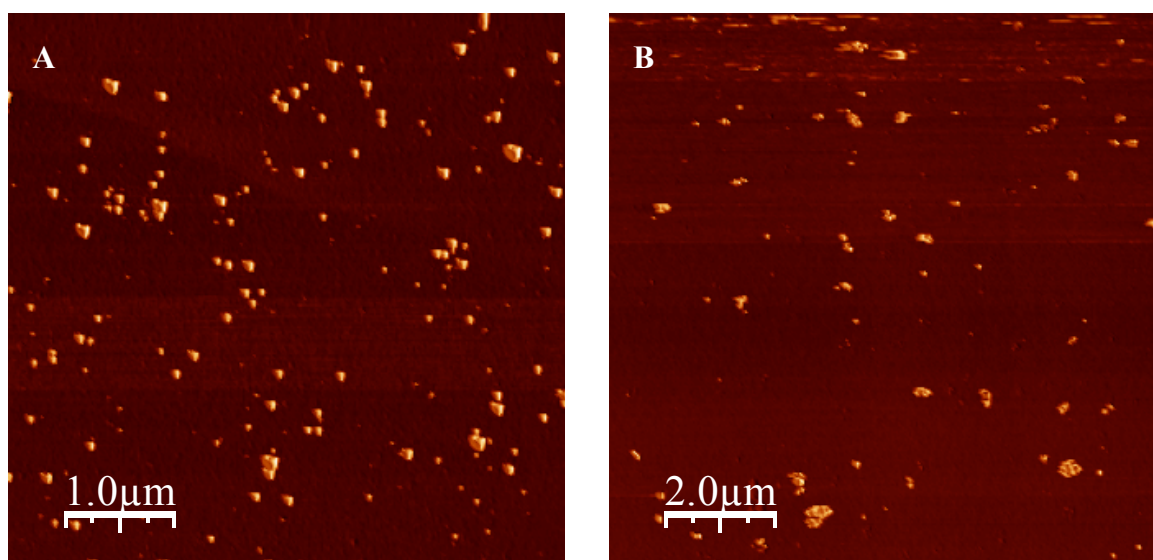


Figure 9.9. AFM pictures of GPS1 and GPS2 aggregates: (A) GPS1 at $0.1\text{mg}\cdot\text{mL}^{-1}$, (B) GPS2 at $0.1\text{mg}\cdot\text{mL}^{-1}$.

9.3. Conclusion

Turbidimetry, MTDSC, HS-DSC, DLS and AFM have been used to investigate the mesoglobular structure and the phase behavior of PMVE-*g*-PS. In water, the graft copolymers with short PS side chains form micellar particles, whereas longer PS side chains produce insolubility of the graft copolymers in water. Aqueous micelle-like aggregates have been prepared from two different PMVE-*g*-PS graft copolymers that contain a thermo-responsive PMVE corona and a high T_g polystyrene core.

The phase behaviour of aqueous PMVE-*g*-PS solutions has first been studied by MTDSC, which demonstrated that the solutions of the graft copolymers follow the typical type III LCST phase behaviour of PMVE at significantly lower demixing temperatures and LCST's. For all samples, spherical mesoglobules resulting from the merging of several individual micelles and aggregates have been observed by DLS and AFM. At low temperature, the copolymers form micelle-like aggregates where their sizes are fairly independent of the concentration. It was found that the solubility of PMVE-*g*-PS in water is limited by the amount of PS grafts but higher solubilities were found compared to block copolymers.

It has been shown by microcalorimetry that the dehydration of the PMVE backbone takes place in all samples but within a broad temperature range. It is concluded that the surface of the hydrophobic core of the small particles is crowded in a way that hinders the compression of the PMVE shell. Moreover, the micellar aggregates were observed to be colloidally stable, and the smaller mesoglobules did not precipitate from water above T_{cp} , whereas the largest ones precipitate.

9.4. References

- [1] (a) Wu C., Li W., Zhu X.X., *Macromolecules*, **2004**, *37*, 4989. (b) Zhang W., Shi L., Wu K., An Y., *Macromolecules*, **2005**, *38*, 5743. (c) Lanson D., Schappacher M., Borsali R., Deffieux A., *Macromolecules*, **2007**, *40*, 9503. (d) Wang F.P., Du X.Z., Wang C., Dong X.L., Yuan L., *J. Appl. Polym. Sci.*, **2008**, *108*, 3677. (e) Suriano F., Coulembier O., Degee P., Dubois P., *J. Polym. Sci., Part A : Polym. Chem.*, **2008**, *46*, 3662. (f) Gao K.J., Li G.T., Shi H.W., Lu X.P., Gao Y.B., Xu B.Q., *J. Polym. Sci., Part A : Polym. Chem.*, **2008**, *46*, 4889.
- [2] (a) Barany G., Zalipsky S., Chang J.L., Albericio F., *React. Polym.*, **1994**, *22*, 243. (b) Zhang L.S., Lin J.P., Lin S.L., *J. Phys. Chem. B*, **2007**, *111*, 9209. (c) Chen L., Hook D.J., Valint P.L., Gardella J.A., *J. Vacuum Sci. & Technol.*, **2008**, *26*, 616. (d) Qi H.F., Zhong C.L., *J. Phys. Chem. B*, **2008**, *112*, 10841. (e) Liu L., Xu X., Guo A.R., Han W., *Carbohydr. Polym.*, **2009**, *75*, 401.
- [3] (a) Selb J., Gallot Y., *Makromol. Chem.*, **1980**, *181*, 809; *182*, 1491. (b) Fessi H., Puissieux F., Devissaguet J.Ph., Ammoury N., Benita S., *Int. J. Pharm.*, **1989**, *55*, R1. (c) Gref R., Minamitake Y., Peracchia M.T., Trubetsky V., Torchilin V., Langer R., *Science*, **1994**, *263*, 1600. (d) Li M., Zhu L., Jiang M., Wu C., *Macromolecules*, **1997**, *30*, 2201.
- [4] (a) Eeckert A.R., Webber S.E., *Macromolecules*, **1996**, *29*, 560. (b) Perrachia M.T., Desmaele D., Couvreur P., d'Angelo J., *Macromolecules*, **1997**, *30*, 846.
- [5] (a) Liu S., Billingham N.C., Armes S.P., *Angew. Chem., Int. Ed.*, **2001**, *40*, 2328. (b) Harada A., Kataoka K., *Macromolecules*, **2003**, *36*, 4995. (c) Dai L., in *'Intelligent Macromolecules for Smart Devices: From Materials Synthesis to Device Applications'*, Springer-Verlag: London, **2004**. (d) Zhang W., Shi L., Gao L., An Y., Li G., Wu K., Liu Z., *Macromolecules*, **2005**, *38*, 6084. (e) Lequieu W., Shtanko N., Du Prez F.E., *J. Membr. Sci.*, **2005**, *256*, 64. (f) Lochhead R.Y., *Cosmetics and Toiletries*, **2006**, *121*, 73. (g) Rinaudo M., Osada Y., *L'Actualité Chimique*, **2006**, *300*, 31. (h) Lynen F., Heijl J., Du Prez F.E., Brown R., Szucs R., Sandra P., *Chromatographia*, **2007**, *66*, 143. (i) Kumar A., Srivastava A., Galaev I.Y., Mattiasson B., *Prog. Polym. Sci.*, **2007**, *32*, 1205. (j) Capadona J.R., Shanmuganathan K., Tyler D.J., Rowan S.J., Weder C., *Science*, **2008**, *319*, 1370.
- [6] Cameron N.S., Corbierre M.K., Eisenberg A., *Can. J. Chem.*, **1999**, *77*, 1311.
- [7] (a) Kwei T.K., Nishi T., Roberts R.F., *Macromolecules*, **1974**, *7*, 667. (b) Nishi T., Wang T.T., Kwei T.K., *Macromolecules*, **1975**, *8*, 227. (c) Nishi T., Kwei T.K., *Polymer*, **1975**, *16*, 285.
- [8] Schappacher M., Deffieux A., Putaux J-L., Viville P., Lazzaroni R., *Macromolecules*, **2003**, *36*, 5776.
- [9] Schappacher M., Putaux J-L., Lefebvre C., Deffieux A., *J. Am. Chem. Soc.*, **2005**, *127*, 2990.
- [10] Bernaerts K., PhD *'Geavanceerde Polymeerarchitecturen met Stimuli-responsieve Eigenschappen Uitgaande van Heterofunctionele Initiatoren'*, academic year **2005**, Gent University, Belgium, Chapter 6.
- [11] Zhao J., Confortini O., Van Assche G., Du Prez F.E., Van Mele B., *Polymer*, **2009**, not yet submitted.
- [12] Hashimoto T., Itakura M., Shimidzu N., *J. Chem. Phys.*, **1986**, *85*, 6773.

- [13] Verbrugghe S., Bernaerts K., Du Prez F.E., *Macromol. Chem. Phys.*, **2003**, *204*, 1217.
- [14] (a) Goethals E.J., Dubreuil M., Wang Y., De Witte I., Christova D., Verbrugghe S., Yanul N., Tanghe L., Mynarczuk G., Du Prez F., *Macromol. Symp.*, **2000**, *153*, 209. (b) Yanul N.A., Kirsh Y.E., Verbrugghe S., Goethals E.J., Du Prez F.E., *Macromol. Chem. Phys.*, **2001**, *202*, 1700. (c) Yanul N.A., Kirsh Y.E., Verbrugghe S., Goethals E.J., Du Prez F.E., in *'Tailored Polymers & Applications'*, Yagci Y., Mishra M.K., Nuyken O., Ito K., Wnek G., Eds. VSH Publishers, **2001**, p. 139.
- [15] (a) Yuk S.H., Cho S.H., Lee S.B., *Macromolecules*, **1997**, *30*, 6856. (b) Shin B.C., Jhon M.S., Lee H.B., Yuk S.H., *Eur. Polym. J.*, **1998**, *34*, 171.,
- [16] Van Durme K., Van Mele B., Bernaerts K., Verdonck B., Du Prez F.E., *J. Polym. Sci., Part B: Polym. Phys.*, **2006**, *44*, 461.
- [17] Schäfer-Soenen H., Moerkerke R., Berghmans H., Koningsveld R., Dušek K., Šolc K., *Macromolecules*, **1997**, *30*, 410.
- [18] Maeda H., *J. Polym. Sci., Part B: Polym. Phys.*, **1994**, *32*, 91.
- [19] Swier S., Van Durme K., Van Mele B., *J. Polym. Sci., Part B: Polym. Phys.*, **2003**, *41*, 1824.
- [20] Aseyev V., Hietala S., Laukkanen A., Nuopponen M., Confortini O., Du Prez F.E., Tenhu H., *Polymer*, **2005**, *46*, 7118.
- [21] Nuopponen M., Ojala J., Tenhu H., *Polymer*, **2004**, *45*, 3643.
- [22] Verdonck B., Goethals E.J., Du Prez F.E., *Macromol. Chem. Phys.*, **2003**, *204*, 2090.
- [23] Folder C., Patrickios C.S., Armes S.P., Billingham N.C., *Macromolecules*, **1996**, *29*, 8160.
- [24] Jada A., Hurtrez G., Siffert B., Riess G., *Macromol. Chem. Phys.*, **1996**, *197*, 3697.

PART IV

Experimental Part

IV.1. Reagents and Materials	209
IV.2. Analytical Methods: Measurements	211
IV.2.1. Atomic Force Microscopy (AFM)	211
IV.2.2. Cloud Point Temperature (T_{cp})	212
IV.2.3. Copolymers Composition	212
IV.2.4. Differential Scanning Calorimetry (DSC)	213
IV.2.5. Dynamic Light Scattering (DLS)	213
IV.2.6. Electrokinetic Sonic Amplitude (ESA)	215
IV.2.7. Elemental Analysis (E.A.)	215
IV.2.8. Fourier Transform Infrared (FT-IR)	215
IV.2.9. Gas Chromatography (GC)	215
IV.2.10. High Sensitivity Differential Scanning Calorimetry (HS-DSC) or Microcalorimetry	216
IV.2.11. Methods of micelle preparation	219
IV.2.12. Modulated Temperature Differential Scanning Calorimetry (MTDSC)	220
IV.2.13. Nuclear Magnetic Resonance (^1H NMR and ^{13}C NMR)	223
IV.2.14. Size Exclusion Chromatography (SEC)	223
IV.2.15. Surface Tension	224
IV.2.16. Ultraviolet-visible spectrophotometer (UV-vis Transmission)	224
IV.3. Syntheses	225
IV.3.1. Synthesis of the Poly(Vinyl Ethers)	225
IV.3.1.1. Synthesis of the Random Copolymers Starting with a Mono-functional Initiator	225
IV.3.1.2. Homopolymerizations of PMVE, PIBVE and PCEVE Starting with a Bi-functional Initiator	227
IV.3.1.3. Synthesis of the Random Copolymers Starting with a Bi-functional Initiator	228
IV.3.1.4. Two-Stage Copolymerizations	229
IV.3.2. Synthesis of the Thermo-responsive PMVE- <i>g</i> -PEO	230
IV.3.2.1. Model Reactions	230
IV.3.2.1.1. By One-step: the Nuyken Method	230
IV.3.2.1.2. By Two-steps: the Finkelstein Method	230
IV.3.2.2. Functionalization of PEO	231
IV.3.2.3. Synthesis of PMVE- <i>g</i> -PEO	233
IV.3.3. Syntheses of PMVE- <i>g</i> -PS and PMVE- <i>g</i> -PMAA by ATRP	234
IV.3.3.1. ATRP Homopolymerization Procedure of St and <i>t</i> BMA	234
IV.3.3.1.1. With CuBr/PMDETA as Metal/Ligand Catalyst	235
IV.3.3.1.2. With NiBr ₂ (PPh ₃) ₂ as Metal Catalyst	235
IV.3.3.2. Synthesis of the Macroinitiator	236
IV.3.3.3. 'Grafting from' Procedure of the Synthesis of the PMVE- <i>g</i> -PS and PMVE- <i>g</i> - P <i>t</i> BMA	237
IV.3.4. References	239

IV.1. Reagents and Materials

Benzylamine (MG = 107.15 gmol⁻¹, ρ = 0.9810, bp = 184°C, 99.5% from Acros Organics) was used as received and degassed under argon during 10 min before use.

n-Butylamine (MG = 73.13 gmol⁻¹, ρ = 0.74, 99.5% from Acros Organics) was used as received and degassed under argon during 10 min before use.

tert-Butyl methacrylate (tBMA, MG = 142.20 gmol⁻¹, ρ = 0.875, bp = 132°C, 98% Aldrich) was distilled in the presence of phenothiazine as inhibitor at low pressure under argon. The monomer was stored at 4°C in the darkness, and filtered through a basic aluminium oxide (Al₂O₃) column twice to remove acid traces just before use.

2-Chloroethyl vinyl ether (CEVE, MG = 106.55 gmol⁻¹, ρ = 1.048, bp = 109°C, 99% from Aldrich) was washed with a 10% aqueous sodium hydroxide solution and then with water, dried overnight with MgSO₄, distilled twice over CaH₂ prior to polymerization and stored under argon at low temperature.

Copper bromide (CuBr, MG = 223.35 g.mol⁻¹, ρ = 4.77, mp = 498°C, 99% from Aldrich) was purified by stirring with acetic acid, then by filtering and washing with ethanol and diethyl ether, and finally by drying in a vacuum oven at 70°C [1].

Copper chloride (CuCl, MG = 134.55 g.mol⁻¹, Aldrich 99%) was purified by washing with acetic acid, filtering with ethanol and drying under vacuum [1].

Dichloromethane HPLC (CH₂Cl₂) was distilled under CaH₂ prior to use.

1,1-Diethoxyethane (DEE, MG = 118.18 gmol⁻¹, ρ = 0.831, bp = 85°C, 99% from Acros Organics) was purified by refluxing 2 hours and distilled over CaH₂ first, then, just before use, distilled over CaH₂.

Anhydrous diethyl ether HPLC (Et₂O, bp = 35°C) was distilled over sodium just before use in the presence of traces of benzophenone as indicator for the presence of H₂O.

Dimethylformamide HPLC (DMF, bp = 153 °C) was stored under molecular sieves 3Å.

Isobutyl vinyl ether (IBVE, MG = 100.16 gmol⁻¹, ρ = 0.768, bp = 83°C, 99.5% from Acros Organics) was washed with a 10% aqueous sodium hydroxide solution and then with water, dried overnight with MgSO₄. Then it was purified by refluxing 4 hours and distilled over CaH₂ first, then distilled again just before use under sodium in the presence of traces of benzophenone as indicator for the presence of H₂O.

Methyl vinyl ether (MVE) (MG = 55.08 g mol⁻¹, bp = 83°C, kindly donated by BASF company, Ludwigshafen) was passed through a CaH₂ trap for drying purposes.

Nickel dibromide triphosphine (Ni(II)Br₂(PPh₃)₂, MG = 743.12 g mol⁻¹, mp = 219-223°C, 99% from Aldrich) was used without purification. It was stored under nitrogen but was weighed in the open air prior polymerization. No catalyst degradation has been noticed even after 2 days in contact with air.

N,N,N',N'',N'''-pentamethyldiethylenetriamine (PMDETA, MG = 173.30 g mol⁻¹, ρ = 0.830, bp = 83-84°C/18 mmHg or 198°C, mp = -20°C, 99+% from Acros) was distilled (85-86°C/12 mmHg), and degassed before use for 1 hour.

Poly(ethylene oxide)monomethyl ether (CH₃O-PEO-OH, M_w = 2000-5000 g mol⁻¹, Aldrich Chemical Company Inc.) was used without further purification except for rigorous drying to remove absorbed water. It was stirred and heated at 70°C for 7 hours under vacuum.

Poly(methyl vinyl ether) (PMVE, M_w = 20 000 g mol⁻¹, T_g = -25°C, from Aldrich Chemical Company Inc.) was dried prior to further handling.

Potassium iodide (KI, MG = 166.01 g mol⁻¹, 99.995% from Acros Organics) was degassed under argon in darkness and dried under vacuum for at least 2 hours before use.

Pyridine (MG = 79.10 g mol⁻¹, ρ = 0.978, bp = 115°C, mp = -42°C 99.5% Avocado) was distilled under CaH₂ prior to use.

Sodium iodide (NaI, MG = 149.89 g mol⁻¹, 99+% from Aldrich) was degassed under argon in darkness and dried under vacuum for at least 2 hours before use.

1,1,3,3-Tetraethoxypropane (TEoP or malonaldehyde bis (diethyl acetal), MG = 220.31 g mol⁻¹, ρ = 0.910, bp = 220°C, 99+%, Acros Organics) was purified by reflux (4 hours), distilled over CaH₂ under reduced pressure and stored under argon at low temperature. It can be used only 5 times. Then, a new purification is necessary.

Tetrahexylaluminium (THA, from Interspe Hamann Group) was dissolved in dry toluene (0.1 M) and stored under argon at low temperature.

Tetrahydrofurane HPLC (THF, bp = 67°C) was purified by refluxing and distillation over sodium in the presence of traces of benzophenone as indicator for the presence of H₂O, then, before use, distilled over sodium in the presence of benzophenone.

2,2,6,6-Tetramethylpiperidine (TMP, MG = 141.26 gmol⁻¹, ρ = 0.837, bp = 152°C, 98% from Acros Organics) was purified by refluxing 4 hours, distilled over CaH₂ under reduced pressure and stored under argon at low temperature.

Toluene HPLC (Fischer Scientific, bp = 110°C) was purified by refluxing and distillation over sodium in the presence of traces of benzophenone as indicator for the presence of H₂O, then, before use, distilled over sodium in the presence of benzophenone.

Triethylamine (Et₃N, MG = 101.19 gmol⁻¹, ρ = 0.726, bp = 89°C, 99.5% from Aldrich) was first purified by reflux (during 2 hours) and then freshly distilled over CaH₂ before use.

Trimethylsilyl iodide (TMSI, MG = 200.10 gmol⁻¹, ρ = 1.406, bp = 106°C, 97% from Aldrich, 5 mL ampoule) was bought at Aldrich in ampoules stabilized by copper. It was used without further purification and stored in the freezer.

Zinc iodide (ZnI₂, MG = 319.18 gmol⁻¹, 99.99+ % of purity, from Aldrich, 5 ml ampoule) was dried under vacuum for at least 12 hours before use under darkness, and stored under argon.

Aluminium oxide (Al₂O₃, Aldrich neutral activated 58 Å), 2-bromoethyl phthalimide (MG = 254.09 gmol⁻¹, 98% from Avocado), *n*-butyl lithium (nBuLi, in a 1.6 M hexane solution, Fluka), lithium borohydride (LiBH₄, 2 M solution in THF, from Acros Organics), potassium-*tert*-butoxide (*t*BuO⁻K⁺, MG = 112.21 gmol⁻¹, 95-99% from Janson Chimica), anhydrous sodium thiosulfate (Na₂S₂O₃) (MG = 105.99 gmol⁻¹, 99% from Aldrich), tetrabutylammonium bromide (TBAB, MG = 322.36 gmol⁻¹, 99+% from Acros Organics), 2,2,2-tribromoethanol (TBE) (MG = gmol⁻¹, from), para-toluenesulfonyl chloride (TsCl, >99%, Fluka), triethylene glycol (TEG, MG = 178 gmol⁻¹ and Aldrich Chemical Company Inc.) were used as received.

All other unspecified reagents and materials were used after distillation or without further treatment.

IV.2. Analytical Methods: Measurements

IV.2.1. Atomic Force Microscopy (AFM)

Samples for AFM analysis were prepared by solvent casting at ambient conditions by spin coating on substrates starting from solutions in water of PMVE-g-PS. Practically, 20 µL of a dilute solution (0.5 mg.mL⁻¹ and 0.1 mg.mL⁻¹) were spin cast on a 2 x 2 cm² Si wafer with rotated monolytic contact probes. Samples were analyzed in liquid state at room temperature. All AFM images were recorded in air with a PicoPlus instrument from Digital imaging (now Agilent) modular Scanning Probe Microscope (SPM), operated in soft tapping mode. The probes were commercially available silicon tips with a spring constant of 40 N/m, a resonance frequency lying

in the 300 kHz. In this work, the images were recorded with the highest sampling resolution available, i.e., 1024 x 1024 data points.

IV.2.2. Cloud Point Temperature (T_{cp})

For T_{cp} measurements, a copolymer solution was dissolved in Milli-Q water at the desired concentration and then put into test tubes and kept at 4°C for 24 hours. The T_{cp} was visually determined by transferring the test tubes into a water bath, and increasing the temperature stepwise with 1°C every 15 min. The T_{cp} was chosen as the temperature when the solution became cloudy. The phase transition temperature of the solutions was also measured by monitoring the transmittance at the wavelength of 540 nm through a 3 cm polystyrene cuvette with a heating rate of 0.1°C.min⁻¹ in between 10 and 50 °C. The transmittance was recorded on a Uvikon 810 UV/VIS spectrophotometer.

The T_{cp} can also be obtained from light scattering and microcalorimetry measurements.

IV.2.3. Copolymers Composition

The DP_n of the copolymers and their compositions were determined from ¹H NMR spectra according to the starting group (DEE or TEoP at 1.1-1.2 ppm) and to characteristic areas of each monomer repeat unit where m corresponds to the number of the repeating units of MVE, n of CEVE and o of IBVE. The ¹H NMR spectra and the results are shown in **Chapter 3**. The methylene unit of the three homopolymers (protons a) appears in the area I_{CH2} between 1.5 – 2.0 ppm. The β-methyl protons adjacent to the oxygen atom, as an ether function, of PMVE (protons b and c) give rise to the signal area I_{MVE} between 3.2 – 3.55 ppm, while those adjacent to the oxygen of PCEVE (protons b, d and e) appear in the range area I_{CEVE} between 3.5 – 3.9 ppm, while also those of PIBVE (protons b and f) appear in the range area I_{IBVE} between 3 – 3.6 ppm. Moreover, IBVE units are also characterized in area I_{CH3} by a single peak (protons h) at 0.9 ppm.

The DP_n and the composition of each copolymers were also calculated from combinations of the integration of both monomers by the three following system equations:

✓ *Case of Poly(MVE-co-CEVE)*

* I_{MVE} + I_{CEVE} = (4 H m + 5 H n + 4 H) * I_H with TEoP/TMSI initiator or I_{MVE} + I_{CEVE} = (4 H m + 5 H n + 3 H) * I_H, with DEE/TMSI initiator (area between 3.1 – 3.9 ppm)

* I_{CH2} = (2 H m + 2 H n + 2 H) * I_H, with TEoP/TMSI initiator or I_{CH2} = (2 H m + 2 H n) * I_H (area between 1.5 – 2.0 ppm)

* I_H = i / 6H, I_H: one proton integration (i: area of the signal at 1.18 ppm).

✓ *Case of Poly(MVE-co-IBVE)*

The equations are the following:

* $I_{MVE} + I_{IBVE} = (4 H m + 3 H o + 4 H) * I_H$ with TEOP/TMSI initiator or $I_{MVE} + I_{IBVE} = (4 H m + 3 H o + 3 H) * I_H$, with DEE/TMSI initiator (area between 3.1 – 3.6 ppm)

* $I_{CH_2} = (2 H m + 3 H o + 2 H) * I_H$, with TEOP/TMSI initiator or $I_{CH_2} = (2 H m + 3 H o) * I_H$ (area between 1.5 – 2.0 ppm)

* $I_{CH_3} = 6 H o$, peak at 0.9 ppm

* $I_H = i / 6H$

✓ *Case of Poly(IBVE-co-CEVE)*

The equations are the following:

* $I_{IBVE} + I_{CEVE} = (5 H n + 3 H o + 4 H) * I_H$ with TEOP/TMSI initiator or $I_{MVE} + I_{IBVE} = (5 H n + 3 H o + 3 H) * I_H$, with DEE/TMSI initiator (area between 3.2 – 3.9 ppm)

* $I_{CH_2} = (2 H n + 3 H o + 2 H) * I_H$, with TEOP/TMSI initiator or $I_{CH_2} = (2 H n + 3 H o) * I_H$ (area between 1.5 – 2.0 ppm)

* $I_{CH_3} = 6 H o$, peak at 0.9 ppm

* $I_H = i / 6H$

The results are listed in table 3 in **Chapter 3**.

IV.2.4. Differential Scanning Calorimetry (DSC)

The thermal analyses were performed on Perkin-Elmer DSC-7 differential scanning calorimeter. The amount of samples was about 10 or 15 mg, a heating rate of $5^{\circ}\text{C}.\text{min}^{-1}$ at the second heating run was used and the temperature and heat capacities were calibrated with indium and n-octane standards.

The glass transition temperature (T_g) of the copolymers was determined by DSC with PERKIN-ELMER thermal analyser DSC-7 with a heating rate of $5^{\circ}\text{C}.\text{min}^{-1}$ during the first and the second heating run with a temperature range from -100 to 140°C . During the measurement, the sample was purged with nitrogen gas. The T_g was defined as the onset of the change in heat capacity during the second heating.

IV.2.5. Dynamic Light Scattering (DLS)

* Principle

DLS also known as quasi-elastic light scattering (QELS), is usually used to determine the particle size and size distribution of colloidal particles. It can be used to characterize latex, ceramic particles and silica, as well as adhesives, toner particles, micelles and microemulsions, among others. Particles that are suspended in a liquid undergo random movement caused by their bombardment by liquid molecules, with smaller particles 'diffusing' through fluid faster than larger particles. This phenomenon is termed Brownian motion after its discoverer Robert Brown, and

can be used to determine the size of the constituent particles. If a coherent and vertically polarized source, such as a laser, is applied to the sample, concentration fluctuations give rise to scattered intensity fluctuations. Variations in the intensity of the light scattered by the particles can be detected at any time by a single photon counting detector, and the size of the particles are derived using an autocorrelator and mathematical algorithms.

* *Theory* [2-3]

In DLS experiments, an autocorrelation function of scattered light intensity $G_2(t) = \langle I(0)I(t) \rangle$ was collected and then converted into an autocorrelation function of scattered electric field $g_1(t)$ using the Siegert's relationship [2]:

$$|g_1(t)| = \beta^{1/2} \sqrt{\frac{G_2(t) - G_2(\infty)}{G_2(\infty)}} \quad \text{Eq.IV.2.5-1}$$

where $G_2(\infty)$ is the experimentally determined baseline, and β is the coherence factor determined by the geometry of the detection (typically $0.5 \leq \beta \leq 0.8$). Characteristic decay times of a field correlation function τ_i and their relative amplitudes $A_i(\tau_i)$ were evaluated via moments of a corresponding distribution function of decay times $A(\tau)$ obtained using an inverse Laplace transform programs CONTIN as

$$g_1(t) = \int_0^{\infty} A(\tau) e^{-1/\tau} d\tau \quad \text{Eq.IV.2.5-2}$$

Corresponding hydrodynamic radii R_{hi} were obtained from relaxation times τ_i via the Stokes-Einstein equation:

$$R_{hi} = \frac{kT}{6\pi n_0} \tau_i q^2 \quad \text{Eq.IV.2.5-3}$$

where k is the Boltzmann constant, T is the absolute temperature, n_0 is the solvent viscosity, q is the scattering vector determined as

$$q = \frac{4\pi n_0}{\lambda_0} \sin \frac{\theta}{2}$$

λ_0 is the wavelength of the incident laser light source; n_0 is the refractive index of the solvent. Mean peak values of hydrodynamic size distributions were used as an average hydrodynamic radius R_h .

* *Experimental*

DLS experiments were performed to investigate properties of intermolecular aggregates on nanometer scale. DLS was also applied to determine the hydrodynamic radius (R_h) and hydrodynamic size distribution of the copolymers synthesized. Methodological aspects of DLS can be found elsewhere [3]. DLS measurements were conducted with a Brookhaven Instruments BIC-200 SM goniometer and a BIC-9000 AT digital correlator. The light source was Spectra Physics model SP127-35 helium/neon laser (632.8 nm, 20 mW). Time correlation functions were analyzed with a Laplace inversion program (CONTIN). Simultaneously, time average intensity of scattered light I was recorded. Intensities measured in counts of photons per second were normalised with respect to the Rayleigh ratio of toluene. The range of graft copolymer

concentrations was 0.02-1 g.L⁻¹ for PMVE-*g*-PEO, and 0.01-10 g.L⁻¹ for PMVE-*g*-PS. The solutions were filtered through Millex membranes PVDF 0.45 µm filter units. The measurement temperature ranged from 10 to 50°C and was controlled by means of a Lauda RC 6C thermostat. Experiments were carried out at a scattering angle range from 40 to 150°. At each temperature, the solutions ($c_p = 0.1 \times \text{mg.mL}^{-1}$) were equilibrated from 30 to 60 min before the measurements. In the DLS, the intensity-intensity time correlation function $G^2(t)$ was recorded, which was used for the determination of the average line width (Γ). The average translational diffusion coefficient $\langle D \rangle$ was further calculated from (Γ/q^2) . Scattering intensity, where the effect of solvent and scattering angle has been taken into consideration can be written as $I_\theta = (I_{\theta, \text{solution}} - I_{\theta, \text{solvent}})\sin \theta$, with $I_{\theta, \text{solution}}$, $I_{\theta, \text{solvent}}$, θ being the scattering intensity of the solution, the scattering intensity of the solvent, and the scattering angle, respectively. I_θ has been presented as a function of q^2 . Scattering function $P(q)$ is written as $P(q) = I_\theta / I_{\theta=0} = 1 - ((R_g^2 q^2)/3)$ where $I_{\theta=0}$ is estimated by extrapolating intensities to zero angle. Thus, $q = (4\pi n_0/\lambda)(\sin(\theta/2))$ is the scattering vector with n_0 and λ are refractive index of solvent and wavelength. It is essential to use the linear part of the scattering function where R_g is proportional its slope, i.e. $q\langle R_g \rangle \leq 1$.

IV.2.6. Electrokinetic Sonic Amplitude (ESA)

The pigment-polymer interaction was investigated by electrokinetic sonic amplitude (ESA) method. ESA measurements were carried out as described earlier [4]. This analytical technique measures the dynamic mobility, which in turn is related to the zeta-potential [4-5].

IV.2.7. Elemental Analysis (E.A.)

For determining the grafting degree of the PEO side chains, all the element values were determined by EA. EA was performed by Solarize in France.

IV.2.8. Fourier Transform Infrared (FT-IR)

FT-IR spectra of graft copolymers were recorded between 4400-600 cm⁻¹ with Bio-Rad 575C enhanced intensity FT-IR spectrometer, using polymer films cast from chloroform solutions onto KBr pellets. The PMVE-*g*-PtBMA was characterized by comparing the FT-IR spectrum of PMVE-*g*-PMAA.

IV.2.9. Gas Chromatography (GC)

GC was performed on a GC8000 from CE instruments with DB-5MS column (60 m x 0.249 mm x 0.25 µm) from J&W scientific. Detection was done with an FID-detector. Injector and detector temperatures were kept constant at 250°C. Starting temperature of the column was 50°C for 3 min, followed by heating rate of 20°C.min⁻¹ until 230°C and kept for 8 min at this temperature. Conversion was determined by using acetone or dichloromethane as internal standard.

IV.2.10. High Sensitivity Differential Scanning Calorimetry (HS-DSC) or Microcalorimetry [6-8]

* Principle

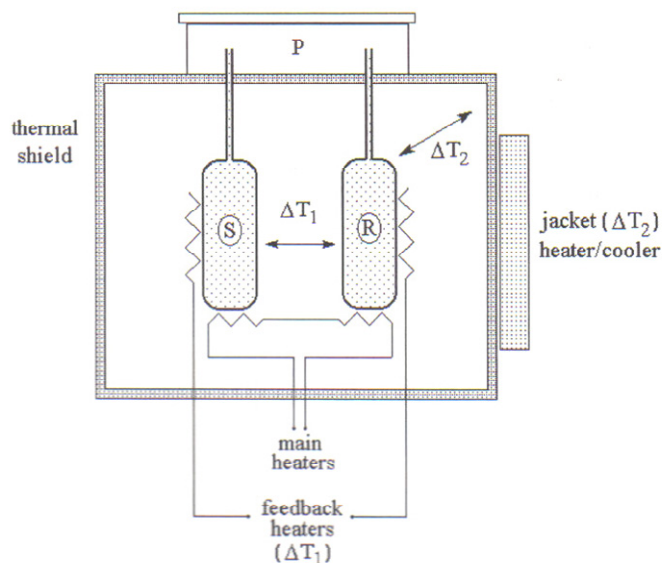


Figure IV.1. Sketch diagram of a typical HS-DSC used for thermal studies of dilute solutions of polymer-biomolecules (adapted from [6]). Identical, total-fill sample (S) and reference (R) cells (typically 0.5-1 mL) containing polymer solution and buffer, respectively, are held under elevated atmospheric or inert gas pressure (P) to inhibit bubble formation during heating. During up-scan operation, power is supplied to the main heaters to raise the temperature of the cells at a steady rate, whilst monitoring the temperature differences between sample reference cells (ΔT_1) and between cells and the surrounding adiabatic jacket (ΔT_2). Feedback through the jacket heater allows the thermal shield temperature to follow that of the cells, and feedback heaters on the cells compensate for any temperature differences between the cells during the scan. Figure taken from reference [7].

A sketch showing the typical layout of a HS-DSC instrument is shown in figure IV.1. A DSC continuously measures the apparent specific heat of a system as a function of temperature. Therefore, HS-DSC can be used to examine a heat induced phase transition or conformational change [8]. A HS-DSC instrument contains two cells suspended in an adiabatic jacket and connected by various heating and temperature/power sensing circuits. In a HS-DSC experiment, a solution of polymer (typically $1 \text{ mg}\cdot\text{mL}^{-1}$ or less in modern instruments) is heated at constant rate in the calorimeter (or sample) cell alongside an identical reference cell containing buffer (H_2O or D_2O) (cell volume = 0.5-1 mL) and the temperature is increased in the range $0.1 - 100^\circ\text{C}$. During a heat induced endothermic transition, the temperature of the sample cell falls behind that of the reference since some of the energy required is used to induce the transition rather than heat the solution. This lag is detected and additional electric power is proportional to the energy associated with the thermally induced transition. Differences in heat energy uptake between the sample and reference cells required to maintain equal temperature, correspond to differences in apparent heat capacity $C_{p,app}$. These differences in heat capacity give direct information about the energetics of thermally-induced processes in the sample. Knowledge of the solute concentration

permits the conversion of the observed electrical against temperature profile to a curve corresponding to an excess heat capacity versus temperature plot.

* Thermodynamics

A single HS-DSC experiment can provide a large amount of thermodynamic information, much of which cannot be obtained by any other technique. Equation Eq.IV.2.10-1 shows that integration of the experimental heat capacity (C_p) curve yields the calorimetric transition enthalpy (ΔH_{cal}):

$$\int C_p dT = \Delta H^0 \quad \text{Eq.IV.2.10-1}$$

This calorimetrically determined enthalpy is model independent and therefore does not depend on the nature of the transition. The temperature at which excess heat capacity ($C_{p,ex}$) is at a maximum defines the transition temperatures or mixing temperatures (T_m). Differences in the initial and final baselines provide a measure of the heat capacity change that accompanies the transition. Equation Eq.IV.2.10-2 shows that by converting the experimental data into a $C_{p,ex}/T$ versus T curve the entropy change (ΔS) for the transition can be determined from the area under such a curve.

$$\Delta S = \int (C_{p,ex} / T) dT \quad \text{Eq.IV.2.10-2}$$

Using these data the value of ΔG can be evaluated at any temperature.

HS-DSC experiments suitably analyzed can also provide important information on the cooperativity of a transition. This can be achieved by comparing the model-dependent van't Hoff enthalpy (ΔH_{vH} obtained by shape analysis of the calorimetric data) and the calorimetric enthalpy (ΔH_{cal}). The advantage of scanning microcalorimetry consists of the fact that both quantities, ΔH_{vH} and ΔH_{cal} , can be determined in a single experiment. If $\Delta H_{vH} = \Delta H_{cal}$ then the transition proceeds in a two-state manner and meaningful thermodynamic data can be obtained by examining the temperature dependence of an equilibrium property. The ratio $\Delta H_{vH}/\Delta H_{cal}$ represents an effective number of cooperative units per polymer molecule and thus provides a quantitative insight into the nature of the transition; specifically, it provides a measure of the fraction of the structure that melts as a single thermodynamic entity, i.e. it defines the size of the cooperative unit. This is a unique advantage of scanning microcalorimetry in the study of biological and polymer molecules.

* Experimental

Microcalorimetry measurements were performed for aqueous polymer solutions with a VP-DSC microcalorimeter (MicroCal Inc) at an external pressure of ca. 180 kPa. The cell volume was 0.507 ml. The instrument response time was set at 5.6 s. Scans were performed from 10 to 100°C at heating rates of 30, 60 and 90°C.h⁻¹. Prior to each scan the sample was kept at 10°C for 15 min. Data were corrected for instrument response time and analysed using the software supplied by the manufacturer. The polymer concentration was 1.0 mg.mL⁻¹, unless otherwise specified. For the present system, the values of T_{demix} are determined with an estimated accuracy

of ± 0.1 °C. The heat of transitions ΔH is given in kilo Joules per moles of repeating units. For PMVE, P(MVE-*stat*-CEVE), PMVE-*g*-PEO and PMVE-*g*-PS, $\Delta C_p = C_p(90^\circ\text{C}) - C_p(25^\circ\text{C})$.

The influence of the scan rate was studied on the PMVE, the backbones and various graft copolymers of PMVE-*g*-PEO and PMVE-*g*-PS. In figures IV.2 and IV.3, the superposition of the curves with the heating rate between 30 and 90°C.h⁻¹ shows that the variation of the scan rate does not cause any systematic change in the thermograms and the T_{cp} values. Moreover, the endothermic transition observed is completely reversible and reproducible (see figure IV.2 and IV.3).

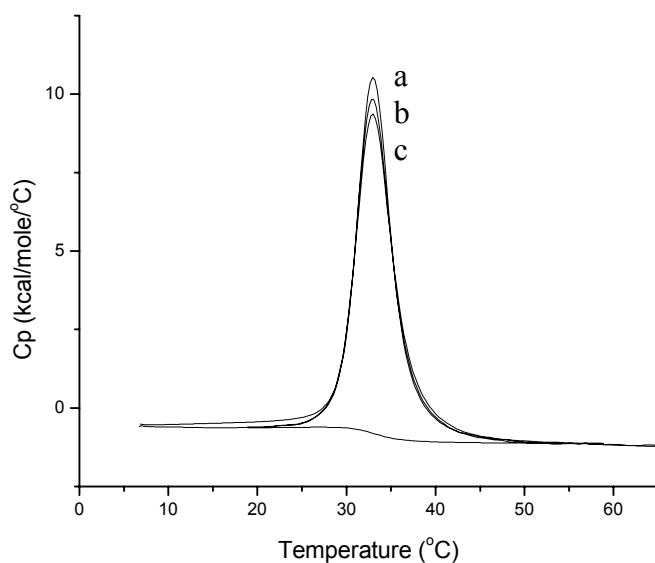


Figure IV.2. Microcalorimetric endotherms for aqueous solutions of PMVE-*g*-PEO with heating rate (a) 90°C.h⁻¹, (b) 60°C.h⁻¹ and (c) 30°C.h⁻¹.

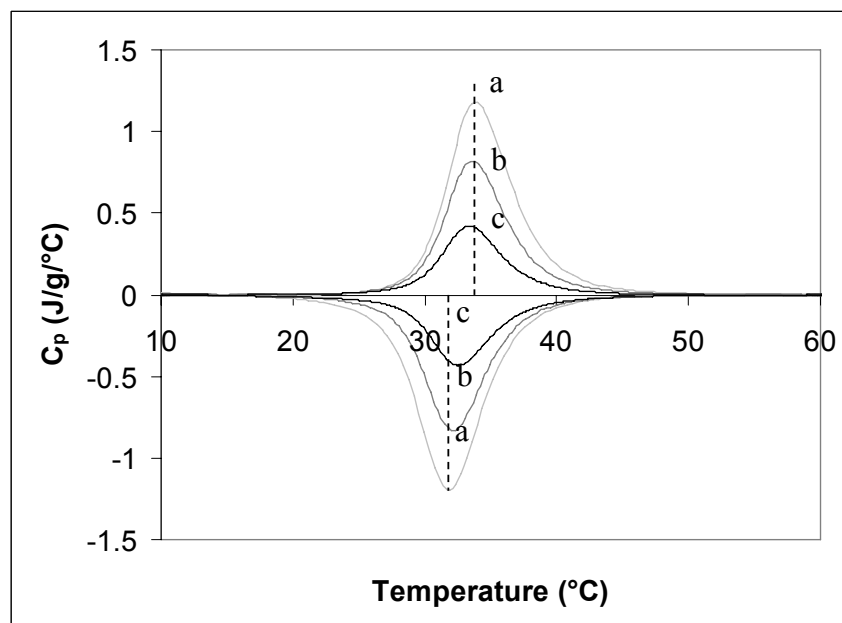


Figure IV.3. Microcalorimetric thermograms for aqueous solutions of PMVE-*g*-PS with heating rate (a) 90°C.h⁻¹, (b) 60°C.h⁻¹ and (c) 30°C.h⁻¹.

The onset temperature (T_{onset}) relates to the starting point of the aggregation process, and the maximal temperature values, at the peak, corresponds to the demixing temperature (T_{demix}). The transition is caused by the dehydration of the polymer chains. Above T_{demix} , the copolymer collapses or precipitates.

For all copolymers the values of the heat capacity (C_p) were the same, within experimental error, before and after the transition. So the faster speed of $90^{\circ}\text{C}\cdot\text{h}^{-1}$ was chosen for all experiments. The reproducibility of the thermograms was demonstrated, proven by the second and subsequent scans with identical run parameters. The transition observed is completely reversible.

IV.2.11. Methods of Micelle Preparation [10-11]

There are two principal methods for the preparation of block copolymer micelles, the direct dissolution method and the dialysis method, as outlined in figure IV.4. The choice of which method to use depends mostly on the solubility of the block copolymer in water. If the copolymer is marginally soluble in water, the direct dissolution method is employed, whereas if the copolymer is poorly soluble in water, the dialysis method is usually employed.

The direct dissolution simply involves adding the PMVE-*g*-PEO copolymer to water. The copolymer and water are mixed at room temperature, and the micelles are formed at elevated temperature.

The dialysis method is used when micelles are to be formed from a copolymer that is not easily soluble in water. In this case, the PMVE-*g*-PS copolymer first dissolved in a common organic solvent, THF, that is miscible with water. Therefore, the preparation method previously introduced by Yu and Eisenberg for 'crew-cut' micelles was applied [10].

First, an initial solution of each copolymer in THF was prepared (concentration $0.8\text{ mg}\cdot\text{mL}^{-1}$) and then deionized water was added dropwise to the solutions with vigorous stirring during three days to induce micellization of the insoluble PMVE-*g*-PS. 15-30 wt-% of water was added depending on polymer. The quality of the solvent became gradually poorer for the hydrophobic chains, this causing the aggregation of the hydrophobic blocks observed as the turbidity of the solutions. Subsequently, the resulting slightly opaque THF/water solutions were dialyzed several times against water to remove THF (Spectra-Por dialysis bags, MWCO: 30 000). The final concentration of the copolymer in pure water was set to $15\text{ mg}\cdot\text{mL}^{-1}$.

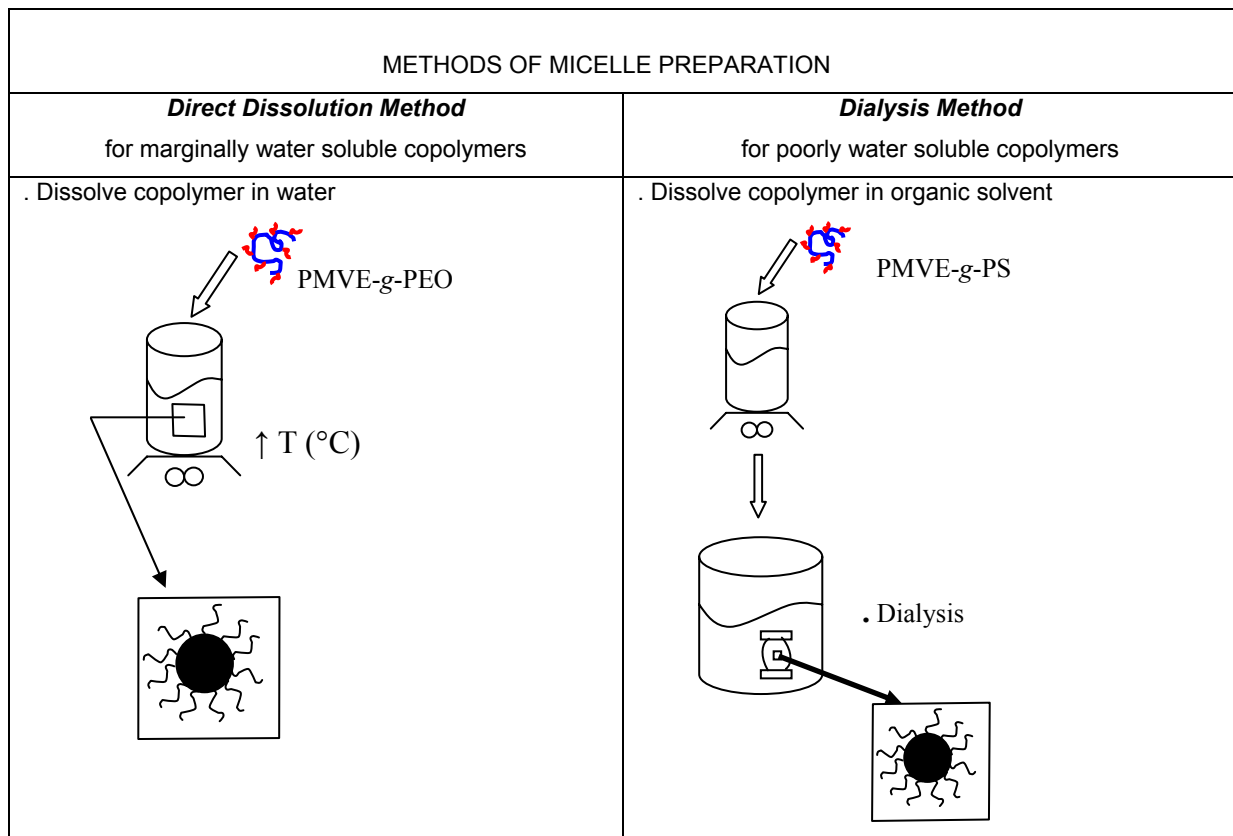


Figure IV.4. Schematic drawing of the two principal methods employed for the preparation of graft copolymer micelles. Figure taken from ref [10].

IV.2.12. Modulated Temperature Differential Scanning Calorimetry (MTDSC)

* *Thermodynamics (taken from [13])*

A MTDSC was applied for measuring the difference in heat flow between a sample and an inert reference, while both were subjected to a temperature program. Such measurements provide information on physical and chemical changes involving endothermic and exothermic process, or changes in heat capacity. The sample was put in a pan that was placed within a furnace, symmetrically to a reference pan. The temperature difference (ΔT) between both pans is related to the heat flow:

$$\frac{dQ}{dt} = \frac{\Delta T}{R} \quad \text{Eq.IV.2.12-1}$$

with dQ the amount of heat transferred to the sample (in J) in a time interval dt and R the thermal resistance of the cell in K.W^{-1} . The resulting heat flow is considered to be a combination of a heating rate dependent term and one related to the absolute temperature. The former is proportional to the heat capacity and the latter contains kinetically driven processes, which can be expressed as:

$$\frac{dQ}{dt} = C_p \frac{dT}{dt} + f(t, T) \quad \text{Eq.IV.2.12-2}$$

with C_p the thermodynamic heat capacity in J.K^{-1} , t the time in min, T the actual temperature and $f(t,T)$ the time- or temperature-dependent kinetic response of any physical or chemical process within the sample in W.

In MTDSC, a sample is subjected to a modulated temperature program obtained by superimposing a sine wave onto an isothermal or linearly changing (underlying) temperature program (figure IV.5) [12]:

$$T = T_0 + \frac{\beta t}{60} + A_T \sin(\omega t) \quad \text{Eq.IV.2.12-3}$$

with β the heating rate in K.min^{-1} , T_0 the initial temperature in K, A_T the temperature modulation amplitude in K and ω the modulation angular frequency in s^{-1} . The modulated heating rate can be written as follows:

$$\frac{dT}{dt} = \frac{\beta}{60} + A_T \omega \cos(\omega t) \quad \text{Eq.IV.2.12-4}$$

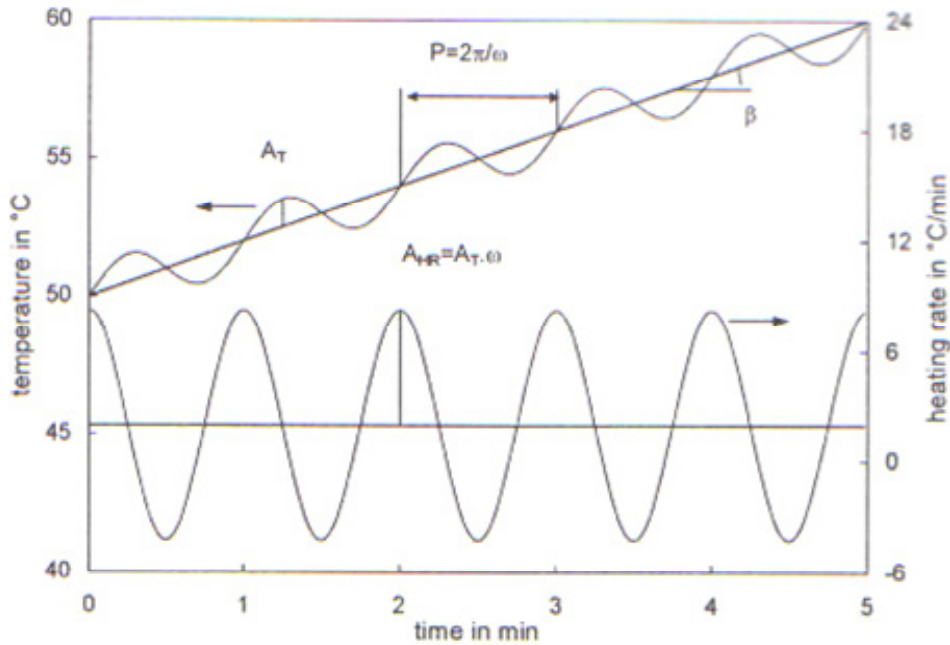


Figure IV.5. MTDSC heating profile, showing the modulated temperature and heating rate for a modulation amplitude of 1°C and a modulation period of 60 s superimposed on the heating ramp with a heating rate of 2°C.min^{-1} . Figure taken from reference [13].

As such, the resulting heat flow is given by:

$$\frac{dQ}{dt} = C_p \left[\frac{\beta}{60} + A_T \omega \cos(\omega t) \right] + f'(T_{UND}, t) + A_K \sin(\omega t) \quad \text{Eq.IV.2.12-5}$$

with $f'(T_{UND}, t)$ in W the average (underlying) response of a kinetic phenomenon to the underlying temperature program, A_K in W the amplitude of the kinetic response to the temperature modulation. This equation contains two contributions: one that depends on the modulation (cyclic) and one that depends on the average temperature (underlying). These signals can be separated as follows:

- The resulting underlying or total heat flow (THF) corresponds to the signal given by conventional DSC:

$$\left. \frac{dQ}{dt} \right|_{TOT} = C_p \frac{\beta}{60} + f'(T_{UND}, t) \quad \text{Eq.IV.2.12-6}$$

- The cyclic heat flow is obtained by subtracting the total heat flow from the modulated heat flow:

$$\left. \frac{dQ}{dt} \right|_{CYCL} = C_p A_T \omega \cos(\omega t) + A_K \sin(\omega t) \quad \text{Eq.IV.2.12-7}$$

The amplitude of the 1st harmonic of this cyclic heat flow and the amplitude of the 1st harmonic of the cyclic component of the modulated heating rate (the actual input) are obtained using a discrete Fourier transformation. They are used to calculate the cyclic heat capacity, which is the ratio between the amplitude of the cyclic heat flow (A_{HF}) and the amplitude of the cyclic heating rate ($A_T \omega$):

$$C_{p,CYCL} = \frac{A_{HF}}{A_T \omega} \quad \text{Eq.IV.2.12-8}$$

Multiplying this heat capacity by the (measured) underlying heating rate β gives the 'reversing heat flow' (RHF in W, Eq.IV.2.12-9), whereas the 'non-reversing heat flow' (NRHF in W, Eq.IV.2.12-10) is calculated by subtracting the reversing heat flow from the total heat flow.

$$RHF = C_{p,CYCL} \beta \quad \text{Eq.IV.2.12-9}$$

$$NRHF = THF - RHF \quad \text{Eq.IV.2.12-10}$$

On the time-scale of the modulation, thermodynamic materials properties and heating rate dependent transitions are found in the reversing signal (e.g. heating/cooling of the material in absence of thermal events). Kinetic properties, dependent on time and absolute temperature, will primarily show up in the non-reversing signal. Changes in the heat capacity due to a Tg, for example, will be found in the reversing heat flow, while a reaction exothermic is found in the non-reversing heat flow [14]. On the other hand, when MTDSC is used for characterizing polymer mixtures, this straightforward deconvolution is no longer valid. Heat effects, coupled with melting/crystallization or mixing/demixing occur during one modulation cycle and thus have a contribution to both signals [15].

* Experimental

1) for PMVE-g-PEO

A first series of MTDSC measurements was performed on a TA Instruments 2920 DSC with the MTDSC™ option and a Refrigerated Cooling System (RCS) cooling accessory. Helium was used as a purge gas (25 mL.min⁻¹). Indium and *n*-decane were used for temperature calibration. The former was also used for enthalpy calibration. Standard modulation conditions are an amplitude of 0.50°C with a period of 60 s. Heat capacity calibration was performed in standard modulation conditions with water, using the heat capacity difference between two temperatures, one above

and one below the melting temperature. In this way, the most accurate measurements of heat capacity changes and excess contributions, $C_{p_{excess}}$, were obtained. Data are expressed as specific heat capacities (or changes) in $\text{J}\cdot\text{g}^{-1}\cdot\text{K}^{-1}$. Non-isothermal experiments were performed at an underlying heating/cooling rate of $0.2^\circ\text{C}\cdot\text{min}^{-1}$.

A second series of MTDSC experiments was performed on a TA Instruments Q1000 (T-zero™ DSC-technology) with a liquid nitrogen cooling system. The calibration and measuring conditions were as stated above. Nitrogen was used as a purge gas ($25\text{ mL}\cdot\text{min}^{-1}$).

2) for PMVE-g-PS

MTDSC measurements were performed on a TA Instruments Q2000 DSC (T-zero™ DSC technique) with the MDSC option, equipped with an RCS cooling accessory and purged with nitrogen ($50\text{ mL}\cdot\text{min}^{-1}$). Baseline, heat capacity, and temperature were calibrated with sapphire and indium. The hermetic crucibles were perforated for the measurements of pure GPS samples. The standard modulation conditions with A_T of 0.5 K and p of 60 s were used unless stated otherwise. Scan rates were 1.0 and $2.5\text{ K}\cdot\text{min}^{-1}$ for phase separation measurements and glass transition measurements, respectively, unless stated otherwise. For phase separation measurements, the solutions were kept isothermally for 30 min at a lower limit temperature of 2°C or -10°C (the latter for the $f_w^{\text{GPS}} > 30\text{ wt}\%$) and for 5 min at an upper limit temperature of 65°C . For glass transition measurements, the solutions were kept isothermally for 10 min at a lower limit temperature of -90°C and for 1 min at an upper limit temperature of 65°C . Three heating-cooling cycles were run to see the reproducibility. For most measurements, all three cooling runs coincide very well. Only the first heating run was slightly different from the subsequent two heating run, which might be due to sample preparation effects. To reduce these effects, the second cycle was used for the analysis of demixing and remixing, while the second cooling and the third heating were used for the analysis of glass transition. Note that $T_{demix}^{threshold}$ corresponds to the first point when polymer solution starts to demix.

IV.2.13. Nuclear Magnetic Resonance (^1H NMR and ^{13}C NMR)

NMR spectra were recorded on a Bruker AC 360 or AC 500 FT NMR-instrument in DMSO-d_6 for PMVE-g-PMAA and in deuterated chloroform CDCl_3 solution for the other products at room temperature.

IV.2.14. Size Exclusion Chromatography (SEC)

** For all the products*

SEC analyses were performed with a Waters instrument equipped with a 60 cm Polymer Laboratories Column, 1000 \AA porosity, with a refractometer index (RI) detection (Melz), and chloroform (CHCl_3) as eluent, and calibrated with polystyrene standards. Therefore, a conversion factor of 0.75 [21] for the backbone and of 0.65 for PMVE-g-PEO was used to compensate the difference in hydrodynamic volume with respect to the polymers synthesized in this work. Hence,

the molar mass distribution (M_w/M_n) and the number-average molar mass (M_n) could be determined.

* *For PMAA and PMVE-g-PMAA*

SEC analyses were performed on a Waters 150-C at 35°C, equipped with Styragel HT3 and HT4 columns. PMAA and PMVE-g-PMAA were measured on three serial missed-B columns (length of each 30 cm, inner diameter 7.5 mm) from Polymer Labs at 40°C using a refractive index detector (2410 Waters). PS standards were used for calibration with N, N-dimethylacetamide (DMA) with added 0.21% LiCl and 0.63% HOAc as eluent at a flow rate of 1.0 mL.min⁻¹.

* *SEC/LS*

SEC with triple detection (refractive index (RI), viscosity and light scattering) was performed on an instrument equipped with two Styragel (mixed C) columns at 40°C. Polystyrene standards were used for calibration, and THF was used as an eluent at a flow rate of 1.0 mL.min⁻¹. A viscotec TS10 detector (scattering angle: 90°, wavelength laser: 670 nm) was used in combination with a Knaub RI detector. The M_w and PDI index were determined using the Trisec software (Viscotec, dn/dc = 0.103).

IV.2.15. Surface Tension

Surface tension measurements were carried out using Cahn Dynamic Contact Angle Analyzer. All the measurements were carried out at 20°C. To confirm precision for our experimental procedures, the surface tension of PMVE-g-PEO solution was measured and its critical aggregate concentration (CAC) determined.

IV.2.16. Ultraviolet-visible spectrophotometer (UV-vis Transmission)

The T_{cp} were determined with a UV-vis spectrophotometer ($\lambda = 630$ nm) for the aqueous solutions with polymer concentration varying from 0.01 to 15 g.L⁻¹. Solutions were heated in a transparent 1 cm³ thin UV cell with a constant rate of 1°C min⁻¹. The T_{cp} was reported at the onset temperature corresponding to an increase of the turbidity. The transmittance was recorded with a Shimadzu 160 1PC UV-vis spectrophotometer equipped with a thermostatic cell holder ETEC-505. The measurements were done in a temperature range of 5-50°C. The temperature was elevated with a step of 5°C. In this work, the heating rate was set to 0.2°C.min⁻¹, and no effect of the heating rate on the signal was observed at low heating rates.

IV.3. Syntheses

IV.3.1. Synthesis of the Poly(Vinyl Ethers)

All glasswork was dried for at least 24 hours in a drying oven at 70°C.

The polymerization was performed in a double jacket reactor provided with magnetic stirrer, an inlet for gaseous MVE, an inlet for solvent, and with a rubber septum-closed neck containing a needle connected with a balloon filled with dry argon.

IBVE and CEVE were added through a rubber septum by means of a hypodermic syringe.

The gaseous MVE flowed stainless tubing into the reactor where it condensed in the cooled toluene solution. The amount and the mass flow of MVE were measured by a mass flow controller (figure IV.6).

For polymerizations performed in the presence of THA, the latter was introduced before the DEE or TEOp and TMSI addition.

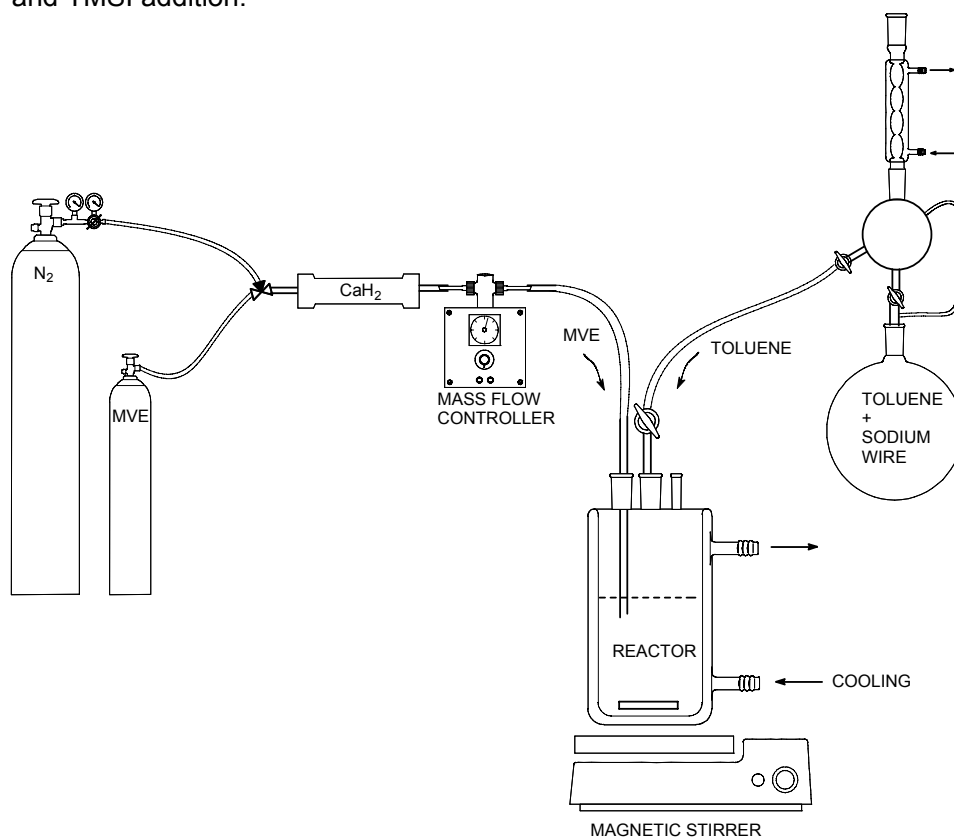


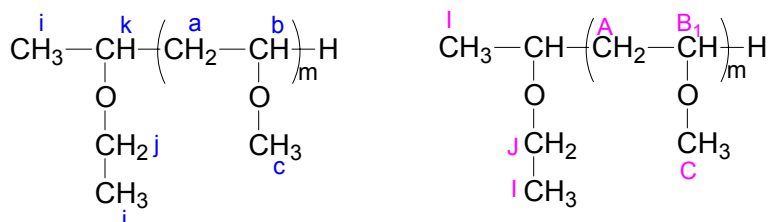
Figure IV.6. The reactor used for the living polymerization of MVE.

IV.3.1.1. Synthesis of the Random Copolymers Starting with a Mono-functional Initiator

Typical copolymerizations conditions were as follows; first, 0.025 M (0.297 mL) of TMSI and 0.021 M (0.245 mL) of DEE were added through the septum to 80 mL of dry toluene under argon atmosphere at -40°C using an equipment describe in reference [16]. After 20 min, 1.036 M (0.086 mol) of a mixture of MVE and CEVE were added. The reactor was warmed to 0°C and the

polymerization was started with the injection of ZnI_2 , dissolved in 3 ml of diethylether. After 2h30min, the polymerization was terminated at -20°C using 1.03 mL (0.002 mol) of LiBH_4 in THF (1.2 mol relative to 1 mol of polymer), and 1.11 mL of deionized water added to decompose residual LiBH_4 .

The quenched reaction mixture was washed with 10% aqueous $\text{Na}_2\text{S}_2\text{O}_3$ solution, then with deionized water, and dried over anhydrous MgSO_4 . The solution was filtered and the solvent was dried under vacuum.

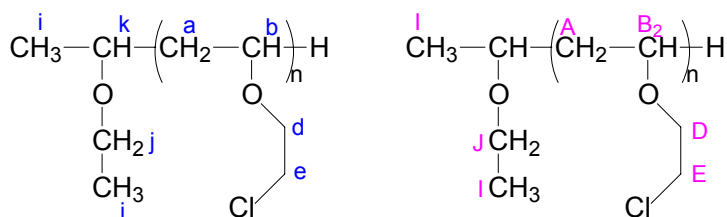


Scheme IV.1. PMVE with DEE/TMSI acetal initiator.

$^1\text{H-NMR}$ (CDCl_3): $\delta = 3.3\text{-}3.5$ ppm (b, c, j, k), $\delta = 1.5\text{-}2.0$ ppm (a), $\delta = 1.18$ ppm (i).

$^{13}\text{C-NMR}$ (CDCl_3): $\delta = 74.5$ ppm (B_1), $\delta = 68.9$ ppm (J), $\delta = 56\text{-}57$ ppm (C), $\delta = 37.6\text{-}39.4$ ppm (A), $\delta = 19.7$ ppm (I).

FT-IR: 2953 cm^{-1} (C-H), 2871 cm^{-1} (C-H), 1114 cm^{-1} (C-O), 1095 cm^{-1} (C-O).

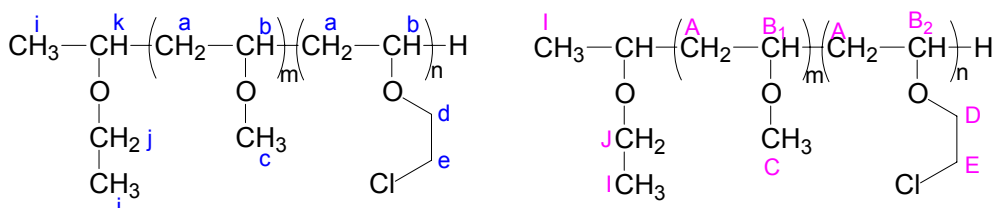


Scheme IV.2. PCEVE with DEE/TMSI acetal initiator.

$^1\text{H-NMR}$ (CDCl_3): $\delta = 3.5\text{-}3.9$ ppm (b, d, e, j, k), $\delta = 1.5\text{-}2.0$ ppm (a), $\delta = 1.18$ ppm (i).

$^{13}\text{C-NMR}$ (CDCl_3): $\delta = 74.5$ ppm (B_1), $\delta = 73.6$ ppm (B_2), $\delta = 68.9$ ppm (J), $\delta = 68.7$ ppm (D), $\delta = 43.7$ ppm (E), $\delta = 39.4\text{-}41.0$ ppm (A), $\delta = 19.7$ ppm (I).

FT-IR: 2953 cm^{-1} (C-H), 2871 cm^{-1} (C-H), 1114 cm^{-1} (C-O), 1095 cm^{-1} (C-O), 732 cm^{-1} (C-Cl), 667 cm^{-1} (C-Cl).



Scheme IV.3. P(MVE-co-CEVE) with DEE/TMSI acetal initiator.

$^1\text{H-NMR}$ (CDCl_3): $\delta = 3.3\text{-}3.9$ ppm (b, c, d, e, j, k), $\delta = 1.5\text{-}2.0$ ppm (a), $\delta = 1.18$ ppm (i).

$^{13}\text{C-NMR}$ (CDCl_3): $\delta = 73.6$ ppm (B_2), $\delta = 68.9$ ppm (J), $\delta = 68.7$ ppm (D), $\delta = 56\text{-}57$ ppm (C), $\delta = 43.7$ ppm (E), $\delta = 39.0\text{-}42.0$ ppm (A), $\delta = 19.7$ ppm (I).

FT-IR: 2953 cm^{-1} (C-H), 2871 cm^{-1} (C-H), 1114 cm^{-1} (C-O), 1095 cm^{-1} (C-O), 732 cm^{-1} (C-Cl), 667 cm^{-1} (C-Cl).

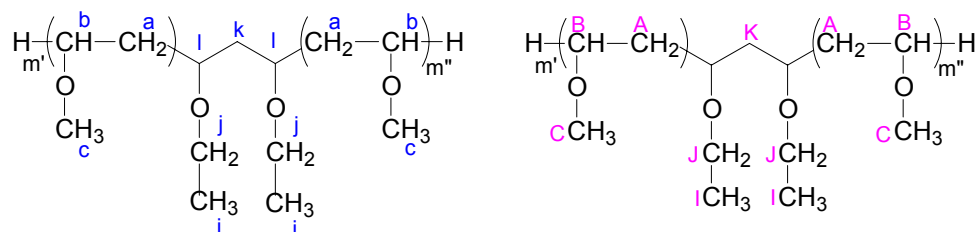
IV.3.1.2. Homopolymerizations of PMVE, PIBVE and PCEVE Starting with a Bi-functional Initiator

Typical homopolymerizations conditions were as follows; first, 2 mL of THA (0.1 M), TMSI and TEoP (table IV.1) were added through the septum to 100 mL of dry toluene under argon atmosphere at -40°C using an equipment described in reference [16]. After 20 min, 0.83 M (0.086 mol) of monomer was added. The reactor was warmed and the polymerization was started with the injection of 5.5 mg ZnI_2 , dissolved in 4 mL of diethylether. After the complete reaction, the polymerization was terminated at -20°C using 1.7 mL (0.2 mol) of LiBH_4 in THF (1.2 mol relative to 1 mol of polymer), and 2 mL of deionized water added to decompose residual LiBH_4 .

The quenched reaction mixture was washed with 10% aqueous $\text{Na}_2\text{S}_2\text{O}_3$ solution, then with deionized water, and dried over anhydrous MgSO_4 . The solution was filtered and the solvent was dried under vacuum.

Table IV.1. Reactions conditions for the homopolymerizations with $[\text{A}]_0/[\text{I}]_0 = 1/33$.

Monomer	$[\text{M}]_0$	$[\text{TEoP}]_0 = [\text{I}]_0$	$[\text{TMSI}]_0$	T_{reaction}	reaction time
MVE	0.83 M (5 g)	0.011 M (18.6 μl)	0.026 M (37.3 μl)	0°C	4 hours
CEVE	0.83 M (8.74 ml)	0.027 M (47.2 μl)	0.066 M (94.3 μl)	0°C	4 hours
IBVE	0.83 M (11.22 ml)	0.027 M (47.2 μl)	0.066 M (94.3 μl)	-40°C	2 h 45 min

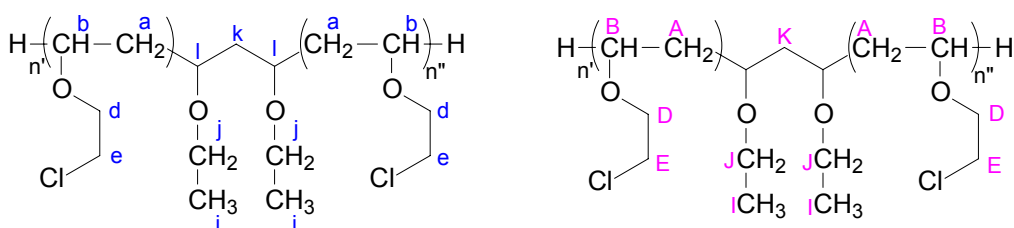


Scheme IV.4. PMVE with TEoP/TMSI bi-acetal initiator.

$^1\text{H-NMR}$ (CDCl_3): $\delta = 4.3$ ppm (l), $\delta = 3.3\text{-}3.5$ ppm (b, c, j), $\delta = 1.5\text{-}2.0$ ppm (a, k), $\delta = 1.18$ ppm (i).

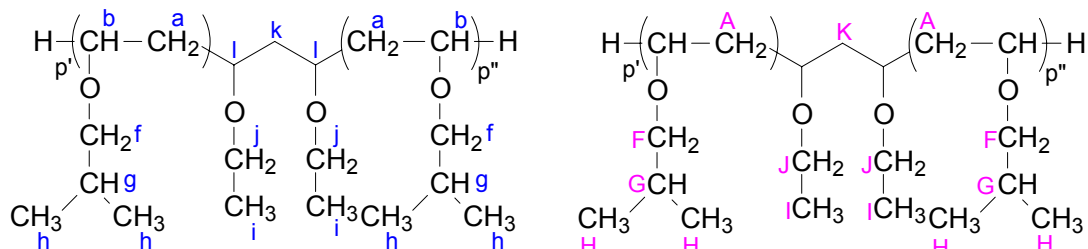
$^{13}\text{C-NMR}$ (CDCl_3): $\delta = 74.5$ ppm (B), $\delta = 68.9$ ppm (J), $\delta = 56\text{-}57$ ppm (C), $\delta = 37.6\text{-}39.4$ ppm (A, K), $\delta = 19.7$ ppm (I).

FT-IR: 2953 cm^{-1} (C-H), 2871 cm^{-1} (C-H), 1114 cm^{-1} (C-O), 1095 cm^{-1} (C-O).



Scheme IV.5. PCEVE with TEoP/TMSI bi-acetal initiator.

$^1\text{H-NMR}$ (CDCl_3): $\delta = 4.3$ ppm (l), $\delta = 3.5\text{-}3.9$ ppm (b, d, e, j), $\delta = 1.5\text{-}2.0$ ppm (a, k), $\delta = 1.18$ ppm (i).
 $^{13}\text{C-NMR}$ (CDCl_3): $\delta = 73.6$ ppm (B), $\delta = 68.7\text{-}68.9$ ppm (D, J), $\delta = 43.7$ ppm (E), $\delta = 39.4\text{-}41.0$ ppm (A, K), $\delta = 19.7$ ppm (I).
 FT-IR: 2953 cm^{-1} (C-H), 2871 cm^{-1} (C-H), 1114 cm^{-1} (C-O), 1095 cm^{-1} (C-O), 732 cm^{-1} (C-Cl), 667 cm^{-1} (C-Cl).



Scheme IV.6. PIBVE with TEOP/TMSI bi-acetal initiator.

$^1\text{H-NMR}$ (CDCl_3): $\delta = 4.3$ ppm (l), $\delta = 3.0\text{-}3.7$ ppm (b, f, j), $\delta = 1.4\text{-}2.0$ ppm (a, g, k), $\delta = 0.9$ ppm (h), $\delta = 1.18$ ppm (i).
 $^{13}\text{C-NMR}$ (CDCl_3): $\delta = 75.8$ ppm (B), $\delta = 68.9$ ppm (F, J), $\delta = 39.4\text{-}41.0$ ppm (A, K), $\delta = 29.0$ ppm (G), $\delta = 19.7$ ppm (H-I).
 FT-IR: 2953 cm^{-1} (C-H), 2871 cm^{-1} (C-H), 1380 cm^{-1} ($\text{C}(\text{CH}_3)_2$), 1365 cm^{-1} ($\text{C}(\text{CH}_3)_2$), 1114 cm^{-1} (C-O), 1095 cm^{-1} (C-O).

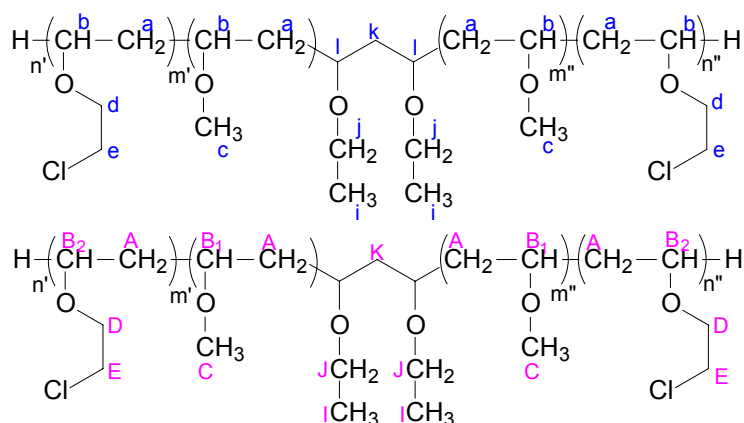
IV.3.1.3. Synthesis of the Random Copolymers Starting with a Bi-functional Initiator

Typical copolymerizations conditions were as follows; first, 0.1 M (2 mL) of THA, 0.066 M (97.8 μL) of TMSI and 0.027 M (47.2 μL) of TEOP were added through the septum to 100 mL of dry toluene under argon atmosphere at -40°C using an equipment described in reference¹. After 20 min, 0.83 M (0.086 mol) of a mixture of MVE/CEVE or IBVE/CEVE were added. The reactor was warmed (table IV.2) and the polymerization was started with the injection of 5.5 mg ZnI_2 , dissolved in 3 ml of diethylether. The polymerization was terminated at -20°C using 1.7 mL (0.2 mol) of LiBH_4 in THF (1.2 mol relative to 1 mol of polymer), and 2 mL of deionized water added to decompose residual LiBH_4 .

The quenched reaction mixture was washed with 10% aqueous $\text{Na}_2\text{S}_2\text{O}_3$ solution, then with deionized water, and dried over anhydrous MgSO_4 . The solution was filtered and the solvent was dried under vacuum.

Table IV.2. Reactions conditions for the copolymerizations with $[\text{A}]_0/[\text{I}]_0 = 1/33$.

<i>Monomer</i>	<i>T_{reaction}</i> °C	<i>reaction time</i>
MVE/CEVE	0°C	4 h
IBVE/CEVE	-30°C	2 h 45

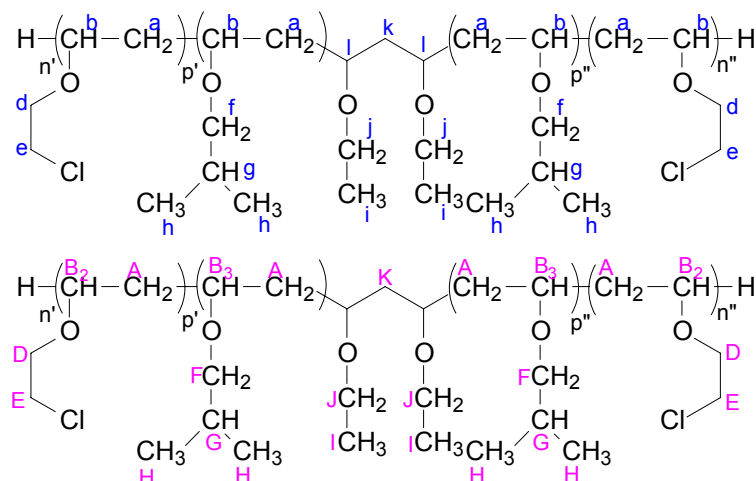


Scheme IV.7. P(MVE-co-CEVE) with TEOP/TMSI bi-acetal initiator.

$^1\text{H-NMR}$ (CDCl_3): $\delta = 4.3$ ppm (l), $\delta = 3.3\text{-}3.9$ ppm (b, c, d, e, j), $\delta = 1.5\text{-}2.0$ ppm (a, k), $\delta = 1.18$ ppm (i).

$^{13}\text{C-NMR}$ (CDCl_3): $\delta = 74.5$ ppm (B_1), $\delta = 73.6$ ppm (B_2), $\delta = 68.7\text{-}68.9$ ppm (D, J), $\delta = 56\text{-}57$ ppm (C), $\delta = 37.6\text{-}41.0$ ppm (A, K), $\delta = 19.7$ ppm (I).

FT-IR: 2953 cm^{-1} (C-H), 2871 cm^{-1} (C-H), 1114 cm^{-1} (C-O), 1095 cm^{-1} (C-O), 732 cm^{-1} (C-Cl), 667 cm^{-1} (C-Cl).



Scheme IV.8. P(IBVE-co-CEVE) with TEOP/TMSI bi-acetal initiator.

$^1\text{H-NMR}$ (CDCl_3): $\delta = 4.3$ ppm (l), $\delta = 3.0\text{-}3.9$ ppm (b, d, e, f, j), $\delta = 1.4\text{-}2.0$ ppm (a, g, k), $\delta = 1.18$ ppm (i), $\delta = 0.9$ ppm (h).

$^{13}\text{C-NMR}$ (CDCl_3): $\delta = 75.8$ ppm (B_3), $\delta = 73.6$ ppm (B_2), $\delta = 68.7\text{-}68.9$ ppm (D, F, J), $\delta = 37.6\text{-}41.0$ ppm (A, K), $\delta = 29.0$ ppm (G), $\delta = 19.7$ ppm (H, I).

FT-IR: 2953 cm^{-1} (C-H), 2871 cm^{-1} (C-H), 1114 cm^{-1} (C-O), 1095 cm^{-1} (C-O), 732 cm^{-1} (C-Cl), 667 cm^{-1} (C-Cl).

IV.3.1.4. Two-stage Copolymerizations

In the case of two-stage copolymerizations, at the time of completion of first-stage polymerization, the second-feed monomer (table IV.3) was injected into the polymerization system by a trans-dermal syringe for IBVE and CEVE, or through the septum by the MVE flow. Then the reaction was terminated and washed as described above.

Table IV.3. Reactions conditions for the two-stage copolymerizations.

<i>First-feed monomer composition</i>	<i>T_{reaction}</i>	<i>End time of first stage product</i>	<i>Second-feed monomer composition</i>	<i>reaction time</i>
MVE/CEVE with 60/40	0°C	2 h 30	MVE/CEVE with 60/40	4 h 10
IBVE/CEVE with 85/15	-30°C	1 h 30	IBVE/CEVE with 95/5	2 h 30

IV.3.2. Synthesis of the Thermo-responsive PMVE-*g*-PEO

IV.3.2.1. Model Reactions

IV.3.2.1.1. By One-step: the Nuyken Method [17-18]

A solution of the corresponding reagents (table IV.4), benzylamine (purged with argon for 10 min), base 1, 2 or 3 (1: TMP, 2: Et₃N and 3: TBuO⁻K⁺) and TBAB only use with the base 3 were dissolved in 30 mL dry DMF and stirred at room temperature for one hour. Subsequently, a solution of 2 g corresponding copolymer P(MVE-*co*-CEVE) ($M_n = 20\,460\text{ g mol}^{-1}$, composition 86.74 mol-% MVE and 13.26 mol-% CEVE) or P(IBVE-*co*-CEVE) ($M_n = 54\,790\text{ g mol}^{-1}$, composition 94.2 mol-% IBVE and 5.8 mol-% CEVE) in 5 mL dry toluene was added dropwise within 30 min. The syringe was washed with 5 mL of dry toluene and the solvent was added to the reaction mixture. This mixture was heated up to 80°C and stirred for 66 hours at this temperature.

After cooling to room temperature, the mixture was filtered to eliminate the solid residues and the solvents were evaporated. The filtrate was dissolved in 25 mL in chloroform, washed three times with deionized water and dried over MgSO₄. The solution was filtered and the solvent was evaporated to dryness under reduced pressure. Then, the pure new copolymer was dried under vacuum.

Table IV.4. Reactions conditions for the nucleophilic substitution.

<i>Copolymer</i>	<i>[Benzylamine]₀</i>	<i>[Base]₀</i>	<i>[TBAB]₀</i>
P(MVE- <i>co</i> -CEVE)	0.1225 M (4.9 mmol)	0.1225 M (4.9 mmol)	0.0025 M (0.098 mmol)
P(IBVE- <i>co</i> -CEVE)	0.0548 M (2.19 mmol)	0.0548 M (2.19 mmol)	0.0011 M (0.044 mmol)

IV.3.2.1.2. By Two-steps: the Finkelstein Method

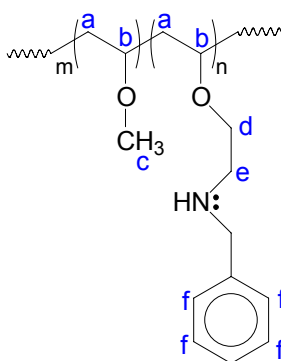
The salts KI and anhydrous Na₂S₂O₃ were suspended in 25 mL dry acetone under argon (table IV.5). The copolymer was solved in 5 mL dry acetone and dropped to the suspension with a syringe whereby the solution changed color to yellow. The syringe was washed with 5 mL acetone and the solvent was added again. The amine was purged with argon for 10 min, then

dissolved in 5 mL dry acetone and added dropwise to the reaction mixture with a syringe. The reaction mixture discolored, was stirred and heated under reflux during 48 hours at 60°C, and cooled down to room temperature under stirring.

Meanwhile precipitation fell out. The precipitate was filtered and the solvent was evaporated to dryness under reduced pressure. The residuum was dissolved in toluene. The quenched reaction mixture was washed with 10% aqueous Na₂S₂O₃ solution and water, dried over anhydrous MgSO₄, filtered, and evaporated to dryness under reduced pressure. Then, the pure copolymer was dried. The product obtained was a bright brown oil, which changed color to dark brown during standing in the lab.

Table IV.5 . Reactions conditions for the nucleophilic substitution.

Copolymer	[Benzylamine] ₀	[KI] ₀	[Na ₂ S ₂ O ₃] ₀
P(MVE-co-CEVE)	0.1225 M	0.074 M	0.147 M
86.74/13.26	(4.9 mmol)	(2.94 mmol)	(5.88 mmol)
P(IBVE-co-CEVE)	0.0548 M	0.034 M	0.066 M
94.2/5.8	(2.19 mmol)	(1.31 mmol)	(2.63 mmol)



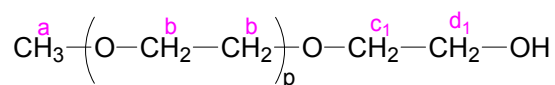
Scheme IV.9. PMVE-g-benzylamine structure.

¹H-NMR (CDCl₃): δ = 7.15-7.35 ppm (f), δ = 4.3 ppm (l), δ = 3.3-3.9 ppm (b, c, d, e, j), δ = 1.5-2.0 ppm (a, k), δ = 1.18 ppm (i).
 FT-IR: 2953 cm⁻¹ (C-H), 2871 cm⁻¹ (C-H), 1114 cm⁻¹ (C-O), 1095 cm⁻¹ (C-O), 732 cm⁻¹ (C-Cl), 667 cm⁻¹ (C-Cl).

IV.3.2.2. Functionalization of PEO

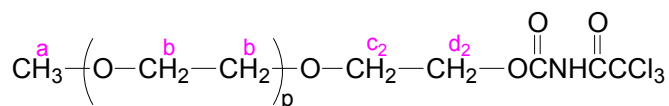
Synthesis of ω-amino-poly(ethylene oxide)-monomethyl ether (CH₃O-PEO-NH₂)

Hydroxyl-ended PEO was first converted to tosylate-functionalized PEO, which was, in the second step, substituted by ammonium to obtain the amino-functionalized PEO.



Scheme IV.10. Structure of CH₃-PEO-OH.

¹H-NMR (CDCl₃): δ = 3.80 ppm (c₁), δ = 3.75 ppm (d₁), δ = 3.55-3.70 ppm (b), δ = 3.37 ppm (a).

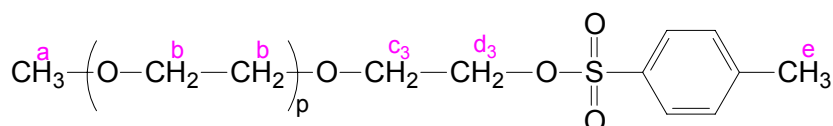


Scheme IV.11. Structure of CH₃- PEO-OH in TAIC.

¹H-NMR (CDCl₃): δ = 4.43 ppm (d₂), δ = 3.80 ppm (c₂), δ = 3.55-3.70 ppm (b), δ = 3.37 ppm (a).

First step: synthesis of PEO-TsCl

50 g (0.01 mol) of hydroxy terminated PEO ($M_w = 5000 \text{ g mol}^{-1}$) was dissolved in 300 mL dry toluene, dried by azeotropic distillation, and concentrated to about 25% of its original volume. A solution of 62.5 mL (0.773 mol) dry pyridine in 125 mL dry CH₂Cl₂ was stirred for 30 min at -5°C. A second solution of 9.5 g (0.050 mol) TsCl was solubilized in 37.5 mL dry CH₂Cl₂ and stirred for 30 min at 0°C. The pyridine solution was added to the PEO/toluene and stirred at 0°C, whereas after 30 min, the TsCl solution was added. The reaction mixture was continuously stirred overnight at 4-6°C under nitrogen atmosphere. Afterwards, it was cooled at 0°C, and 7.5 g ice were added to destroy the unreacted TsCl under stirring for 30 min. The pyridine was removed in the aqueous phase by addition of 97.5 mL of 0.3 N aqueous HCl solution, 250 g of ice and 10 mL of CH₂Cl₂ under stirring. On the other hand, the organic phase was extensively washed with: i) 3 M aqueous HCl solution at 0°C, ii) two times with a saturated NaCl solution, and iii) with a saturated NaHCO₃ solution. Next, the organic phase was dried under MgSO₄, then concentrated. PEO was precipitated several times by dropwise addition in cool Et₂O. This mixture was kept overnight at 0°C to facilitate recrystallization. Finally, the precipitate was filtered off, and dried in oven overnight to eliminate Et₂O. Yield 45 g.



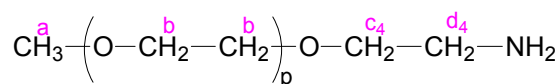
Scheme IV.12. Structure of CH₃- PEO-OTs.

¹H-NMR (CDCl₃): δ = 4.15 ppm (d₃), δ = 4.10 ppm (c₃), δ = 3.55-3.70 ppm (b), δ = 3.37 ppm (a).
 E. A. Calcd for PEO₅₀₀₀: C, 54.43 wt-%; H, 8.96 wt-%; O, 35.98 wt-%. Found: C, 54.39 wt-%; H, 8.92 wt-%; O, 36.06 wt-%.
 FT-IR (KBr): 2877 (ν C-H), 1458 (ν C-CH₂), 1182 (ν S-O-C), 1114 (ν CH₂-O-CH₂), 1106 (ν C-O-C), 665 (ν C-Cl), no absorption for OH at 3500 cm⁻¹.

Second step: synthesis of PEO-NH₂ (2)

40 g (0.008 mol) of PEO-TsCl ($M_w = 5000 \text{ g mol}^{-1}$) was dissolved in 220 mL NH₃ (25% in water) and heated for 72 hours at 70°C under reflux in an autoclave (500 ml, Schott, Mainz). After cooling to room temperature, the autoclave was carefully opened. After concentrating the mixture by rotatory evaporation, ethanol was stepwise added and removed till no residual NH₃ could be detected. The PEO was redissolved in CH₂Cl₂ and washed with 15 mL of 2 N aqueous NaOH solution, after which toluene (1v/10v toluene/CH₂Cl₂) was added to separate the emulsion phases. The organic phase was washed with half saturated NaCl solution; dried under MgSO₄, and filtered off. Finally, the solution was concentrated and redissolved in toluene, allowing crystallization at 0°C at least overnight. Once precipitation took place, the crystals were washed

with cool diethyl ether several times and the solid material was dried in vacuum oven. Yield 36 g. The yield of amination was 100 % as determined by the amount of TsCl by NMR.



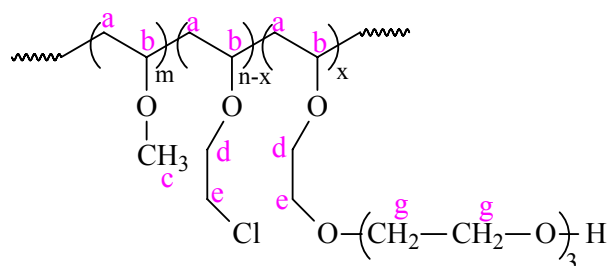
Scheme IV.13. Structure of CH₃-PEO-NH₂.

¹H-NMR (CDCl₃): δ = 3.50 ppm (c₄), δ = 3.55-3.70 ppm (b), δ = 3.37 ppm (a), δ = 2.95 ppm (d₄).
E. A. Calcd for PEO₅₀₀₀: C, 54.45 wt-%; H, 9.13 wt-%; N, 0.28 wt-%; O, 36.14 wt-%. Found: C, 54.39 wt-%; H, 9.19 wt-%; N, 0.34 wt-%; O, 36.05 wt-%.
FT-IR (KBr): 3420 (ν N-H), 2877 (ν C-H), 1580 (ν N-H), 1458 (ν C-CH₂), 1114 (ν CH₂-O-CH₂) and 1106 (ν C-O-C), no absorption for S-O-C 1182 and for Cl at 665 cm⁻¹.

This hydrophilic polymer is soluble in many solvents, e.g. water, ethanol, pyridine, dioxane, toluene, dichloromethane, chloroform, tetrahydrofurane, and insoluble in diethylether and petroleum ether.

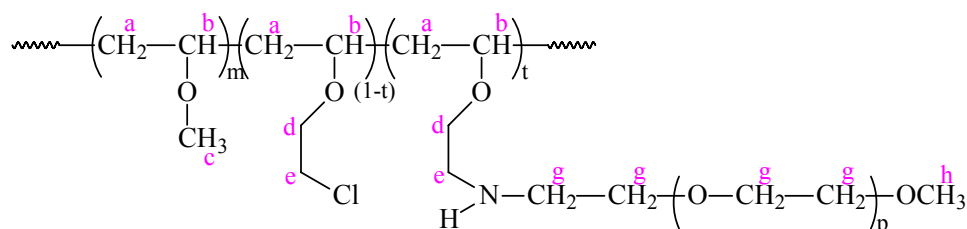
IV.3.2.3. Synthesis of PMVE-g-PEO

2.64 mL (4.22 mmol) *n*BuLi were slowly added to a solution of 8.43 g (4.22 mmol) CH₃-PEO-NH₂ (2) (M_w = 2000 g mol⁻¹) dissolved in 150 ml dry THF under argon atmosphere at -78°C, and stirred for 30 min. 4 g (1.40 mmol Cl) P(MVE-*stat*-CEVE) (234MVE/5CEVE, M_n = 14 230 g mol⁻¹) (1) was dissolved in 20 mL of dry toluene. Then, the solution (1) of P(MVE-*stat*-CEVE) was dropwise added to the reaction mixture of (2) stirred at room temperature for 72 hours. The syringe used was rinsed out with 5 mL of dry toluene, which are added to the reaction mixture. After this period, the chlorine ions were detected as a white precipitate by addition of silver nitrate aqueous solution into the system. The solvents were evaporated and the product (3) was dissolved in CH₂Cl₂. The strong *n*BuLi base was destroyed with acetic acid at low temperature. Then, the solution was neutralized with a NaHCO₃ saturated solution washed several times by pure water, dried over MgSO₄ and filtered off. The graft product was precipitated in cold diethyl ether, and then purified by dialysis (MWCO 7-10000, two weeks) in water to remove the remaining PEO. Dialysis in water yielded pure PMVE-*g*-PEO as sticky or white powder depending on the PMVE wt-%. The success of purification process was shown by the disappearance of the homo-PEO peak in the SEC chromatograms.



Scheme IV.14. PMVE-*g*-TEG structure.

¹H-NMR (CDCl₃): δ = 5.6 ppm (g), δ = 4.3 ppm (l), δ = 3.3-3.9 ppm (b, c, d, e, j), δ = 1.5-2.0 ppm (a, k), δ = 1.18 ppm (i).
FT-IR: 2953 cm⁻¹ (C-H), 2871 cm⁻¹ (C-H), 1114 cm⁻¹ (C-O), 1095 cm⁻¹ (C-O), 732 cm⁻¹ (C-Cl), 667 cm⁻¹ (C-Cl).



Scheme IV.15. Structure of PMVE-*g*-PEO.

$^1\text{H-NMR}$ (CDCl_3): $\delta = 4.3$ ppm (l), $\delta = 3.3\text{--}3.9$ ppm (b, c, d, e, g, h, j), $\delta = 1.5\text{--}2.0$ ppm (a, k), $\delta = 1.18$ ppm (i).

FT-IR (KBr): 3420 (ν N-H), 2953 and 2871 (ν C-H), 1580 (ν N-H), 1458 (ν C-CH₂), 1114 (ν C-O), 1106 (ν C-O-C), 1095 (ν C-O) and 732 (ν C-Cl) cm^{-1} .

IV.3.3. Syntheses of PMVE-*g*-PS and PMVE-*g*-PtBMA by ATRP

IV.3.3.1. ATRP Homopolymerization Procedure of St and tBMA

All experiments were conducted according to the Schlenck method. In a typical ATRP experiment, the appropriate amounts of initiator, monomer, solvent and magnetic bar were introduced in a glass tube, which was then closed by a three-way stopcock and placed under nitrogen flow to remove oxygen molecules during 45 min. In a second, dry 10 mL three-neck round-bottom flask, catalyst system was charged, and the flask was sealed with a rubber septum. This activator was also bubbled with argon for 45 min to remove traces of oxygen. Then, the catalyst system was added under nitrogen with a syringe to the monomer solution and placed in an oil bath preheated and maintained at the desired temperature.

When high temperature and/or long reaction time were required, the tubes were sealed under vacuum. For the polymerization in acetone, the tube was frozen in liquid nitrogen and three “pump-freeze-thaw” cycles were then performed. To study the kinetics of the polymerization, samples were taken using a degassed syringe during the course of reaction and diluted with ethyl acetate. Part of the solution was used for GC and ^1H NMR to determine monomer conversion, while the remaining part was used for SEC analysis. After completion of the reaction, ethyl acetate (10 mL) was added to the flask. The resulting green catalyst (Cu^{II} or Ni^{II} complex) colored polymer solution was passed through a aluminium oxide (Al_2O_3) column to remove the copper or nickel complex. The resulting colorless polymer solution was concentrated by rotavaporation, after which the polymer was purified by precipitation. After evaporation of the solvent, PS was dissolved in THF and recovered by precipitation into cold methanol, filtered and dried under vacuum until constant weight. In the case of PtBMA, the product was dissolved in a small quantity of chloroform, and then added dropwise to a solution of ethanol/water (90/10) under stirring and left precipitating overnight. Afterwards, water was added dropwise to accelerate the precipitation of the product. The final product was filtrated, washed with water and dried in vacuum oven. The PtBMA, depending on the M_n and polydispersity, could also be dissolved in THF and precipitate in cold hexane.

IV.3.3.1.1. With CuBr/PMDETA as Metal/Ligand Catalyst

For the homopolymerization of *t*BMA, CuBr catalyst (265.0 mg, 1.85 mmol), TBE (523.0 g, 1.85 mmol), *t*BMA (15 mL, 92.3 mmol, $DP_n^{\text{theoretical}} = 50$) and 15 mL THF (50/50 v/v) and were charged to a dry 100 mL three-neck round-bottom flask, and the flask was sealed with a rubber septum. The reaction mixture was bubbled with argon gas for 45 min to remove traces of oxygen. In a second, dry 10 mL three-neck round-bottom flask, PMDETA (385.0 μ L, 1.85 mmol) was degassed 45 min before use to remove traces of oxygen. Then, PMDETA was added via a degassed syringe to the monomer solution and immersed in oil bath at 60°C to start the polymerization.

The same procedure was used for PS polymerization. The table IV.6 recapitulates the experimental data of *Pt*BMA and PS syntheses.

Table IV.6. Data from *Pt*BMA and PS syntheses.

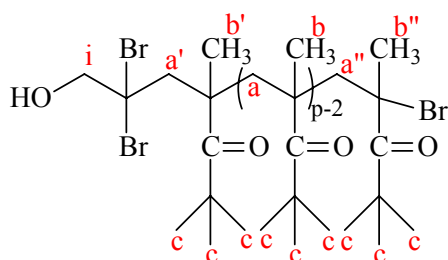
<i>monomer</i>	$[M]_0$ <i>mol, mL</i>	$[TBE]_0$ <i>mmol, mg</i>	$[CuBr]_0$ <i>mmol, mg</i>	$[PMDETA]_0$ <i>mmol, μL</i>	<i>temperature</i> $(^\circ\text{C})$	<i>vol solvent</i> <i>(mL)</i>
<i>t</i> BMA	50 0.092; 15	1 1.85; 523	1 1.85; 265	1 1.85; 385	90	15
	50 0.138; 22.5	1 2.8; 792	1 2.8; 402	1 2.8; 585	70	7.5
<i>St</i>	50 0.196; 22.5	1 3.93; 1103	1 3.93; 559	1 3.93; 814	110	7.5
	50 0.196; 22.5	1 3.93; 1103	0.75 2.95; 423	0.75 2.95; 615	110	7.5
	50 0.196; 22.5	1 3.93; 1103	0.5 1.97; 280	0.5 1.97; 407	110	7.5

IV.3.3.1.2. With NiBr₂(PPh₃)₂ as Metal Catalyst

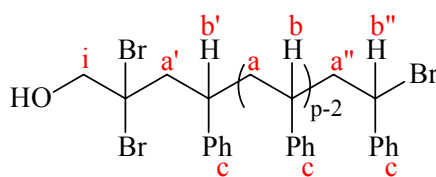
The procedure was the same as discussed in the previous homopolymerization with CuBr/PMDETA except that NiBr₂(PPh₃)₂ was added instead of CuBr, and TBE was added in the second flask instead of PMDETA to start the polymerization. The table IV.7 recapitulates the experimental data of *Pt*BMA and PS syntheses.

Table IV.7. Data from PtBMA and PS syntheses.

<i>monomer</i>	<i>[M]₀</i> <i>mol, mL</i>	<i>[TBE]₀</i> <i>mmol, mg</i>	<i>[NiBr₂(PPh₃)₂]₀</i> <i>mmol, mg</i>	<i>temperature</i> <i>(°C)</i>	<i>vol solvent</i> <i>(mL)</i>
tBMA	200 0.092; 15	1 4.6; 130	1 4.6; 343	70	5
St	250 0.131; 15	1 0.52; 148	0.5 0.26; 194	90	/
	250 0.131; 15	1 0.52; 148	0.2 0.10; 77.7	90	/

**Scheme IV.16.** Structure of PtBMA.

¹H-NMR (CDCl₃): δ = 4.68 ppm (i), δ = 2.18 ppm (a'), δ = 1.70-2.13 ppm (a, b''), δ = 1.30-1.51 ppm (a'', b', c), δ = 0.88–1.21 ppm (b).

**Scheme IV.17.** Structure of PS.

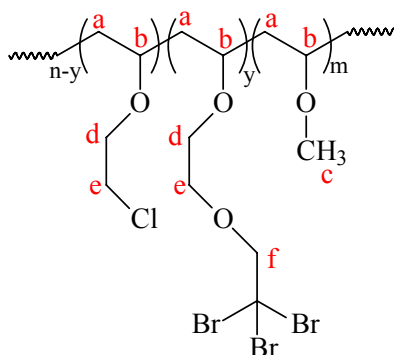
¹H-NMR (CDCl₃): δ = 6.30-7.30 ppm (c), δ = 4.8 ppm (b''), δ = 4.45 ppm (i), δ = 4.24 ppm (a''), δ = 2.76 ppm (b, b'), δ = 2.38 ppm (a'), δ = 1.25–2.25 ppm (a).

IV.3.3.2. Synthesis of the Macroinitiator

TBE (5.54 g, 19.6 mmol) was dissolved in 20 mL THF under stirring under argon atmosphere. When the solution temperature was decreased to -78 °C, *n*BuLi (12.25 mL, 19.6 mmol) (1.6 mol in hexane relative to 1 mol of chlorine group) was added slowly during 1 hour under stirring. The mixture was heated to room temperature and a solution of P(MVE-*stat*-CEVE) (30 g, 16.3 mmol of chlorine groups), previously dissolved in 100 mL dry THF during one hour, was added dropwise to the basic mixture. After three days, the solvent was evaporated. The product was dissolved in toluene, then washed several times with deionized water, dried over anhydrous MgSO₄ and filtrated. The solvent was evaporated and the product was dried overnight under vacuum oven. Table IV.8 recapitulates the macroinitiator syntheses data.

Table IV.8. Data from the macroinitiator syntheses.

<i>backbone</i>				<i>TBE</i>		<i>nBuLi</i>	
<i>name</i>	<i>m (mg)</i>	<i>nb CEVE</i>	<i>n CEVE (mmol)</i>	<i>n (mmol)</i>	<i>m (g)</i>	<i>n (mmol)</i>	<i>V (mL)</i>
B4	20	4	4.0	4.8	1.36	4.8	3.00
B5	30	10	16.3	19.6	5.54	19.6	12.25
B6	27	11	17.6	21.2	5.98	21.2	13.23

**Scheme IV.18.** Structure of the macroinitiator PMVE-*g*-TBE.

$^1\text{H-NMR}$ (CDCl_3): $\delta = 4.3$ ppm (l), $\delta = 4.25$ ppm (f), $\delta = 3.3\text{-}3.9$ ppm (b, c, d, e, j), $\delta = 1.5\text{-}2.0$ ppm (a, k), $\delta = 1.18$ ppm (i).

IV.3.3.3. ‘Grafting from’ Procedure of the Synthesis of the PMVE-*g*-PS and PMVE-*g*-PtBMA

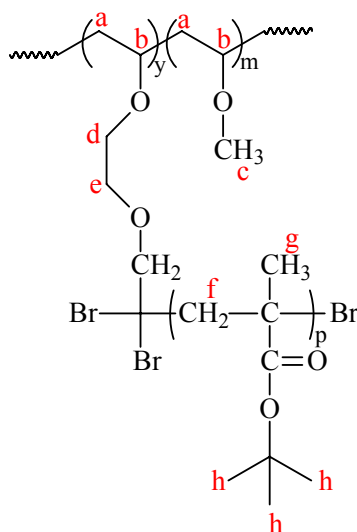
CuBr/PMDETA or $\text{NiBr}_2(\text{PPh}_3)_2$ were used as catalyst for the graft copolymer synthesis. The procedure was the same as discussed in the previous homopolymerization except that a macroinitiator (203 mg, $M_n = 20\,930\text{ g}\cdot\text{mol}^{-1}$, 0.009 mmol, theoretical degree of polymerization 200) and solvent (toluene, 4.45 mL) were added to the flask initially. PMVE modified with TBE as a graft initiator (called the macroinitiator), and the solvent were placed into a dry 100 mL three-neck round-bottom flask, and the flask was sealed with a rubber septum. Once the macroinitiator was completely dissolved, the monomer (St, 0.081 mL, 7.76 mmol) and catalyst were added. The solution was bubbled with argon for 45 min to remove traces of oxygen. Then, the monomer solution was immersed in an oil bath at the desired reaction temperature to start the copolymerization. Samples were taken and analyzed for monomer conversion by GC and ^1H NMR. The obtained graft copolymer was purified as described above. PMVE-*g*-PS was precipitated in cold methanol whereas PMVE-*g*-PtBMA precipitated in ethylene glycol.

Table IV.9. Data from PMVE-*g*-P*t*BMA and PMVE-*g*-PS syntheses with CuBr/PMDETA as catalyst from the macroinitiator M_3 .

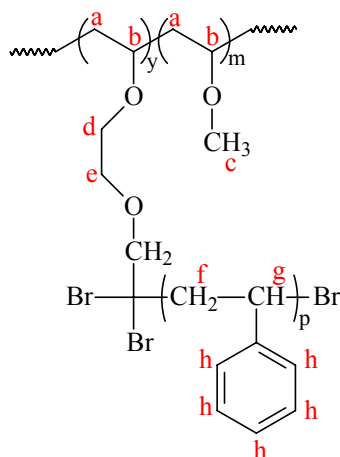
<i>monomer</i>	$[M_3]_0$ mmol, mg	$[M]_0$ mmol, mL	$[TBE]_0$ mmol	$[CuBr]_0$ mmol, mg	$[PMDETA]_0$ mmol, μ L	<i>T</i> (°C)	<i>vol solvent</i> (mL)
<i>tBMA</i>	0.026; 0.51	250 58.5; 9.5	1 0.234	1 0.234; 34	1 0.234; 49	60	4.45
<i>St</i>	0.025; 0.49	250 57.8; 6.04	1 0.231	1 0.231; 33	1 0.231; 48	90	3.02

Table IV.10. Data from PMVE-*g*-PS syntheses with $NiBr_2(PPh_3)_3$ as metal catalyst with $DP_n = 200$.

<i>macroinitiator</i>	$[Macro]_0$ mmol, mg	$[M]_0$ mmol, mL	$[TBE]_0$ mmol	$[NiBr_2(PPh_3)_2]_0$ mmol, mg	<i>T</i> (°C)	<i>vol solvent</i> (mL)
M_1	0.009; 203	200 7.76; 0.81	1 0.039	1 0.039; 288	75	0.81
M_2	0.008; 166	200 12.8; 1.34	1 0.064	0.5 0.064; 47.5	75	1.34

**Scheme IV.19.** Structure of PMVE-*g*-P*t*BMA.

1H -NMR ($CDCl_3$): $\delta = 4.3$ ppm (l), $\delta = 3.3$ -3.9 ppm (b, c, d, e, j), $\delta = 1.70$ -2.13 ppm (f), $\delta = 1.5$ -2.0 ppm (a, k), $\delta = 1.30$ -1.51 ppm (h), $\delta = 1.18$ ppm (i), $\delta = 0.88$ -1.21 ppm (g).



Scheme IV.20. Structure of PMVE-*g*-PS.

$^1\text{H-NMR}$ (CDCl_3): $\delta = 6.30\text{--}7.30$ ppm (h), $\delta = 4.3$ ppm (l), $\delta = 3.3\text{--}3.9$ ppm (b, c, d, e, j), $\delta = 2.76$ ppm (g), $\delta = 1.25\text{--}2.25$ ppm (a, f, k), $\delta = 1.18$ ppm (i).

IV.4. References

- [1] Keller R., Wycoff H., *Inorg. Syn.*, **1947**, 2, 1.
- [2] Berne B., Pecora R., in *'Dynamic Light Scattering'*, Wiley: New York, **1976**.
- [3] Brown W.; in *'Dynamic Light Scattering: The Method and some Application'*, Clarendon Press, Oxford, **1993**.
- [4] Eisenbach C.D., Schaller Ch., Schauer T., Dirnberger K., *ACS Symposium Series 881 'Particle Sizing and Characterization'*, ACS **2004**, 215.
- [5] (a) O'Brien R.W., *J. Fluid. Mech.*, **1988**, 190, 71. (b) Miller N.P., Berg J.C., *Colloids and Surfaces*, **1991**, 59, 119. (c) Schaller C., Schauer T., Dirnberger K., Eisenbach C.D., *Eur. Phys. J.*, **2001**, E 6, 365.
- [6] Haq I., *Arch. Biochem. Biophys.*, **2002**, 403, 1.
- [7] Cooper A., Nutley A., Wadwood A., in *"Protein-ligand Interactions: Hydrodynamics"* in chapter *'Calorimetry Differential Scanning Microcalorimetry'*, in, S.E. Harding and B.Z. Chowdhry (Eds), Oxford University Press, Oxford New York, **2000**, p 287-318.
- [8] (a) Tiktopulo E.I., Bychkova V.E., Rička J., Ttitsyn O.B., *Macromolecules*, **1994**, 27, 2879. (b) O'Brien R., Haq I., in *'Biocalorimetry 2'*, John E. Ladbury and Michael Doyle Edition, John Wileys & Sons, **2004**, chapter 1.
- [9] Plotnikov V.V., Brandts J.M., Lin L.N., Brandts J.F., *Anal. Biochem.*, **1997**, 250, 237.
- [10] Allen C., Maysinger D., Eisenberg A., *Colloids and Surfaces B: Biointerf.*, **1999**, 16, 3.
- [11] Yu K., Eisenberg A., *Macromolecules*, **1996**, 29, 6359.
- [12] (a) Reading M., *Trends Polymer Sci.*, **1993**, 1, 248. (b) Baur H., Wunderlich B., *J. Therm. Anal. Calorim.*, **1998**, 54, 437. (c) Hill V., Craig D.Q.M., Feely L.C., *Int. J. Pharm.*, **1999**, 192, 21.
- [13] Van Durme Kurt, in *'Phase Separation Kinetics of Aqueous Polymer Systems by means of Modulated Temperature DSC'*, PhD from Vrij Universiteit Brussel, Belgium, **2005**.

- [14] (a) Van Assche G., Van Hemelrijck A., Rahier H., Van Mele B., *Thermochim. Acta*, **1995**, 268, 121. (b) Van Hemelrijck A., Van Mele B., *J. Therm. Anal. Calorim.*, **1997**, 49, 437. (c) Swier S., Van Assche G., Van Hemelrijck A., Rahier H., Verdonck E., Van Mele B., *J. Therm. Anal. Calorim.*, **1998**, 54, 558.
- [15] (a) Dreezen G., Groeninckx, Swier S., Van Mele B., *Polymer*, **2001**, 42, 1449. (b) Swier S., Pieters R., Van Mele B., *Polymer*, **2002**, 43, 3611. (c) Swier S., Van Durme K., Van Mele B., *J. Polym. Sci., Part B: Polym. Phys.*, **2003**, 41, 1824. (d) Van Durme K., Van assche G., Van Mele B., *Macromolecules*, **2004**, 37, 9596.
- [16] Reyntjens W.G., Goethals E.J., *Design. Monom. Polym.*, **2001**, 4(2), 195.
- [17] (a) Nuyken O., Rieß G., Loontjens J.A., van der Linde R., *Macromolecular Reports*, **1995**, A32 (Suppls. 1&2), 217. (b) and A32 (Suppls. 4), 459.
- [18] Nuyken O., Ingrish S., *Macromol. Chem. Phys.*, **1998**, 199, 711.

CONCLUSION

The progress results from the smart application of the experience.

Elbert Hubbard

Conclusion

A representative variety of thermo-responsive graft copolymers of controlled architecture with fascinating properties has been the topic of this research. What has emerged from this work is that the controlled/living polymerization methods developed so far eliminate the limits in the design of novel types of graft copolymers with potential applications such as drug carriers, switchable amphiphiles, mineralization templates, etc... Interdisciplinary research was needed in order to get advantage of the high potential of these thermo-responsive graft copolymers towards specific applications.

Thermo-responsive PMVE was chosen as the backbone of the graft copolymer structures. A statistical copolymerization of VE with a small amount of CEVE was synthesized by living cationic copolymerization techniques (**Chapter 3**). The pendant chlorine groups have been used for the coupling reaction with telechelic PEO with the *grafting onto* method (**Chapter 5**). Based on the same idea, the pendant chlorine groups were capable to initiate the controlled radical polymerization (ATRP) of styrene and *t*BMA via the *grafting from* method (**Chapter 8**). All these polymers were well-defined with regard to the molecular weights of the backbone and the branches, as well as the number of branches. They could have narrow molecular weight distribution but the position of the branches is random.

To introduce PEO as side chains, it was necessary to use an excess of homopolymer to efficiently graft it onto the functionalized PMVE main chain, and the remaining fraction was removed with dialysis in order to obtain pure graft copolymers (**Chapter 5**).

In comparison to the *grafting onto* approach with coupling reaction by nucleophilic substitution, the *grafting from* method by ATRP offers convenient and mild radical reactive sites and generally results in little or no excess of the graft homopolymer. On the other hand, the prediction of the molecular weight of the growing side chain is problematic in this case. Some homopolymerizations of St and *t*BMA were first investigated with a new ATRP initiator, tribromoethanol (TBE), by two different metal catalyst systems, CuBr/PMDETA and NiBr₂(PPh₃)₂ (**Chapter 8**). It was confirmed that ATRP is a particularly suitable polymerization technique for both St and *t*BMA with CuBr/PMDETA. On the other hand, the NiBr₂(PPh₃)₂ metal catalyst system was proved to be efficient only for St homopolymerization.

First of all, to control the syntheses of PMVE-*g*-PS and PMVE-*g*-PMAA by the *grafting from* method via ATRP, the PMVE backbone was converted into a macroinitiator, bearing ATRP initiating

groups as side groups in each repeating unit, which is obtained by the nucleophilic substitution of the chlorine groups, followed by transformation of the precursor polymer into PMVE-*g*-TBE. In this way, this efficient macroinitiator permitted St and *t*BMA to be *grafted from* the backbone *via* ATRP (**Chapter 8**).

In the case of *t*BMA, which was chosen as precursor monomer of methacrylic acid, complications have been encountered due to (1) uncontrolled radical formation with CuBr/PMDETA catalyst system, and (2) the immiscibility between *t*BMA and NiBr₂(PPh₃)₂ metal catalyst. Thus, attempts were done to obtain bi-responsive PMVE-*g*-PMAA graft copolymers, after deprotection of the P*t*BMA side chains but, unfortunately, this polymerization procedure was unsuccessful as a result of the ill-defined control (**Chapter 8**).

For the PS-containing graft copolymers, both copper and nickel-mediated ATRP were found to be possible. In the case of the use of CuBr/PMDETA as catalyst, low molecular weights were obtained because of transfer reactions occurring during the polymerization. PMVE-*g*-PS graft copolymers with higher molecular weights have been successfully synthesized with the Ni catalyst.

From the number of research and review papers published over the last decade, it turns out that graft copolymer micellization, which is a unique example to achieve self-assembled nanoparticles with well-defined morphologies, is an area of increasing interest for the fundamental understanding and in view of practical application possibilities. Once the desirable structure was developed, properties of the aqueous solutions of thermo-responsive copolymers were investigated (**Chapter 6 and 9**).

MTDSC proved to be an excellent tool to evaluate the miscibility of the binary polymer mixtures studied, especially using its sensitivity for measuring T_g. The PMVE-*g*-PEO/water system does not show improved phase separation kinetics in comparison with PMVE (**Chapter 6**). This is due to the fact that PMVE does not vitrify (at T_{demix}) nor seems to be miscible with PEO. This difference in thermo-responsive behaviour also affects the change in demixing temperature upon grafting the backbone materials. It is generally assumed that grafting a hydrophilic polymer onto a thermo-responsive polymer enhances the solubility properties in water, which is thought to increase the demixing temperature. This hypothesis holds as long as the polymer concentration is very low, i.e. the mixture contains a substantial amount of bulk water [1]. However, when investigating the entire composition range, using MTDSC, the T_{demix} of PMVE-*g*-PEO was clearly lowered upon grafting. This originates from the thermo-responsive backbone to interact with the surrounding water, resulting in a weakening of the water-polymer interaction and thus lowering T_{demix} . The introduction of a hydrophilic component also influences the kinetics of phase separation. Both the rate of demixing and remixing became instantaneous upon grafting linear PMVE with PEO and PS.

Introduction of different hydrophilic/hydrophobic groups, such as CEVE-pendant groups, Br nucleophilic groups, PEO and PS grafts, proved to have a large influence on the type III LCST phase behaviour of PMVE in water. In all cases, statistical and graft copolymers with PMVE shift

the miscibility gap to lower temperatures. Hence, the solubility behaviour of PMVE in water gets worse as the content of CEVE, Br, PEO and PS increases.

Moreover, the aggregate formation was investigated by DLS and HS-DSC (**Chapter 6 and 9**). In the case of PMVE-*g*-PEO copolymers, it was found that above the demixing temperatures, a core shell nano-structure was formed, in which the core consists of collapsed PMVE chains, whereas the PEO chains form the shell. The attained particle dimensions do not allow quantifying the core and shell size. This is explained by a substantial amount of residual water in the core. In contrast, PMVE-*g*-PS formed micelles with a PS core and PMVE shell at any temperature.

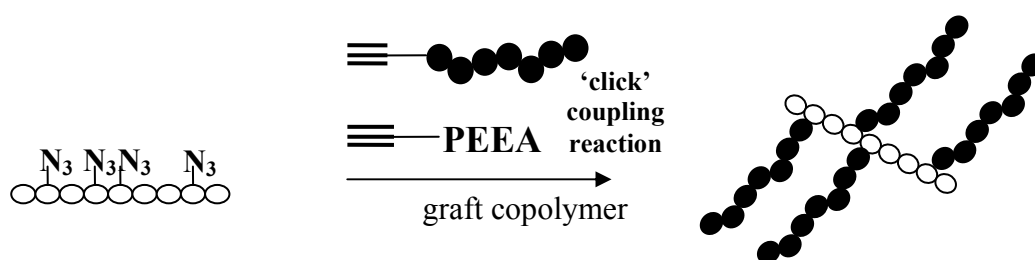
For all samples, spherical mesoglobules resulting from the merging of several individual micelles and aggregates have been observed, similar as for the PMVE homopolymer. At low temperature, the copolymers form micelle-like aggregates with sizes that are fairly independent of the concentration. Further investigation revealed that size aggregates of PMVE-*g*-PEO and PMVE-*g*-PS do not change when the number or the length of the grafts increased. This indicates that the formation of aggregates is due to intramolecular interaction between the grafts and the backbone on one hand, and between each graft copolymer on the other hand. This intramolecular aggregation is less likely to happen upon lowering the polymer concentration. A comparison of all these data revealed that the formation of the PMVE-*g*-PEO and of the PMVE-*g*-PS nanoparticles with a 'core-shell' structure actually involves two processes: the intrachain 'coil-to-globule' transition just below T_{cp} , and the interchain aggregation. Nevertheless, R_h values determined by DLS have shown that the interchain aggregation is dominant.

Aqueous polymer systems that display large conformational changes in response to temperature variations have attracted much attention in recent years covering a wide range of applications. Although these materials are very promising, usually the response rate is too slow. This can be overcome by introducing grafts on the thermo-responsive PMVE backbone. As general conclusion, PMVE-*g*-PEO and PMVE-*g*-PS graft copolymers have proved to have suitable thermo-responsive properties. For example, PMVE-*g*-PEO has been shown to act as efficient dispersants and stabilizers for carbon black, a good model for sludge [2]. From the industrial viewpoint, pigment or inorganic particle stabilization in water has a huge potential due to the public demand for products friendly to the environment. We expect that our work could help chemists as well as non-chemists to develop new applications which could be reliably utilized in real life application.

With regard to future developments, we assume the opportunity for the synthesis of the desired bi-responsive graft copolymers. After our research on the PMVE-*g*-PMAA system, the use of 1-ethoxyethyl as the protecting group for (meth)acrylic acid has been studied in our research group. Poly(1-ethoxyethyl methacrylate) (PEEMA) and poly(1-ethoxyethyl acrylate) (PEEA) are novel precursors for poly(methacrylic acid) (PMAA) and poly(acrylic acid) (PAA),

respectively [3]. They have the unique property that deprotection is carried out by a heating step, with the loss of ethyl vinyl ether (bp: 33°C) as a gas, preventing the need of an additional purification step after deprotection.

A different synthetic strategy towards graft copolymer architectures could rely on a combination of ATRP and “click” chemistry. Recently, in our research group, a combination of ATRP of EEA and the Cu(I) catalyzed “click” chemistry 1,3-dipolar cycloaddition reaction of azides and terminal alkynes was evaluated as a method to synthesize diverse amphiphilic copolymer structures [4]. Using 1-ethoxy protecting group strategy as precursor of PAA segments, polymers with alkyne as well as azide functionalities have been synthesized. These polymers were subsequently “clicked” together to yield block copolymers. Moreover, it is well-known that the bromide ends of polymers prepared by ATRP can easily be transformed into azides by nucleophilic substitution and subsequently reacted with functional alkynes. Based on this scheme, a new strategy could be used for preparing well-defined bi-responsive PMVE-*g*-P(M)AA graft copolymers, consisting of the synthesis of a PMVE-macroinitiator with a suitable pendant azide functional compound, followed by the “click” coupling grafting reaction of the alkyne-terminated PEE(M)A (see scheme C1).



Scheme C1. Schematic depiction of the synthesis of graft copolymers using ‘click’ chemistry. Figure taken from ref [4].

References

- [1] (a) Virtanen J., Tenhu H., *Macromolecules*, **2000**, *33*, 5970. (b) Berlinova I.V., Dimitrov I.V., Vladimirov N.G., Samichkov V., Ivanov Y., *Polymer*, **2001**, *42*, 5963. (c) Gan D.J., Lyon L.A., *Macromolecules*, **2002**, *35*, 9634.
- [2] Bulychev N., Confortini O., Kopold P., Dirnberger K., Schauer T., Du Prez F. E., Zubov V., Eisenbach C. D., *Polymer*, **2007**, *48*, 2636.
- [3] (a) Van Camp W., Du Prez F.E., Bon S.A.F., *Macromolecules*, **2004**, *37*, 6673. (b) Van Camp Wim, in ‘*Novel Routes for the Design of Poly((meth)acrylic acid) Containing Polymer Structures by Controlled Radical Polymerization*’, PhD in **2007**, Ghent University, Belgium.
- [4] Van Camp W., Germonpré V., Mespouille L., Dubois Ph., Goethals E.J. and Du Prez F., *React. Functional Polym.*, **2007**, *67*, 1168.

APPENDIX

Appendix I: COPOINT program

COPOINT program [1] is a simple program that fits integrated copolymerization equations to experimental monomer / copolymer composition data. The program applies numeric integration techniques that allow the user to introduce a wide variety of copolymerization equations in their differential form. The applied grid search algorithm ensures to find the global minimum of the square difference sum within the user-defined search limits.

By evaluation of the statistical error of the square difference sum, the probable error ranges of the fitted copolymerization parameters are estimated, which allows the user to estimate the reliability of the fit [2-7]. Hence COPOINT rapidly enables the user to decide which model equation approximates his data best, or if his set of data is sufficiently accurate.

The new version of the program in which the azeotropic point is enabled to be integrated, is given by Source code of COPOINT, written in Microsoft QuickBasic 4.5.

References

- [1] Beginn U., *e-polymers*, **2005**, no. 073.
- [2] O'Driscoll K.F., Reilly P.M., *Makromol. Chem., Macromol. Symp.*, **1987**, 10/11, 355.
- [3] Tirrell D.A., 'Copolymerization' in *Encycl. Polym. Sci. Eng.*, Kroschwitz J.I. editor, Vol. 4, pp. 192 - 233, Wiley, New York, **1985**.
- [4] Cote A.L., Davis T.P., *Prog. Polym. Sci.*, **2000**, 24, 1217.
- [5] Davis T.P., *J. Polym. Sci., Part A : Polym. Chem.*, **2001**, 39, 597.
- [6] Hagiopol C. editor, 'Copolymerization: toward a Systematic Approach', Kluwer Academic/Plenum Publishers, New York, **2000**.
- [7] Kuchanov S.I., *Adv. Polym. Sci.*, **1992**, 103, 1.

Appendix II: Basic Program for the Tidwell-Mortimer Method

The use of statistically invalid procedures on otherwise good data resulted in tremendous diversity of tabulated reactivity ratios.

To determine r_1 and r_2 , a non-linear method least-squares analysis was used where the sum of squares of residuals SS between measured and predicted conversion (eq. AII.1) are minimized by changing r_1 and r_2 :

$$SS(r_1, r_2) = \sum_{i=1}^n (m_i - f_{real}(r_1, r_2)_i)^2 \quad (\text{eq. AII.1})$$

where m_i is the mole fraction of the copolymerized monomers at the i th experimental data point, $f_{real}(r_1, r_2)_i$ is the value of Mayo-Lewis equation (eq. 2.2, **Chapter 2.2.**) at the i th experimental data point calculated from measured M_i .

For the least-squares procedure, the use of the 'sum-of-squares space' (SSspace) approach was opted, which is less likely to converge to a local minimum (the surface is inspected visually). Adapting this approach to our calculations, the Joint Confidence Intervals (JCI) is calculated from eq. AII.2:

$$SS(r_1, r_2) \leq SS(r_1'', r_2'') + \sigma^2 F_{0.95;2}^{n-2}(2, n-2) \quad (\text{eq. AII.2})$$

where $SS(r_1, r_2)$ is the value of eq. AII.1 at a given r_1, r_2 value, $SS(r_1'', r_2'')$ is the value of eq. AII.1 at the point estimates for the monomer reactivity ratios, and $\sigma^2 F_{0.95;2}^{n-2}(2, n-2)$ is the product of the variance of monomer conversion (estimated to be 9×10^{-4} for our reactions) and $F_{0.95;2}^{n-2}(2, n-2)$ at the 95% confidence interval for 2 degrees of freedom and n experimental data.

To construct the SSspace, eq. AII.1 was evaluated for a range of r_1 and r_2 values for a given data set in EXCEL 7.0 using a looping structure written in an Excel Visual Basic program.

The Excel program

First the experimental parameters M_1 and m_1 were written in a table AII.1 and f_{theo} and values were calculated from the Lewis-Mayo equation (eq. 2.2, **Chapter 2.2.**).

In sheet 1, the grid was designed by placing r_1 values in a single column (occupying several rows) and the r_2 values in a single row (occupying several columns). The first macro 'SSspace', made in Microsoft Visual Basic, was then executed by clicking on Tools → Macro → Macros... → SSspace → Run.

This code generates a 200 x 255 matrix of sum-of-squares values from which the minimum can be selected. One can obtain the least-squares sum $SS(r_1, r_2)$ at the best set of parameters by just keeping track of the lowest sum of squares value (SS_{real}) during the calculation of the sum of squares array.

It is difficult to graph the numbers corresponding to the JCI in this format since they are not arranged in a x,y-column format. Therefore, a short macro 'Matrixconvert' was written which can convert a matrix into an x,y,z-column format. So, the r_1, r_2 and SS values were copied in sheet 2 ('blad 3') in three columns on clicking on Tools → Macro → Macros... → Matrixconvert → Run.

Finally, an algorithm 'Verschil' was written to construct the JCI displaying the r_1 and r_2 values for which the corresponding sum-of-squares value corresponds to the joint

confidence condition, which can be represented by an ellipsoid because of the sum of squares space. You click on Tools → Macro → Macros... → Verschil → Run.

Table AII.1. Experimental and calculated data from the copolymerization of MVE with IBVE.

x or $M1$	Y or $m1$	f_{theo}	$(m_1 - f_{theo})^2$	f_{real}	$(m_1 - f_{real})^2$
0,1	0,16923	0,082458771	0,007529246	0,12059	0,002365892
0,2	0,24242	0,185185185	0,003275824	0,239292	9,78534E-06
0,3	0,33823	0,303265941	0,001222485	0,354501	0,00026473
0,4	0,44286	0,429447853	0,000179886	0,464997	0,000490062
0,5	0,54794	0,555555556	5,79967E-05	0,569923	0,000483268
0,6	0,6962	0,674157303	0,00048588	0,668734	0,000754396
0,7	0,78313	0,779816514	1,09792E-05	0,761145	0,00048332
0,8	0,84001	0,869565217	0,000873511	0,847084	5,00453E-05
0,9	0,92708	0,942668137	0,00024299	0,926635	1,97719E-07

The Excel Visual Basic Program

This program was made by the PhD student Bart Dervaux from the Ghent university (colleague of my laboratory) with the help of ref [1,2].

References

- [1] van Herk A.M., *J. Chem. Edu.*, **1995**, *72*, 138,
 [2] Arehart S.V., Matyjaszewski K., *Macromolecules*, **1999**, *32*, 2221.

Appendix III: Determination of the Degree of Functionalization of PMVE-*g*-PEO by Elemental Analysis and the Non-linear Least-squares Analysis

The degree of grafting was determined by E.A. and the non-linear least-squares analysis from data coming from the PhD's Frederic Mercier of the university of Free University of Brussels (VUB) in the laboratory of Professor Willem [1-2].

The degree of the grafting t is a very important parameter characterizing to which extent PEO side chains are grafted. Maximal degree of grafted PEO chains on the PMVE backbone could be represented as $(\text{PMVE})_m\text{-(P-Cl)}_{1-t}\text{-(P-NH-CH}_2\text{-CH}_2\text{-(O-CH}_2\text{-CH}_2\text{)}_p\text{OCH}_3)_t$, in which P-Cl stands for PCEVE and t the molar fraction of CEVE units on which the pendent chlorine group is substituted by functional $\text{NH}_2\text{-PEO-OCH}_3$ chains.

1. Determination of the degree of grafting from E.A. results

The degree of grafting can be calculated from E.A. results. Major attention was paid to the calculation of t using these data, especially because the results obtained were not always easy to understand. For this purpose, the basics behind this method will be worked out here in order to provide a clear scope of the origin of the problems met.

The principle

E.A. provides the mass fractions of the different elements in the compound investigated. Considering a compound with molecular formula containing atoms of the elements α, β, θ and χ , the mass fractions for these elements can be written as:

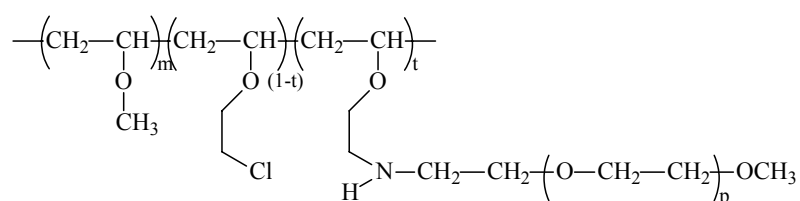
$$\text{Fraction.}\alpha = \frac{(\text{number.of.atoms.}\alpha) \times (\text{atomic.mass.}\alpha)}{\sum_{\mu} [(\text{number.of.atoms.}\mu) \times (\text{atomic.mass.}\mu)]}$$

$$\text{Fraction.}\beta = \frac{(\text{number.of.atoms.}\beta) \times (\text{atomic.mass.}\beta)}{\sum_{\mu} [(\text{number.of.atoms.}\mu) \times (\text{atomic.mass.}\mu)]}$$

$$\text{Fraction.}\theta = \frac{(\text{number.of.atoms.}\theta) \times (\text{atomic.mass.}\theta)}{\sum_{\mu} [(\text{number.of.atoms.}\mu) \times (\text{atomic.mass.}\mu)]}$$

$$\text{Fraction.}\chi = \frac{(\text{number.of.atoms.}\chi) \times (\text{atomic.mass.}\chi)}{\sum_{\mu} [(\text{number.of.atoms.}\mu) \times (\text{atomic.mass.}\mu)]}$$

In this case, four equations can thus be written down, in which each of them contains only one single parameter t . This is demonstrated with two examples, the first one being compound PMVE-*g*-PEO, represented as in scheme AIII.1.



Scheme AIII.1. Representation of compound PMVE-*g*-PEO.

The relative mass of each of the elements in compound PMVE-*g*-PEO (with $m = 284$, $n = 5$ and $p = 114$) can be expressed as:

$$C: [5 + 284 \times 3 + (5 \times 4) (1 - t) + (5 \times 227) t] \times 12.011 = [857 + 20 (1 - t) + 1135 t] \times 12.011 \quad (\text{eq. AIII.1})$$

$$H: [12 + 284 \times 6 + (5 \times 7) (1 + t) + (5 \times 455) t] \times 1.008 = [1716 + 35 (1 + t) + 2275 t] \times 1.008 \quad (\text{eq. AIII.2})$$

$$O: [2 + 284 + 5 + (5 \times 114) t] \times 15.999 = [291 + 570 t] \times 15.999 \quad (\text{eq. AIII.3})$$

$$Cl: [5 (1 - t)] \times 35.453 \quad (\text{eq. AIII.4})$$

The total relative mass can then be written as:

$$\begin{aligned} \text{Total mass} &= \text{mass of C} + \text{mass of H} + \text{mass of O} + \text{mass of Cl} \\ &= [857 + 20 (1 - t) + 1135 t] \times 12.011 + [1716 + 35 (1 + t) + 2275 t] \times 1.008 \\ &\quad + [291 + 570 t] \times 15.999 + [5 (1 - t)] \times 35.453 \\ &= 17\,131.639 + 24\,867.943 t \end{aligned} \quad (\text{eq. AIII.5})$$

For compound PMVE-*g*-PEO, an example of mass fractions obtained from E.A. was: C: 59.11 %, H: 9.99 %, O: 30.72 % and Cl: 0.31 %. Combining equations (eq. AIII.1 - 4) with (eq. AIII.5), defines the mass fraction of the different elements as a function of the single parameter t :

$$\gamma_C = \frac{[857 + 20(1-t) + 1135t] \times 12.011}{17131.639 + 24867.943t} = 0.5911 \quad (\text{eq. AIII.6})$$

$$\gamma_H = \frac{[1716 + 35(1+t) + 2275t] \times 1.008}{17131.639 + 24867.943t} = 0.999 \quad (\text{eq. AIII.7})$$

$$\gamma_O = \frac{[291 + 570t] \times 15.999}{17131.639 + 24867.943t} = 0.3072 \quad (\text{eq. AIII.8})$$

$$\gamma_{Cl} = \frac{[5(1-t)] \times 35.453}{17131.639 + 24867.943t} = 0.0031 \quad (\text{eq. AIII.9})$$

Equations (eq. AIII.6-9) constitute an overdetermined system of four equations in one single parameter t . Hence, four independent values of t can be obtained:

$$(\text{eq. AIII.6}): \quad t = 0.384 \quad \text{using C}$$

$$(\text{eq. AIII.7}): \quad t = 0.408 \quad \text{using H}$$

$$(\text{eq. AIII.8}): \quad t = 0.406 \quad \text{using O}$$

$$(\text{eq. AIII.9}): \quad t = 0.499 \quad \text{using Cl}$$

Using the equation for C, O, H or Cl, good and realistic results are obtained, values being in the same range of 0.4.

It is also possible to determine the confidence interval t , given that the confidence interval on the E.A. results are known. The smallest difference in the value of γ_i results in a rather large confidence on the value obtained for t . Moreover, as the equation used is non-linear, the resulting confidence interval on t is not symmetric. Common use of E.A. results in structural chemistry makes confidence ranges of $\pm 0.3\%$ for C, of $\pm 0.04\%$ for H, of $\pm 0.5\%$ for O and of $\pm 0.2\%$ for Cl.

2. The non-linear least-squares analysis

The method will be explained for the determination of the functionalization degree t of compound $(\text{PMVE})_m\text{-(P-Cl)}_{1-t}\text{-(P-NH-CH}_2\text{-CH}_2\text{-(O-CH}_2\text{-CH}_2\text{)}_p\text{OCH}_3)_t$ with $m = 284$, $n = 5$ and $M_w \text{PEO} = 5000 \text{ gmol}^{-1}$.

The carbon mass fraction γ_C for this compound can be written as:

$$\gamma_C = \frac{[857 + 20(1-t) + 1135t] \times 12.011}{[857 + 20(1-t) + 1135t] \times 12.011 + [1716 + 35(1+t) + 2275] \times 1.008 + [291 + 570t] \times 15.999 + [5(1-t)] \times 35.453} \quad (\text{eq. AIII.10})$$

where 12.011, 1.008, 15.999 and 35.453 are the atomic masses of carbon, hydrogen, oxygen and chlorine respectively. This implies that for every element i , γ_i obeys an equation of the general form:

$$\gamma_i = \frac{a_i + b_i t}{p + q t} = f_i(t) \quad (\text{eq. AIII.11})$$

Since only the parameter t is to be optimized, the system is overdetermined since equations of type (eq. AIII.11) can be written for each element present in the compounds, e.g. for the PMVE-*g*-PEO above, four elemental analysis results (C, H, O, Cl) for a single unknown t . The optimal t value is, accordingly, determined by non-linear least-squares analysis [3] of the set of equations of type (eq. AIII.11), using the expressions:

$$\frac{f_i(t) - \gamma_i}{\sigma_i} = e_i(t) \quad i = 1, \dots, n \quad (\text{eq. AIII.12})$$

with n = number of equations

t = parameter to be calculated

γ_i = experimental mass fraction of element i

σ_i = standard deviation on the mass fraction γ_i

$e_i(t)$ = weighted residue on the mass fraction γ_i

The costfunction $V(t)$ to be minimized in the non-linear least squares analysis is given by:

$$V(t) = \frac{1}{2} \sum_{i=1}^n e_i^2(t) \quad (\text{eq. AIII.13})$$

or in matrix form:

$$V(t) = \frac{1}{2} e^T \cdot e \quad (\text{eq. AIII.14})$$

where:

$$e = \begin{bmatrix} e_1 \\ \vdots \\ e_n \end{bmatrix}$$

is the column matrix of the e_i values, and e^T its transposed. Minimizing the costfunction implies solving the equation:

$$\frac{dV(t)}{dt} = \left(\frac{de}{dt} \right)^T e = 0 \quad (\text{eq. AIII.15})$$

The numerical solution of equation (eq. AIII.15) is found by applying an iterative Newton-Raphson process [4]:

$$\frac{d^2V(t)}{dt^2} \Delta t^{(j+1)} = - \frac{dV(t)}{dt} \quad (\text{eq. AIII.16})$$

Where j represents the iteration counting label and $\Delta t^{(j+1)} = t^{(j+1)} - t^{(j)}$ (eq. AIII.17), where ideally converges to zero, in practice to a predefined numerical threshold. All the calculations on the t values from E.A. data, as described above, have been performed with the software MATLAB [5]. The program used for obtaining the costfunction and t can be found in the next section.

In this method, a costfunction is obtained for the set of equations associated with a given compound. From this costfunction, the value of t with its confidence interval is calculated. A typical costfunction for the PMVE- g -PEO is given in figure AIII.1.

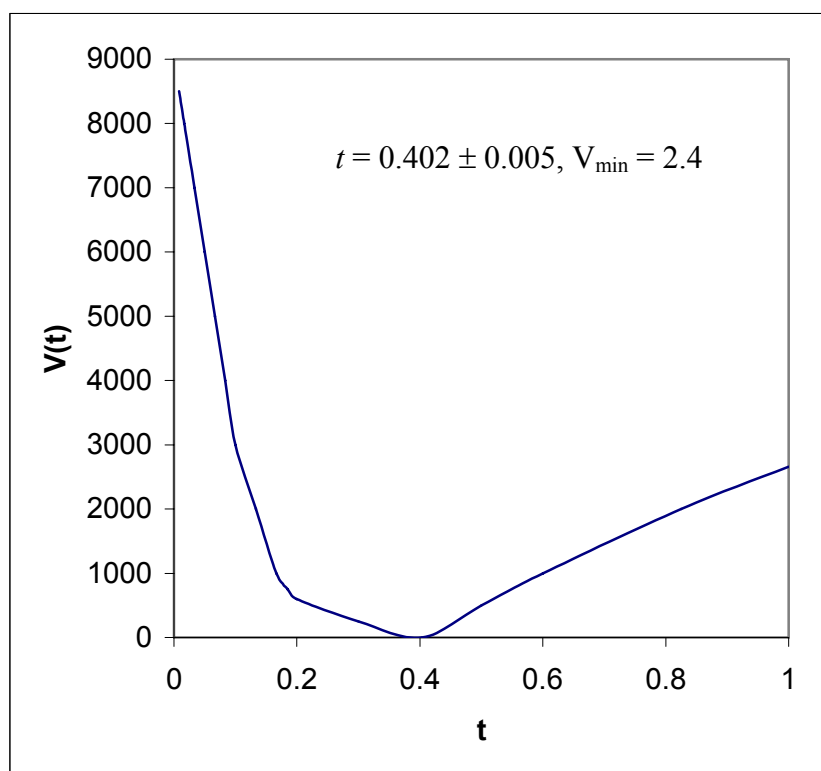


Figure AIII.1. Costfunction for compound PMVE- g -PEO.

From this figure it is clear how t is obtained by minimization of the costfunction. Only one minimum of the costfunction is found, meaning that any starting value of t can be used in the Newton-Raphson iteration procedure to find the actual t value.

3. MATLAB Routines

MATLAB routine and subroutines for the calculation of t , σ_t and V_{\min} for compound $(\text{PMVE})_m\text{-(P-Cl)}_{1-t}\text{-(P-NH-CH}_2\text{-CH}_2\text{-(O-CH}_2\text{-CH}_2\text{)}_p\text{OCH}_3)_t$:

MAIN PROGRAM

```
p=[61.487;57.539;10.302;9.662;27.177;32.799;1.035;0]; (mol fraction of the atom C, H, O
and Cl of first (P-Cl)1-t; secondly of (P-NH-CH2-CH2-(O-CH2-CH2)pOCH3)t)
m=[0.389;0.376;0.412;0.499]; (t values of C, H, O and Cl from E.A. results)
f=[0.003;0.0004;0.005;0.002]/2; (incertitude of each element C, H, O and Cl)
prec=10^(-10);
MaxI++=100;
[t,vart,V]=estimatet (p,m,prec,MaxI++,f);
t
sqrt (vart)
V
```

SUB ROUTINES

```

function [t,vart,V]=estimatet (p,m,prec,MaxItt,f);
(%starting value)
Points = 100;
s=zeros (Points,1);
for jj=1:Points
    s (jj)=costfunction ((jj/points),m,p,f);
end
figure (1)
plot (s)
[dummy,jjmin]=min (s);
t=jjmin/Points;
ii=0;
dt=1
while (ii< MaxItt) & (abs (dt/t) >prec)
ii=ii+1;
e=TheError (t,m,p,f);
j=jacobian (t,p,f);
dt=-1/ (j.*j) * (j.*e);
t=t+dt;
V=costfunction (t,m,p,f);
end
vart=1/ (j.*j);

function V=costfunction (t,m,p,f);
e=TheError (t,m,p,f);
V=0.5*e.*e;

function e=TheError (t,m,p,f);

L=length (f);
for x=1:L
    e (x,1) = (((p (((2*x) -1)) +p ((2*x)) *t) / (p (((2*L) +1)) +p (((2*L)) *t) - m(x)) / f(x));
end

function j=jacobian (t,p,f);
L=length (f);
for x=1:L
    j (x,1) = (((p (((2*L) +1)) *p ((2*x))) - (p (((2*L) +2)) *p (((2*x) - 1)))) / (f (x) * ((p
(((2*L) +1)) +p (((2*L) +2)) *t) ^2 ))) ;
end

```

4. References

- [1] F. Mercier, PhD in , Free University Brussels, Belgium, **2004**, Chap. 5.
[2] Mercier, F.A.G.; Biesemans, M.; Altmann, R.; Willem, R. *Organometallics*, **2001**, *20*, 58
[3] Champ M.A., Seligman P.F., in '*Organotin: Environmental Fate and Effects*', Chapman & Hall, London, **1996**.

-
- [4] Piotto M., Boudonneau M., Furrer J., Raya J., Elbayed K., *J. Magn. Reson.*, **2001**, *149*, 114.
- [5] Griesinger C., Schwalbe H., Sleucher J., Sattler M., in '*Two-dimensional NMR Spectroscopy - Applications for Chemists and Biochemists*', Croasmun W.R., Carlson R.M.K. Eds., VCH, New York, **1994**, p. 457.

Appendix IV: Abbreviations

[A]₀: activator concentration
AFM: atomic force microscope
AIBN: azo-(bis)-isobutyronitrile
Al₂O₃: aluminium oxide
AlR₃: trialkylaluminium
ARGET: activator regenerated by electron transfer
ATRP: atom transfer radical polymerization
nBuLi: n-butyl lithium
tBuO⁻K⁺: potassium-tert-butoxide
bipy: 2,2'-bipyridine
CAC: critical aggregate concentration
CaH₂: calcium hydride
CCl₄: tetrachloroethane
CH₂Cl₂: dichloromethane
CDCl₃: chloroform deuterated
CMC: critical micelle concentration
CRP: controlled radical polymerization
Cu: copper
CuBr: copper bromide
CuPc: copper phthalocyanine
DEE: 1,1-diethoxyethane
 ΔG_m : Gibbs free energy of mixing
 ΔG_m^0 : standard free energy of micellization
 ΔH_m : enthalpy of mixing
 ΔH_m^0 : standard enthalpy
DLS: dynamic light scattering
DMF: dimethylformamide
 ΔS_m : entropy of mixing
 ΔS_m^0 : standard entropy
DP_n: number-average degree of polymerization
DSC: differential scanning calorimetry
E.A.: elemental analysis
ESA: electrokinetic sonic amplitude
Et: ethyl
Et₂O: diethyl ether
EtOH: ethanol
Et₃N: triethylamine
f: initiation efficiency
*f*_i: mole fraction of comonomer in the feed
*F*_i: mole fraction of the comonomer in the copolymer
*F*_n: number-average end-functionality
FDA: Food and Drug Administration
FT-IR: Fourier Transform Infrared
GC: gas chromatography
h: hour
HB: protonic acid
HI: hydrogen iodide

HLB: hydrophilic-hydrophobic-balance or hydrophilic-lipophilic-balance
HPLC: high performance liquid chromatography
HS-DSC: high sensitive - differential scanning calorimetry or microcalorimetry
I: intensity of light
[I]₀: initiator concentration
I₂: iodine
JCI: join confidence intervals
k_a: rate constant of activation
k_d: rate constant of deactivation
K_{eq}: magnitude equilibrium constant
KI: potassium iodide
k_p: rate constant of propagation
L.A.: Lewis Acid
LCST: Lower Critical Solution Temperature LiBH₄: lithium borohydride
[M]: concentration of monomer
M₆TREN: N,N,N',N'',N''-hexamethyl-tris(2-aminomethyl) amine
Me: methyl
MeOH: methanol
MEK: methyl ethyl ketone or acetone
MgSO₄: sulphate magnesium
M_i: monomer i
min: minute
M_n: number-average-molecular weight
Mⁿ: transition metal complex
[Mⁿ]: concentration of catalyst at low oxidation state
M_w: molecular weight
M_w/M_n: molecular weight distribution
MX_n: metal halide
mol-%: mol percent
MTDSC: modulated temperature differential scanning calorimetry
NaI : sodium iodide
Na₂S₂O₃ : sodium thiosulfate
Ni: nickel
Ni(II)Br₂(PPh₃)₂ : nickel (II) bis(triphenylphosphine) dibromide
NMP: nitroxide mediated polymerization
NMR: nuclear magnetic resonance
p: molar monomer conversion
[P*]: concentration of polymer radical
PDI: polydispersity PMDETA: N,N,N',N'',N''-pentamethyldiethylene-triamine
iPr: isopropyl
PRE: persistent radical effect
r_i, r₁, r₂: monomer reactivity ratio of monomer i, 1 and 2
RAFT: reversible addition-fragmentation chain transfer
R_h: apparent hydrodynamic radius
R_p: rate of propagation
RX: alkyl halide
s: second
SEC: size exclusion chromatography
SFRP: stable free radical polymerization

SS: sum of squares
t: grafting degree
TAIC: trichloroacetyl isocyanate
TBAB: tetrabutylammonium bromide
TBE: 2,2,2-tribromoethanol
TCE: 2,2,2-chloroethanol
 T_{cp} : cloud point temperature
 T_{demix} : demixing temperature
TEG: triethylene glycol
TEoP: 1,1,3,3-tetraethoxypropane
 T_g : glass transition temperature
THA: trihexylaluminium
THF: tetrahydrofuran
 TiO_2 : titanium dioxide
TMP: 1,1,5,5-tetramethyl piperidine
TMSI: trimethylsilyl iodide
TsCl: para-toluenesulfonyl chloride
UCST: upper critical solution temperature
wt-%: weight percent
X: halogen
 X_i : mole fraction of monomer i
 $[X-Mt^{n+1}]$: concentration of oxidized metal complexes as persistent radicals
 ZnI_2 : zinc iodide

Monomers

AA: acrylic acid
AMPS: 2-acrylamido-2-methyl-1-propansulfonate
tBu: tert-butyl
nBA: n-butyl acrylate
nBAc: n-butyl acetate
nBMA: n-butyl methacrylate
tBMA: tert-butyl methacrylate
nBVE: n-butyl vinyl ether
tBuVE: tert-butyl vinyl ether
CEMA: cinnamoyloxyethylmethacrylate
CEVE: 2-chloroethyl vinyl ether
EVE: ethyl vinyl ether
HEMA-TMS: 2-(trimethylsilyloxy)ethyl methacrylate
IBVE: isobutyl vinyl ether
MA: methacrylate
MAA: methacrylic acid
MEMA: 2-(N-morpholino) ethyl methacrylate
MMA: methyl methacrylate
MVE: methyl vinyl ether
NIPAAm: N-isopropylacrylamide
ODVE: octadecyl vinyl ether
iPrVE: isopropyl vinyl ether
St: styrene
VBA: 4-vinylbenzoic acid

VE: vinyl ether

VP: N-vinyl-2-pyrrolidone

Homopolymers

CH₃-PEO-OH: α -methoxy- ω -hydroxyl-poly(ethylene oxide) or monomethyl ether poly(ethylene oxide)

CH₃O-PEO-NH₂: α -amino- ω -monomethyl ether-poly(ethylene oxide)

CH₃O-PEO-OTs: α -tosylate- ω -monomethyl ether poly(ethylene oxide)

PAA: poly(acrylic acid)

PAEVE : poly(aminoethyl vinyl ether)

P_nBA: poly(n-butyl acrylate)

PtBMA: poly(tert-butyl methacrylate)

PBPEM: poly(hydroxy methyl acrylate-2-(2-bromopropionyl-oxy)ethyl methacrylate)

PCEVE: poly(2-chloroethyl vinyl ether)

PCPFA: isopropyl pentachlorophenyl fumarate

PDMAEMA: poly(2-(N,N-dimethylamino) ethylmethacrylate))

PEEA: poly(1-ethoxyethyl acrylate)

PEEMA: poly(1-ethoxyethyl methacrylate)

PEG: poly(ethylene glycol)

mPEG: monomethoxy poly(ethylene glycol)

PEMA: poly(ethyl methacrylate)

PEO: poly(ethylene oxide)

PEtOx: poly(2-ethyl-2-oxazoline)

PEVE: poly(ethyl vinyl ether)

PIBVE: poly(isobutyl vinyl ether)

PMA: polymethacrylate

PMAA: poly(methacrylic acid)

PMeOXA: poly(2-methyl-2-oxazoline)

PMMA: poly(methyl methacrylate)

PMO: poly(methylene oxide)

PMVE: poly(methyl vinyl ether)

PNIPAAm: poly(N-isopropylacrylamide)

PODVE: poly(octadecyl vinyl ether)

PPO: poly(propylene oxide)

PS: polystyrene

PVCL: poly(N-vinyl caprolactam)

PVDF: poly(vinylidene fluoride)

PVE: poly(vinyl ether)

Copolymers

PAA-*b*-PMVE: poly(acrylic acid)-*block*-poly(methyl vinyl ether)

PAA-*g*-PMVE: poly(acrylic acid)-*graft*-poly(methyl vinyl ether)

PB-*g*-PEO: poly(butadiene)-*graft*-poly(ethylene oxide)

P(*t*BS-*alt*-MA) : poly((4-*tert*-butylstyrene)-*alternating*-maleic anhydride)

PEG-*b*-PNIPAAm: poly(ethylene glycol)-*block*-poly(N-isopropylacrylamide)

PEG-*g*-PNIPAAm: poly(ethylene glycol)-*graft*-poly(N-isopropylacrylamide)

PEO-*b*-PLGA-*b*-PEO: poly(ethylene oxide)-*block*-poly(lactic acid-*co*-glycolic acid)-*block*-poly(ethylene oxide)

PIBVE-*b*-PCEVE: poly(isobutyl vinyl ether)-*block*-poly(2-chloroethyl vinyl ether)

P(IBVE-*co*-CEVE): poly(isobutyl vinyl ether -*co*-(2-chloroethyl vinyl ether))
PMEMA-*b*-PDMAEMA: poly(2-(N-morpholinoethyl)methacrylate)-*block*-poly(diethylaminoethylmethacrylate)
PMMA-*b*-P*n*BMA-*b*-PMMA: poly(methyl methacrylate)-*block*-poly(*n*-butyl methacrylate)-*block*-poly(methyl methacrylate)
PMVE-*b*-PIBVE: poly(methyl vinyl ether)-*block*-poly(isobutyl vinyl ether)
PMVE-*b*-PIBVE-*b*-PMVE: poly(methyl vinyl ether)-*block*-poly(isobutyl vinyl ether)-*block*-poly(methyl vinyl ether)
PMVE-*b*-PMTEGVE: poly(methyl vinyl ether)-*block*-poly(methyl(triethylene glycol) vinyl ether)
PMVE-*b*-PVA: poly(methyl vinyl ether)-*block*-poly(vinyl alcohol)
PMVE-*b*-PS: poly(methyl vinyl ether)-*block*-polystyrene
P(MVE-*co*-CEVE): poly(methyl vinyl ether-*co*-(2-chloroethyl vinyl ether))
P(MVE-*co*-IBVE): poly(methyl vinyl ether-*co*- isobutyl vinyl ether)
P(MVE-*co*-ODVE): poly(methyl vinyl ether-*co*-octadecyl vinyl ether)
P(MVE-*stat*-CEVE): poly(methyl vinyl ether-*statistical*-(2-chloroethyl vinyl ether))
PMVE-*g*-PEO: poly(methyl vinyl ether)-*graft*-poly(ethylene oxide)
PMVE-*g*-PMAA: poly(methyl vinyl ether)-*graft*- poly(methacrylic acid)
PMVE-*g*-PS: poly(methyl vinyl ether)-*graft*-polystyrene
PMVE-*g*-TBE: poly(methyl vinyl ether)-*graft*-(2,2,2-tribromoethanol)
PNIPAAm-*b*-P*t*BMA: poly(N-isopropyl acrylamide)-*block*-poly(*ter*-butyl methacrylate)
PNIPAAm-*b*-PS: poly(N-isopropyl acrylamide)-*block*-polystyrene
PNIPAAm-*g*-P2VP: poly(N-isopropyl acrylamide)-*graft*-poly(2-vinyl pyridine)
PS-*b*-PAA: polystyrene-*block*-poly(acrylic acid)
PS-*b*-PMAA: polystyrene-*block*-poly(methacrylic acid)
P(St-*alt*-MA): poly(styrene-*alternating*-maleic anhydride)
PS-*g*-PCEVE: polystyrene-*graft*-poly(2-chloroethyl vinyl ether)
PS-*g*-PEO: polystyrene-*graft*-poly(ethylene oxide)
PVBA-*b*-PMEMA: poly(4-(vinylbenzoic acid))-*block*-poly(2-(N-morpholino) ethyl methacrylate)

Publication List

- Confortini O., Verdonck B., Goethals E., "Living Cationic Copolymerizations of Methyl Vinyl Ether with Isobutyl Vinyl Ether: Copolymerization Parameters and Properties of the Copolymers", *e-polymers*, **2002**, n° 043.
- Aseyev V., Hietala S., Laukkanen A., Nuopponen M., Confortini O., Du Prez F.E., Tenhu H., "Mesoglobules of Thermo-Responsive Polymers in Dilute Aqueous Solutions above the LCST", *Polymer*, **2005**, 46, 7118.
- V. Bulychev N., Confortini O., Arutunov I., Dirnberger K., Schauer T., Du Prez F.E., Zubov V., Eisenbach C.D., "Application of Thermo-responsive Poly(Methyl Vinyl Ether) Containing Copolymers in Combination with Ultrasonic Treatment for Pigment Surface Modification in Pigment Dispersions", *Polymer*, **2007**, 48(9), 2636.
- Confortini O., Du Prez F.E., "Functionalized Thermo-responsive Poly(Vinyl Ether) by Living Cationic Random Copolymerization of Methyl Vinyl Ether and 2-chloroethyl Vinyl Ether", *Macromol. Chem. Phys.*, **2007**, 208, 1871.
- Confortini O., Van Durme K., El Ouaamari I., Van Mele B., Du Prez F.E., "Design and Evaluation of Novel Thermo-responsive and Amphiphilic Poly(Methyl Vinyl Ether)-*g*-Poly(Ethylene Oxide) Graft Copolymers", *Polymer*, **2009**, *submitted*.
- Gabriel S., Confortini O., Stach M., Zhang T., Gilbert Y., Du Prez F.E., Jérôme R., Duwez A.S., Jérôme C., "One Step Electrographing of Thermo-responsive PMVE Films onto Conductive Surfaces", *Macromolecules*, **2009**, *manuscript in preparation*.
- Confortini O., Aseyev V., Laukkanen A., Tenhu H., Du Prez F.E., "Novel Thermo-responsive Poly(Methyl Vinyl Ether) Graft Copolymers as Revealed by Dynamic Light Scattering, Microcalorimetry and Pressure Perturbation Calorimetry", *manuscript in preparation*.
- Confortini O., Aseyev V., Tenhu H., Du Prez F.E., "Aggregates Formation of Thermo-responsive of Poly(Methyl Vinyl Ether)-*g*-Polystyrene Graft Copolymers Synthesized by ATRP", *manuscript in preparation*.
- Zhao J., Confortini O., Van Assche G., Du Prez F.E., Van Mele B., "Demixing and Remixing Kinetics in Aqueous Solutions of Poly(Methyl Vinyl ether)-*g*-Polystyrene Studied by Means of Modulated Temperature Differential Scanning Calorimetry", *manuscript in preparation*.

International Oral Presentations

**University of Helsinki, Laboratory of Professor H. Tenhu, Finland
28/04/2004**

"Synthesis of Functional Graft Copolymers with Poly(Ethylene Oxide) Side Chains onto Poly(Vinyl Ethers) Backbones"

**Workshop on Poly(methyl vinyl ether) in collaboration with China academia, Leuven, Belgium
3 - 4/11/2004**

"Design and Evaluation of Poly(Methyl Vinyl Ether)-Containing Graft Copolymers"

**6th Advanced Polymers via Macromolecular Engineering (APME 2005), Istanbul, Turkey
10 - 15/08/2005**

"Smart Graft Copolymers with Poly(Methyl Vinyl Ether) Backbone"

**STIPOMAT Conference 2005, ESF congress, Obernai, France
27 - 30/10/2005**

"Thermo-responsive Graft Copolymers with Poly(Methyl Vinyl Ether) Backbone"

**University of Helsinki, Laboratory of Professor H. Tenhu, Finland
30/11/2005**

"Thermo-responsive Properties of Poly(Methyl Vinyl Ether)-*g*-Polystyrene Graft Copolymers Synthesized by ATRP"

**STIPOMAT Conference 2006, ESF congress, Seggau, Austria
30 - 31/10/2006**

"Molecular Design and Aggregate Formation of Thermo-responsive Poly(Methyl Vinyl Ether)-*g*-Polystyrene Graft Copolymers"